

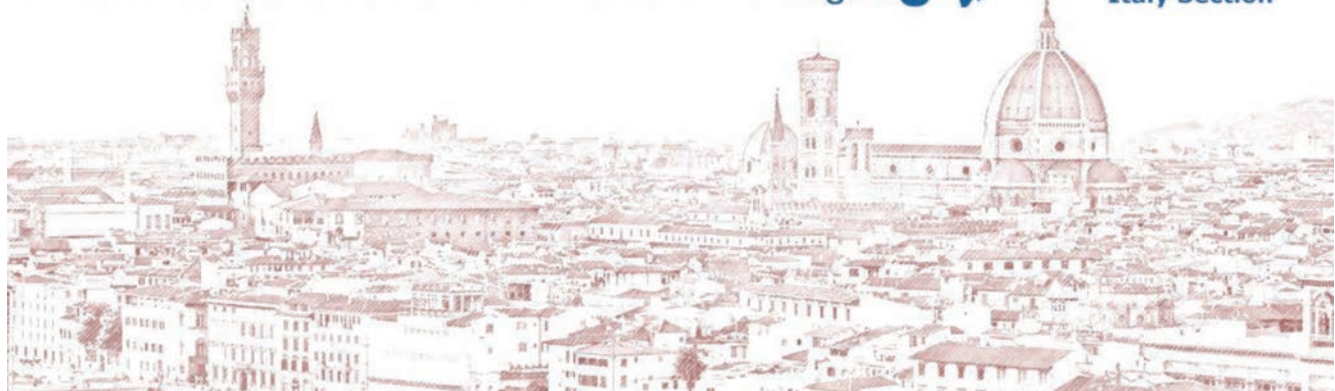
IEEE **Antennas & PROPAGATION**

Magazine

TIME-VARYING METAMATERIALS

Embracing the Temporal Dimension





HISTELCON 2023

Florence, Italy - 7-9 September 2023

SCIENCE AND TECHNOLOGY OR TECHNOLOGY AND SCIENCE?

FIRST ANNOUNCEMENT AND CALL FOR PAPERS

HISTELCON is a flagship conference series of the IEEE Region 8 held every two years and is dedicated to any aspects of the history of electrical engineering, electronics, computing and their impact on social and economical development.

HISTELCON 2023 will be the eighth HISTELCON conference, coming back to Italy after the 2012 Pavia edition. It will be a hybrid event, held both live and online. The conference official language is English, and all presentations will be oral. The conference will be hosted in the magnificent city of Florence, Italy, in the *Antica Canonica di San Giovanni*, in Florence Cathedral Square.

CALL FOR PAPERS

In addition to the relations between **Technology and Science**, the conference is open to other topics, including:

- **Technology museums**
- **Computers and microprocessors**
- **Device and system vulnerability**
- **Foundational research and Big Science**
- **Measurement systems and units**
- **Big corporations**
- **Radio astronomy**
- **Humanistic studies and technology**

Save the date and join us in Florence!

Important dates

15 April 2023 – Paper Submission

20 May 2023 – Paper review notification

17 June 2023 – Final Camera-ready paper submission

28 June 2023 – Early bird registration expires

Papers can either be **one-page abstracts** or **two to four pages full papers**. Both will undergo the same review process with the same deadlines, but only full papers will be considered for publication in IEEE Xplore. To this aim, each accepted paper must be presented by a registered author. Not more than two papers can be presented by a single author. A charge applies to the second paper.

2023.ieee-histelcon.org
histelcon2023@ieeesezioneitalia.it

Organizers

Honorary Chair

Vincenzo Piuri, *Region 8 Director 2023-2024, University of Milan*

General Chairs

Massimo Guarneri, *IEEE History Activity Committee Italy Section chair, University of Padua*

Giuseppe Pelosi, *University of Florence*

Technical Program Chair

Stefano Selleri, *University of Florence*

Treasurer

Pisana Placidi, *University of Perugia*

Publication Chair

Monica Righini, *University of Florence*

Steering Committee

Martin Bastiaans, *Region 8 History Activities Chair, Eindhoven University of Technology*

Antonio Savini, *IEEE History Committee Chair and Italy Section LM Affinity Group Chair, University of Pavia*

Anthony C. Davies, *HISTELCON2019 Chair, Potters Bar, Herts, UK*

Victor Fouad Hanna, *1st HISTELCON Chair, University of Paris 6*

Gianfranco Chicco, *IEEE Italy Section chair, Politecnico di Torino Sergio Rapuano, IEEE Italy Section past-chair, University of Sannio*

Tiziana Tambosso - *Region 8 Conference Coordination Committee Chair*

Donatella Lippi, *Fondazione Scienza e Tecnica*

Webmaster

Gianluca Mazzilli, *Athena Srl*

IEEE Antennas & PROPAGATION Magazine



IMAGE LICENSED BY INGRAM PUBLISHING

FEATURES

- 10 A Tutorial on the Basics of Time-Varying Electromagnetic Systems and Circuits**

Grigorii Ptitsyn, Mohammad Sajjad Mirmoosa, Amirhosein Sotoodehfar, and Sergei A. Tretyakov

- 21 Scattering at Temporal Interfaces**

Shixiong Yin, Emanuele Galiffi, Gengyu Xu, and Andrea Alù

- 29 Using Time-Varying Systems to Challenge Fundamental Limitations in Electromagnetics**

Zeki Hayran and Francesco Monticone

- 39 Merging Effective Medium Concepts of Spatial and Temporal Media**

Victor Pacheco-Peña and Nader Engheta

- 50 Generalized Space-Time Engineered Modulation (GSTEM) Metamaterials**

Christophe Caloz, Zoé-Lise Deck-Léger, Amir Bahrami, Oscar Céspedes Vicente, and Zhiyu Li

- 61 4D Wave Transformations Enabled by Space-Time Metasurfaces**

Sajjad Taravati and George V. Eleftheriades



ON THE COVER

This issue of *IEEE Antennas and Propagation Magazine* includes an interesting and informative special issue on time-varying metamaterials with a great roster of astonishingly high-quality articles from top experts of the discipline.

©SHUTTERSTOCK.COM/SVARUN

MISSION STATEMENT:

IEEE Antennas and Propagation Magazine publishes feature articles and columns that describe engineering activities within its scope, taking place in industry, government, and universities. All feature articles are subject to peer review. Emphasis is placed on providing the reader with a general understanding of either a particular subject or of the technical challenges being addressed by various organizations as well as their capabilities to cope with these challenges. Review, tutorial, and historical articles are welcome.

DEPARTMENTS

- 4 EDITOR'S COMMENTS**
Everything Flows
- 6 SPECIAL SERIES: GUEST EDITORIAL**
Metamaterials Embrace the Temporal Dimension
- 76 MEETINGS & SYMPOSIA**
- 78 COURSES**
- 79 BIOELECTROMAGNETICS**
Body Feature Intercomparison of Specific Absorption Rate Induced by High-Power, Portable, and Broadband Electromagnetic Sources
- 92 TURNSTILE**
Don't Leave Home Without It
- 93 STAND ON STANDARDS**
Why Every Member of the AP-S Should Own a Copy of the Antenna Measurement Standard IEEE Standard 149
- 99 HISTORICALLY SPEAKING**
The Role of History in Technology Fields
- 102 WOMEN IN ENGINEERING**
Up Close and Personal
- 105 YOUNG PROFESSIONALS**
Resonating Journeys
- 112 INDUSTRY ACTIVITIES**
10 Questions ...
- 116 AP-S COMMITTEES & ACTIVITIES**
EuCAP 2023, AP-S Chapter Activities, COPE Corner, and Distinguished Lecturers
- 126 IN MEMORIAM**
Remembering Prof. Rodolfo S. Zich
- 128 HIDDEN WORD**

IEEE ANTENNAS AND PROPAGATION MAGAZINE EDITORIAL BOARD

Editor-in-Chief

Francesco P. Andriulli
Politecnico di Torino, Italy
apm-eic@ieee.org

Editorial Assistant

Christina Tang-Bernas
University of Southern California,
California, USA
tangbern@usc.edu

Associate Editors for Feature Articles

Simon Adrian
University of Rostock, Germany
simon.adrian@uni-rostock.de

Eva Antonino-Daviu
Technical University of Valencia, Spain
evanda@upvnet.upv.es

Hakan Bagci
King Abdullah University of Science and Technology, Saudi Arabia
hakan.bagci@kaust.edu.sa

Yaniv Brick
Ben-Gurion University of the Negev,
Beer-Sheva, Israel
ybrick@bgu.ac.il

Daniilo Brizi
University of Pisa, Italy
daniilo.brizi@unipi.it

Ruisi He
Beijing Jiaotong University, China
ruisi.he@bjtu.edu.cn

Yejun He
Shenzhen University, China
yjhe@szu.edu.cn

Wonbin Hong
Pohang University of Science and Technology, South Korea
whong@postech.ac.kr

Mengmeng Li
Nanjing University of Science and Technology, China
limengmeng@just.edu.cn

Adrien Merlini
IMT Atlantique, France
adrien.merlini@imt-atlantique.fr

Sima Noghanian
PAPT, Inc., USA
sima_noghanian@ieee.org

Paolo Rocca
University of Trento, Italy
paolo.rocca@unitn.it

Felix Vega
Directed Energy Research Center
Technology Innovation Institute
Abu Dhabi, United Arab Emirates
felix.vega@ieee.org

Hao Xin
University of Arizona, Arizona, USA
hxin@email.arizona.edu

Abdulkadir Yucel

Nanyang Technological University,
Singapore
acyucel@ntu.edu.sg

Columns and Departments

Bioelectromagnetics

Asimina Kiourtzi
The Ohio State University, Ohio, USA
kiourtzi.1@osu.edu

Book Reviews

Kristof Cools
Ghent University, Belgium
kristof.cools@ugent.be

Chapter News

Meisong Tong
Tongji University, China
mstong@tongji.edu.cn

COPE Corner

Anisha Apte
Synergy Microwave Corporation,
New Jersey, USA
anisha_apte@ieee.org

Distinguished Lecturers

Kwai Man Luk
City University of Hong Kong,
Hong Kong
eekmluk@cityu.edu.hk

Education Corner

Sean Hum
University of Toronto, Canada
sean.hum@utoronto.ca

Electromagnetic Perspectives

Christophe Caloz
KU Leuven, Belgium
christophe.caloz@kuleuven.be

EM Programmer's Notebook

Matthys Botha
Stellenbosch University, South Africa
mmbotha@sun.ac.za

From the Screen of Stone

Ross Stone
Stoneware Limited, California, USA
r.stone@ieee.org

Hidden Word

Fred Gardiol
fred.gardiol@hispeed.ch

Historically Speaking

Trevor Bird
Antengenuity, Australia
tsbird@optusnet.com.au

Industry Activities

Rod Waterhouse
Octane Wireless, Maryland, USA
rwwaterhouse@octanewireless.com

Measurements Corner

Debatosh Guha
Institute of Radio Physics & Electronics, India
dguha@ieee.org

Meetings & Symposia

Short Courses

Raymond Wasky
John Hopkins University, Maryland, USA
raymond.wasky@jhuapl.edu

Stand on Standards

Vikass Monebhurrun
CentraleSupélec, France
vikass.monebhurrun@supelec.fr

Turnstile

Rajeev Bansal
University of Connecticut, USA
rajeev@engr.uconn.edu

Women in Engineering

Francesca Vipiana
Polytechnic University of Turin, Italy
francesca.vipiana@polito.it

Young Professionals

C.J. Reddy
Altair Engineering, Inc., Virginia, USA
cjreddy@ieee.org

Past Editors-in-Chief

Ross Stone
Founding Editor-in-Chief
Stoneware Limited, California, USA
r.stone@ieee.org

Mahta Moghaddam

University of Southern California,
California, USA
mahta@usc.edu

IEEE Periodicals

Magazines Department

445 Hoes Lane, Piscataway, NJ 08854 USA
Pilar Etuk,
Journals Production Manager

Katie Sullivan,
Senior Manager, Journals Production

Janet Duder, Senior Art Director

Gail A. Schnitzer,

Associate Art Director

Theresa L. Smith, Production Coordinator

Mark David, Director, Business

Development—Media & Advertising

Tel: +1 732 465 6473

Fax: +1 732 981 1855

m.david@ieee.org

Felicia Spagnoli, Advertising

Production Manager

Peter M. Tuohy, Production Director

Kevin Lisankie, Editorial Services Director

Dawn M. Melley, Senior Director,

Publishing Operations

IEEE prohibits discrimination, harassment, and bullying.

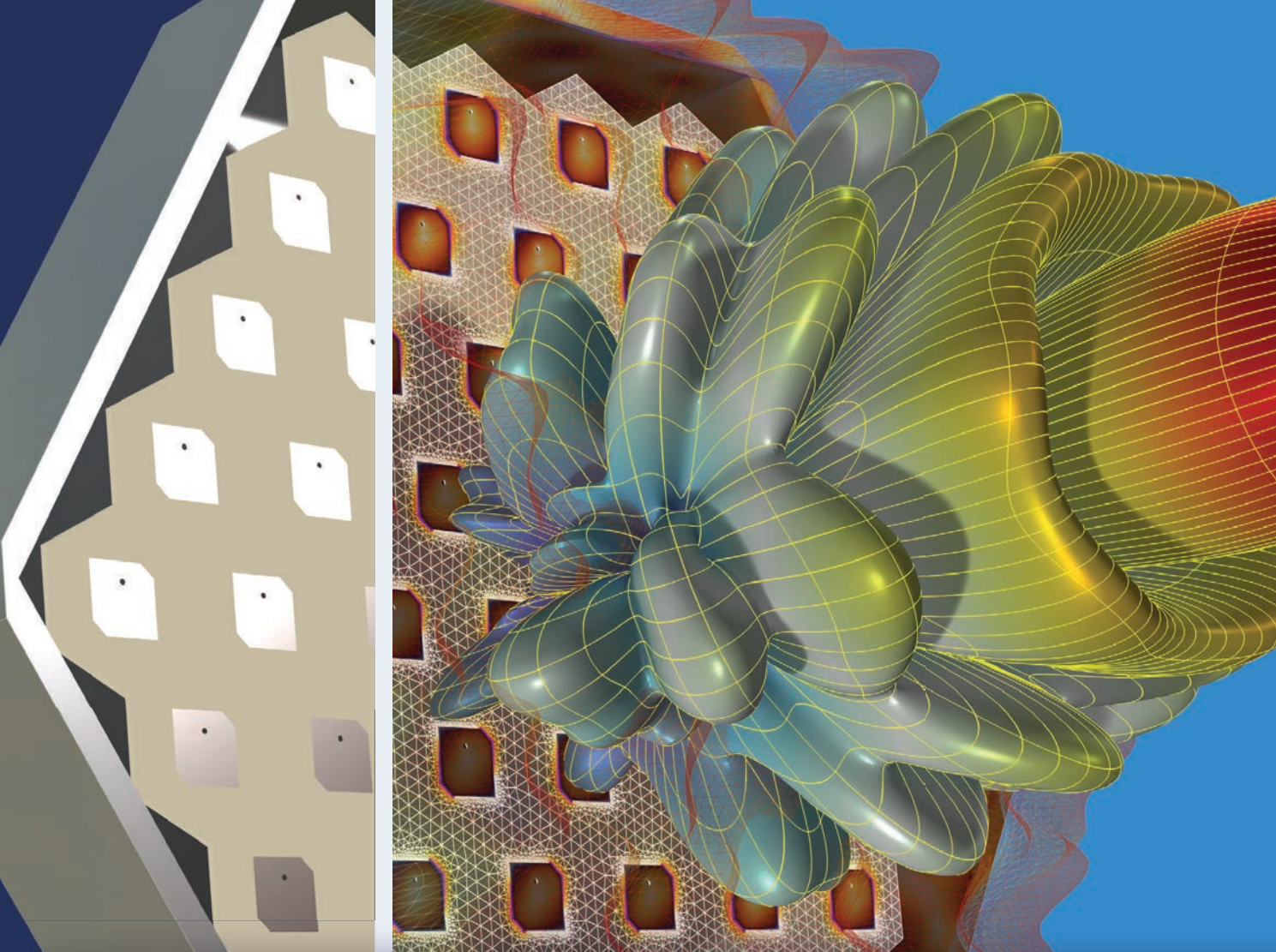
For more information, visit <http://www.ieee.org/web/aboutus/whatis/policies/p9-26.html>.

Address editorial correspondence to the Editor-in-Chief Francesco P. Andriulli, Dept. Electronics and Telecommunications, Politecnico di Torino, Corso Duca degli Abruzzi 24 10129, Turin, Italy; e-mail: apm-eic@ieee.org

General information for contributors: Contributions to *IEEE Antennas and Propagation Magazine* are accepted through ScholarOne Manuscripts at <https://mc.manuscriptcentral.com/apm-ieee>. Contributors are encouraged to contact the magazine editor-in-chief before submitting their articles to inquire whether their prospective submission is within the scope of the magazine. Article formatting requirements vary based on the type of article. The authors are asked to consult <http://ieeearthorcenter.ieee.org/> and <https://www.ieeeaps.org/publications/ieee-antennas-and-propagation-magazine> for general instructions. Manuscripts should be in English. The editor-in-chief reserves the right to accept, reject, and/or edit any and all material submitted. Submission of material will be interpreted as assignment and release of copyright and any and all other rights as if the standard IEEE copyright and US Export Control Compliance Forms had been signed by the copyright owner. All material associated with contributions may be discarded after the issue containing the contribution goes to press, unless otherwise requested. The nominal deadline for material not requiring peer review or extensive editing is 120 days prior to the start of the month of publication. Contact the editor-in-chief if you have timely material that cannot make this deadline. All feature articles are subject to full peer review per IEEE policy. There is a limit of ten double-column printed pages for all articles. All contributions to

departments are reviewed by the associate editor(s) for that department, with additional peer review as deemed necessary by the associate editor. Conference reports should be no more than two pages and contain no more than five figures.

IEEE Antennas and Propagation Magazine (ISSN1045 9243) is published bimonthly by The Institute of Electrical and Electronics Engineers, Inc. Headquarters: 3 Park Avenue, 17th Floor, New York, NY 10016-5997, U.S.A. +1 212 419 7900. Responsibility for the contents rests upon the authors and not upon the IEEE, the Society, or its members. The magazine is a membership benefit of the IEEE Antennas and Propagation Society, and subscriptions are US\$6.00 per member per year (included in Society fee). Replacement copies for members are available for US\$20 (one copy only). Nonmembers can purchase individual copies for US\$135. Nonmember subscription prices are available on request. Copyright and Reprint Permissions: Abstracting is permitted with credit to the source. Libraries are permitted to photocopy beyond the limits of the U.S. Copyright law for private use of patrons: 1) those post-1977 articles that carry a code at the bottom of the first page, provided the per-copy fee is paid through the Copyright Clearance Center, 222 Rosewood Drive, Danvers, MA 01970, U.S.A.; and 2) pre-1978 articles without fee. For other copying, reprint, or republication permission, write to: Copyrights and Permissions Department, IEEE Service Center, 445 Hoes Lane, Piscataway NJ 08854 U.S.A. Copyright © 2023 by The Institute of Electrical and Electronics Engineers, Inc. All rights reserved. Periodicals postage paid at New York, NY, and at additional mailing offices. Postmaster: Send address changes to IEEE Antennas and Propagation Magazine, IEEE, 445 Hoes Lane, Piscataway, NJ 08854 U.S.A. Canadian GST #125634188. Printed in U.S.A.



Take the Lead in RF Design

with COMSOL Multiphysics®

Multiphysics simulation is expanding the scope of RF analysis to higher frequencies and data rates. Accurate models of microwave, mmWave, and photonic designs are obtained by accounting for coupled physics effects, material property variation, and geometry deformation. Ultimately, this helps you more quickly see how a design will perform in the real world.

» comsol.com/feature/rf-innovation



Francesco Andriulli

Everything Flows

Can you step twice in the same river? "Surely not!" would answer Heraclitus of Ephesus, the famous Ionian philosopher. If everything in nature flows, however, why should you trust your metamaterial to always stay the same? You shouldn't, indeed, as we learn in this issue of the magazine! Prof. Andrea Alù, in fact, is our guest editor for an incredibly interesting and informative special issue on time-varying metamaterials. I am very grateful to Prof. Alù for his successful efforts in collecting a great roster of astonishingly high-quality articles from top experts of the discipline, providing an impactful overview of the topic. Enjoy the reading!

BE THE NEXT GUEST EDITOR OF A NEW SPECIAL ISSUE, SECTION, OR SERIES!

Are you enjoying the special issues of the magazine? The next could come from you! Special issues and sections

I am very grateful to Prof. Alù for his successful efforts in collecting a great roster of astonishingly high-quality articles from top experts of the discipline.

include up to six articles to appear in a single issue of the magazine. Special series, instead, run for several issues (one or two articles per issue). The focus of special issues/sections/series could be on either established or emerging research topics relevant to the IEEE Antennas and Propagation Society. It goes without saying that we are also quite interested in interdisciplinary topics. You can send your proposal to apm-eic@ieee.org with 1) a title and a short abstract; 2) a list of prospective guest editors, with affiliations; and 3) a tentative list of potential contributors. We are looking forward to hearing from you!

Digital Object Identifier 10.1109/MAP.2023.3286758
Date of current version: 8 August 2023

REMEMBERING THE COLLEAGUES WHO LEFT US

It is with sorrow that we have learned of the passing of Prof. Rodolfo Zich, from Politecnico di Torino. Our thoughts and prayers go to him, his family, and his friends. Prof. Zich is honored in this issue of the magazine with an "In Memoriam" column [A1] from Prof. Roberto Graglia, on page 126.

In the final phases of preparing this issue, we also learned of the passing of Prof. Matteo Pastorino, from the University of Genoa. Prof. Pastorino had been an associate editor of the magazine, and this news leaves the entire editorial board in deep sadness. An "In Memoriam" column honoring him will appear in a future issue of the magazine.

APPENDIX: RELATED ARTICLE

[A1] R. D. Graglia, "Remembering Prof. Rodolfo S. Zich," *IEEE Antennas Propag. Mag.*, vol. 65, no. 4, pp. 126–127, Aug. 2023, doi: 10.1109/MAP.2023.3281988.



RF Testing Equipment That's Built to Last



SunAR RF Motion products give you the competitive edge with the long-lasting durability that AR products are known for. The SunAR product line includes:

- Antennas
 - Wireless & EMC testing
 - Distributed antenna systems (DAS)
- System controllers
- Turntables
- Reverberation chamber stirrers
- Antenna masts / positioners / stands

Many SunAR products can be customized to your specifications.

To learn more about customization options for masts, positioners, stirrers, and turntables, visit www.arworld.us/sunarrfmotion or call us at 215-723-8181.



sunar rf motion

Other **ar** divisions: **rf/microwave instrumentation** • **modular rf** • **ar europe**



IMAGE LICENSED BY INGRAM PUBLISHING



Andrea Alù 

Metamaterials Embrace the Temporal Dimension

Over the past 20 years, metamaterials have evolved into a powerful platform for wave manipulation, demonstrating a plethora of exciting functionalities relevant to a wide range of technologies. Yet, most of the work on metamaterials to date has been limited to carefully patterning materials in space, enabled by advances in micro- and nanofabrication and in the understanding of complex wave-matter interactions at subwavelength scales. The complex wave transformations enabled by metamaterials are typically associated with multiple scattering events, driving complex interference and resonance phenomena associated with the multiple spatial interfaces that form their microstructure. Spatial metamaterials are, however, fundamentally limited in the way they can transform and control waves; in the linear regime, the frequency content of the incoming waves is conserved, and time-reversal symmetry, reciprocity, and passivity impose further constraints [1]. Recent developments have demonstrated that many of these limitations may be bypassed by adding time as a relevant “fourth” dimension—beyond the three spatial ones—in the design of metamaterials. For instance, tailored time variations can break time-reversal symmetry and reciprocity [2], and they can transform frequencies and impart gain through parametric effects.

Such a time interface sustains phenomena, such as time reflection and time refraction, that are somewhat related to the familiar scattering processes occurring at a spatial interface.

These concepts have recently been converging into a new paradigm for metamaterials in which space and time can be combined together to drastically expand the palette of degrees of freedom available for wave control [3].

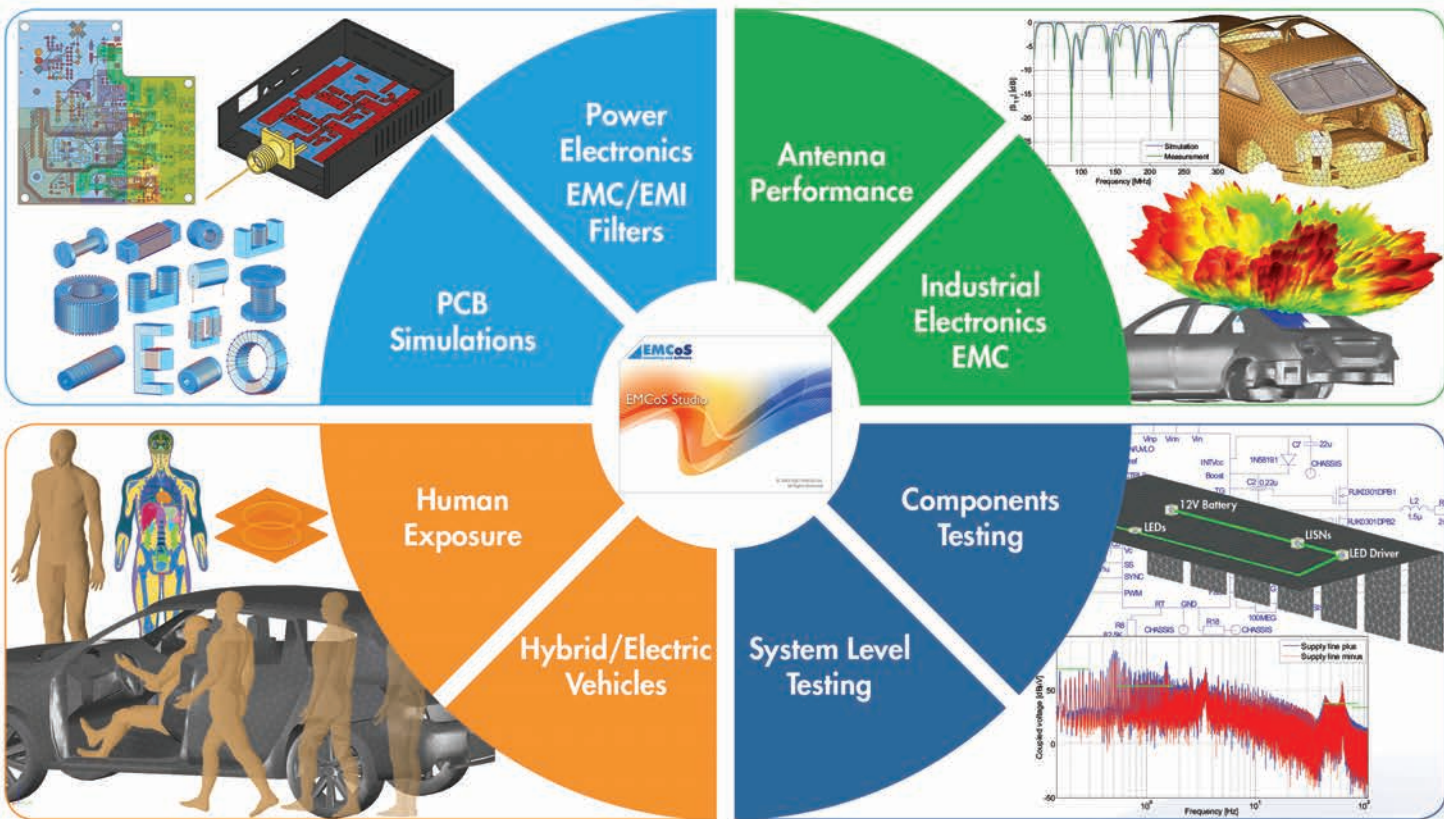
The idea of using time as a dimension for wave control can be traced back to the late 1950s, when Morgensthaler [4] introduced the concept of a *time interface*. Dual to the familiar concept of a spatial interface, which consists of a sharp transition in space that does not change in time, a time interface is everywhere in space, but it exists only at one instant in time. It is formed when the material properties of the medium supporting an input wave are abruptly and largely changed. Such a time interface sustains phenomena, such as time reflection and time refraction, that are somewhat related to the familiar scattering processes occurring at a spatial interface. At a time interface, backward and forward

waves are generated, but their frequency and energy are not conserved, providing an efficient and inherently fast platform to realize signal amplification and frequency transformations. In addition, time-reflected signals are time-reversed without distortions, offering a frequency-agnostic and efficient form of phase conjugation, relevant for applications from imaging to communications and computing.

Progress in the technologies that allow us to change and control the material properties in time has recently revived interest in these phenomena, supporting the fast and efficient tuning of the electromagnetic response of circuit elements and materials. In turn, exciting proposals to leverage these phenomena for exotic wave control have been appearing in the recent literature [5], [6], [7]. Inspired by how combinations of spatial interfaces enable sophisticated wave manipulation, e.g., sharp resonances and bandgaps in photonic crystals, combinations of time interfaces have been shown to support new forms of wave interference and resonances, and when combined, they can form the basis for time crystals [8] and time metamaterials [9]. The recent experimental demonstration of a time interface for electromagnetic waves, obtained in a transmission-line metamaterial loaded with a dense array of switches and reservoir capacitors, has

EMCoS Studio

One software product for multiple solutions!



www.emcos.com
E-mail: info@emcos.com

EMCoS
Consulting and Software

enabled the observation of the powerful opportunities of these concepts, for instance, realizing broadband, fast phase conjugation, and frequency conversion [10], spearheading further excitement in this field of research. The overarching vision consists of combining tailored spatial and temporal interfaces in 4D metamaterials, enabling seamless wave transformations in space, time, frequency, and momentum, and hence, opening unchartered opportunities for the future of metamaterials.

Within this background, it has been exciting to edit this special issue that aims to offer an overview of these recent advances and an introduction to this emerging field of research for the benefit of the broad antennas and propagation community. G. Ptitsyn et al. [A1] present an excellent tutorial on the basics of time-varying systems and circuits, pointing out the relevant opportunities that time variations offer in the quest of manipulating electromagnetic signals and the new challenges that emerge in their modeling. S. Yin et al. [A2] discuss time interfaces and wave interference enabled by their combinations in the framework of scattering and transmission-line theory, shedding physical insights on the associated phenomena within a framework that can be accessible to electrical and antenna engineers. Z. Hayran and F. Monticone [A3] showcase ways in which, by adding the temporal dimension, we can overcome some of the inherent limitations of linear time-invariant structures, offering a vista over the new opportunities that time- and space-time metamaterials may offer. V. Pacheco-Peña and N. Engheta [A4] discuss homogenization principles and effective-medium theory for time metamaterials, comparing them with classical homogenization schemes for layered media and offering interesting physical insights into the new phenomena enabled by periodic combinations of time interfaces. C. Caloz et al. [A5] discuss the opportunities enabled by the combination of space and time interfaces in space-time metamaterials, unveiling physical insights and engineering perspectives for applications. Finally, S. Taravati and G. V. Eleftheriades [A6] present the modeling, design, and applications of space-time

At a time interface, backward and forward waves are generated, but their frequency and energy are not conserved, providing an efficient and inherently fast platform to realize signal amplification and frequency transformations.

metasurfaces, which tailor waves by combining variations in space and time over a thin platform. As a collection, this series of articles aims at providing an introduction to these topics for the benefit of the broad electrical engineering and antennas and propagation communities, offering a snapshot of the state of the art and a perspective on the evolution of this field.

I would like to take this opportunity to thank all the authors and reviewers of these articles, which form a great collection. Sincere thanks also go to *IEEE Antennas and Propagation Magazine* Editor-in-Chief Prof. Francesco Andriulli for encouragement and support and to Editorial Assistant Christina Tang-Bernas for all of the support and patience. I hope that many of you will enjoy reading this collection and that it may be useful to introduce the broad readership of this journal to a topic that is rapidly becoming an exciting direction in the context of electromagnetic wave manipulation and of metamaterials.

AUTHOR INFORMATION

Andrea Alù (aalù@gc.cuny.edu) is with the Photonics Initiative, Advanced Science Research Center, City University of New York, New York, NY 10031 USA and with the Physics Program, Graduate Center, City University of New York, New York, NY 10016 USA.

APPENDIX: RELATED ARTICLES

[A1] G. Ptitsyn, M. S. Mirmoosa, A. Sotoodehfar, and S. A. Tretyakov, "A tutorial on the basics of time-varying electromagnetic systems and circuits: Historic overview and basic concepts of time-modulation," *IEEE Antennas Propag. Mag.*, vol. 65, no. 4, pp. 10–20, Aug. 2023, doi: 10.1109/MAP2023.3261601.

[A2] S. Yin, E. Galiffi, G. Xu, and A. Alù, "Scattering at temporal interfaces: An overview from an antennas and propagation engineering perspective," *IEEE Antennas Propag. Mag.*, vol. 65, no. 4, pp. 21–28, Aug. 2023, doi: 10.1109/MAP2023.3254486.

[A3] Z. Hayran and F. Monticone, "Using time-varying systems to challenge fundamental limitations in electromagnetics: Overview and summary of applications," *IEEE Antennas Propag. Mag.*, vol. 65, no. 4, pp. 29–38, Aug. 2023, doi: 10.1109/MAP2023.3236275.

[A4] V. Pacheco-Peña and N. Engheta, "Merging effective medium concepts of spatial and temporal media: Opening new avenues for manipulating wave-matter interaction in 4D," *IEEE Antennas Propag. Mag.*, vol. 65, no. 4, pp. 39–49, Aug. 2023, doi: 10.1109/MAP2023.3254480.

[A5] C. Caloz, Z.-L. Deck-Léger, A. Bahrami, O. C. Vicente, and Z. Li, "Generalized space-time engineered modulation (GSTEM) metamaterials: A global and extended perspective," *IEEE Antennas Propag. Mag.*, vol. 65, no. 4, pp. 50–60, Aug. 2023, doi: 10.1109/MAP2022.3216773.

[A6] S. Taravati and G. V. Eleftheriades, "4D wave transformations enabled by space-time metasurfaces: Foundations and illustrative examples," *IEEE Antennas Propag. Mag.*, vol. 65, no. 4, pp. 61–74, Aug. 2023, doi: 10.1109/MAP2022.3201195.

REFERENCES

- [1] A. Krasnok, N. Nefedkin, and A. Alù, "Parity-time symmetry and exceptional points," *IEEE Antennas Propag. Mag.*, vol. 63, no. 6, pp. 110–121, Dec. 2021, doi: 10.1109/MAP2021.3115766.
- [2] A. Kord and A. Alù, "Magnetless circulators based on synthetic angular-momentum bias: Recent advances and applications," *IEEE Antennas Propag. Mag.*, vol. 63, no. 6, pp. 51–61, Dec. 2021, doi: 10.1109/MAP2020.3043437.
- [3] N. Engheta, "Four-dimensional optics using time-varying metamaterials," *Science*, Vol. 379, No. 6638, pp. 1190–1191, Mar. 2023, doi: 10.1126/science.adf1094.
- [4] R. Morgenthaler, "Velocity modulation of electromagnetic waves," *IRE Trans. Microw. Theory Techn.*, vol. 6, no. 2, pp. 167–172, Apr. 1958, doi: 10.1109/TMTT.1958.1124533.
- [5] A. Akbarzadeh, N. Chamanara, and C. Caloz, "Inverse prism based on temporal discontinuity and spatial dispersion," *Opt. Lett.*, vol. 43, no. 14, pp. 3297–3300, Jul. 2018, doi: 10.1364/ol.43.003297.
- [6] V. Pacheco-Peña and N. Engheta, "Antireflection temporal coatings," *Optica*, vol. 7, no. 4, pp. 323–331, Apr. 2020, doi: 10.1364/optica.381175.
- [7] E. Galiffi et al., "Photonics of time-varying media," *Adv. Photon.*, vol. 4, no. 1, Feb. 2022, Art. no. 014002, doi: 10.1117/1.AP.4.1.014002.
- [8] K. Sacha and J. Zakrzewski, "Time crystals: A review," *Rep. Prog. Phys.*, vol. 81, no. 1, Jan. 2018, Art. no. 016401, doi: 10.1088/1361-6633/aa8b38.
- [9] S. Yin, E. Galiffi, and A. Alù, "Floquet metamaterials," *eLight*, vol. 2, no. 1, May 2022, Art. no. 8, doi: 10.1186/s43593-022-00015-1.
- [10] H. Moussa, G. Xu, S. Yin, E. Galiffi, Y. Ra'di, and A. Alù, "Observation of temporal reflection and broadband frequency translation at photonic time interfaces," *Nature Phys.*, early access, 2023, doi: 10.1038/s41567-023-01975-y.



ORDER OF MAGNITUDE AHEAD

WiPL-D Pro CAD 2023 *released!*

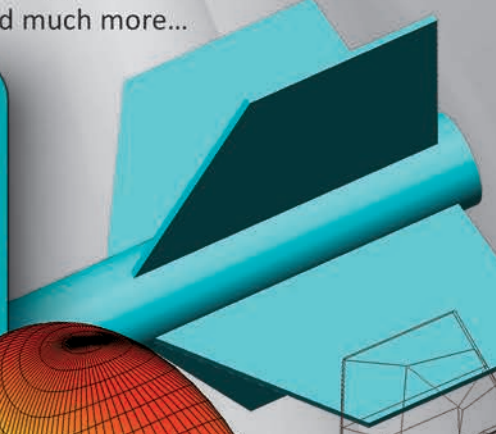
*Efficient modeling
of flexible antennas
and circuits*

New:

- Validate command - automatic validation and robust error fixing adaptive to changes in model topology
- Wrapping of flat bodies over arbitrary developable surfaces
- Imported WIPL-D Pro files are now simulation-ready
- Accelerated modeler – smooth work with highly complex geometries
- Region selection mode
- Support for:
 - Frequency and Sweep parallel run
 - Periodic Boundary Condition
- Automatic deletion of auxiliary Point Bodies in Snap to Topology/Geometry modes
- And much more...

Features:

- Solid modeling using built-in primitives (curves, surface bodies and solids)
- Import from and export to various CAD formats with efficient model repair and defeaturing
- Easy manipulations and Boolean Operations
- Quadrilateral mesher optimized for HOBFs
- Full support for symbolic modeling, symmetry, GPU acceleration and other standard WIPL-D features



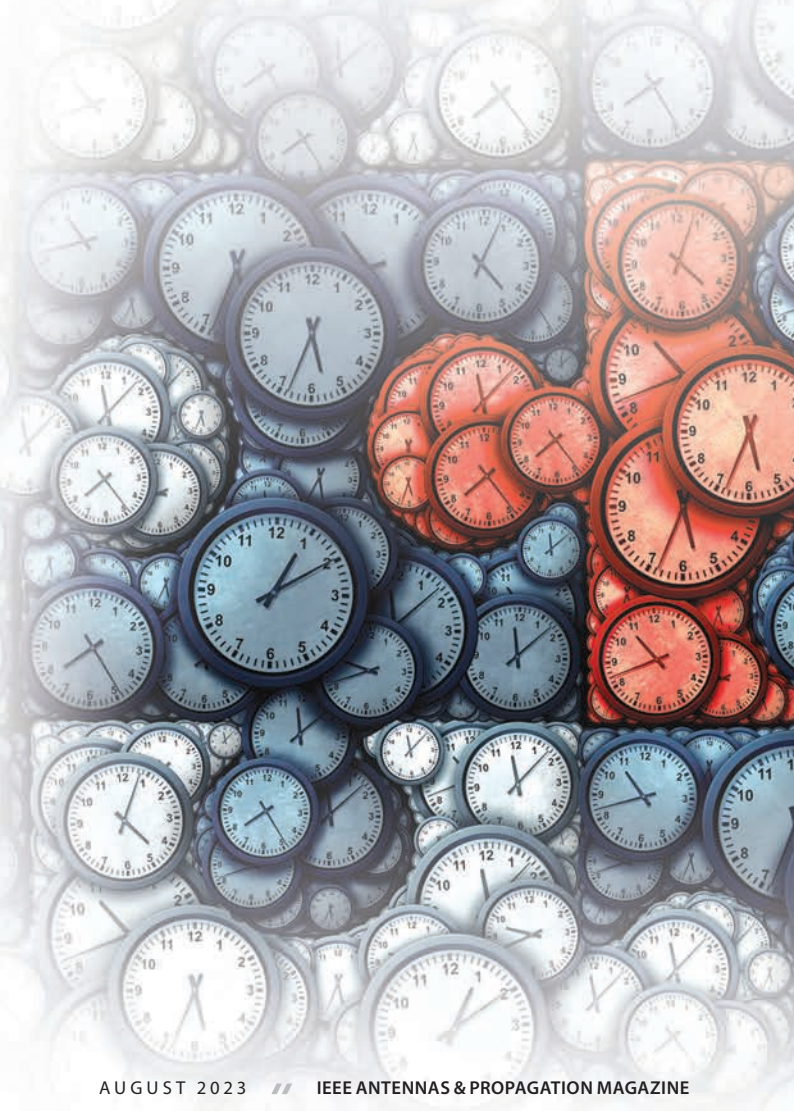
A Tutorial on the Basics of Time-Varying Electromagnetic Systems and Circuits

Historic overview and basic concepts of time-modulation.

During the last decade, possibilities to realize new phenomena and create new applications by varying system properties in time have gained increasing attention in many research fields. Although the interest in using time-modulation techniques for engineering electromagnetic (EM) response has become revitalized only in recent years, the field originates from the middle of the previous century, and a multitude of works have been published ever since. In this tutorial article, we provide a historical picture and review the basic concepts in this field. In particular, we introduce the general theory of linear time-varying (LTV) systems and discuss the means to properly account for frequency dispersion of nonstationary systems. Also, we elucidate models of time-varying electrical circuits and materials and discuss some useful effects that can be achieved by time modulation of circuit or material parameters.

INTRODUCTION

Dynamic changes of properties of a system made by an external force remove limitations on system response imposed by invariance under time translations. This is sometimes an unwanted feature that is inevitably present and whose effects should be



mitigated by some means. For instance, cars in motion and people walking in the streets dynamically alter propagation channels of telecommunication systems, or, control equipment on a plane constantly experiences dynamic changes of the environment. Researchers in fields such as signal processing, communications, radio wave propagation, information theory, and control engineering are familiar with the practical importance of this problem [1]. In EMs and microwave and antenna engineering, however, nonstationarity can be importantly used as an additional degree of freedom for controlling signals and waves in the desired way. In the past two decades, applied physicists and EM engineers have attempted to manipulate waves by designing artificial materials and surfaces: metamaterials and metasurfaces. In particular, they studied how the geometry of inclusions (forming an artificial material or surface) and the distances between them modify and engineer wave-matter interactions. As a follow-up step, why not assume that the properties of such inclusions change in time. Taking this fourth dimension into account helps us realize new and exotic effects in interactions of waves with materials or surfaces and enhance the functionalities of devices. For instance, in the microwave range, one can use mechanically moving parts of electrical devices or

employ electronic components such as varactors and transistors. At short wavelengths, it can be optical pumping at an extremely high speed, which can even be considered a step-like change. An illustration of various means that realize time modulation is given in Figure 1.

Note that despite the broad variety of problems and various frequency ranges, the fundamental formulation of EM problems for time-varying systems is common. In this tutorial article, we overview the foundations and basic methods used for the analysis and engineering of microwave and optical time-varying systems. We begin by presenting a historical overview of the development of time-modulation techniques from approximately 1950 until 2022. We start from the work published by Lotfi A. Zadeh in 1950 and gradually move toward developments in antenna engineering, electric circuits, and EM media, where researchers investigated time-varying systems for enhancement of bandwidth, amplification, realizing nonreciprocity, frequency mixing, and so forth. Next, we present and discuss the general basic concepts associated with linear and causal time-varying systems. We scrutinize systems that possess memory and are temporally dispersive. In the last part, we discuss the general theory of electric circuits, consisting of time-varying elements or

dielectrics with time-varying permittivity. In this introductory tutorial, we focus on only circuits, but actually, this knowledge can be effectively used in many branches of antenna and microwave engineering.

Before continuing, it is important to clarify the difference between time modulation and tuning (reconfiguration) of devices. Tunable systems are capable of switching between several operational regimes, and in each of the regimes, parameters of the system remain constant. For example, reconfigurable antennas can be shifted to different resonance frequencies using a switchable capacitance bank. Another example are reconfigurable intelligent surfaces that can be dynamically adjusted, optimizing propagation channels. For tunable systems, intermediate (transient) states are usually not taken into account, and only steady-state operational regimes are of interest. In contrast to that, time-modulated structures capitalize exactly on the transient regime, which is realized when system parameters change in time. Such systems are within the focus of this tutorial.

HISTORICAL OVERVIEW

Despite the recent burst of research interest in the field of time modulation, its historical origin goes back to the middle of the previous century. Interestingly, the problem of dynamic variations of a

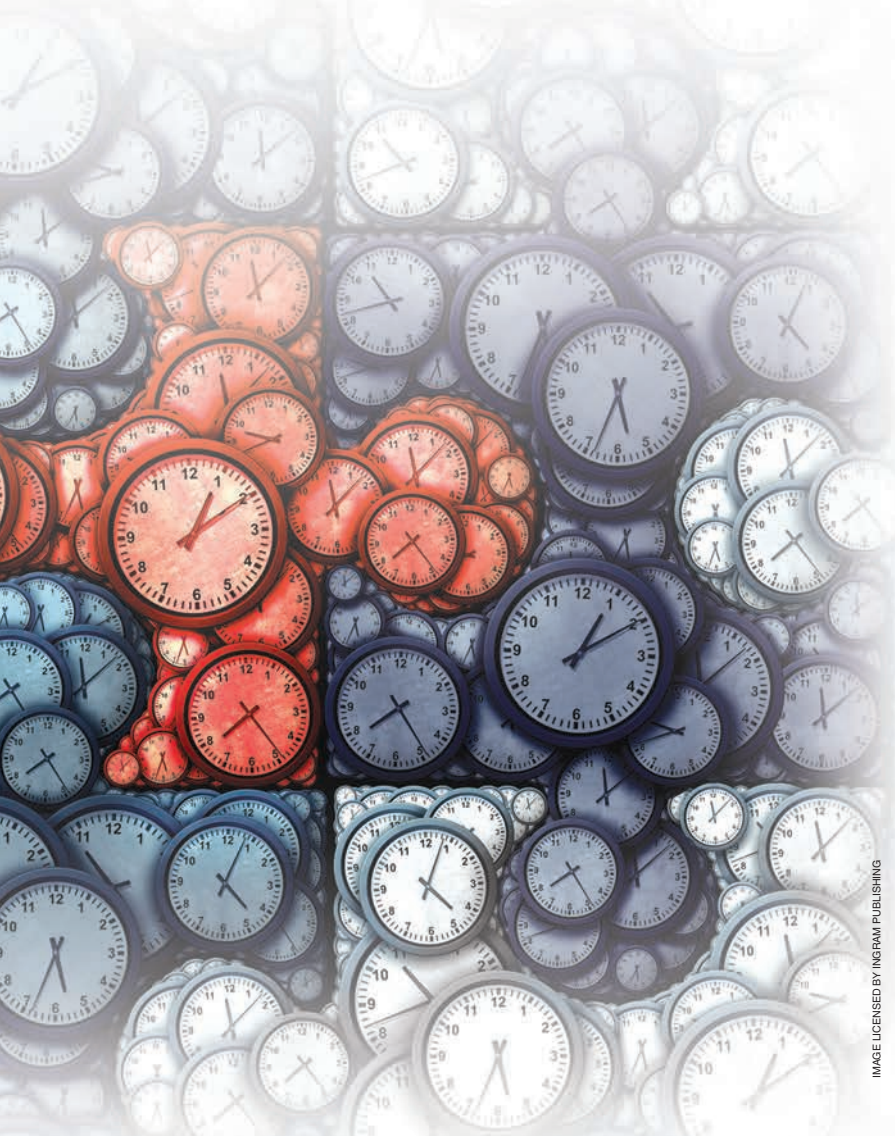


IMAGE LICENSED BY INGRAM PUBLISHING

system's parameters was not allocated to a single research field. Probably one of the first papers on this topic appeared in communication theory. Zadeh (1921–2017), the father of fuzzy logic and one of the pioneers of artificial intelligence, described “frequency analysis of variable networks” in 1950 [2], [3]. Zadeh extended the frequency analysis techniques that were conventionally used and proposed a “system function” defined in a joint time-frequency domain to characterize LTV systems. Zadeh comprehensively tackled the problem and studied such aspects as stability [4], pulse response [3], and power spectra of variable networks [5]. These ideas were further developed by Kailath by discussing possible simplifications [6] and experimental issues [7]. General theoretical investigations of time-varying systems were further continued by Gersho [8], [9], where he studied such a fundamental property as “time-frequency” duality, which was also later investigated by Bello [10]. In addition to that, Bello considered randomly time-variant channels and introduced the assumption of wide-sense, stationary uncorrelated scattering, which gathered huge attention [11].

TIME-VARYING EM SYSTEMS: 1950–1980

In the newly born field of radio engineering, scientists were focused on overcoming practical issues such as small bandwidth and large antenna size, and time modulation of antennas was considered one of the possible resolutions to these problems. Several antenna geometries were proposed and tested for efficient information transfer, however, only in the

Time-modulated structures capitalize exactly on the transient regime, which is realized when system parameters change in time.

1950s was a general understanding of fundamental limitations on small antennas formulated by Wheeler [12] and Chu [13]. In these works, the authors proved that for linear, passive, and time-invariant antennas, their size, bandwidth, and efficiency cannot be optimized simultaneously. Naturally, to overcome Chu's limitation, one needs to utilize either active, nonlinear, or time-varying systems. One of the first attempts to overcome Chu's

limitation was performed by Jacob and Brauch [14]. They used so-called “antenna keying,” where nonlinear properties of ferrite materials are utilized to modulate the resonance frequency of a small antenna using a time-varying inductor. It indeed helped transmit signals in the kilohertz frequency range beyond the fundamental limitation, however, the presence of a ferrite core in the structure hindered applicability of this system at higher frequencies because the saturation effect of ferrite cores sets the maximal modulation speed of such inductors. This problem was later resolved using a switchable capacitor bank that was used as a time-varying capacitor [15]. Time-varying components were used also in [16] and [17]. Worth mentioning is that the antenna-keying approach was later reinvented and renamed *direct antenna modulation* [18], [19], [20], keeping all of its essential features.

In the years to come, antenna engineers preferred to move (and still are moving) toward higher frequencies where higher bandwidth and smaller antenna sizes could be obtained, often sacrificing antenna efficiency. Obviously, this development cannot continue indefinitely. In addition to that, low-frequency

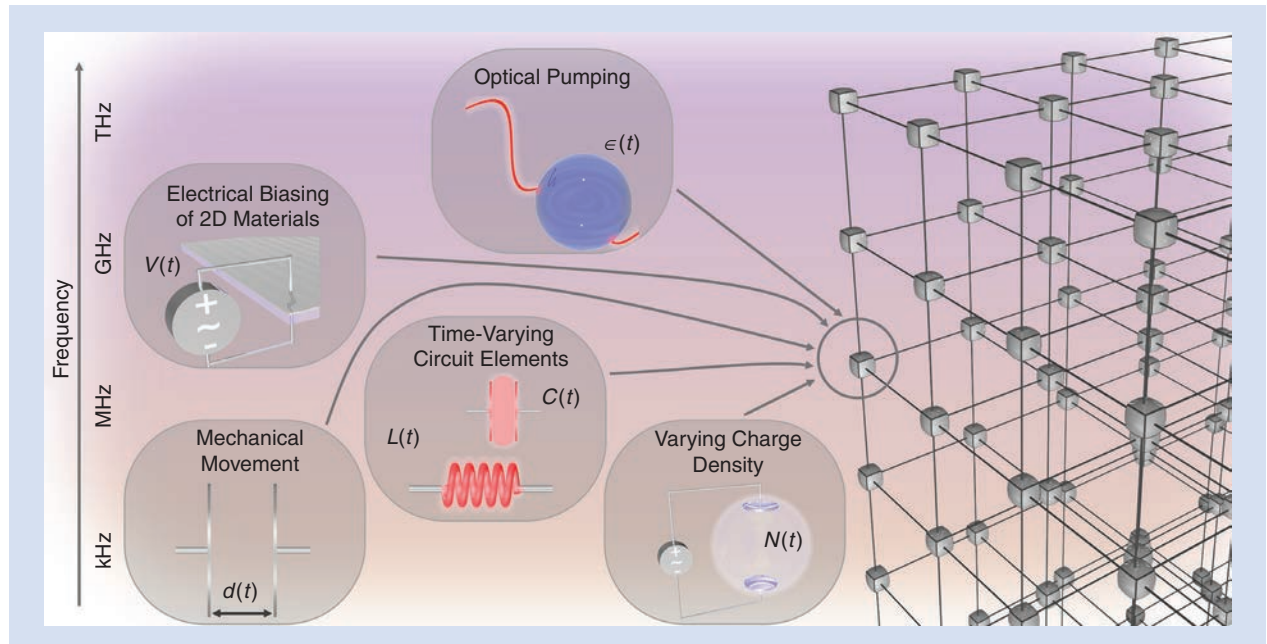


FIGURE 1. The possible ways to realize time modulation of circuits and media.

applications as well as the need for electrically small antennas with a wide bandwidth still create a strong demand for nonlinear, active, and/or time-varying antennas.

Studies of electrical circuits with time-varying parameters probably began with the works of Cullen [21], Tien [22], and Tien and Suhl [23]. Cullen and Suhl considered time-modulated electrical circuits with distributed parameters and noticed that they were capable of parametric amplification when

the phase velocity of the modulation wave is the same as the wave-phase velocity (called *luminal metamaterials* in [24]). Tien found frequency mixing and envisaged many other phenomena that can occur in parametric circuits with spatially distributed parameters. Studies of amplification in these structures continued [25], together with the discovery of a new functionality: nonreciprocity. In [26], Kamal proposed and experimentally tested a parametric device made of just two time-varying circuit elements that was capable of nonreciprocal wave transmission. Nonreciprocity is essential for many applications, and time modulation brings a new way to realize it [27].

Possibly the earliest work on media with time-varying parameters dates back to 1958, when Morgenthaler [28] considered propagation of EM waves through a dielectric material sample with time-varying permittivity or permeability and found a solution for the case when the impedance of the medium remains constant. He noticed that an abrupt jump of permittivity creates forward- and backward-propagating waves, analogous to a spatial discontinuity. Traveling-wave modulation was studied from the general perspectives of Simon [29] and Oliner et al. [30] in 1961. They considered the problem of EM wave propagation in media with a progressive sinusoidal disturbance. Later, Felsen and Whitman [31] considered slow and abrupt modulations of unbounded media and focused their attention on the excitation problem, and on the source-dependent phenomena. Interestingly, they even incorporated special cases of dispersion in their analysis and found a focusing effect in an abruptly changing medium. In the same year, Fante [32] studied a time-varying half-space and considered slow and abrupt modulations as well as included dispersion in his description. A very peculiar property of time-varying materials was found in [33] by Holberg and Kunz. They studied fields inside a time-varying slab and discovered exponential amplification of waves with certain wavenumbers.

In the Soviet Union, the field of time-varying media was heavily studied in the plasma community. The community studied the problem from various different perspectives, such as wave propagation in moving media [34], [35], [36], transformation of waves on moving boundaries [37] and inside media with slowly varying parameters [37], [38], [39], reflection and refraction of waves on moving inhomogeneous plasma structures [40], [41], [42], energy relations in time-varying media

Many research techniques try to use time-modulation techniques to overcome certain fundamental limitations imposed for passive structures.

[43], and more. In one of his pioneering papers [44], Stepanov considered the dielectric constant of unsteady plasma. For convenience of the analysis, Stepanov performed a Fourier transform of plasma susceptibility and introduced a new material parameter of plasma that simultaneously depends on time and frequency, thus incorporating frequency dispersion in his model of nonstationary plasma.

All of these studies (and others) provide a solid platform for current research. Many of these works are being developed further or reworked for technologies available today. Let us now briefly review the current status of research on time-modulated structures.

TIME-VARYING EM SYSTEMS: 1981–2022

Various phenomena and effects have been investigated theoretically and experimentally over the last 40 years. For instance, the role of frequency dispersion in time-modulated systems is of utmost importance because materials whose properties can be altered dynamically are usually highly dispersive. This problem was actively studied by Mirmoosa et al. [45], Engheta [46], Solis and Engheta [47], and Sloan et al. [48]. In [45], Mirmoosa et al. further developed the theoretical approach proposed by Zadeh [2]. They coined the term *temporal complex polarizability* to describe light-particle interactions when the properties of a sub-wavelength particle change in time. Their definition is exactly what Zadeh wrote in equation (2) in his paper [2]. Pacheco-Peña and Engheta [49], [50] exploit complementary roles of space and time in Maxwell's equations to find temporal analogues to spatial phenomena. Other very distinct methods are investigated in Derode et al. [51], Fink [52], Przadka et al. [53], and Popoff et al. [54], where time-reversal symmetry of EM waves are uniquely capitalized. Many research techniques try to use time-modulation techniques to overcome certain fundamental limitations imposed for passive structures [12], [13], [55]. For instance, breaking limitations on antenna performance was studied, for example, by Hadad et al. [56], Li et al. [57], and Mostafa et al. [58]. The breaking of Lorentz reciprocity using time-varying structures was studied actively in many research groups, including Galiffi et al. [24], Taravati et al. [59], Chamanara et al. [60], Caloz et al. [61], Sounas and Alù [62], Correas-Serrano et al. [63], Dinc et al. [64], Fleury et al. [65], Song et al. [66], Lira et al. [67], Yu and Fan [68], Shi et al. [69], Wang et al. [70], Asadchy et al. [71], Shaltout et al. [72], Shaltout et al. [73], Koutserimpas and Fleury [74], Zhang et al. [75], Taravati and Kishk [76], Ramaccia et al. [77], Ramaccia et al. [78], Li et al. [79], and many more.

In addition to nonreciprocity, numerous other applications and models were studied, such as frequency conversion [80], [81], [82], [83], [84], [85], [86], [87], [88], amplification [74], [89], [90], Doppler shift [91], [92], [93], extreme accumulation

of energy [94], instantaneous control of radiation and scattering [95], [96], Fresnel drag [97], negative refraction [98], effective medium models [99], [100], control of diffusion [101], pulse compression [102], camouflage [103], [104], temporal birefringence [105], [106], temporal photonic crystals [107], [108], [109], space-time crystals [110], [111], [112], power combiners [113], Wood anomalies [114], and more. This is not a complete list of applications and groups working on time modulation. The number of works that have appeared in the recent decades is massive, and the general interest toward this research topic has only grown (see, for example, the review papers in [115], [116]).

LTV SYSTEMS

Any classical physical system can be modeled by a differential equation or set of differential equations. That is, temporal variations of a certain dynamic variable or variables $O(t)$ (for example, an electric field at some point of space or current in a conductor) under the action of some external excitation $I(t)$ (for example, an external electromotive force of a voltage source, or the field of an incident wave) can be found as the solution of equation

$$\mathcal{L}_t O(t) = I(t) \quad (1)$$

where \mathcal{L}_t is a differential operator that acts on function $O(t)$. The solution to this equation for an excitation in form of the Dirac delta function is called *Green's function* $G(\gamma, t)$:

$$\mathcal{L}_t G(\gamma, t) = \delta(\gamma). \quad (2)$$

Here, t represents the observation time, and γ is the delay between t and time moment τ when the excitation arrives, i.e., $\gamma = t - \tau$. Note that the following derivations can be performed, equivalently, also in terms of the time variable τ instead of the delay parameter γ . Sometimes, G is called the *impulse response of a system* as it is a reaction of the system to the input in the form of a delta-function pulse [117]. Sometimes, it is also called the *fundamental solution of an operator* as any input can be viewed as a summation of weighted delta functions.

Most importantly, for linear systems, the response to excitations that arbitrarily vary in time can be found in terms of the Green function. Here we discuss LTV systems. Let us prove this property of Green's function by multiplying (2) by an arbitrary function of time $I(t - \gamma)$ and integrating over γ :

$$\int_{-\infty}^{\infty} \mathcal{L}_t G(\gamma, t) I(t - \gamma) d\gamma = \int_{-\infty}^{\infty} \delta(\gamma) I(t - \gamma) d\gamma = I(t). \quad (3)$$

Because the operator \mathcal{L}_t acts at the variable t and it is a linear operator (we consider linear systems), we can take the operator outside of the integral:

$$\mathcal{L}_t \int_{-\infty}^{\infty} G(\gamma, t) I(t - \gamma) d\gamma = I(t). \quad (4)$$

By comparing (1) and (4), we see that the output of the system is given by

$$O(t) = \int_0^{\infty} G(\gamma, t) I(t - \gamma) d\gamma. \quad (5)$$

Mathematically, the integration in (5) would be performed over the retardation time γ from $-\infty$ to ∞ , but we restrict the integration to only nonnegative values. Negative retardation time means that excitations that will happen at future moments of time affect the output at present. This is against an extremely fundamental empirical law of nature: causality. The causality principle says that the state of a system is defined by its evolution in the past, and it cannot be affected by events at future moments of time.

Let us see how this equation simplifies for linear time-invariant systems when the operator \mathcal{L}_t that describes the system does not change in time. It means that shifting the input by some time interval also shifts the output by the same interval because the system is immutable. Thus, the output depends only on the time interval γ between the moment when the input is applied and the moment when we observe the resulting output, which allows us to write

$$O(t) = \int_0^{\infty} G(\gamma) I(t - \gamma) d\gamma. \quad (6)$$

Despite the very similar forms of (5) and (6), the first is far more complicated to use because the response function is explicitly dependent on two time variables. Because for stationary systems the integral in (6) is a convolution, we can make a Fourier transform and write in the frequency domain a simple linear relationship between the input and output variables: $O(\Omega) = G(\Omega)I(\Omega)$. This familiar frequency-domain method is not possible to use for time-varying systems because the integral in (5) is not a conventional convolution.

INSTANTANEOUS RESPONSE

To be able to use (5), one can make assumptions about the system and simplify the theory accordingly. One of these assumptions is instantaneous response, which simplifies the theory immensely. Under this assumption, Green's function is expressed as

$$G^{ir}(\gamma, t) = \delta(\gamma) G(t) \quad (7)$$

where superscript "ir" stands for "instantaneous response." One can immediately see how easy and compact the relationship between the input and output becomes

$$O(t) = G(t)I(t). \quad (8)$$

Written in this form, the equation is very convenient and easy to use. However, this simplicity comes at a high cost. For example, regarding EM media, instantaneous response means that atoms get polarized instantaneously without inertia, which, strictly speaking, is never the case. In systems where the transition time is negligible compared to the period of the incident

field oscillations, it is possible to use the instantaneous response approximation. In other words, (8) remains valid if the input interacts with the system that is modulated slowly enough such that it can be practically treated as static at all moments of time. In this approximation, frequency dispersion of materials is completely neglected.

TIME-VARYING CIRCUITS

Next we explain how these basic concepts are used to analyze electric circuits with lumped time-varying elements. We concentrate on time-varying capacitors and describe their salient characteristics. The interested reader can repeat the same procedure for other elements such as inductors and resistors.

GENERAL DESCRIPTION OF TIME-VARYING CAPACITANCE

Conventionally, *capacitance* is defined as the electric charge divided by the voltage. However, in general, this definition does not provide a complete picture, even in the time-invariant scenario, as it is valid only in the assumption that the capacitor exhibits an instantaneous response. In general, the electric charge $Q(t)$ and the voltage $v(t)$ over a capacitor should be related as in (5):

$$Q(t) = \int_0^\infty C(\gamma, t)v(t - \gamma)d\gamma. \quad (9)$$

Based on this general linear and causal relationship, we aim to find a formula that connects the electric current and voltage fully in the frequency domain. Using the Fourier transform, we write the instantaneous voltage based on its frequency-domain counterpart. Accordingly, (9) becomes $Q(t) = 1/2\pi \int_{-\infty}^{+\infty} C_T(\omega, t)V(\omega)\exp(j\omega t)d\omega$, where we define the temporal complex capacitance as

$$C_T(\omega, t) = \int_0^{+\infty} C(\gamma, t)\exp(-j\omega\gamma)d\gamma \quad (10)$$

which is the Fourier transform of the capacitance kernel ($C(\gamma, t) = 0$ for $\gamma < 0$ due to causality). The electric current flowing through the capacitor is the time derivative of the electric charge. Thus,

$$i(t) = \frac{1}{2\pi} \int_{-\infty}^{+\infty} Y_T(\omega, t)V(\omega)\exp(j\omega t)d\omega \quad (11)$$

where

$$Y_T(\omega, t) = \frac{dC_T(\omega, t)}{dt} + j\omega C_T(\omega, t) \quad (12)$$

can be called *temporal complex admittance* modeling of the nonstationary capacitance. Interestingly, this parameter is complex valued. In the aforementioned relationship, the first

In systems where the transition time is negligible compared to the period of the incident field oscillations, it is possible to use the instantaneous response approximation.

term is associated with the time derivative of the temporal complex capacitance. In the stationary scenario, this time derivative vanishes and the admittance is determined only by the conventional second term.

EXAMPLE: AN RLC CIRCUIT

Suppose that a voltage source $v_s(t)$ with a series resistance R is connected to a time-varying capacitor and a stationary inductor. From the circuit theory, we know that $v_s(t) = Ri(t) + Ldi/dt + v(t)$, where $v(t)$ is the voltage across the capacitor, and L represents the

inductance. The current and voltage in a time-varying capacitor are related to each other as in (11). Taking the Fourier transform of (11), we have

$$I(\Omega) = \frac{1}{2\pi} \int_{-\infty}^{+\infty} Y(\omega, \Omega - \omega)V(\omega)d\omega \quad (13)$$

in which

$$Y(\omega, \Omega) = \int_{-\infty}^{\infty} Y_T(\omega, t)e^{-j\Omega t}dt = j(\Omega + \omega)C(\omega, \Omega). \quad (14)$$

Here, $Y(\omega, \Omega)$ and $C(\omega, \Omega)$ are the Fourier transforms of the temporal complex admittance and capacitance, respectively. How the admittance and the capacitance are associated with each other fully in the frequency domain is something intriguing. In fact, it is very similar to the time-invariant scenario. However, in a nonstationary case, we have two angular frequencies that are added. Equation (13) can be written as

$$I(\Omega) = \frac{j\Omega}{2\pi} \int_{-\infty}^{+\infty} C(\omega, \Omega - \omega)V(\omega)d\omega. \quad (15)$$

Using this equation, we can finally find that

$$V_s(\Omega) = j\Omega \left(\frac{R + j\Omega L}{2\pi} \right) \int_{-\infty}^{+\infty} C(\omega, \Omega - \omega)V(\omega)d\omega + V(\Omega). \quad (16)$$

This is an integral equation that is solvable, at least numerically, if the capacitance kernel is known.

If we assume the instantaneous response of a time-varying capacitor, the capacitance kernel becomes a multiplication of Dirac delta function $\delta(\gamma)$ and a function of time variable t . Thus, $C(\omega, \Omega)$ is invariant with respect to the first argument, and therefore, (16) becomes

$$V_s(\Omega) = j\Omega \left(\frac{R + j\Omega L}{2\pi} \right) \int_{-\infty}^{+\infty} C(\Omega - \omega)V(\omega)d\omega + V(\Omega). \quad (17)$$

The integrals in (15)–(17) reduce to convolutions, and the inverse Fourier transform of (15) gives us the usual,

instantaneous relationship $i(t) = d/dt[C(t)v(t)]$. Many works on time-modulated structures start from assuming that circuit or material parameters (such as capacitance, inductance, permittivity, and permeability) are functions of time, as in this relationship between the current and voltage, and solve the corresponding equations in the time domain. It is important to remember that this approach completely neglects frequency dispersion of all materials from which the device is made. As an example, for a capacitor, this is a valid assumption if the capacitor is made of perfectly conducting plates with a vacuum between them, and the capacitance is modulated by mechanical movements of the plates.

As another limiting case, let us suppose that the capacitor is static (time invariant). In this scenario, the capacitance kernel depends on only the time-delay variable γ , and, as a result, $C(\omega, \Omega) = 2\pi C(\omega)\delta(\Omega)$. Hence, (16) is simplified to $V_s(\Omega) = (1 + j\Omega RC(\Omega) - \Omega^2 LC(\Omega))V(\Omega)$, which is the usual frequency-domain expression for an RLC circuit.

Finally, we note that the same theory is applicable to other linear and causal relations of EM theory. For example, the general relationship between displacement vector (**D**) and electric field (**E**) in time-modulated dielectrics or metamaterials has the form

$$\mathbf{D}(\mathbf{r}, t) = \int_0^\infty \epsilon(\gamma, t) \mathbf{E}(\mathbf{r}, t - \gamma) d\gamma \quad (18)$$

which is exactly the same as the general relationship defining time-modulated capacitance [see (9)].

PERIODICALLY MODULATED SYSTEMS

Many useful features in time-modulated systems are realized with time-periodic modulations. Importantly, periodicity of modulation allows us to use the Floquet theorem, which was introduced by Gaston Floquet (1847–1920) in 1883 [118]. The Floquet theorem is applicable to any linear structure with periodically varied properties, including spatial and temporal variations. In the case of spatially varied parameters, this theorem is known as *Bloch's theorem* [119], [120]. The theorem is quite general, and it can be applied to vector and scalar quantities for unbounded media, slabs, and boundaries. Here, we consider an unbounded homogeneous dielectric medium whose permittivity $\epsilon(t)$ periodically varies in time with the period T . For simplicity, we assume an instantaneous response of the medium. As the medium is homogeneous in space and there is no preferred direction, let us assume that there is an EM wave propagating in the z direction. Fields are governed by the wave equation

$$\frac{\partial^2}{\partial z^2} \mathbf{u}(z, t) - \frac{1}{c^2} \frac{\partial^2}{\partial t^2} [\epsilon(t) \mathbf{u}(z, t)] = 0 \quad (19)$$

The Floquet theorem is applicable to any linear structure with periodically varied properties, including spatial and temporal variations.

where c is the speed of light in a vacuum, and $\mathbf{u}(z, t)$ represents a transverse electric field in the time domain. Without loss of generality, we can assume a certain polarization of $\mathbf{u}(z, t)$ that lies in the xy -plane and further consider only the field amplitude. As a mathematical solution of (19), $\mathbf{u}(z, t)$ can be a complex-valued function. As the medium is modulated only in time, we can separate the variables and consider spatial dependency as that of a plane wave, e^{-jkz} ,

where k denotes the wavenumber. Thus, we look for solutions in form

$$u(z, t) = u_t(t) e^{-jkz} \quad (20)$$

which reduces (19) to

$$\frac{1}{c^2} \frac{d^2}{dt^2} [\epsilon(t) u_t(t)] + k^2 u_t(t) = 0. \quad (21)$$

This equation is convenient to rewrite as

$$\frac{d^2}{dt^2} y(t) + K(t) y(t) = 0 \quad (22)$$

where $y(t) = u_t(t)\epsilon(t)$ and $K(t) = k^2 c^2 / \epsilon(t)$. Interestingly, in this form, (22) as a second-order differential equation with a time-dependent coefficient can be clearly recognized as Hill's equation [121]. The Floquet theorem, whose detailed proof is given in the supplementary materials available at <https://www.doi.org/10.1109/MAP.2023.3261601>, states that the two linearly independent solutions of this second-order equation, $y_1(t)$ and $y_2(t)$, can be found in form

$$y_1(t) = e^{j\alpha t} p_1(t), \quad y_2(t) = e^{-j\alpha t} p_2(t) \quad (23)$$

where α is a constant, and $p_{1,2}$ are periodic functions with the period T .

As $p_{1,2}(t)$ are periodic, it is possible to present them as an infinite Fourier series of frequency harmonics:

$$p_{1,2}(t) = \sum_{n=-\infty}^{+\infty} p_n e^{-jn\frac{2\pi}{T}t} \quad (24)$$

where p_n denote the amplitudes of harmonics. For convenience, let us represent $2\pi/T$ as the modulation angular frequency ω_M . By using the expression in (24), the solution $y_1(t)$ in (23), for example, can be rewritten as

$$y_1(t) = \sum_{n=-\infty}^{+\infty} p_n e^{j(\alpha - n\omega_M)t}. \quad (25)$$

Worth noting is that $y_1(t)$ is a complex-valued function, and the real-valued solution can be obtained by taking the real part

of it. Equation (25) shows that the solution of the wave (19) can be written as an infinite series of frequency harmonics that are separated in frequency by ω_M . Let us further consider a simple example that shows how useful the Floquet theorem is.

INSTANTANEOUS PERIODICALLY TIME-VARYING CAPACITANCE

The most noticeable case that people have been studying is associated with approximately instantaneous and periodic time-varying capacitance or permittivity as this allows us to create devices such as parametric amplifiers. In the following, we use the general theory presented in the previous section and draw important conclusions for this particular case. Because the response is assumed to be instantaneous, the capacitance kernel is equal to the Dirac delta function, which is multiplied by a function that depends on only the time variable t . In other words, we have $C(\gamma, t) = \delta(\gamma)h(t)$, in which $h(t)$ is periodic, meaning that it can be expanded into a Fourier series as

$$C_T(t) = h(t) = \sum_{n=-\infty}^{+\infty} a_n \exp(jn\Omega_p t). \quad (26)$$

It is clear that the temporal complex capacitance is real valued, and it does not depend on the angular frequency ω because the system is dispersionless. In (26), a_n are the Fourier coefficients, and Ω_p represents the angular frequency associated with the periodicity of $h(t)$. Now we need to make a Fourier transform of the temporal complex capacitance. This simply results in a summation of the Dirac delta functions as

$$C(\Omega) = 2\pi \sum_{n=-\infty}^{+\infty} a_n \delta(\Omega - n\Omega_p). \quad (27)$$

Next, we substitute this relation into (15) to deduce a general expression that relates the electric current to the voltage. After some small manipulations, we arrive at

$$I(\Omega) = \sum_{n=-\infty}^{+\infty} j\Omega a_n V(\Omega - n\Omega_p). \quad (28)$$

Let us suppose that the capacitor is connected to a time-harmonic voltage source, i.e., $v(t) = A \cos(\omega_0 t + \phi)$ or $V(\Omega) = \pi A [\exp(j\phi) \delta(\Omega - \omega_0) + \exp(-j\phi) \delta(\Omega + \omega_0)]$. Using this expression, we see that

$$\begin{aligned} I(\Omega) &= j\pi A \sum_{n=-\infty}^{+\infty} \Omega a_n [\exp(j\phi) \delta(\Omega - n\Omega_p - \omega_0) \\ &\quad + \exp(-j\phi) \delta(\Omega - n\Omega_p + \omega_0)]. \end{aligned} \quad (29)$$

Making the inverse Fourier transform, we find

$$\begin{aligned} i(t) &= \frac{A}{2} \sum_{n=-\infty}^{+\infty} [j(\omega_0 + n\Omega_p) a_n \exp(j(\omega_0 t + n\Omega_p t + \phi)) \\ &\quad - j(\omega_0 - n\Omega_p) a_n \exp(-j(\omega_0 t - n\Omega_p t + \phi))]. \end{aligned} \quad (30)$$

At a quick glance, we observe that there are two exponential functions (multiplied by some coefficients) that are not complex conjugate to each other due to the opposite signs of the terms $\pm n\Omega_p$. However, we notice that the integer n changes from $-\infty$ to $+\infty$. By having this small but important point in mind,

and by paying attention to the fact that $a_n^* = a_{-n}$ (because the time-varying capacitance is a real-valued function), we conclude that

$$i(t) = A \cdot \text{Re} \left[\sum_{n=-\infty}^{+\infty} j(\omega_0 + n\Omega_p) \exp(j\phi) a_n \exp(j(\omega_0 + n\Omega_p)t) \right] \quad (31)$$

where $\text{Re}[\dots]$ denotes the real part. In (31), if we define I_n as the complex coefficient that is multiplied by the exponential function, the equation finally reduces to

$$i(t) = \text{Re} \left[\sum_{n=-\infty}^{+\infty} I_n \exp(j\omega_n t) \right] \quad (32)$$

in which $\omega_n = \omega_0 + n\Omega_p$. This gives us the message that in such instantaneous periodic systems there are oscillations at infinitely many frequencies that become far from the fundamental frequency ω_0 with the increasing index n . Using this result, if this time-varying capacitance is part of a more complex electric circuit, we can write the voltage over the capacitance as

$$v(t) = \text{Re} \left[\sum_{n=-\infty}^{+\infty} V_n \exp(j\omega_n t) \right]. \quad (33)$$

Equations (32) and (33) are used to introduce an admittance matrix modeling time-modulated circuit components. Let us derive this matrix, which helps solve complicated problems. We should substitute the expressions in (32) and (33) into (28) and attempt to find a way to relate I_n to V_n . By doing this, we realize that for every integer l ($l = 0, \pm 1, \pm 2, \dots$) we have $I_l = \sum_m \sum_n j[\omega_0 + (n+m)\Omega_p] a_m V_n$. Here, the key point is that the summations are with respect to all possible values of m and n such that $m + n = l$. For example, if $l = 2$, the possible values are $(m, n) = \dots(-1, +3), (0, +2), (+1, +1) \dots$. As a result, if we restrict ourselves to N values for m , there are N different values for n . It is simple to play with the aforementioned relationship and present it as the following:

$$\begin{pmatrix} I_{-N} \\ I_{-N+1} \\ \vdots \\ I_N \end{pmatrix} = \begin{pmatrix} j\omega_{-N} a_0 & j\omega_{-N} a_{-1} & \cdots & j\omega_{-N} a_{-2N} \\ j\omega_{-N+1} a_1 & j\omega_{-N+1} a_0 & \cdots & \vdots \\ \vdots & \vdots & \ddots & \vdots \\ j\omega_N a_{2N} & j\omega_N a_{2N-1} & \cdots & j\omega_N a_0 \end{pmatrix} \begin{pmatrix} V_{-N} \\ V_{-N+1} \\ \vdots \\ V_N \end{pmatrix}. \quad (34)$$

The matrix multiplied by the voltage vector on the right side is the admittance matrix. Contemplating this matrix, we see that it is a square matrix $(2N + 1 \times 2N + 1)$ whose diagonal is associated with the dc component of the modulated signal a_0 .

In a similar way, matrix relations can be written for other periodically time-modulated circuit components [122] or impedance parameters of metasurfaces [123]. We see that circuits and metasurfaces with time-modulated elements can be studied using familiar circuit-theory methods, except that scalar voltages and currents become vector amplitudes of frequency harmonics, and scalar relations between voltages and currents are replaced by matrix relations. In the supplementary materials available at <https://www.doi.org/10.1109/MAP.2023.3261601>, we

also discuss the power and energy relationships in time-varying capacitors.

CONCLUSIONS

In this short introductory tutorial, we focused on the most fundamental notions of the theory of LTV circuits and systems. Under the assumption of linearity, the general causal relationships between currents and voltages or fields and polarizations take the form of integral relationships where the kernel depends on two time variables: observation and delay time. In the frequency domain, we deal with two frequency variables: one to account for frequency dispersion and the other for the signal spectrum. Importantly, currents oscillating at a certain frequency become coupled to voltages at all frequencies, and the circuit-theory relationships take a matrix form. Although some phenomena, like frequency conversion, are similar to nonlinear phenomena, it is important to stress that all of the circuit and field equations remain linear, which greatly simplifies their solutions but does not allow realization of nonlinear effects. On the other hand, external time modulations break the time-reversal symmetry of field equations, allowing realization of nonreciprocal devices. In addition, time-modulated systems are not conservative because power can be exchanged with the external device that changes some of the system components in time. This property allows realization of various parametric amplifiers. Solutions of the linear matrix or integral equations for time-varying structures reveal possibilities for multiple applications of time-modulated circuit components and materials, starting from classical mixers or parametric amplifiers, to magnetless nonreciprocal devices or antennas working beyond fundamental limits set for linear passive devices.

ACKNOWLEDGMENT

This work was supported by the Academy of Finland under grant 330260. This article has supplementary downloadable material available at <https://www.doi.org/10.1109/MAP.2023.3261601>, provided by the authors.



AUTHOR INFORMATION

Grigorii Ptitsyn (ptitcyn@seas.upenn.edu) is with Aalto University, 02150 Espoo, Finland. His main research interests include electromagnetics of complex media, metasurfaces, time-modulated structures, and reconfigurable surfaces.

Mohammad Sajjad Mirmoosa (mirmoosa@protonmail.com) is with Aalto University, 02150 Espoo, Finland. His main research interests include theories of electromagnetism and wave-matter interaction.

Amirhosein Sotoodehfar (amirhossein.sotoodeh@ucalgary.ca) is with the University of Calgary, Calgary, AB T2N 1N42500, Canada. His main research interests are quantum materials and quantum chemistry.

Sergei A. Tretyakov (sergei.tretyakov@aalto.fi) is with Aalto University, 02150 Espoo, Finland. His main scientific interests are electromagnetic field theory, complex media electromagnetics, and microwave engineering.

REFERENCES

- [1] G. Matz and F. Hlawatsch, "Fundamentals of time-varying communication channels," in *Wireless Communications Over Rapidly Time-Varying Channels*. New York, NY, USA: Academic, 2011, pp. 1–63.
- [2] L. A. Zadeh, "Frequency analysis of variable networks," *Proc. IRE*, vol. 38, no. 3, pp. 291–299, Mar. 1950, doi: 10.1109/JRPROC.1950.231083.
- [3] L. A. Zadeh, "The determination of the impulsive response of variable networks," *J. Appl. Phys.*, vol. 21, no. 7, pp. 642–645, 1950, doi: 10.1063/1.1699724.
- [4] L. A. Zadeh, "On stability of linear varying-parameter systems," *J. Appl. Phys.*, vol. 22, no. 4, pp. 402–405, 1951, doi: 10.1063/1.1699972.
- [5] L. A. Zadeh, "Correlation functions and power spectra in variable networks," *Proc. IRE*, vol. 38, no. 11, pp. 1342–1345, Nov. 1950, doi: 10.1109/JRPROC.1950.234427.
- [6] T. Kailath, "Sampling models for linear time-variant filters," *Res. Lab. Electron., Massachusetts Inst. Technol.*, Cambridge, MA, USA, Tech. Rep. 352, May 1959.
- [7] T. Kailath, "Measurements on time-variant communication channels," *IEEE Trans. Inf. Theory*, vol. 8, no. 5, pp. 229–236, Sep. 1962, doi: 10.1109/TIT.1962.1057748.
- [8] A. Gershoff, "Characterization of time-varying linear systems," School Elect. Eng., Cornell Univ., Ithaca, NY, USA, Tech. Rep. AD0420573, Feb. 1963.
- [9] A. Gershoff, "Properties of time-varying linear systems," School Elect. Eng., Cornell Univ., Ithaca, NY, USA, Tech. Rep. EE552, 1962.
- [10] P. Bello, "Time-frequency duality," *IEEE Trans. Inf. Theory*, vol. 10, no. 1, pp. 18–33, Jan. 1964, doi: 10.1109/TIT.1964.1053640.
- [11] P. Bello, "Characterization of randomly time-variant linear channels," *IEEE Trans. Commun. Syst.*, vol. 11, no. 4, pp. 360–393, Dec. 1963, doi: 10.1109/TCOM.1963.1088793.
- [12] H. A. Wheeler, "Fundamental limitations of small antennas," *Proc. IRE*, vol. 35, no. 12, pp. 1479–1484, Dec. 1947, doi: 10.1109/JRPROC.1947.226199.
- [13] L. J. Chu, "Physical limitations of omni-directional antennas," *J. Appl. Phys.*, vol. 19, no. 12, pp. 1163–1175, May 1948, doi: 10.1063/1.1715038.
- [14] M. Jacob and H. Brauch, "Keying VLF transmitters at high speed," *Electronics*, vol. 27, no. 12, pp. 148–151, 1954.
- [15] H. Wolff, "High-speed frequency-shift keying of LF and VLF radio circuits," *IRE Trans. Commun. Syst.*, vol. 5, no. 3, pp. 29–42, Dec. 1957, doi: 10.1109/TCOM.1957.1097513.
- [16] J. Galejs, "Switching of reactive elements in high-Q antennas," *IEEE Trans. Commun. Syst.*, vol. 11, no. 2, pp. 254–255, Jun. 1963, doi: 10.1109/TCOM.1963.1088740.
- [17] H. Hartley, "Analysis of some techniques used in modern LF-VLF radiation systems," *IEEE Trans. Commun. Technol.*, vol. 16, no. 5, pp. 690–700, Oct. 1968, doi: 10.1109/TCOM.1968.1089913.
- [18] V. F. Fusco and Q. Chen, "Direct-signal modulation using a silicon microstrip patch antenna," *IEEE Trans. Antennas Propag.*, vol. 47, no. 6, pp. 1025–1028, Jun. 1999, doi: 10.1109/8.777127.
- [19] W. Yao and Y. Wang, "Direct antenna modulation - A promise for ultra-wideband (UWB) transmitting," in *Proc. IEEE MTT-S Int. Microw. Symp. Dig.*, 2004, vol. 2, pp. 1273–1276, doi: 10.1109/MWSYM.2004.1339221.
- [20] A. Babakhani, D. B. Rutledge, and A. Hajimiri, "Near-field direct antenna modulation," *IEEE Microw. Mag.*, vol. 10, no. 1, pp. 36–46, Feb. 2009, doi: 10.1109/MMM.2008.930674.
- [21] A. Cullen, "A travelling-wave parametric amplifier," *Nature*, vol. 181, no. 4605, pp. 332–332, Feb. 1958, doi: 10.1038/181332a0.
- [22] P. Tien, "Parametric amplification and frequency mixing in propagating circuits," *J. Appl. Phys.*, vol. 29, no. 9, pp. 1347–1357, Sep. 1958, doi: 10.1063/1.1723440.
- [23] P. Tien and H. Suhl, "A traveling-wave ferromagnetic amplifier," *Proc. IRE*, vol. 46, no. 4, pp. 700–706, Apr. 1958, doi: 10.1109/JRPROC.1958.286770.
- [24] E. Galiffi, P. A. Huidobro, and J. B. Pendry, "Broadband nonreciprocal amplification in luminal metamaterials," *Phys. Rev. Lett.*, vol. 123, no. 20, Nov. 2019, Art. no. 206101, doi: 10.1103/PhysRevLett.123.206101.
- [25] M. Currie and R. Gould, "Coupled-cavity traveling-wave parametric amplifiers: Part I-analysis," *Proc. IRE*, vol. 48, no. 12, pp. 1960–1973, Dec. 1960, doi: 10.1109/JRPROC.1960.287564.
- [26] A. Kamal, "A parametric device as a nonreciprocal element," *Proc. IRE*, vol. 48, no. 8, pp. 1424–1430, Aug. 1960, doi: 10.1109/JRPROC.1960.287569.
- [27] B. Anderson and R. Newcomb, "On reciprocity and time-variable networks," *Proc. IEEE*, vol. 53, no. 10, pp. 1674–1674, Jul. 1965, doi: 10.1109/PROC.1965.4321.
- [28] F. R. Morgenthaler, "Velocity modulation of electromagnetic waves," *IRE Trans. Microw. Theory Techn.*, vol. 6, no. 2, pp. 167–172, Apr. 1958, doi: 10.1109/TMTT.1958.1124533.

- [29] J.-C. Simon, "Action of a progressive disturbance on a guided electromagnetic wave," *IRE Trans. Microw. Theory Techn.*, vol. 8, no. 1, pp. 18–29, Jan. 1960, doi: 10.1109/TMTT.1960.1124657.
- [30] A. Oliner and A. Hessel, "Wave propagation in a medium with a progressive sinusoidal disturbance," *IRE Trans. Microw. Theory Techn.*, vol. 9, no. 4, pp. 337–343, 1961, doi: 10.1109/TMTT.1961.1125340.
- [31] L. Felsen and G. Whitman, "Wave propagation in time-varying media," *IEEE Trans. Antennas Propag.*, vol. 18, no. 2, pp. 242–253, Mar. 1970, doi: 10.1109/TAP.1970.1139657.
- [32] R. Fante, "Transmission of electromagnetic waves into time-varying media," *IEEE Trans. Antennas Propag.*, vol. 19, no. 3, pp. 417–424, May 1971, doi: 10.1109/TAP.1971.1139931.
- [33] D. Holberg and K. Kunz, "Parametric properties of fields in a slab of time-varying permittivity," *IEEE Trans. Antennas Propag.*, vol. 14, no. 2, pp. 183–194, Mar. 1966, doi: 10.1109/TAP.1966.1138637.
- [34] S. Averkov and N. Stepanov, "Wave propagation in systems with a traveling parameter," *Izvestiya Vysshikh Uchebnykh Zavedenii, Radiofizika*, vol. 2, no. 2, pp. 203–212, Mar. 1959.
- [35] V. Gavrilenko, G. Lupanov, and N. Stepanov, "Dynamo-optical effects in a plasma," *Radiophys. Quantum Electron.*, vol. 15, no. 2, pp. 138–143, Feb. 1972, doi: 10.1007/BF02209107.
- [36] V. Gavrilenko, G. Lupanov, and N. Stepanov, "Electromagnetic waves in nonuniformly moving media (electromagnetic wave reflection from region with variable drift velocity and polarization of waves propagating in nonuniformly moving medium, applying to isotropic plasma)," in *Proc. Electromagn. Wave Theory*, 1971, pp. 518–525.
- [37] L. Ostrovskii and N. Stepanov, "Nonresonance parametric phenomena in distributed systems," *Radiophys. Quantum Electron.*, vol. 14, no. 4, pp. 387–419, Apr. 1971, doi: 10.1007/BF01030725.
- [38] N. Stepanov, "Adiabatic transformation of a wave spectrum in a nonstationary medium with dispersion," *Radiophys. Quantum Electron.*, vol. 12, no. 2, pp. 227–234, Feb. 1969, doi: 10.1007/BF01031285.
- [39] V. Pikulin and N. Stepanov, "The kinetic theory of electromagnetic waves in an electron plasma with slowly varying parameters," *Izvestiya Vysshikh Uchebnykh Zavedenii, Radiofizika*, vol. 16, pp. 1138–1145, Aug. 1973, doi: 10.1007/BF01031619.
- [40] N. Stepanov, "On wave reflection from arbitrary moving inhomogeneity," *Izvestiya Vysshikh Uchebnykh Zavedenii, Radiofizika*, vol. 5, pp. 908–916, May 1962.
- [41] Y. M. Sorokin and N. Stepanov, "The reflection and refraction of electromagnetic waves in a moving inhomogeneous plasma," *Radiophys. Quantum Electron.*, vol. 14, no. 1, pp. 17–23, Jan. 1971, doi: 10.1007/BF01032902.
- [42] N. Stepanov and Y. M. Sorokin, "Kinetic theory of electromagnetic wave reflection from a moving inhomogeneous plasma sheath," *Soviet Phys. Tech. Phys.*, vol. 17, p. 456, Sep. 1972.
- [43] Y. M. Sorokin, "On a certain energy relationship for waves in systems having traveling parameters," *Radiophys. Quantum Electron.*, vol. 15, no. 1, pp. 36–39, Jan. 1972, doi: 10.1007/BF02209239.
- [44] N. Stepanov, "Dielectric constant of unsteady plasma," *Radiophys. Quantum Electron.*, vol. 19, no. 7, pp. 683–689, Jul. 1976, doi: 10.1007/BF01034233.
- [45] M. Mirmoosa, T. Koutserimpas, G. Ptitsyn, S. Tretyakov, and R. Fleury, "Dipole polarizability of time-varying particles," *New J. Phys.*, vol. 24, no. 6, Jun. 2022, Art. no. 063004, doi: 10.1088/1367-2630/ac6b4c.
- [46] N. Engheta, "Metamaterials with high degrees of freedom: Space, time, and more," *Nanophotonics*, vol. 10, no. 1, pp. 639–642, 2021, doi: 10.1515/nanoph-2020-0414.
- [47] D. M. Solís and N. Engheta, "Functional analysis of the polarization response in linear time-varying media: A generalization of the Kramers-Kronig relations," *Phys. Rev. B*, vol. 103, no. 14, Apr. 2021, Art. no. 144303, doi: 10.1103/PhysRevB.103.144303.
- [48] J. Sloan, N. Rivera, J. D. Joannopoulos, and M. Soljačić, "Casimir light in dispersive nanophotonics," *Phys. Rev. Lett.*, vol. 127, no. 5, Jul. 2021, Art. no. 053603, doi: 10.1103/PhysRevLett.127.053603.
- [49] V. Pacheco-Peña and N. Engheta, "Temporal equivalent of the Brewster angle," *Phys. Rev. B*, vol. 104, no. 21, Dec. 2021, Art. no. 214308, doi: 10.1103/PhysRevB.104.214308.
- [50] V. Pacheco-Peña and N. Engheta, "Temporal aiming," *Light, Sci. Appl.*, vol. 9, no. 1, pp. 1–12, Jul. 2020, doi: 10.1038/s41377-020-00360-1.
- [51] A. Derode, A. Tourin, J. de Rosny, M. Tanter, S. Yon, and M. Fink, "Taking advantage of multiple scattering to communicate with time-reversal antennas," *Phys. Rev. Lett.*, vol. 90, no. 1, Jan. 2003, Art. no. 014301, doi: 10.1103/PhysRevLett.90.014301.
- [52] M. Fink, "From Loschmidt daemons to time-reversed waves," *Philosophical Trans. Roy. Soc. A, Math., Phys. Eng. Sci.*, vol. 374, no. 2069, Jun. 2016, Art. no. 20150156, doi: 10.1098/rsta.2015.0156.
- [53] A. Przadka, S. Feat, P. Petitjeans, V. Pagneux, A. Maurel, and M. Fink, "Time reversal of water waves," *Phys. Rev. Lett.*, vol. 109, no. 6, Aug. 2012, Art. no. 064501, doi: 10.1103/PhysRevLett.109.064501.
- [54] S. M. Popoff, A. Aubry, G. Lerosey, M. Fink, A.-C. Boccara, and S. Gigan, "Exploiting the time-reversal operator for adaptive optics, selective focusing, and scattering pattern analysis," *Phys. Rev. Lett.*, vol. 107, no. 26, Dec. 2011, Art. no. 263901, doi: 10.1103/PhysRevLett.107.263901.
- [55] M. Manteghi, "Fundamental limits, bandwidth, and information rate of electrically small antennas: Increasing the throughput of an antenna without violating the thermodynamic Q-factor," *IEEE Antennas Propag. Mag.*, vol. 61, no. 3, pp. 14–26, Jun. 2019, doi: 10.1109/MAP.2019.2907892.
- [56] Y. Hadad, J. C. Soric, and A. Alù, "Breaking temporal symmetries for emission and absorption," *Proc. Nat. Acad. Sci.*, vol. 113, no. 13, pp. 3471–3475, Mar. 2016, doi: 10.1073/pnas.1517363113.
- [57] H. Li, A. Mekawy, and A. Alù, "Beyond Chu's limit with Floquet impedance matching," *Phys. Rev. Lett.*, vol. 123, no. 16, Oct. 2019, Art. no. 164102, doi: 10.1103/PhysRevLett.123.164102.
- [58] M. H. Mostafa, G. Ptitsyn, and S. Tretyakov, "Dipole antennas with time-varying body and shape," in *Proc. 14th Int. Congr. Artif. Mater. Novel Wave Phenomena (Metamater.)*, 2020, pp. 63–65, doi: 10.1109/Metamaterals49557.2020.9285128.
- [59] S. Taravati, N. Chamanara, and C. Caloz, "Nonreciprocal electromagnetic scattering from a periodically space-time modulated slab and application to a quasiconic isolator," *Phys. Rev. B*, vol. 96, no. 16, Oct. 2017, Art. no. 165144, doi: 10.1103/PhysRevB.96.165144.
- [60] N. Chamanara, S. Taravati, Z.-L. Deck-Léger, and C. Caloz, "Optical isolation based on space-time engineered asymmetric photonic band gaps," *Phys. Rev. B*, vol. 96, no. 15, Oct. 2017, Art. no. 155409, doi: 10.1103/PhysRevB.96.155409.
- [61] C. Caloz, A. Alù, S. Tretyakov, D. Sounas, K. Achouri, and Z.-L. Deck-Léger, "Electromagnetic nonreciprocity," *Phys. Rev. Appl.*, vol. 10, no. 4, Oct. 2018, Art. no. 047001, doi: 10.1103/PhysRevApplied.10.047001.
- [62] D. L. Sounas and A. Alù, "Angular-momentum-biased nanorings to realize magnetic-free integrated optical isolation," *ACS Photon.*, vol. 1, no. 3, pp. 198–204, Feb. 2014, doi: 10.1021/ph400058y.
- [63] D. Correas-Serrano, J. Gomez-Diaz, D. Sounas, Y. Hadad, A. Alvarez-Melcon, and A. Alù, "Nonreciprocal graphene devices and antennas based on spatiotemporal modulation," *IEEE Antennas Wireless Propag. Lett.*, vol. 15, pp. 1529–1532, 2016, doi: 10.1109/LAWP.2015.2510818.
- [64] D. Dinc, M. Tymchenko, A. Nagulu, D. Sounas, A. Alù, and H. Krishnaswamy, "Synchronized conductivity modulation to realize broadband lossless magnetic-free non-reciprocity," *Nature Commun.*, vol. 8, no. 1, pp. 1–9, Oct. 2017, doi: 10.1038/s41467-017-00798-9.
- [65] R. Fleury, D. Sounas, and A. Alù, "Non-reciprocal optical mirrors based on spatio-temporal acousto-optic modulation," *J. Opt.*, vol. 20, no. 3, Feb. 2018, Art. no. 034007, doi: 10.1088/2040-8986/aaa3e.
- [66] A. Y. Song, Y. Shi, Q. Lin, and S. Fan, "Direction-dependent parity-time phase transition and nonreciprocal amplification with dynamic gain-loss modulation," *Phys. Rev. A*, vol. 99, no. 1, Jan. 2019, Art. no. 013824, doi: 10.1103/PhysRevA.99.013824.
- [67] H. Lira, Z. Yu, S. Fan, and M. Lipson, "Electrically driven nonreciprocity induced by interband photonic transition on a silicon chip," *Phys. Rev. Lett.*, vol. 109, no. 3, Jul. 2012, Art. no. 033901, doi: 10.1103/PhysRevLett.109.033901.
- [68] Z. Yu and S. Fan, "Complete optical isolation created by indirect interband photonic transitions," *Nature Photon.*, vol. 3, no. 2, pp. 91–94, Jan. 2009, doi: 10.1038/nphoton.2008.273.
- [69] Y. Shi, S. Han, and S. Fan, "Optical circulation and isolation based on indirect photonic transitions of guided resonance modes," *ACS Photon.*, vol. 4, no. 7, pp. 1639–1645, Jun. 2017, doi: 10.1021/acsphotonics.7b00420.
- [70] X. Wang et al., "Nonreciprocity in bianisotropic systems with uniform time modulation," *Phys. Rev. Lett.*, vol. 125, no. 26, Dec. 2020, Art. no. 266102, doi: 10.1103/PhysRevLett.125.266102.
- [71] V. S. Asadchy, M. S. Mirmoosa, A. Díaz-Rubio, S. Fan, and S. A. Tretyakov, "Tutorial on electromagnetic nonreciprocity and its origins," *Proc. IEEE*, vol. 108, no. 10, pp. 1684–1727, Oct. 2020, doi: 10.1109/JPROC.2020.3012381.
- [72] A. M. Shaltout, A. Kildishev, and V. Shalaev, "Time-varying metasurfaces and Lorentz non-reciprocity," *Opt. Mater. Exp.*, vol. 5, no. 11, pp. 2459–2467, Jul. 2015, doi: 10.1364/OME.5.002459.
- [73] A. M. Shaltout, V. M. Shalaev, and M. L. Brongersma, "Spatiotemporal light control with active metasurfaces," *Science*, vol. 364, no. 6441, May 2019, Art. no. eaat3100, doi: 10.1126/science.aat3100.
- [74] T. T. Koutserimpas and R. Fleury, "Nonreciprocal gain in non-Hermitian time-Floquet systems," *Phys. Rev. Lett.*, vol. 120, no. 8, Feb. 2018, Art. no. 087401, doi: 10.1103/PhysRevLett.120.087401.
- [75] L. Zhang et al., "Breaking reciprocity with space-time-coding digital metasurfaces," *Adv. Mater.*, vol. 31, no. 41, Aug. 2019, Art. no. 1904069, doi: 10.1002/adma.201904069.

- [76] S. Taravati and A. A. Kishk, "Dynamic modulation yields one-way beam splitting," *Phys. Rev. B*, vol. 99, no. 7, Feb. 2019, Art. no. 075101, doi: 10.1103/PhysRevB.99.075101.
- [77] D. Ramaccia, D. L. Sounas, A. V. Marini, A. Toscano, and F. Bilotti, "Electromagnetic isolation induced by time-varying metasurfaces: Nonreciprocal Bragg grating," *IEEE Antennas Wireless Propag. Lett.*, vol. 19, no. 11, pp. 1886–1890, Nov. 2020, doi: 10.1109/LAWP.2020.2996275.
- [78] D. Ramaccia, D. L. Sounas, A. Alù, F. Bilotti, and A. Toscano, "Nonreciprocity in antenna radiation induced by space-time varying metamaterial cloaks," *IEEE Antennas Wireless Propag. Lett.*, vol. 17, no. 11, pp. 1968–1972, Sep. 2018, doi: 10.1109/LAWP.2018.2870688.
- [79] A. Li, Y. Li, J. Long, E. Forati, Z. Du, and D. Sievenpiper, "Time-modulated nonreciprocal metasurface absorber for surface waves," *Opt. Lett.*, vol. 45, no. 5, pp. 1212–1215, Mar. 2020, doi: 10.1364/OL.382865.
- [80] M. Liu, D. A. Powell, Y. Zarate, and I. V. Shadrivov, "Huygens' metadevices for parametric waves," *Phys. Rev. X*, vol. 8, no. 3, Sep. 2018, Art. no. 031077, doi: 10.1103/PhysRevX.8.031077.
- [81] K. Lee et al., "Linear frequency conversion via sudden merging of meta-atoms in time-variant metasurfaces," *Nature Photon.*, vol. 12, no. 12, pp. 765–773, Dec. 2018, doi: 10.1038/s41566-018-0259-4.
- [82] M. M. Salary, S. Jafar-Zanjani, and H. Mosallaei, "Electrically tunable harmonics in time-modulated metasurfaces for waveform engineering," *New J. Phys.*, vol. 20, no. 12, Dec. 2018, Art. no. 123023, doi: 10.1088/1367-2630/aaf47a.
- [83] K. Lee et al., "Electrical control of terahertz frequency conversion from time-varying surfaces," *Opt. Exp.*, vol. 27, no. 9, pp. 12,762–12,773, Apr. 2019, doi: 10.1364/OE.27.012762.
- [84] X. Zou, Q. Wu, and Y. E. Wang, "Monolithically integrated parametric mixers with time-varying transmission lines (TVTLs)," *IEEE Trans. Microw. Theory Techn.*, vol. 68, no. 10, pp. 4479–4490, Oct. 2020, doi: 10.1109/TMTT.2020.3011116.
- [85] Y. Zhou et al., "Broadband frequency translation through time refraction in an epsilon-near-zero material," *Nature Commun.*, vol. 11, no. 1, pp. 1–7, May 2020, doi: 10.1038/s41467-020-15682-2.
- [86] K. Pang et al., "Adiabatic frequency conversion using a time-varying epsilon-near-zero metasurface," *Nano Lett.*, vol. 21, no. 14, pp. 5907–5913, Jul. 2021, doi: 10.1021/acs.nanolett.1c00550.
- [87] J. Yang et al., "Simultaneous conversion of polarization and frequency via time-division-multiplexing metasurfaces," *Adv. Opt. Mater.*, vol. 9, no. 22, Sep. 2021, Art. no. 2101043, doi: 10.1002/adom.202101043.
- [88] B. Apffel and E. Fort, "Frequency conversion cascade by crossing multiple space and time interfaces," *Phys. Rev. Lett.*, vol. 128, no. 6, Feb. 2022, Art. no. 064501, doi: 10.1103/PhysRevLett.128.064501.
- [89] N. Wang, Z.-Q. Zhang, and C. T. Chan, "Photonic Floquet media with a complex time-periodic permittivity," *Phys. Rev. B*, vol. 98, no. 8, Aug. 2018, Art. no. 085142, doi: 10.1103/PhysRevB.98.085142.
- [90] S. Lee et al., "Parametric oscillation of electromagnetic waves in momentum band gaps of a spatiotemporal crystal," *Photon. Res.*, vol. 9, no. 2, pp. 142–150, 2021, doi: 10.1364/PRJ.406215.
- [91] Y. Xiao, G. P. Agrawal, and D. N. Maywar, "Spectral and temporal changes of optical pulses propagating through time-varying linear media," *Opt. Lett.*, vol. 36, no. 4, pp. 505–507, Feb. 2011, doi: 10.1364/OL.36.000505.
- [92] D. Ramaccia, D. L. Sounas, A. Alù, A. Toscano, and F. Bilotti, "Doppler cloak restores invisibility to objects in relativistic motion," *Phys. Rev. B*, vol. 95, no. 7, Feb. 2017, Art. no. 075113, doi: 10.1103/PhysRevB.95.075113.
- [93] Z. Wu and A. Grbic, "Serrodyne frequency translation using time-modulated metasurfaces," *IEEE Trans. Antennas Propag.*, vol. 68, no. 3, pp. 1599–1606, Mar. 2020, doi: 10.1109/TAP.2019.2943712.
- [94] M. Mirmoosa, G. Ptiteyn, V. Asadchy, and S. Tretyakov, "Time-varying reactive elements for extreme accumulation of electromagnetic energy," *Phys. Rev. Appl.*, vol. 11, no. 1, Jan. 2019, Art. no. 014024, doi: 10.1103/PhysRevApplied.11.014024.
- [95] G. Ptiteyn, M. S. Mirmoosa, and S. A. Tretyakov, "Time-modulated meta-atoms," *Phys. Rev. Res.*, vol. 1, no. 2, Sep. 2019, Art. no. 023014, doi: 10.1103/PhysRevResearch.1.023014.
- [96] M. S. Mirmoosa, G. A. Ptiteyn, R. Fleury, and S. A. Tretyakov, "Instantaneous radiation from time-varying electric and magnetic dipoles," *Phys. Rev. A*, vol. 102, no. 1, Jul. 2020, Art. no. 013503, doi: 10.1103/PhysRevA.102.013503.
- [97] P. A. Huidobro, E. Galiffi, S. Guenneau, R. V. Craster, and J. Pendry, "Fresnel drag in space-time-modulated metamaterials," *Proc. Nat. Acad. Sci.*, vol. 116, no. 50, pp. 24,943–24,948, Nov. 2019, doi: 10.1073/pnas.1915027116.
- [98] V. Bruno et al., "Negative refraction in time-varying strongly coupled plasmonic-antenna-epsilon-near-zero systems," *Phys. Rev. Lett.*, vol. 124, no. 4, Jan. 2020, Art. no. 043902, doi: 10.1103/PhysRevLett.124.043902.
- [99] V. Pacheco-Peña and N. Engheta, "Effective medium concept in temporal metamaterials," *Nanophotonics*, vol. 9, no. 2, pp. 379–391, 2020, doi: 10.1515/nanoph-2019-0305.
- [100] P. A. Huidobro, M. G. Silveirinha, E. Galiffi, and J. Pendry, "Homogenization theory of space-time metamaterials," *Phys. Rev. Appl.*, vol. 16, no. 1, Jul. 2021, Art. no. 014044, doi: 10.1103/PhysRevApplied.16.014044.
- [101] M. Camacho, B. Edwards, and N. Engheta, "Achieving asymmetry and trapping in diffusion with spatiotemporal metamaterials," *Nature Commun.*, vol. 11, no. 1, pp. 1–7, Jul. 2020, doi: 10.1038/s41467-020-17550-5.
- [102] H. Barati Sede, M. M. Salary, and H. Mosallaei, "Optical pulse compression assisted by high-Q time-modulated transmissive metasurfaces," *Laser Photon. Rev.*, vol. 16, no. 5, Mar. 2022, Art. no. 2100449, doi: 10.1002/lpor.202100449.
- [103] M. Liu, A. B. Kozyrev, and I. V. Shadrivov, "Time-varying metasurfaces for broadband spectral camouflage," *Phys. Rev. Appl.*, vol. 12, no. 5, Nov. 2019, Art. no. 054052, doi: 10.1103/PhysRevApplied.12.054052.
- [104] X. Wang and C. Caloz, "Spread-spectrum selective camouflaging based on time-modulated metasurface," *IEEE Trans. Antennas Propag.*, vol. 69, no. 1, pp. 286–295, 2020, doi: 10.1109/TAP.2020.3008621.
- [105] A. Akbarzadeh, N. Chamanara, and C. Caloz, "Inverse prism based on temporal discontinuity and spatial dispersion," *Opt. Lett.*, vol. 43, no. 14, pp. 3297–3300, 2018, doi: 10.1364/OL.43.003297.
- [106] V. Pacheco-Peña and N. Engheta, "Spatiotemporal isotropic-to-anisotropic meta-atoms," *New J. Phys.*, vol. 23, no. 9, Sep. 2021, Art. no. 095006, doi: 10.1088/1367-2630/ac21df.
- [107] E. Lustig, Y. Sharabi, and M. Segev, "Topological aspects of photonic time crystals," *Optica*, vol. 5, no. 11, pp. 1390–1395, Nov. 2018, doi: 10.1364/OPTICA.5.001390.
- [108] Y. Sharabi, E. Lustig, and M. Segev, "Disordered photonic time crystals," *Phys. Rev. Lett.*, vol. 126, no. 16, Apr. 2021, Art. no. 163902, doi: 10.1103/PhysRevLett.126.163902.
- [109] A. M. Shaltout, J. Fang, A. V. Kildishev, and V. M. Shalaev, "Photonic time-crystals and momentum band-gaps," in *Proc. Conf. Lasers Electro-Opt.*, 2016, pp. 1–2.
- [110] N. Chamanara, Z.-L. Deck-Léger, C. Caloz, and D. Kalluri, "Unusual electromagnetic modes in space-time-modulated dispersion-engineered media," *Phys. Rev. A*, vol. 97, no. 6, Jun. 2018, Art. no. 063829, doi: 10.1103/PhysRevA.97.063829.
- [111] Z.-L. Deck-Léger, N. Chamanara, M. Skorobogatiy, M. G. Silveirinha, and C. Caloz, "Uniform-velocity spacetime crystals," *Adv. Photon.*, vol. 1, no. 5, Oct. 2019, Art. no. 056002, doi: 10.1117/1.AP.1.056002.
- [112] J. Park and B. Min, "Spatiotemporal plane wave expansion method for arbitrary space-time periodic photonic media," *Opt. Lett.*, vol. 46, no. 3, pp. 484–487, Feb. 2021, doi: 10.1364/OL.411622.
- [113] X. Wang, V. S. Asadchy, S. Fan, and S. Tretyakov, "Space-time metasurfaces for perfect power combining of waves," *ACS Photon.*, vol. 8, no. 10, pp. 3034–3041, May 2021, doi: 10.1021/acspophotonics.1c00981.
- [114] E. Galiffi, Y.-T. Wang, Z. Lim, J. B. Pendry, A. Alù, and P. A. Huidobro, "Wood anomalies and surface-wave excitation with a time grating," *Phys. Rev. Lett.*, vol. 125, no. 12, Sep. 2020, Art. no. 127403, doi: 10.1103/PhysRevLett.125.127403.
- [115] D. L. Sounas and A. Alù, "Non-reciprocal photonics based on time modulation," *Nature Photon.*, vol. 11, no. 12, pp. 774–783, Nov. 2017, doi: 10.1038/s41566-017-0051-x.
- [116] E. Galiffi et al., "Photonics of time-varying media," *Adv. Photon.*, vol. 4, no. 1, Jan. 2022, Art. no. 014002, doi: 10.1117/1.AP.4.014002.
- [117] A. V. Oppenheim, A. S. Willsky, and S. Nawab, *Signals and Systems*. Englewood Cliffs, NJ, USA: Prentice Hall, 1996.
- [118] G. Floquet, "Sur les équations différentielles linéaires à coefficients périodiques," *Annales Scientifiques de L'École Normale Supérieure*, vol. 12, no. 2, pp. 47–88, 1883, doi: 10.24033/asens.220.
- [119] F. Bloch, "Über die quantenmechanik der elektronen in kristallgittern," *Zeitschrift für Physik*, vol. 52, nos. 7–8, pp. 555–600, Jul. 1929, doi: 10.1007/BF01339455.
- [120] A. Ishimaru, *Electromagnetic Wave Propagation, Radiation, and Scattering: From Fundamentals to Applications*. Hoboken, NJ, USA: Wiley, 2017.
- [121] W. Magnus and S. Winkler, *Hill's Equation*. New York, NY, USA: Dover, 1979.
- [122] P. Jayathurathnage, F. Liu, M. S. Mirmoosa, X. Wang, R. Fleury, and S. A. Tretyakov, "Time-varying components for enhancing wireless transfer of power and information," *Phys. Rev. Appl.*, vol. 16, no. 1, Jul. 2021, Art. no. 014017, doi: 10.1103/PhysRevApplied.16.014017.
- [123] X. Wang, A. Díaz-Rubio, H. Li, S. A. Tretyakov, and A. Alù, "Theory and design of multifunctional space-time metasurfaces," *Phys. Rev. Appl.*, vol. 13, no. 4, Apr. 2020, Art. no. 044040, doi: 10.1103/PhysRevApplied.13.044040.



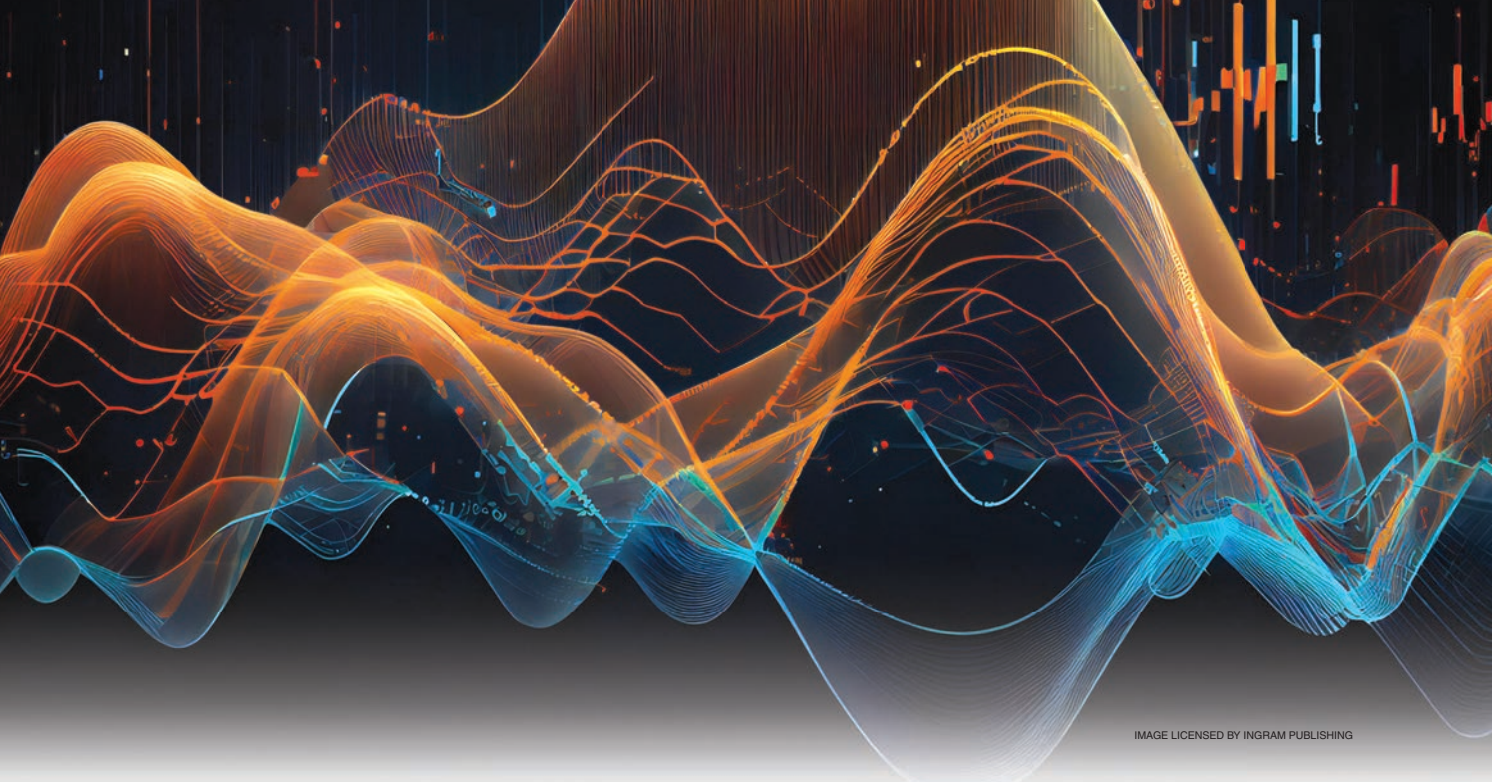


IMAGE LICENSED BY INGRAM PUBLISHING

Shixiong Yin , Emanuele Galiffi, Gengyu Xu, and Andrea Alù 

Scattering at Temporal Interfaces

An overview from an antennas and propagation engineering perspective.

Recent years have witnessed a surge of interest in exotic electromagnetic (EM) wave propagation in time-varying systems. An interesting concept is the one of a temporal interface, the time-analogue of a spatial interface, formed by an abrupt and uniform change of the EM properties of the host medium in time. A time interface scatters the incident wave in a dual fashion compared to its spatial counterpart, conserving momentum but transforming frequency and exchanging energy with the wave. This article provides an overview of the wave-scattering features induced by time interfaces from an antennas and propagation engineering perspective. We first discuss the dualities of wave propagation across spatial and temporal

interfaces, by recasting the telegrapher equations in a linear time-variant (LTV) transmission line (TL). Then, we introduce the scattering matrix to describe temporal scattering processes, and derive the conditions for reciprocity and momentum conservation. Understanding temporal scattering through the lens of conventional microwave engineering theory may facilitate the analysis and implementation of next-generation metamaterials encompassing temporal degrees of freedom.

INTRODUCTION

Scattering is at the basis of most EM wave phenomena, from the red glow we see at sunset to the multipath propagation in wireless communications. From a physics standpoint, it emerges at spatial discontinuities where the impedances of the two involved media are mismatched. As a result, a portion

of the impinging wave is rerouted to different directions in space, as in the case of the reflection and refraction phenomena illustrated in Figure 1(a). Morgenthaler envisioned in [1] that a wave can also be scattered by a discontinuity in time, as shown in Figure 1(b), at which the entire medium undergoes an abrupt change of its constitutive parameters. Dual to its spatial counterpart, two scattered waves are launched at this time interface, propagating in the new medium. The time-refracted signal travels forward, while the time-reflected one travels backward in space by conjugating its phase, hence time-reversing the incident signal.

In the past decades, temporal reflection and refraction phenomena have attracted broad attention from numerous communities interested in wave physics, including microwave [1], [2], [3], optics [4], mechanics [5], plasma [6], and quantum physics [7]. Many promising applications leveraging time interfaces have been proposed, e.g., the inverse prism [8], broadband impedance matching, energy trapping and absorption [9], [10], [11], [12], [13], [14], temporal aiming [15], and phase conjugation [16]. An extended recent review on time-varying media can be found in [17]. In this article, we focus on wave scattering at temporal discontinuities, drawing analogies with familiar concepts and terminologies in the antennas and propagation community. In the “Temporal TL Model” section, we derive the telegrapher equations for the charge and flux waves in a homogenous LTV TL and we examine the duality between spatial and temporal reflection coefficients, and between energy and momentum conservation at spatial and temporal interfaces. In the “Temporal Network Analysis” section, we introduce the duality of the scattering matrix for temporal interfaces, and we formulate temporal network analysis. To exemplify its broad applicability, we investigate cascaded temporal networks, reciprocity constraints, and momentum conservation conditions. Finally, we conclude by envisioning opportunities that temporal scattering may offer in various applications.

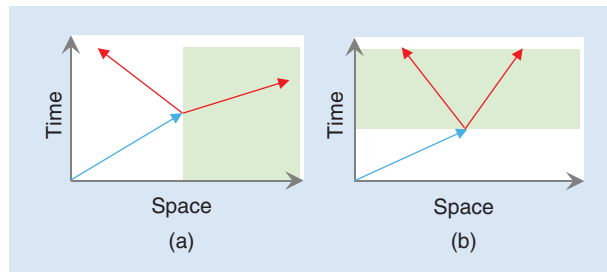


FIGURE 1. (a) Reflection and refraction at a spatial interface. (b) Temporal scattering at a time interface.

In the past decades, temporal reflection and refraction phenomena have attracted broad attention from numerous communities interested in wave physics.

TEMPORAL TL MODEL

TELEGRAPHER EQUATIONS IN TIME-VARYING MEDIA

As a prominent model in microwave engineering, the TL model replaces the minute description of fields with terminal quantities in circuits, by translating Maxwell's equations into the telegrapher equations. Figure 2(a) shows a conventional microwave TL in the form of a parallel-plate waveguide carrying a transverse EM (TEM) mode and featuring a spatial inhomogeneity. The nonzero field components E_x and H_y satisfy $\partial_z E_x = -\mu(z)\partial_t H_y$ and $\partial_z H_y = -\epsilon(z)\partial_t E_x$, where ϵ and μ are the time-invariant permittivity and permeability of the medium between the conductors, respectively. Introducing the voltage across the plates $V \propto E_x$ and the current on the plates $I \propto H_y$, we obtain the telegrapher equations [18]:

$$\begin{aligned} \frac{\partial V}{\partial z} &= -L(z) \frac{\partial I}{\partial t} \\ \frac{\partial I}{\partial z} &= -C(z) \frac{\partial V}{\partial t} \end{aligned} \quad (1)$$

where $C \propto \epsilon$ and $L \propto \mu$ are the capacitance and inductance per unit length, and their z dependence indicates the two media before and after the interface. Since the system is linear and time-invariant (LTI), the frequency ω is conserved, while the wavenumber $k(z) = \pm \omega \sqrt{L(z)C(z)}$ is different in the two regions.

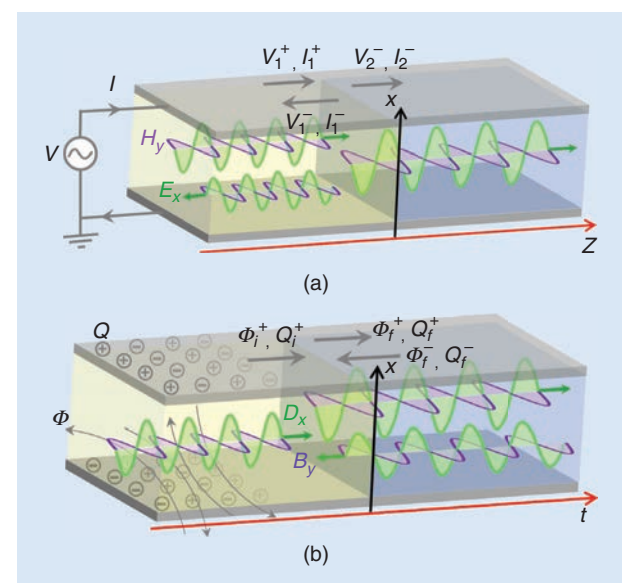


FIGURE 2. (a) A TL featuring a spatial interface. (b) A TL featuring a temporal interface, at which the medium is abruptly switched in time and uniformly in space.

An incident wave (V_1^+, I_1^+) impinging on the spatial interface at $z=0$, as shown in Figure 2(a), is partially reflected (V_1^-, I_1^-) and transmitted (V_2^-, I_2^-) with different wavelengths but identical frequencies. The input-side characteristic impedance $Z_1 = V_1^+/I_1^+ = -V_1^-/I_1^-$ and the load-side impedance $Z_2 = V_2^-/I_2^-$ determine the spatial reflection coefficient $\Gamma = V_1^-/V_1^+$ [18] through:

$$\Gamma = \frac{Z_2 - Z_1}{Z_2 + Z_1} \quad (2)$$

which can be derived from Kirchhoff's voltage and current laws, and is consistent with Fresnel scattering coefficients at the interface.

Dually, we can consider a parallel-plate waveguide filled by a spatially homogeneous but time-varying permittivity $\epsilon(t)$ and permeability $\mu(t)$. Maxwell's curl equations for the TEM wave read $\partial_t D_x = -\mu^{-1}(t) \partial_z B_y$ and $\partial_t B_y = -\epsilon^{-1}(t) \partial_z D_x$, where $D_x = \epsilon(t) E_x$ and $B_y = \mu(t) H_y$ if the material dispersion is negligible. Dual to a spatial boundary with vanishing thickness and infinite extent, an ideal temporal interface is formed when the distributed capacitance and/or inductance experience a discontinuity in time, as shown in Figure 2(b). The equivalent circuit quantities now become the electric charge per unit length $Q = C(t)V$ and the magnetic flux per unit length $\Phi = L(t)I$, yielding the telegrapher equations with time-varying characteristic parameters [2]:

$$\begin{aligned} \frac{\partial Q}{\partial t} &= -\frac{1}{L(t)} \frac{\partial \Phi}{\partial z} \\ \frac{\partial \Phi}{\partial t} &= -\frac{1}{C(t)} \frac{\partial Q}{\partial z}. \end{aligned} \quad (3)$$

The wavenumber k in this LTV system is preserved due to translational symmetry in space, hence it must be the same before and after the temporal interface, while the frequency follows $\omega(t) = \pm k/\sqrt{L(t)C(t)}$, and it abruptly changes after $t=0$. An incident wave denoted by (Φ_i^+, Q_i^+) is scattered by such an ideal temporal interface—at which L and C abruptly change to different values uniformly across the entire TL—inducing two counterpropagating waves: one propagates forward $[(\Phi_f^+, Q_f^+)]$, while the other is coupled to the negative frequency $-\omega_f$, hence it is time-reflected and propagates backward in space $[(\Phi_f^-, Q_f^-)]$. Physically, the time-reflected wave corresponds to the “echo” of a signal produced by the time interface, played backward in time while keeping the original spatial profile.

The temporal reflection and transmission coefficients can be defined for the charge waves as $R = Q_f^-/Q_i^+$ and $T = Q_f^+/Q_i^+$, respectively. If no shock current or voltage appears at this time interface ($\partial Q/\partial t$ and $\partial \Phi/\partial t$ are assumed finite), the electric charge density Q and magnetic flux density Φ (or equivalently the fields D_x and B_y) are continuous [1], which yields:

$$\begin{aligned} 1 &= T + R \\ Z_i &= Z_f T - Z_f R. \end{aligned} \quad (4)$$

Note that the two scattered waves both must experience the new characteristic impedance $Z_f = \Phi_f^+/Q_f^+ = -\Phi_f^-/Q_f^-$, since they both exist after the time interface. The initial impedance $Z_i = \Phi_i^+/Q_i^+$ and final impedance Z_f are related by the ratio of backward to forward wave amplitude $\rho = R/T$ [19] through:

$$\rho = \frac{Z_f - Z_i}{Z_f + Z_i}. \quad (5)$$

Comparing (5) to (2) reveals that, by replacing the spatial reflection coefficient Γ with the temporal backward-to-forward wave amplitude ratio ρ , we can employ conventional TL theory formulas for temporal interfaces. It is possible to use a conventional Smith chart to predict the backward-to-forward wave amplitude ratio ρ by considering impedance transformations in temporal slabs, rather than in spatial ones. By engineering impedance transformation networks through multiple tailored temporal interfaces, it is then possible to realize the desired momentum spectrum of ρ , as recently shown for temporal quarter-wave plates [10]. Leveraging the equivalence between Γ and ρ , we recently showed in [19] that broadband impedance matching and frequency conversion can be realized by temporally tapered interfaces, in analogy with Klopfenstein tapers in the spatial domain [20].

ENERGY AND MOMENTUM DUALITY

The frequency-wavenumber duality discussed so far alludes to an analogous relationship between energy and momentum at spatial and temporal interfaces. In a passive TL, the spatial reflection coefficient satisfies $|\Gamma| \leq 1$. Based on the duality between Γ and ρ , we similarly conclude that $|\rho| = |R/T| \leq 1$, i.e., $|R| \leq |T|$, in a “passive” temporal TL. However, we should stress that the total energy in an LTV system is generally not conserved, since a switching event may impart energy to the system. Hence, here *passivity* actually refers to the fact that the net momentum, rather than the energy, cannot exceed its initial value. In this section, we formally derive the energy-momentum duality between spatial and temporal interfaces.

Across a lossless spatial interface, as shown in Figure 2(a), the conservation of power (energy) demands that the time-averaged net power flow must be conserved:

$$P_{\text{net},1} = P_{\text{net},2} \Leftrightarrow \frac{1}{Z_1} - \frac{|\Gamma|^2}{Z_1} = \frac{|T|^2}{Z_2} \quad (6)$$

where T is the spatial transmission coefficient. Yet, discontinuous charge and flux across the spatial interface implies that the linear momentum of the wave is not conserved, and the ratio of the time-averaged net momentum densities $g = \Re\{Q^*\Phi\}/2$ in the two media is:

$$\frac{g_{\text{net},2}}{g_{\text{net},1}} = \frac{k_2^2}{k_1^2}. \quad (7)$$

By contrast, across a charge- and flux-continuous temporal interface, as shown in Figure 2(b), the momentum density is conserved, while the net power flow averaged in space over a wavelength $P_{\text{net}} = \Re\{V^*I\}/2$ (more details can be found

in the supplementary material, available at <https://doi.org/10.1109/MAP.2023.3254486>) is modified by a factor:

$$\frac{P_{\text{net},f}}{P_{\text{net},i}} = \frac{\omega_f^2}{\omega_i^2}. \quad (8)$$

For the energy balance, the reader is referred to [9]. Dual to the power conservation at a spatial interface in (6), we can also write the condition for momentum conservation at a time-interface in terms of net momentum, which reads:

$$g_{\text{net},i} = g_{\text{net},f} \Leftrightarrow Z_i = Z_f |T|^2 - Z_f |R|^2. \quad (9)$$

The derivation of (6) to (9) can be found in the supplementary materials (available at <https://doi.org/10.1109/MAP.2023.3254486>). These results demonstrate the energy/

The wavenumber k in this LTV system is preserved due to translational symmetry in space, hence it must be the same before and after the temporal interface.

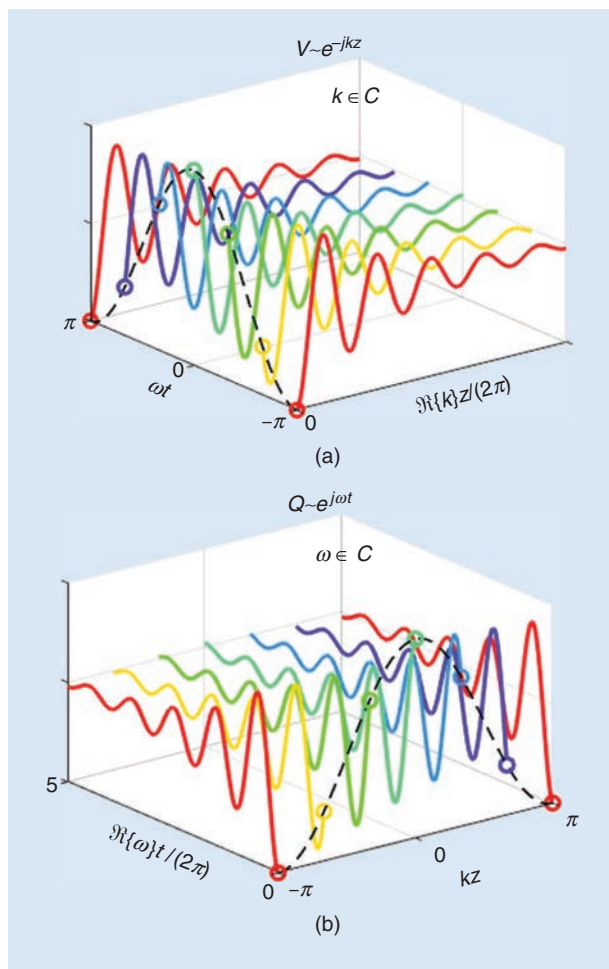


FIGURE 3. (a) Voltage waves with complex wavenumber and different temporal phases in a lossy TL within a spatial TL model. (b) Charge waves with complex frequency and different spatial phases in a lossy TL for a temporal TL model.

momentum duality associated with spatial/temporal scattering. It should also be noted that the conservation of wavenumber k at a temporal interface (dual of the conservation of ω at a spatial one) does not necessarily ensure conservation of wave momentum (energy). An evident example is that a lossy LTI system does conserve frequency but not energy. Similarly, we can impart or extract wave momentum in a space-invariant (hence k -conservative) system if it exchanges momentum with the environment while maintaining spatial transla-

tional symmetry. For instance, recently we realized a TL metamaterial with periodically loaded shunt capacitors, in which a charge-discontinuous temporal interface was realized by switching off the loads and grounding the charges in the capacitors [21]. The inclusion of such “momentum baths” can produce different forms of temporal scattering and interference compared to the more conventional examples in [1] and [10].

LOSSY TEMPORAL Tls

Loss in a nondispersive TL can be modeled by a series resistance and shunt conductance [18], corresponding to magnetic and electric conduction loss of the material, respectively. For simplicity, here we consider just the electric conductance per unit length, assuming that the loss is concentrated in the electric response of the material. In a conventional TL, if we assume a harmonic time dependence $e^{j\omega t}$, the telegrapher equations with loss can be hence written as:

$$\begin{aligned} \frac{dV}{dz} &= -j\omega LI \\ \frac{dI}{dz} &= -(G + j\omega C)V \end{aligned} \quad (10)$$

which corresponds to a complex wavenumber $k = \pm \omega \sqrt{c_r LC}$ with $c_r = 1 + G/(j\omega C)$. It is common in this TL model to assume ω to be real, which is the quantity conserved at the interface, while k is complex-valued. As an example, a voltage wave $V \sim e^{-jkz}$ propagating along the $+z$ direction is plotted in Figure 3(a), showing a decay factor in space due to loss, yet with a steady amplitude at each point in space as time varies (different curves in the figure) due to the temporal variation $e^{j\omega t}$.

In a temporal TL in the presence of loss, the telegrapher equations with spatial harmonic dependence e^{-jkz} read:

$$\begin{aligned} \frac{d\Phi}{dt} &= \frac{jk}{C} Q \\ \frac{dQ}{dt} &= \frac{jk}{L} \Phi - \frac{G}{C} Q. \end{aligned} \quad (11)$$

Here, given the dual nature of the conserved quantities, it is convenient to let the frequency ω assume complex values,

given by the dispersion relation $\omega\sqrt{c_rLC} = k$, while k is real. As shown in Figure 3(b), this implies that an incoming signal is uniform in space with dependence e^{-jkz} , but it decays in time. Because the electric and magnetic fields of a wave in lossy media are not in phase, the energy exchanges at a temporal interface can exhibit nontrivial features [22]. Consider a time-refracted wave with amplitude $T(t) \sim e^{j\omega t}$, where $\Re\{\omega\} > 0$, living in a material with complex impedance $Z = \sqrt{L/(c_rC)}$. Then, the time-reflected component $R(t) \sim e^{-j\omega^*t}$ takes negative and complex conjugated frequency and thus experiences the conjugate wave impedance Z^* . The space-averaged net power flow

$$P_{\text{net}}(t) = \frac{\Re\{c_r^{-1}\}}{\sqrt{LC}} \frac{|T|^2 - |R|^2}{2C} = \frac{\Re\{V^*I\}}{2} \quad (12)$$

is proportional to the Poynting vector averaged in space [22], while the total power flow is the sum of the flows carried by the two waves in opposite directions:

$$P_{\text{tot}}(t) = \frac{\Re\{c_r^{-1}\}}{\sqrt{LC}} \frac{|T|^2 + |R|^2}{2C}. \quad (13)$$

The space-averaged energy density consists of two parts [22]:

$$w(t) = U_t(t) + U_i(t). \quad (14)$$

The first term $U_t(t) = \Re\{1 + c_r^{-1}\}(|T|^2 + |R|^2)/(2C)$ is directly proportional to the total power flow, as expected, but the second one $U_i(t) = \Re\{T^*R(1 - c_r^{-1})\}$ arises from the interference between the counterpropagating waves, which are nonorthogonal in a lossy TL. As a result, the total power flow in the forward and backward waves after one or more time interfaces in the presence of material loss are not just determined by the energy imparted or subtracted by the switching events, but also by the energy exchanges between the waves as they interact with each other, potentially inducing highly unusual phenomena [22].

TEMPORAL NETWORK ANALYSIS

TEMPORAL SCATTERING MATRIX

To facilitate the analysis of wave scattering at temporal interfaces, especially in the presence of multiple such interfaces, it is convenient to develop a temporal network formalism in analogy with the spatial case. Figure 4(a) shows a conventional LTI two-port network in space, where the incident signals

Similarly, we can impart or extract wave momentum in a space-invariant (hence k -conservative) system if it exchanges momentum with the environment while maintaining spatial translational symmetry.

impinge from both sides ($z < z_1$ with impedance Z_1 and $z > z_2$ with impedance Z_2), and generate scattered signals in both directions. In contrast, a temporal scattering network, shown in Figure 4(b), does not allow propagation from the future ($t > t_f$ with impedance Z_f) to the past ($t < t_i$ with impedance Z_i). Once we assume a spatial harmonic dependence e^{-jkz} across the entire medium, a signal that travels backward in space can emulate incidence along the $-t$ axis by taking the negative frequency e^{-jkz} . As opposed to the nomenclature in spatial scattering networks, in temporal scattering we assign a superscript “ \pm ” to a wave propagating

along the $\pm z$ direction, while the subscripts “ i ” and “ f ” denote the (initial) incident and (final) scattered waves, respectively. For example, the backward-propagating signal (Q_i^-, Φ_i^-) in Figure 4(b), which appears to be traveling “back in time,” is generated by an incident wave propagating along $-z$, dual to (V_i^-, I_i^-) in Figure 4(a). Similarly, the signal (Q_f^-, Φ_f^-) plays the role of a temporally scattered wave rather than a spatially incident one, such as (V_2^+, I_2^+) in Figure 4(a). This different causality relation is also illustrated by the different signal flows in Figure 4: the coupling between two ports in a spatial network is bidirectional in space [Figure 4(a)], while only forward scattering in time is allowed in a temporal network [Figure 4(b)], and multiple

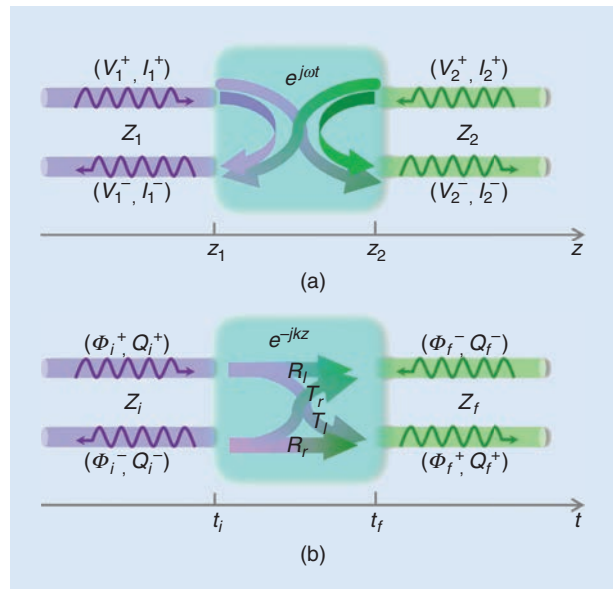


FIGURE 4. (a) A spatial two-port network. The arrows in the box illustrate the bidirectional scattering between the two ports. (b) A temporal two-port network with characteristic impedance changing from Z_i at $t = t_i$ to Z_f at $t = t_f$ uniformly in space. The temporal scattering occurs only forward in time due to causality.

scattering can only be achieved through additional switching processes.

Wave scattering by the spatial network shown in Figure 4(a) can be described by a 2×2 scattering matrix S relating $(V_1^-, V_2^-)^T = S(V_1^+, V_2^+)^T$. Analogously, we can define the temporal scattering matrix for the corresponding time-interface, shown in Figure 4(b), at which the impedance is uniformly changed from Z_i to Z_f during the time interval $t_i < t < t_f$, e.g., being switched abruptly [1], sequentially, or smoothly [19], [23]. The scattering matrix determines the amplitude and phase of the scattered waves for arbitrary excitations from the two directions. We define the temporal scattering matrix in terms of the wave amplitudes of electric charge density:

$$\begin{pmatrix} Q_f^+ \\ Q_f^- \end{pmatrix} = S \begin{pmatrix} Q_i^+ \\ Q_i^- \end{pmatrix}, \text{ where } S = \begin{pmatrix} T_l & R_r \\ R_l & T_r \end{pmatrix}, \quad (15)$$

where the subscript $l(r)$ denotes the propagation direction of the incident wave $+z(-z)$.

As a concrete example, Figure 5(a) illustrates a two-port temporal network consisting of a single temporal interface. In the left panels of Figure 5(a), we assume an incident wave of unitary charge amplitude, propagating along $+z$. The wave impedance Z_i is determined by the parameters of a lossy TL

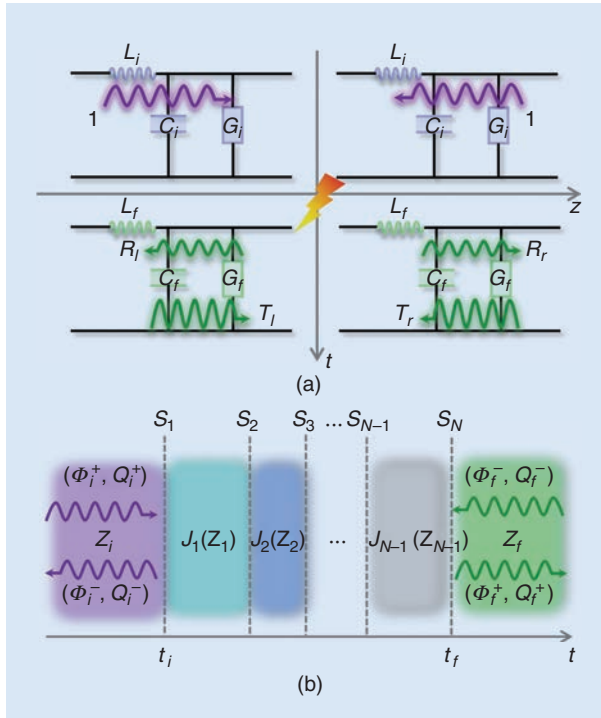


FIGURE 5. (a) A TL with initial characteristic inductance L_i , capacitance C_i and conductance G_i supports unitary (charge) waves impinging from opposite directions. After the temporal interface (lighting icon), two counterpropagating waves are generated in both cases with different amplitudes. (b) A temporal multilayer structure consisting of N temporal interfaces. The initial impedance Z_i is switched sequentially in time, through Z_1, Z_2, \dots, Z_{N-1} to its final value Z_f .

as detailed in the “Lossy Temporal TLs” section. After the time interface, with the impedance abruptly switched to its final value, temporal refraction and reflection occur. Their amplitudes T_l and R_l can be derived from the temporal boundary conditions given by (4), with the impedance in front of the reflection coefficient being conjugated in the presence of loss, yielding:

$$T_l = (Z_f^* + Z_i)/(2\Re\{Z_f\}), \quad R_l = (Z_f - Z_i)/(2\Re\{Z_f\}). \quad (16)$$

On the other hand, when the incident wave travels from the right and sees impedance Z_i^* , as shown in the right panels in Figure 5(a), the temporal scattering coefficients become:

$$T_r = \frac{Z_f + Z_i^*}{2\Re\{Z_f\}}, \quad R_r = \frac{Z_f^* - Z_i^*}{2\Re\{Z_f\}}. \quad (17)$$

The temporal scattering matrix for the network shown in Figure 5(a) can then be explicitly written as:

$$S = \frac{1}{2\Re\{Z_f\}} \begin{pmatrix} Z_f^* + Z_i & Z_f^* - Z_i^* \\ Z_f - Z_i & Z_f + Z_i^* \end{pmatrix}. \quad (18)$$

Another example that has been recently studied is the one of a temporal multilayer structure, in which the impedance of the entire medium is switched sequentially in time, forming the building block of time-metamaterials and photonic time crystals [24], [25], [26]. A temporally layered medium is depicted in Figure 5(b), consisting of N time interfaces characterized by temporal scattering matrices S_m with $m = 1, 2, \dots, N$. During each layer of impedance Z_m , the wave propagation can be described by a scattering matrix $J_m = \text{diag}(e^{j\omega_m \tau_m}, e^{-j\omega_m \tau_m})$, where ω_m is the complex frequency and τ_m is the duration of each layer. Since the incident and scattered signals are separated on the two sides of (15), the scattering matrix also behaves as the transfer matrix defined for the amplitudes of counterpropagating waves, which implies that the total scattering matrix of this cascaded temporal network equals the chain-product of the individual scattering matrices:

$$S_{\text{tot}} = S_N \prod_{m=1}^{N-1} J_{N-m} S_{N-m}. \quad (19)$$

With the matrix formalism of temporal scattering, we are now ready to study the general constraints on temporal scattering, such as reciprocity and momentum conservation.

RECIPROCAL TIME NETWORKS

Lorentz reciprocity [27] in the Rayleigh–Carson form implies that the electric field induced at a receiver located at a certain point in space and created by a current source at another location are the same when we interchange the positions of source and receiver (see [28, Chapter 1.10]). Breaking reciprocity can be achieved using a dc magnetic bias in magneto-optical materials [29], [30], and more recently it has been explored

using asymmetric nonlinearities [31], [32], [33] and space-time modulation [34], [35], [36]. In a reciprocal LTI system, the spatial scattering matrix is symmetric: $S(\omega)^T = S(\omega)$. In the presence of temporal interfaces, however, causality implies different properties for the temporal scattering matrix. If the involved phenomena are reciprocal, Lorentz reciprocity implies that an arbitrary temporal interface scatters a wave incident from one direction in the same manner as an opposite traveling wave. Mathematically, we can conclude from (16) and (17) that $T_l = T_r$ and $R_l = R_r^*$ for a reciprocal temporal interface, or expressed compactly in terms of the temporal S matrix:

$$\sigma_x S^* = S \sigma_x \quad (20)$$

where $\sigma_x = (0, 1; 1, 0)$ is the first Pauli matrix that interchanges the rows (columns) of its succeeding (preceding) matrix; (20) also applies to the cascaded matrices of temporal multilayers, as shown in Figure 5(b). To prove this, we first verify that $\sigma_x J_m^* = J_m \sigma_x$ and $\sigma_x S_m^* = S_m \sigma_x$ if all the layers are reciprocal. Then, by inserting the involutory Pauli matrix $\sigma_x = \sigma_x^{-1}$, we obtain:

$$\begin{aligned} \sigma_x S_{\text{tot}}^* &= (\sigma_x S_N^*) \sigma_x (\sigma_x J_{N-1}^*) \sigma_x \cdots (\sigma_x J_1^*) \sigma_x (\sigma_x S_1^*) \\ &= [(S_N \sigma_x) \sigma_x (J_{N-1} \sigma_x) \sigma_x \cdots (J_1 \sigma_x) \sigma_x S_1] \sigma_x. \\ &= S_{\text{tot}} \sigma_x \end{aligned} \quad (21)$$

[37] considered more complex scenarios involving anisotropic and nonreciprocal media.

MOMENTUM-CONSERVING NETWORKS

As discussed in the “Energy and Momentum Duality” section, the linear momentum of an EM wave upon temporal scattering in a uniform medium is dual to the energy in a time-invariant spatial scattering scenario. Considering two counterpropagating waves ($\Phi_{i,f}^\pm, Q_{i,f}^\pm$) as in the temporal scattering network shown in Figure 4(b), the net momentum density of the waves is (more details can be found in the supplementary material, available at <https://doi.org/10.1109/MAP.2023.3254486>):

$$g_{i,f} = \Re\{Z_{i,f}\}(|Q_{i,f}^+|^2 - |Q_{i,f}^-|^2). \quad (22)$$

If there is no external shock current or voltage that alters the total charge or flux in the system, then the net momentum is conserved during the temporal scattering, i.e., $g_i = g_f$. Substituting the temporal scattering matrix given by (15), we find:

$$a|Q_i^+|^2 - b|Q_i^-|^2 + 2\Re\{cQ_i^+(Q_i^-)^*\} = 0 \quad (23)$$

where $a = |S_{11}|^2 - |S_{21}|^2 - \Re\{Z_i\}/\Re\{Z_f\}$, $b = |S_{22}|^2 - |S_{12}|^2 - \Re\{Z_i\}/\Re\{Z_f\}$, and $c = S_{11}S_{12}^* - S_{22}^*S_{21}$. For arbitrary incident waves Q_i^\pm , (23) must hold. Thus, all three coefficients should vanish. In particular, the relation $a = b = 0$ is dual to the power (energy) conservation condition ubiquitous in spatial scattering, which reads $|S_{11}|^2 + |S_{21}|^2 = |S_{22}|^2 + |S_{12}|^2 = 1$. The “–” sign in a, b stems from the vectorial nature of momentum, and the impedance ratio is due to our definition of the

temporal scattering matrix in terms of electric charge density, which requires renormalization when converting the wave amplitude to its momentum. In analogy with $S^\dagger S = \mathbf{1}$ (identity matrix) for energy conservation in the spatial case, we express the condition $a = b = c = 0$ in matrix form as:

$$\Re\{Z_f\}(\sigma_z S)^\dagger(\sigma_z S) = \Re\{Z_i\} \mathbf{1} \quad (24)$$

where \dagger denotes conjugate transpose and $\sigma_z = (1, 0; 0, -1)$ is the third Pauli matrix. We have hence obtained a constraint for the scattering matrix consistent with a momentum-conserving temporal network. If the system is also lossless (with real-valued impedances) and reciprocal ($S_{11} = S_{22}^*$, $S_{21} = S_{12}^*$), then (24) simplifies to (9) derived from the temporal boundary conditions.

CONCLUSIONS

In summary, we have discussed wave scattering at temporal interfaces from a microwave engineering perspective. Starting from the dual form of the telegraphers’ equations in the presence of time-varying constitutive parameters, we have showcased several space-time dualities, including those between frequency and wavenumber, energy and momentum, and the reflection coefficients associated with spatial and temporal boundaries. We then introduced the temporal scattering matrix formalism, which exhibits dual symmetries to the spatial case, as well as distinct properties stemming from causality. The scattering framework presented in this article can serve as a tool to shed light on more sophisticated temporal scattering processes [38], [39], [40]. We believe that this tool can provide fertile ground for both wave physics and EM engineering. For instance, wave interference in a lossy temporal TL can enhance the field of non-Hermitian physics [22]. From the engineering standpoint, temporal scattering can join forces with space-time and Floquet metamaterials [41], [42] to enhance the growing field of reconfigurable intelligent surfaces [43], implying exciting opportunities for antennas and propagation applications, such as broadband frequency translation [21] and signal amplification.

ACKNOWLEDGMENT

This work was supported by the Air Force Office of Scientific Research and the Simons Foundation. E.G. acknowledges funding from the Simons Foundation through a Junior Fellowship of the Simons Society of Fellows (855344). More details regarding mathematical details and derivations of a few equations in the main text, including the averaging of energy and momentum density, power and momentum balance, and the net momentum in a lossy, can be found in the supplementary material (available at <https://doi.org/10.1109/MAP.2023.3254486>).



AUTHOR INFORMATION

Shixiong Yin (syin000@citymail.cuny.edu) is a Ph.D. student in the Department of Electrical Engineering, City College of The City University of New York, New York, NY 10031, USA.

Emanuele Galiffi (egaliffi@gc.cuny.edu) is a postdoctoral research fellow with the Photonics Initiative, the Advanced Science Research Center at The City University of New York, New York, NY 10031, USA.

Gengyu Xu (gxy@gc.cuny.edu) is a postdoctoral researcher with the Photonics Initiative, the Advanced Science Research Center at The City University of New York, New York, NY 10031, USA.

Andrea Alù (aalu@gc.cuny.edu) is a distinguished professor at the City University of New York (CUNY), the Founding Director of the Photonics Initiative, the CUNY Advanced Science Research Center, and the Einstein professor of physics at the CUNY Graduate Center, New York, NY 10016, USA; and a professor of Electrical Engineering at the City College of New York, New York, NY 10031, USA.

REFERENCES

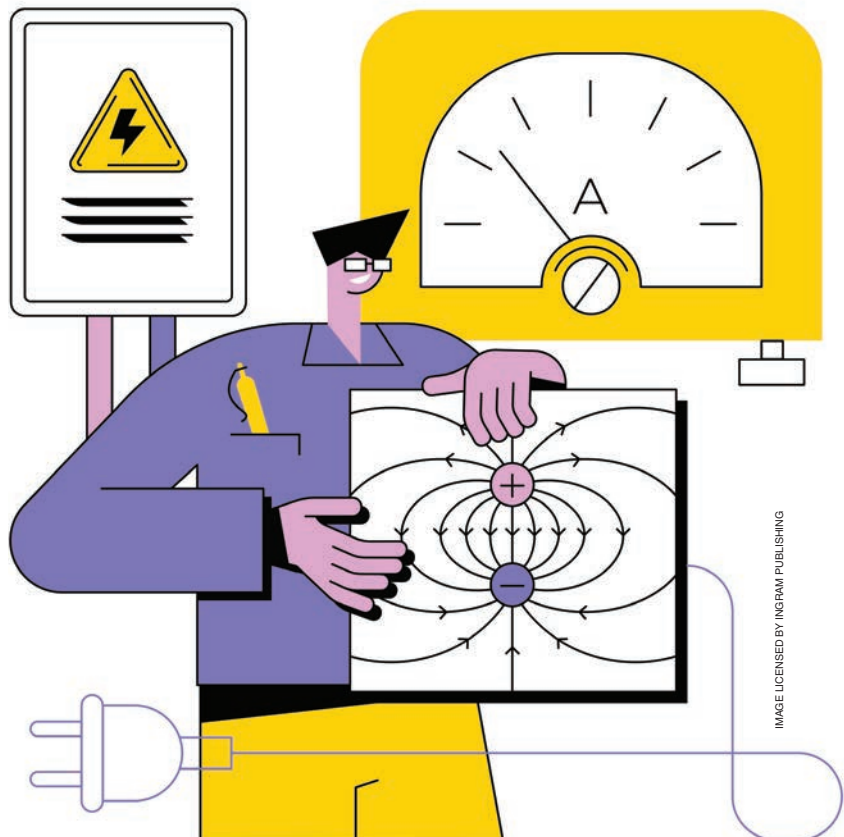
- [1] F. R. Morgenthaler, "Velocity modulation of electromagnetic waves," *IRE Trans. Microw. Theory Techn.*, vol. 6, no. 2, pp. 167–172, Apr. 1958, doi: 10.1109/TMTT.1958.1124533.
- [2] B. A. Auld, J. H. Collins, and H. R. Zapp, "Signal processing in a nonperiodically time-varying magnetoelastic medium," *Proc. IEEE*, vol. 56, no. 3, pp. 258–272, Mar. 1968, doi: 10.1109/PROC.1968.6270.
- [3] D. K. Kalluri, *Electromagnetics of Time Varying Complex Media: Frequency and Polarization Transformer*. Boca Raton, FL, USA: CRC Press, 2010.
- [4] B. W. Plasiniis, W. R. Donaldson, and G. P. Agrawal, "What is the temporal analog of reflection and refraction of optical beams?" *Phys. Rev. Lett.*, vol. 115, no. 18, Oct. 2015, Art. no. 183901, doi: 10.1103/PhysRevLett.115.183901.
- [5] V. Bacot, M. Labousse, A. Eddi, M. Fink, and E. Fort, "Time reversal and holography with spacetime transformations," *Nature Phys.*, vol. 12, no. 10, pp. 972–977, Oct. 2016, doi: 10.1038/nphys3810.
- [6] J. T. Mendonça, *Theory of Photon Acceleration Series in Plasma Physics*. Bristol, U.K.: IOP Publishing, 2001.
- [7] J. T. Mendonça, A. M. Martins, and A. Guerreiro, "Temporal beam splitter and temporal interference," *Phys. Rev. A*, vol. 68, no. 4, Oct. 2003, Art. no. 043801, doi: 10.1103/PhysRevA.68.043801.
- [8] Akbarzadeh, N. Chamanara, and C. Caloz, "Inverse prism based on temporal discontinuity and spatial dispersion," *Opt. Lett.*, vol. 43, no. 14, 2018, Art. no. 3297, doi: 10.1364/ol.43.00.
- [9] A. Shlivinski and Y. Hadad, "Beyond the Bode-Fano bound: Wideband impedance matching for short pulses using temporal switching of transmission-line parameters," *Phys. Rev. Lett.*, vol. 121, no. 20, Nov. 2018, Art. no. 204301, doi: 10.1103/PhysRevLett.121.204301.
- [10] V. Pacheco-Peña and N. Engheta, "Antireflection temporal coatings," *Optica*, vol. 7, no. 4, pp. 323–331, Apr. 2020, doi: 10.1364/optica.381175.
- [11] H. Li and A. Alù, "Temporal switching to extend the bandwidth of thin absorbers," *Optica*, vol. 8, no. 1, pp. 24–29, Jan. 2021, doi: 10.1364/optica.408399.
- [12] C. Firestein, A. Shlivinski, and Y. Hadad, "Absorption and scattering by a temporally switched lossy layer: going beyond the Rozanov bound," *Phys. Rev. Appl.*, vol. 17, no. 1, Jan. 2022, Art. no. 014017, doi: 10.1103/PhysRevApplied.17.014017.
- [13] X. Yang, E. Wen, and D. F. Sievenpiper, "Broadband time-modulated absorber beyond the Bode-Fano limit for short pulses by energy trapping," *Phys. Rev. Appl.*, vol. 17, no. 4, Apr. 2022, Art. no. 044003, doi: 10.1103/PhysRevApplied.17.044003.
- [14] Z. Hayran and F. Monticone, "Capturing broadband light in a compact bound state in the continuum," *ACS Photon.*, vol. 8, no. 3, pp. 813–823, Mar. 2021, doi: 10.1021/acspophotonics.0c01696.
- [15] V. Pacheco-Peña and N. Engheta, "Temporal aiming," *Light Sci. Appl.*, vol. 9, no. 1, pp. 1–12, Jul. 2020, doi: 10.1038/s41377-020-00360-1.
- [16] S. Yin and A. Alù, "Efficient phase conjugation in a space-time leaky waveguide," *ACS Photon.*, vol. 9, no. 3, pp. 979–984, Feb. 2022, doi: 10.1021/acspophotonics.1c01836.
- [17] E. Galiffi et al., "Photonics of time-varying media," *Adv. Photon.*, vol. 4, no. 1, Feb. 2022, Art. 014002, doi: 10.1117/1.AP4.1.014002.
- [18] D. M. Pozar, *Microwave Engineering*, 4th ed. Hoboken, NJ, USA: Wiley, 2011.
- [19] E. Galiffi, S. Yin, and A. Alù, "Tapered photonic switching," *Nanophotonics*, vol. 11, no. 16, pp. 3575–3581, Sep. 2022, doi: 10.1515/nanoph-2022-0200.
- [20] R. W. Klopfenstein, "A transmission line taper of improved design," *Proc. IRE*, vol. 44, no. 1, pp. 31–35, Jan. 1956, doi: 10.1109/JRPROC.1956.274847.
- [21] H. Moussa, G. Xu, S. Yin, E. Galiffi, Y. Radi, and A. Alù, "Observation of temporal reflections and broadband frequency translations at photonic time-interfaces," *Nat. Phys.*, Mar. 2023, doi: 10.1038/s41567-023-01975-y.
- [22] H. Li, S. Yin, E. Galiffi, and A. Alù, "Temporal parity-time symmetry for extreme energy transformations," *Phys. Rev. Lett.*, vol. 127, no. 15, Oct. 2021, Art. no. 153903, doi: 10.1103/physrevlett.127.153903.
- [23] Y. Hadad and A. Shlivinski, "Soft temporal switching of transmission line parameters: wave-field, energy balance, and applications," *IEEE Trans. Antennas Propag.*, vol. 68, no. 3, pp. 1643–1654, Mar. 2020, doi: 10.1109/TAP.2020.2967302.
- [24] E. Lustig, M. Segev, and Y. Sharabi, "Topological aspects of photonic time crystals," *Optica*, vol. 5, no. 11, pp. 1390–1395, Nov. 2018, doi: 10.1364/OPTICA.5.001390.
- [25] Y. Sharabi, E. Lustig, and M. Segev, "Disordered photonic time crystals," *Phys. Rev. Lett.*, vol. 126, no. 16, Mar. 2021, Art. no. 163902, doi: 10.1103/PhysRevLett.126.163902.
- [26] G. Castaldi, M. Moccia, N. Engheta, and V. Galdi, "Herpin equivalence in temporal metamaterials," *Nanophotonics*, vol. 11, no. 20, pp. 4479–4488, Sep. 2022, doi: 10.1515/nanoph-2022-0338.
- [27] H. A. Lorentz, "The theorem of Poynting concerning the energy in the electromagnetic field and two general propositions concerning the propagation of light," *Amsterdammer Akad. Wet.*, vol. 4, 1896, Art. no. 176.
- [28] R. E. Collin, *Field Theory of Guided Waves*. New York, NY, USA: Wiley, 1990.
- [29] G. Buchta, "Magnetically scanned reciprocal and nonreciprocal leaky-wave antennas," *Proc. IEEE*, vol. 52, no. 5, pp. 625–626, May 1964, doi: 10.1109/PROC.1964.3023.
- [30] L. Sounas and C. Caloz, "Gyrotropy and nonreciprocity of graphene for microwave applications," *IEEE Trans. Microw. Theory Techn.*, vol. 60, no. 4, pp. 901–914, Apr. 2012, doi: 10.1109/TMTT.2011.2182205.
- [31] L. Sounas, J. Soric, and A. Alù, "Broadband passive isolators based on coupled nonlinear resonances," *Nature Electron.*, vol. 1, no. 2, pp. 113–119, Feb. 2018, doi: 10.1038/s41928-018-0025-0.
- [32] M. Cotrufo, S. A. Mann, H. Moussa, and A. Alù, "Nonlinearity-induced nonreciprocity—Part I," *IEEE Trans. Microw. Theory Techn.*, vol. 69, no. 8, pp. 3569–3583, Aug. 2021, doi: 10.1109/TMTT.2021.3079250.
- [33] N. Bender et al., "Observation of asymmetric transport in structures with active nonlinearities," *Phys. Rev. Lett.*, vol. 110, no. 23, Jun. 2013, Art. no. 234101, doi: 10.1103/PhysRevLett.110.234101.
- [34] L. Sounas, T. Kodera, and C. Caloz, "Electromagnetic modeling of a magnetless nonreciprocal gyrotropic metasurface," *IEEE Trans. Antennas Propag.*, vol. 61, no. 1, pp. 221–231, Jan. 2013, doi: 10.1109/TAP.2012.2214997.
- [35] D. Ramaccia, D. L. Sounas, A. Alù, F. Biliotti, and A. Toscano, "Nonreciprocal horn antennas using angular momentum-biased metamaterial inclusions," *IEEE Trans. Antennas Propag.*, vol. 63, no. 12, pp. 5593–5600, Dec. 2015, doi: 10.1109/TAP.2015.2496105.
- [36] S. Taravati and C. Caloz, "Mixer-duplexer-antenna leaky-wave system based on periodic space-time modulation," *IEEE Trans. Antennas Propag.*, vol. 65, no. 2, pp. 442–452, Feb. 2017, doi: 10.1109/TAP.2016.2632735.
- [37] H. Li, S. Yin, and A. Alù, "Nonreciprocity and faraday rotation at time interfaces," *Phys. Rev. Lett.*, vol. 128, no. 17, Apr. 2022, Art. no. 173901, doi: 10.1103/PhysRevLett.128.173901.
- [38] D. M. Solis, R. Kastner, and N. Engheta, "Time-varying materials in the presence of dispersion: Plane-wave propagation in a Lorentzian medium with temporal discontinuity," *Photon. Res.*, vol. 9, no. 9, Sep. 2021, Art. no. 1842, doi: 10.1364/prj.427368.
- [39] E. Galiffi, P. A. Huidobro, and J. B. Pendry, "An Archimedes' screw for light," *Nature Commun.*, vol. 13, no. 1, May 2022, Art. no. 2523, doi: 10.1038/s41467-022-30079-z.
- [40] E. Galiffi, Y. T. Wang, Z. Lim, J. B. Pendry, A. Alù, and P. A. Huidobro, "Wood anomalies and surface-wave excitation with a time grating," *Phys. Rev. Lett.*, vol. 125, no. 12, Sep. 2020, Art. no. 127403, doi: 10.1103/PhysRevLett.125.127403.
- [41] C. Caloz and Z.-L. Deck-Leger, "Spacetime metamaterials—Part II: Theory and applications," *IEEE Trans. Antennas Propag.*, vol. 68, no. 3, pp. 1583–1598, Mar. 2020, doi: 10.1109/TAP.2019.2944216.
- [42] S. Yin, E. Galiffi, and A. Alù, "Floquet metamaterials," *eLight*, vol. 2, no. 1, Dec. 2022, Art. no. 8, doi: 10.1186/s43593-022-00015-1.
- [43] Q. Ma, Q. Xiao, Q. R. Hong, X. Gao, V. Galdi, and T. J. Cui, "Digital coding metasurfaces: From theory to applications," *IEEE Antennas Propag. Mag.*, vol. 64, no. 4, pp. 96–109, Aug. 2022, doi: 10.1109/MAP.2022.3169397.



Using Time-Varying Systems to Challenge Fundamental Limitations in Electromagnetics

Overview and summary of applications.

Time-varying systems open intriguing opportunities to explore novel approaches in the design of efficient electromagnetic devices. While such explorations date back to more than half a century ago, recent years have experienced a renewed and increased interest into the design of dynamic electromagnetic systems. This resurgence has been partly fueled by the desire to surpass the performance of conventional devices, and to enable systems that can challenge various well-established performance bounds, such as the Bode–Fano limit, the Chu limit, and others. Here, we give an overview of this emerging research area and provide a concise and systematic summary of the most relevant applications for which the relevant performance bounds can be overcome through time-varying elements. In addition to enabling devices with superior performance metrics,



such research endeavors may open entirely new opportunities and offer insight towards future electromagnetic and optical technologies.

INTRODUCTION

The study of electromagnetic wave interactions with time-varying media dates back to more than half a century ago, when several pioneering works [1], [2], [3], [4], [5], [6], [7], [8], [9], [10] revealed the rich physics arising in such systems. Although in the following decades several other works have further explored the implications of wave propagation in dynamic media [11], [12], [13], [14], it was not until recently that the field gained considerable momentum [15], partly owing to the improved fabrication and characterization techniques in various frequency regimes [16], [17], [18]. Consequently, it was soon discovered that time-dependent systems can enable many interesting and novel phenomena, such as interband photonic transitions [19], [20], nonreciprocal systems [21], [22], efficient frequency conversion [23], [24], [25], [26], temporal aiming [27], Fresnel drag [28], negative extinction [29], entangled photon generation [30], [31], parametric oscillations [32], synthetic dimensions [33], topological phase transitions [34], and nonreciprocal gain [35], among others [36]. Several recent publications also further investigated the fundamental aspects of wave propagation in time-varying media, such as [37], [38], [39], [40], [41], [42], thus providing a better understanding of the physical implications of these systems.

Apart from enabling novel effects, time-varying materials and components may also be used to improve a given device to achieve better performance in terms of operational bandwidth, size, efficiency of the relevant process, and other metrics [36]. In some cases, such improvements may even exceed what is normally allowed by well-established performance bounds, as physical bounds and fundamental limits in electromagnetics are typically derived under the assumption of linearity and time invariance (LTI systems). Indeed, as mentioned above, time variance in the system properties may enable various functionalities not present in a conventional setting, such as parametric gain [35] or spectral changes [19], [23], [24], [25], [26], [43], which are not accounted for when deriving bounds for LTI systems, and can therefore be exploited to bypass such physical limits. Consequently, time-varying materials and components provide exceptional opportunities to realize superior devices not restricted by various conventional limits.

APPLICATIONS

In this section we provide a concise overview of the most relevant applications of time-varying designs to overcome various physical bounds of conventional LTI electromagnetic systems. In this regard, this section is divided into various subsections, each of which focuses on a specific application or research topic, with the goal to systematically guide the reader through this

It was soon discovered that time-dependent systems can enable many interesting and novel phenomena.

emerging research area. We will not discuss some major research directions that also seek to overcome various constraints of conventional systems and broaden their functionality, such as the possibility to break reciprocity [21], [22] or create synthetic dimensions [33] based on time modulation, since these topics are already covered in detail in the literature. Instead, we

will focus on certain topics of particular interest to the IEEE Antennas and Propagation community, including how time-varying systems impact the fundamental limitations of antennas [44], broadband impedance-matching networks [45], and radar absorbers [46].

IMPEDANCE MATCHING

Efficient power transfer from a source to a load with minimal reflections is arguably one of the most important tasks in electromagnetic engineering. Thus, when designing impedance-matching networks to minimize reflections, it becomes essential to identify the limitations and the optimal configurations of the system. In this regard, a matching-bandwidth limit was introduced for linear, time-invariant, passive systems by Bode in 1945 [47], which was later generalized by Fano for arbitrary load impedances [45]. The resulting Bode–Fano limit provides a theoretical upper bound on the bandwidth over which a certain reflection reduction can be attained, independent of the complexity of the employed matching network (only assumed to be LTI, passive, and reactive), and it is therefore a very powerful tool to assess the maximum possible bandwidth of various electromagnetic systems, such as antennas [48] or optical invisibility cloaks [49]. To overcome this limitation, one strategy that has been explored in the literature is to break the underlying assumption of passivity. Indeed, several proposals utilizing active “non-Foster” elements have shown that the bandwidth of small antennas [50] and cloaking devices [51], [52], [53], [54] can be extended beyond what would be possible with a passive system. However, active elements typically increase the noise level of the system [55] and can lead to instabilities (unbounded oscillations in time) [54], [56], [57], thereby disrupting the desired functionality.

An alternative option to go beyond the Bode–Fano limit is to break the assumption of time invariance, i.e., allow temporal variation in the system properties. In this context, [58] employed time-varying matching networks to achieve a better bandwidth performance compared to their time-invariant counterparts by exploiting information about the incident signal. More recently, [59] provided another interesting method, which involves switching the system parameters while a broadband signal (a pulse) is within the matching network and before it reaches the load, as shown in Figure 1(a) and (b). The temporal switching would generally lead to reflected waves due to the temporal discontinuity (temporal interface) [60]; however, it was shown that the matching efficiency (defined

as the ratio between the power dissipated on the load and the maximal available power from the source plus the total power provided by the modulation) can still be maximized over a broad bandwidth by optimizing several parameters, including the characteristic impedance of the matching transmission line and the phase velocity of the pulse within the matching line before and after the switching event [59]. Since temporal switching increases the number of free parameters that can be tuned compared to the time-invariant case, one may achieve performance metrics that are otherwise out of reach in a conventional time-invariant setting, especially for large load-source impedance contrast values [see Figure 1(c)] [59]. This proposal was further extended from “hard” (abrupt) to “soft” temporal switching in [61], which could be more feasible to implement in practice. An adverse byproduct of the temporal switching operation is the spectral compression or broadening of the pulse, which necessitates the use of additional analog or digital devices to restore the original pulse spectrum, and thus may complicate the overall matching system. Moreover, this method is feasible only for short time signals (as quasi-monochromatic signals would require impractically long matching lines), and requires knowledge that the pulse is present within the time-switched matching line (which implies the presence of some fast detection mechanism able to trigger the switching event). Even with these limitations, this approach shows a realistic path toward broadband matching networks beyond the Bode–Fano constraints.

For the quasi-monochromatic regime, on the other hand, a transmission-line system where the load impedance itself is varied in time has been used to impedance-match a time-harmonic source to a purely reactive load and to accumulate and release energy on demand [see Figure 1(d)–(g)] [62]. Specifically, it was shown that, while a time-invariant reactive load would fully reflect an incident wave, a time-modulated reactance can emulate a resistance and can, therefore, act as a “virtual” absorber [62]. An intuitive explanation of this effect is that

temporally modulating the reactance with a suitable tangent function is equivalent to a short-circuited transmission line with the shorted end moving away from the source with the same velocity as the phase velocity of the incident signal [62].

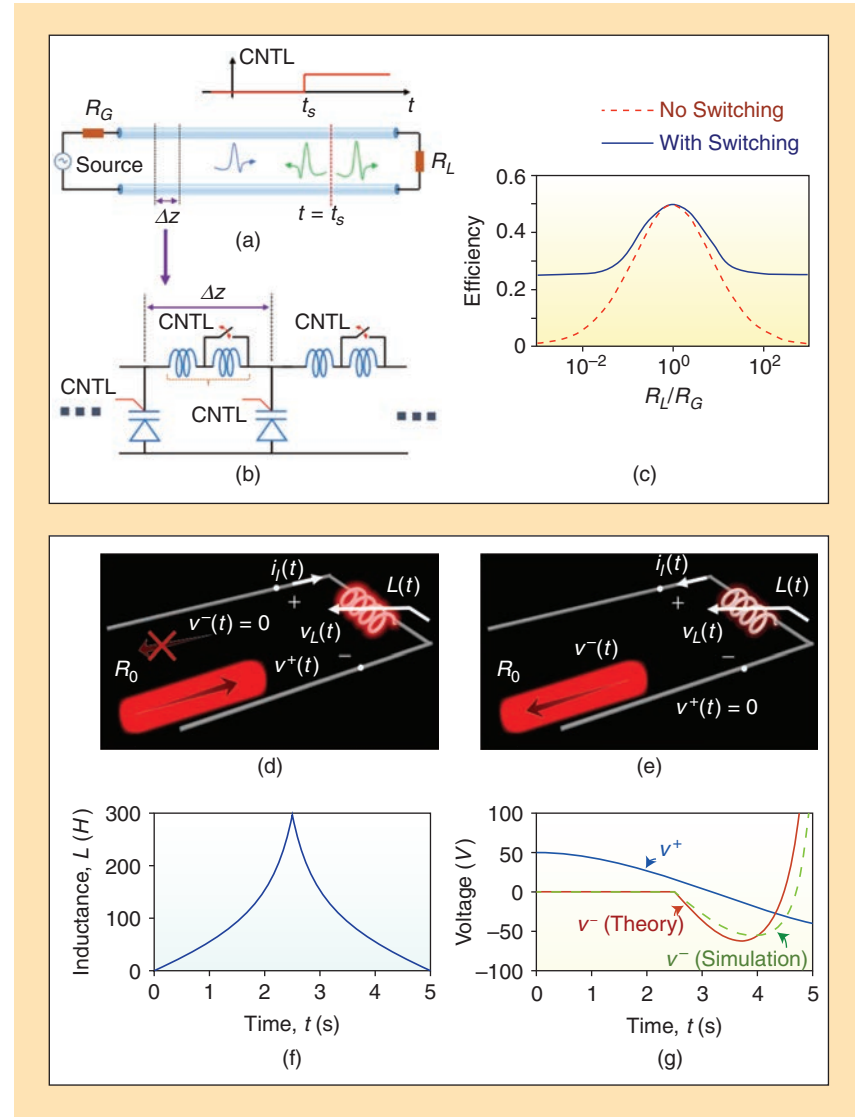


FIGURE 1. (a) A temporally switched transmission line can be employed to match a source impedance R_G to a load impedance R_L surpassing the Bode–Fano limit. (b) Such a switched matching line can be realized with parallel varactor diodes and banks of series inductors, whose properties are changed abruptly in time at $t = t_s$. (c) The maximum transmission efficiency for various R_L/R_G values shows that the temporally switched case (solid blue) provides better performance compared to the nonswitched time-invariant case (dashed red line), especially for large source-load impedance contrast values. (d) and (e) A transmission line terminated with a time-varying inductance $L(t)$. (d) Using a suitable time modulation, the inductor can accumulate energy without any reflections. (e) By time-reversing the temporal modulation in (d), the energy trapped by the inductor can be released. (f) Time-modulation profile of the inductance, comprising both the trapping (before $t = 2.5$ s) and releasing regimes (after $t = 2.5$ s). (g) Temporal variation of the incident signal V^+ and the reflected signal V^- at the load position (obtained theoretically and through simulations) for a load inductance temporally modulated as in (f). CNTL: control. Panels (a)–(c) are reproduced with permission from [59], American Physical Society. Panels (d)–(g) are reproduced with permission from [62], American Physical Society.

Therefore, the incident wave does not reflect back since it never appears to “reach” the reflecting termination. Consequently, energy from a time-harmonic source can be trapped with no reflections and released on demand [see Figure 1(f) and (g)].

Along similar lines, another interesting application of temporal modulation in the context of impedance matching is related to the problem of capturing and trapping an incident electromagnetic wave into a lossless resonant cavity, with no reflections. This can be achieved by temporally modulating the radiation leakage from the cavity, such that it perfectly cancels the direct reflection from the cavity at all time instants [63]. In this regard, we have also shown that by temporally modulating the shell of a compact core-shell scatterer (acting as an open cavity supporting a nonradiating mode), an incident broadband pulse can be captured within the cavity with no reflection, effectively forcing a broadband signal into a narrowband resonator with ideal efficiency (this may also be interpreted as spectrum compression through temporal modulation with the additional constraint of zero reflections) [64]. Further details can be found in the supplementary material, available at <https://doi.org/10.1109/MAP.2023.3236275>.

ANTENNA PERFORMANCE ENHANCEMENT

Antenna miniaturization is another major research area within the applied electromagnetics community with many potential benefits for various applications, such as communication systems, sensor networks, implanted medical devices, and navigation systems. While it is generally possible to reduce the size of an antenna down to subwavelength dimensions for a given design frequency, this typically comes at the price of reduced bandwidth, directivity, and radiation efficiency. In this regard, the fundamental tradeoffs between size and bandwidth for electrically small antennas were investigated more than half a century ago in several seminal papers by Wheeler [65], Chu [66], and later by Harrington [67], resulting in, as it is known today, *the Chu–Harrington limit* [68]. The limit as derived by Chu is based on an equivalent circuit model for the radial wave impedance of the lowest-order spherical wave generated by a generic LTI lossless antenna enclosed within a spherical volume. This equivalent circuit becomes more reactive as the size of the spherical volume is reduced, leading to a higher Q factor (consistent with the fact that, for example, a short wire dipole has a strongly reactive input impedance). Then, as recognized by Chu, while the inverse of the Q factor may be interpreted as the fractional bandwidth of the antenna at a single resonance, a more accurate definition is in terms of the tolerable reflection coefficient over the operating band using a suitable matching network, and therefore the antenna bandwidth is limited by the Bode–Fano

Consequently, time-varying materials and components provide exceptional opportunities to realize superior devices not restricted by various conventional limits.

limit (see “Impedance Matching” section, above) [69] applied to Chu’s equivalent circuit. In other words, these results define a tradeoff between antenna bandwidth and realized gain (gain taking into account the efficiency associated with reflection losses), and quantify how the product between bandwidth and realized gain is decreased by miniaturization. These analyses were later refined by other researchers (e.g., [44], [70], [71], [72]), further underscoring the fact that for a linear time-invariant passive electrically small antenna one cannot simultaneously minimize size and maximize bandwidth and efficiency.

Following Chu’s work [66], antenna engineers realized early the need for active (i.e., nonpassive) designs, nonlinear materials, or time-varying components to increase the bandwidth of wireless systems based on electrically small antennas. In this context, for example, nonlinear ferrite materials were exploited to realize time-varying inductors, which were used to overcome the limitations of small antennas in very low frequency transmitters by shifting the carrier frequency [73]. Subsequent works (see, for instance, [74], [75], [76], [77], [78]) further demonstrated the unique opportunities enabled by time-varying “switched” elements to design antennas with improved bandwidth characteristics.

More recently, with the renewed surge of interest in temporal modulation in electromagnetic systems, research into electrically small time-varying antennas has been reinvigorated. For example, [79] confirmed that the antenna bandwidth can be increased significantly through impedance modulation. Another more recent work employed “Floquet” impedance matching [80] [Figure 2(a)–(c)] to overcome the Chu–Harrington limit by imparting parametric gain into the system [32] through a periodic modulation of the matching network components at twice the frequency of the antenna resonant frequency. A realistic simulation of the proposed design was also demonstrated based on a small loop antenna [Figure 2(b)] that includes periodically modulated variable capacitors (varactors). Through numerical calculations [Figure 2(c)], it was shown that the bandwidth-efficiency product can be significantly enhanced owing to the temporal modulation compared to the time-invariant case, and can even surpass the predictions of the Bode–Fano limit applied to the Chu–Harrington equivalent circuit, which is a rather remarkable result given the fact that parametric phenomena are typically narrowband.

A possible drawback of schemes of this type is that the parametric gain may potentially lead to instabilities. However, unlike antenna systems based on active non-Foster elements [81], [82], [83], the dispersion of the parametric gain can be more easily controlled through the modulation properties to bring the system into the stable regime. Moreover, it was also pointed out

that deliberately inducing an impedance mismatch by modifying the source impedance can act as negative feedback to help ensure stability and increase the operational bandwidth at the same time [80]. Indeed, a stable parametric enhancement effect was later experimentally demonstrated in [84] in a fabricated

time-varying loop antenna operating at radio frequencies. In this context, other recent studies also investigated the use of time-varying parametric amplifiers with the aim of broadening the bandwidth of electrically small antennas [85], [86] [Figure 2(d) and (e)]. Similar to [80] and [84], this was achieved by first

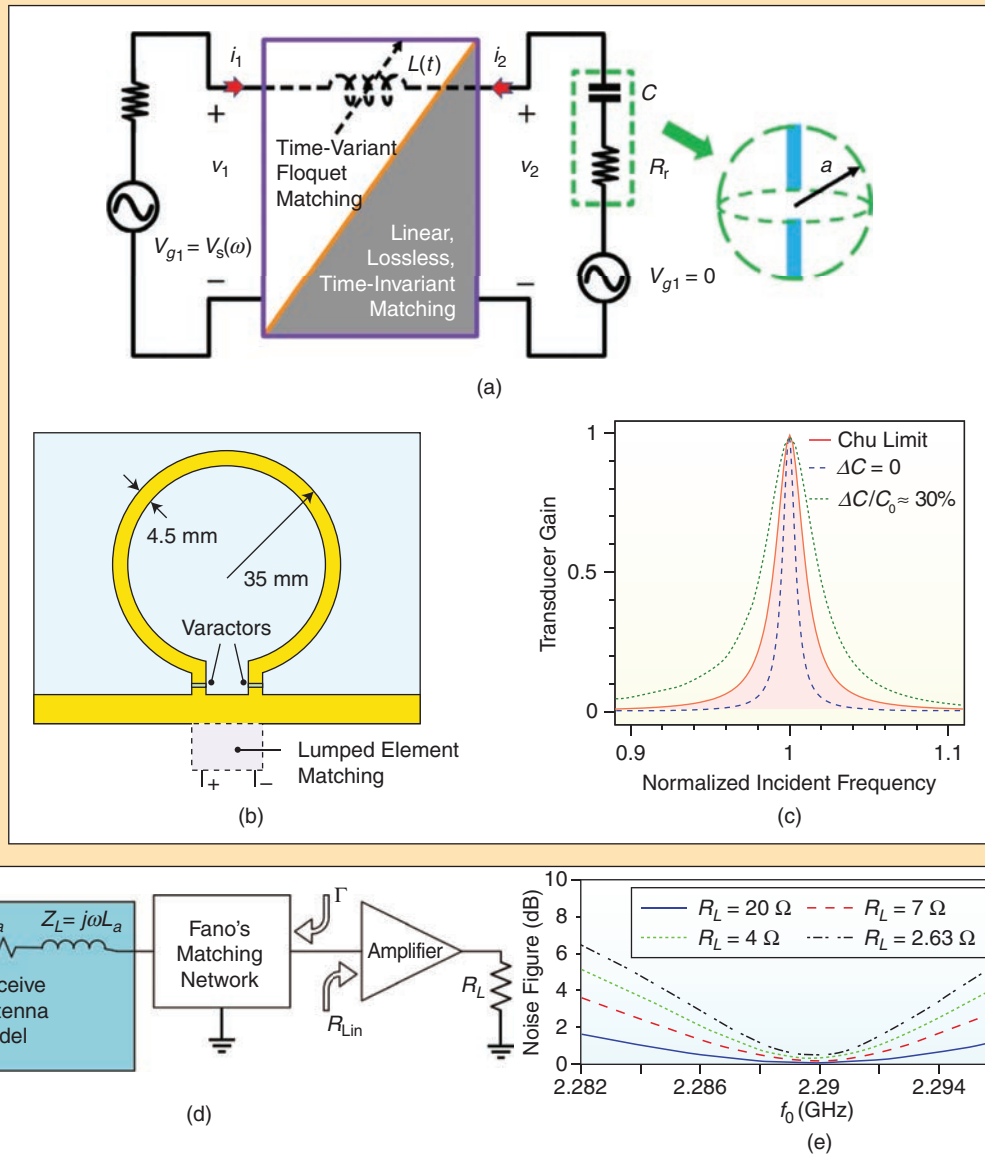


FIGURE 2. (a) A “Floquet” matching network with periodically time-varying elements can be employed to increase the efficiency-bandwidth product of an electrically small antenna by imparting parametric gain to the system. (b) An electrically small loop antenna (at the design frequency of 300 MHz) matched with periodically driven variable capacitors (varactors). (c) Transducer gain profiles (efficiency taking into account mismatch losses) obtained through numerical simulations show that the bandwidth of the time-modulated antenna (green dotted line) can exceed the maximum bandwidth predicted by the Chu–Harrington limit (red solid line). The time-invariant antenna (blue dashed line), on the other hand, is bounded by this limit. The incident frequency is normalized to the antenna design frequency. ΔC denotes the capacitance modulation amplitude, while C_0 (~ 3 pF) is the static capacitance. (d) Schematic for a different example of (receiving) antenna with an enhanced efficiency-bandwidth product. By deliberately inducing a mismatch between the antenna and the load, hence increasing reflection losses, the antenna bandwidth can be widened. The decrease in efficiency associated with mismatch losses can then be compensated through a parametric amplifier. (e) The inherently low-loss nature of parametric amplification can help bring the noise figure down while still maintaining a high bandwidth enhancement. Panels (a)–(c) are reproduced with permission from [80], American Physical Society. Panels (d)–(e) are reproduced with permission from [86], IEEE.

trading realized gain with bandwidth, in line with the Bode–Fano limit, by detuning the system from the ideal impedance-matched condition, hence increasing reflections, and subsequently using a parametric up-converter amplifier based on time-varying reactive elements to compensate for these mismatch losses. Different from [80] and [84], however, in [85] and [86] the authors placed a particular focus on assessing the noise properties of the system and studied a specific circuit configuration in which a receiving antenna is connected to an amplifier [Figure 2(d)] with real input impedance several times greater than the real part of the input impedance of the antenna, as this allows achieving an optimal tradeoff between increased bandwidth and added noise [Figure 2(e)].

ELECTROMAGNETIC ABSORPTION

Electromagnetic wave absorption plays a crucial role in various electromagnetic and optical systems, ranging from solar energy harvesting to scattering minimization for radar applications or anechoic chamber measurements. A key limitation of conventional electromagnetic absorbers is the typical tradeoff between the absorption bandwidth, i.e., the bandwidth over which a certain level of absorption can be maintained, and the thickness of the absorbing material or structure. Within this context, using the analytical properties of the reflection coefficient, Rozanov [46] showed that this tradeoff is in fact fundamental, and there exists an ultimate thickness to bandwidth ratio $\Delta\lambda/d$ for passive LTI absorbers backed by a perfect conductor. Specifically, for the case of a nonmagnetic absorber, the upper limit for this ratio is $\Delta\lambda/d < 16/|\ln \rho_0|$, where ρ_0 is the maximum tolerable reflection within the operating bandwidth. Clearly, the absorption bandwidth can therefore be widened by increasing the thickness of the absorber or the tolerable reflection. Prominent examples of broadband absorbers include cascaded [88], [89] or adiabatically tapered [90], [91], [92] lossy structures, which typically have thicknesses on the order of several wavelengths. However, for many applications, such as radar absorption or solar energy harvesting, creating the thinnest possible absorber with the widest possible bandwidth is highly desirable, which motivates the significant interest in overcoming the “Rozanov bound.” In this direction, it was shown in [87] that temporally switching the relative permittivity of the absorbing material can be used to extend the bandwidth of thin absorbers beyond what is possible with time-invariant structures [Figure 3(a)], similar to the use of temporally switched transmission lines for broadband impedance matching, as discussed in the “Impedance Matching” section, above. An important drawback of these approaches is that, while reflections are reduced within the bandwidth of the incident wave, significant reflections may be induced outside

With the renewed surge of interest in temporal modulation in electromagnetic systems, research into electrically small time-varying antennas has been reinvigorated.

this frequency range as the temporal switching can lead to strong frequency conversion. While this may not pose a problem for certain narrowband applications, it would become an issue in the context of, for example, broadband radar systems and stealth technology, as the target may become even more easily detectable due to the increased reflections outside the original signal bandwidth, which could then be picked up by sufficiently broadband or multiband detectors.

To overcome this problem, a possible strategy is to modulate

both the real and imaginary part of the permittivity in such a way that the modulation spectrum becomes “unilateral” (or “spectrally causal”), as we theoretically demonstrated in a recent publication [43]. Such an approach ensures that back-reflections due to the temporal modulations are prohibited over a very wide frequency range and, therefore, the incident wave is perfectly absorbed with no reflections over wide bandwidths [Figure 3(b) and (c)]. Along similar lines, a recent work theoretically demonstrated, through a Green’s function analysis and numerical optimizations, that a suitable switching of both the conductivity and permittivity leads to a reduction of reflection over the whole frequency spectrum [93]. As an alternative strategy, a recent experimental work [94] also demonstrated broadband absorption by creating an energy-trap through switched electronic components triggered by the pulse entering the absorbing region. While the strategies described so far work for short broadband pulses and are based on nonperiodic temporal modulations (e.g., “switching”), perfect absorption for quasi-monochromatic signals has also been realized by employing periodic temporal modulations [95]. Specifically, it was shown that perfect absorption can be achieved even with infinitesimal losses due to coherent multichannel illumination with Floquet time-periodic driving schemes.

OTHER APPLICATIONS

Our list of applications that can benefit from time-varying systems is certainly not exhaustive. In the supplementary material (available at <https://doi.org/10.1109/MAP.2023.3236275>), we provide several other application examples that might be of interest to readers also from different backgrounds, such as optics and photonics.

OUTLOOK

Although the study of time-varying electromagnetic systems dates back more than half a century, recent years have seen a surge of renewed interest in this topic, largely motivated by the need to realize novel electromagnetic systems that are superior to conventional LTI ones for various applications, from high-speed full-duplex communication systems, to broadband stealth technology, to high-efficiency energy harvesting and energy

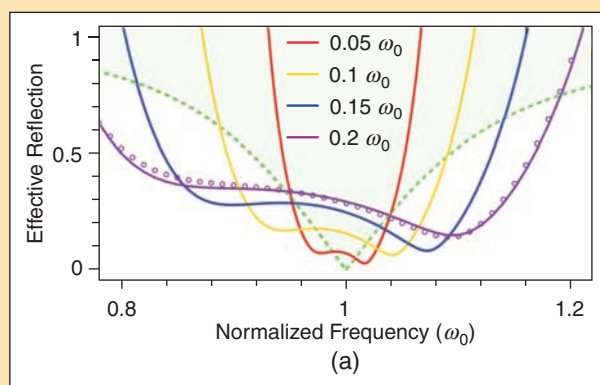
transfer. However, while recent progress in this field has been promising, we believe several challenges should be taken into consideration and carefully addressed before such systems can be adopted into practical use.

Since a time-varying system requires external power to operate, such active systems might become susceptible to instabilities (unbounded oscillations) that can disrupt the desired functionality. Thus, especially for systems involving parametric amplification, a

Creating the thinnest possible absorber with the widest possible bandwidth is highly desirable, which motivates the significant interest in overcoming the “Rozanov bound.”

careful analysis is essential to assess and ensure stability [80]. Moreover, the additional energy pumped into the system [96] should be carefully taken into account when determining the figure of merits (such as efficiency) of the design [97] and also to assess whether the external power required by the temporal modulation is beyond practical reach and/or may damage the system [98].

Frequency dispersion is another fundamental property of physical materials, constrained by



(a)

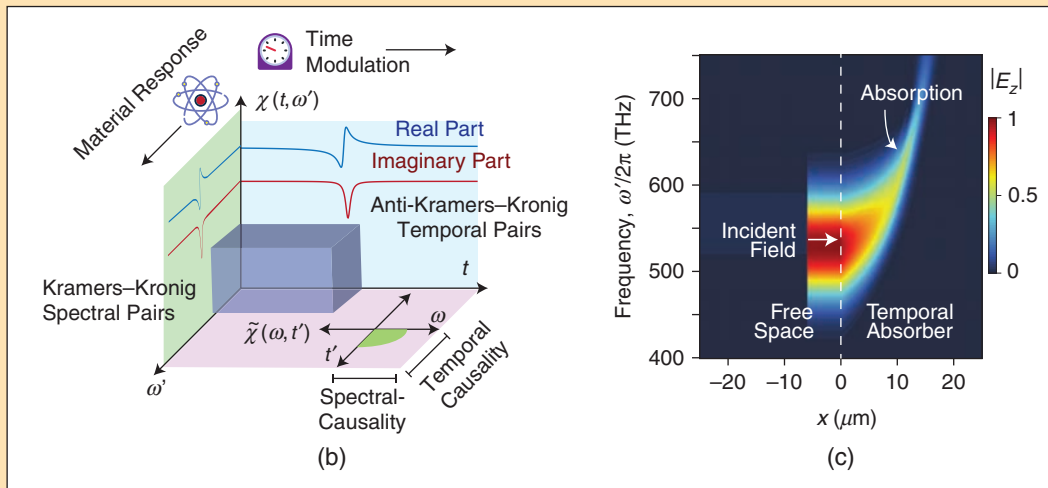


FIGURE 3. (a) An electromagnetic absorber with a time-switched permittivity can be employed to extend the absorption bandwidth beyond the time-invariant case (shown by the green dashed line). Different reflection spectra are shown, corresponding to incident Gaussian pulses with different widths. (b) Alternatively, one may temporally modulate the complex permittivity (both its real and imaginary parts simultaneously) such that the modulation spectrum becomes one-sided (or “spectrally causal”), which implies that frequency down-conversion and back-reflections due to the temporal modulation are prohibited over a broad bandwidth. (c) Such a complex modulation may potentially increase the bandwidth of electromagnetic absorbers, as in the time-switched case, but without inducing any reflection within or outside the operational bandwidth (as seen in the figure, the field is fully transmitted, frequency up-shifted, and absorbed, with no reflections, at any frequency). Panel (a) is reproduced with permission from [87], Optical Society of America. Panels (b) and (c) are reproduced with permission from [43], Optical Society of America.

the implications of the causality principle expressed by the Kramers-Kronig relations. Hence, any realistic system involves, to some degree, frequency variations in the material constitutive parameters. However, especially for numerical studies involving time-varying structures, such dispersion effects are often ignored and the time variation is assumed to be independent of frequency [20]. As a result, any realistic implementation of such proposals will necessarily experience performance deterioration due to frequency dispersion of the material properties. We note that several recent works [98], [99], [100], [101] have now started studying material dispersion effects more systematically in the context of time-varying systems. However, we believe further investigations in this area are important to improve our understanding of time-varying materials and may lead to improved designs and more accurate performance predictions.

For schemes requiring synchronization between the incident wave and the temporal variation, another significant challenge is that fast detectors and switching mechanisms are essential to trigger the modulation in the presence of the incident wave. Such additional components might complicate the design and reduce its practical applicability. Hence, more research is needed to integrate such components into time-varying systems in a practically useful manner.

Dissipation, unless desired to realize absorbers, is another challenge that needs to be addressed for various practical applications that involve time-varying systems. For instance, epsilon-near-zero materials have recently become the subject of increasing interest to realize deep and fast modulations at optical frequencies, as they can be efficiently controlled through external optical pumps [18]. However, such materials still suffer from high losses around their epsilon-near-zero wavelengths. Hence, the search for better epsilon-near-zero materials with lower losses is an important area of research (note that, theoretically, nothing prevents the existence of an epsilon-near-zero material that is dissipationless, albeit frequency-dispersive, within a certain frequency window). Alternatively, one could exploit (rather than eliminate or compensate) the losses in such materials to realize time-dependent loss profiles that accompany the time-varying refractive-index profiles. In this context, we recently provided a general strategy to exploit the synergy between these two time-modulation profiles for various applications [43]. Investigations along these directions may also enhance our understanding of wave dynamics in complex (“non-Hermitian”) time-varying media.

Despite the challenges outlined here, we believe that the use of time-varying materials and components to overcome

It would be safe to say that the new insights and the new tools provided by the field of time-varying electromagnetic systems will enable further advances and possible revolutions in the next decades.

the limitations of conventional LTI electromagnetic/photonics systems is an exciting and promising research area that might lead to novel and superior devices and, as more research is conducted, a deeper understanding of the actual fundamental limits in electromagnetics. Spatially varying engineered structures, such as frequency-selective surfaces, photonic crystals, and metamaterials have revolutionized the field of electromagnetics in recent decades. Along the same vein, it would be safe to say that the new insights and the new tools provided by the field of time-varying electromagnetic systems will enable further advances and possible revolutions in the next decades.

ACKNOWLEDGMENT

The authors acknowledge support from the Air Force Office of Scientific Research with Grant FA9550-19-1-0043 through Dr. Arje Nachman. This article has supplementary downloadable material available at <https://doi.org/10.1109/MAP.2023.3236275>, provided by the authors.



AUTHOR INFORMATION

Zeki Hayran (zh337@cornell.edu) is a Ph.D. candidate at the School of Electrical and Computer Engineering, Cornell University, Ithaca, New York 14853, USA. His research interests include time-varying metamaterials, non-Hermitian optics, and topological photonics. He is a Student Member of IEEE.

Francesco Monticone (francesco.monticone@cornell.edu) is an assistant professor of Electrical and Computer Engineering at Cornell University, Ithaca, New York 14853, USA. His research interests are applied electromagnetics, metamaterials/metasurfaces, and nanophotonics. He is a Member of IEEE and an associate editor of *IEEE Transactions on Antennas and Propagation*.

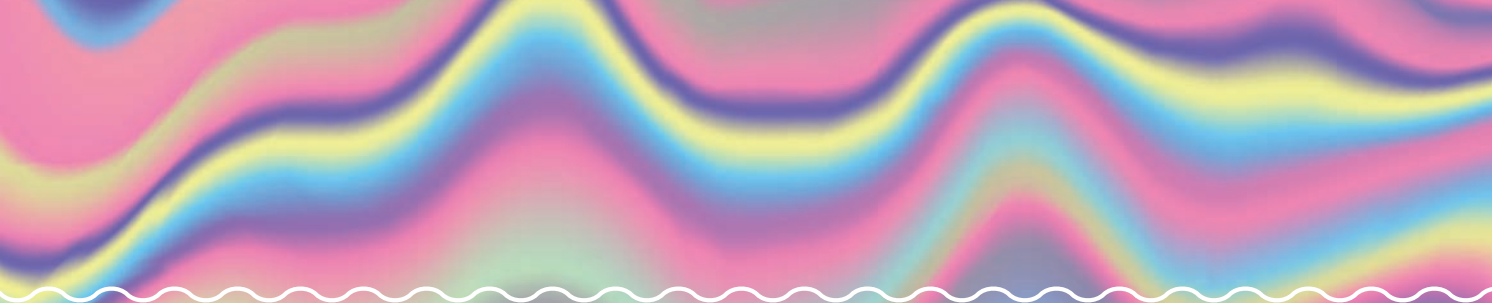
REFERENCES

- [1] F. R. Morgenstahler, “Velocity modulation of electromagnetic waves,” *IRE Trans. Microw. Theory Techn.*, vol. 6, no. 2, pp. 167–172, Apr. 1958, doi: 10.1109/TMTT.1958.1124533.
- [2] J.-C. Simon, “Action of a progressive disturbance on a guided electromagnetic wave,” *IRE Trans. Microw. Theory Techn.*, vol. 8, no. 1, pp. 18–29, Jan. 1960, doi: 10.1109/TMTT.1960.1124657.
- [3] E. S. Cassey and A. A. Oliner, “Dispersion relations in time-space periodic media: Part I-Stable interactions,” *Proc. IEEE*, vol. 51, no. 10, pp. 1342–1359, Oct. 1963, doi: 10.1109/PROC.1963.2566.
- [4] E. S. Cassey, “Waves guided by a boundary with time-Space periodic modulation,” *Proc. Inst. Elect. Eng.*, vol. 112, no. 2, pp. 269–279, Feb. 1965, doi: 10.1049/piee.1965.0040.
- [5] D. Holberg and K. Kunz, “Parametric properties of fields in a slab of time-varying permittivity,” *IEEE Trans. Antennas Propag.*, vol. 14, no. 2, pp. 183–194, Mar. 1966, doi: 10.1109/TAP.1966.1138637.

- [6] E. S. Cassedy, "Dispersion relations in time-space periodic media part II—Unstable interactions," *Proc. IEEE*, vol. 55, no. 7, pp. 1154–1168, Jul. 1967, doi: 10.1109/PROC.1967.5775.
- [7] B. Auld, J. H. Collins, and H. Zapp, "Signal processing in a nonperiodically time-varying magnetoelastic medium," *Proc. IEEE*, vol. 56, no. 3, pp. 258–272, Mar. 1968, doi: 10.1109/PROC.1968.6270.
- [8] L. Felsen and G. Whitman, "Wave propagation in time-varying media," *IEEE Trans. Antennas Propag.*, vol. 18, no. 2, pp. 242–253, Mar. 1970, doi: 10.1109/TAP.1970.1139657.
- [9] R. Fante, "Transmission of electromagnetic waves into time-varying media," *IEEE Trans. Antennas Propag.*, vol. 19, no. 3, pp. 417–424, May 1971, doi: 10.1109/TAP.1971.1139931.
- [10] R. Chu and T. Tamir, "Wave propagation and dispersion in space-time periodic media," *Proc. Inst. Electr. Eng.*, vol. 119, no. 7, pp. 797–806, Jul. 1972, doi: 10.1049/piee.1972.0169.
- [11] E. Yablonovitch, "Spectral broadening in the light transmitted through a rapidly growing plasma," *Physical Rev. Lett.*, vol. 31, no. 14, Oct. 1973, Art. no. 0777, doi: 10.1103/PhysRevLett.31.877.
- [12] N. Stepanov, "Dielectric constant of unsteady plasma," *Radiophysics Quantum Electron.*, vol. 19, no. 7, pp. 683–689, Jul. 1976, doi: 10.1007/BF01034233.
- [13] D. Kalluri and V. Goteti, "Frequency shifting of electromagnetic radiation by sudden creation of a plasma slab," *J. Appl. Phys.*, vol. 72, no. 10, pp. 4575–4580, Nov. 1992, doi: 10.1063/1.352111.
- [14] N. Stepanov, "Waves in nonstationary media," *Radiophysics Quantum Electron.*, vol. 36, no. 7, pp. 401–409, Jul. 1993, doi: 10.1007/BF01040254.
- [15] C. Caloz and Z.-L. Deck-Léger, "Spacetime metamaterials—Part I: General concepts," *IEEE Trans. Antennas Propag.*, vol. 68, no. 3, pp. 1569–1582, Mar. 2020, doi: 10.1109/TAP.2019.2944225.
- [16] A. M. Shaltout, V. M. Shalaev, and M. L. Brongersma, "Spatiotemporal light control with active metasurfaces," *Science*, vol. 364, no. 6441, May 2019, Art. no. eaat3100, doi: 10.1126/science.aat3100.
- [17] S. Taravati and A. A. Kishk, "Space-time modulation: Principles and applications," *IEEE Microw. Mag.*, vol. 21, no. 4, pp. 30–56, Apr. 2020, doi: 10.1109/MMM.2019.2963606.
- [18] O. Reshef, I. De Leon, M. Z. Alam, and R. W. Boyd, "Nonlinear optical effects in epsilon-near-zero media," *Nature Rev. Mater.*, vol. 4, no. 8, pp. 535–551, Aug. 2019, doi: 10.1038/s41578-019-0120-5.
- [19] J. N. Winn, S. Fan, J. D. Joannopoulos, and E. P. Ippen, "Interband transitions in photonic crystals," *Physical Rev. B*, vol. 59, no. 3, Jan. 1999, Art. no. 1551, doi: 10.1103/PhysRevB.59.1551.
- [20] Z. Yu and S. Fan, "Complete optical isolation created by indirect interband photonic transitions," *Nature Photon.*, vol. 3, no. 2, pp. 91–94, Feb. 2009, doi: 10.1038/nphoton.2008.273.
- [21] D. L. Sounas and A. Alù, "Non-reciprocal photonics based on time modulation," *Nature Photon.*, vol. 11, no. 12, pp. 774–783, Dec. 2017, doi: 10.1038/s41566-017-0051-x.
- [22] I. A. Williamson, M. Minkov, A. Dutt, J. Wang, A. Y. Song, and S. Fan, "Integrated nonreciprocal photonic devices with dynamic modulation," *Proc. IEEE*, vol. 108, no. 10, pp. 1759–1784, Sep. 2020, doi: 10.1109/JPROC.2020.3023959.
- [23] M. Notomi and S. Mitsuji, "Wavelength conversion via dynamic refractive index tuning of a cavity," *Physical Rev. A*, vol. 73, no. 5, May 2006, Art. no. 051803, doi: 10.1103/PhysRevA.73.051803.
- [24] S. F. Preble, Q. Xu, and M. Lipson, "Changing the colour of light in a silicon resonator," *Nature Photon.*, vol. 1, no. 5, pp. 293–296, May 2007, doi: 10.1038/nphoton.2007.72.
- [25] Y. Zhou et al., "Broadband frequency translation through time refraction in an epsilon-near-zero material," *Nature Commun.*, vol. 11, no. 1, pp. 1–7, May 2020, doi: 10.1038/s41467-020-15682-2.
- [26] J. B. Khurgin et al., "Adiabatic frequency shifting in epsilon-near-zero materials: The role of group velocity," *Optica*, vol. 7, no. 3, pp. 226–231, Mar. 2020, doi: 10.1364/OPTICA.374788.
- [27] V. Pacheco-Peña and N. Engheta, "Temporal aiming," *Light, Sci. Appl.*, vol. 9, no. 1, pp. 1–12, Jul. 2020, doi: 10.1038/s41377-020-00360-1.
- [28] P. A. Huidobro, E. Galiffi, S. Guenneau, R. V. Craster, and J. Pendry, "Fresnel drag in space–Time-modulated metamaterials," *Proc. Nat. Acad. Sci.*, vol. 116, no. 50, pp. 24,943–24,948, Dec. 2019, doi: 10.1073/pnas.1915027116.
- [29] M. R. Shcherbakov et al., "Time-variant metasurfaces enable tunable spectral bands of negative extinction," *Optica*, vol. 6, no. 11, pp. 1441–1442, Nov. 2019, doi: 10.1364/OPTICA.6.001441.
- [30] M. Cirone, K. Rzaz-Dotewski, and J. Mostowski, "Photon generation by time-dependent dielectric: A soluble model," *Physical Rev. A*, vol. 55, no. 1, Jan. 1997, Art. no. 62, doi: 10.1103/PhysRevA.55.62.
- [31] J. Sloan, N. Rivera, J. D. Joannopoulos, and M. Soljačić, "Casimir light in dispersive nanophotonics," *Physical Rev. Lett.*, vol. 127, no. 5, Jul. 2021, Art. no. 053603, doi: 10.1103/PhysRevLett.127.053603.
- [32] S. Lee et al., "Parametric oscillation of electromagnetic waves in momentum band gaps of a spatiotemporal crystal," *Photon. Res.*, vol. 9, no. 2, pp. 142–150, Feb. 2021, doi: 10.1364/PRJ.406215.
- [33] L. Yuan, A. Dutt, and S. Fan, "Synthetic frequency dimensions in dynamically modulated ring resonators," *APL Photon.*, vol. 6, no. 7, Jul. 2021, Art. no. 071102, doi: 10.1063/5.0056359.
- [34] T. Ozawa et al., "Topological photonics," *Rev. Modern Phys.*, vol. 91, no. 1, Mar. 2019, Art. no. 015006, doi: 10.1103/RevModPhys.91.015006.
- [35] T. T. Koutsiperidis and R. Fleury, "Nonreciprocal gain in non-hermitian time-Floquet systems," *Physical Rev. Lett.*, vol. 120, no. 8, Feb. 2018, Art. no. 087401, doi: 10.1103/PhysRevLett.120.087401.
- [36] C. Caloz and Z.-L. Deck-Léger, "Spacetime metamaterials—Part II: Theory and applications," *IEEE Trans. Antennas Propag.*, vol. 68, no. 3, pp. 1583–1598, Mar. 2020, doi: 10.1109/TAP.2019.2944216.
- [37] A. B. Shvartsburg, "Optics of nonstationary media," *Phys.-Uspekhi*, vol. 48, no. 8, Aug. 2005, Art. no. 797, doi: 10.1070/PU2005v04n08ABEH002119.
- [38] F. Biancalana, A. Amann, A. V. Uskov, and E. P. O'reilly, "Dynamics of light propagation in spatiotemporal dielectric structures," *Physical Rev. E*, vol. 75, no. 4, Apr. 2007, Art. no. 046607, doi: 10.1103/PhysRevE.75.046607.
- [39] Y. Xiao, G. P. Agrawal, and D. N. Maywar, "Spectral and temporal changes of optical pulses propagating through time-varying linear media," *Opt. Lett.*, vol. 36, no. 4, pp. 505–507, Feb. 2011, doi: 10.1364/OL.36.000505.
- [40] M. Bakunov and A. Maslov, "Reflection and transmission of electromagnetic waves at a temporal boundary: Comment," *Opt. Lett.*, vol. 39, no. 20, pp. 6029–6029, Oct. 2014, doi: 10.1364/OL.39.006029.
- [41] B. Plansinis, W. Donaldson, and G. Agrawal, "What is the temporal analog of reflection and refraction of optical beams?" *Physical Rev. Lett.*, vol. 115, no. 18, Oct. 2015, Art. no. 183901, doi: 10.1103/PhysRevLett.115.183901.
- [42] B. W. Plansinis, W. R. Donaldson, and G. P. Agrawal, "Spectral splitting of optical pulses inside a dispersive medium at a temporal boundary," *IEEE J. Quantum Electron.*, vol. 52, no. 12, pp. 1–8, Nov. 2016, doi: 10.1109/JQE.2016.2626081.
- [43] Z. Hayran, A. Chen, and F. Monticone, "Spectral causality and the scattering of waves," *Optica*, vol. 8, no. 8, pp. 1040–1049, Aug. 2021, doi: 10.1364/OPTICA.423089.
- [44] R. C. Hansen, "Fundamental limitations in antennas," *Proc. IEEE*, vol. 69, no. 2, pp. 170–182, Feb. 1981, doi: 10.1109/PROC.1981.11950.
- [45] R. M. Fano, "Theoretical limitations on the broadband matching of arbitrary impedances," *J. Franklin Inst.*, vol. 249, no. 1, pp. 57–83, Jan. 1950, doi: 10.1016/0016-0032(50)90006-8.
- [46] K. N. Rozanov, "Ultimate thickness to bandwidth ratio of radar absorbers," *IEEE Trans. Antennas Propag.*, vol. 48, no. 8, pp. 1230–1234, Aug. 2000, doi: 10.1109/8.884491.
- [47] H. Bode, *Network Analysis and Feedback Amplifier Design* (Bell Telephone Laboratories Series). New York, NY, USA: Van Nostrand, 1945.
- [48] M. Gustafsson and S. Nordebo, "Bandwidth, Q factor, and resonance models of antennas," *Prog. Electromagn. Res.*, vol. 62, pp. 1–20, Jan. 2006, doi: 10.2528/PIER06033003.
- [49] F. Monticone and A. Alù, "Invisibility exposed: Physical bounds on passive cloaking," *Optica*, vol. 3, no. 7, pp. 718–724, Jul. 2016, doi: 10.1364/OPTICA.3.000718.
- [50] S. E. Sussman-Fort and R. M. Rudish, "Non-Foster impedance matching of electrically-small antennas," *IEEE Trans. Antennas Propag.*, vol. 57, no. 8, pp. 2230–2241, Aug. 2009, doi: 10.1109/TAP.2009.2024494.
- [51] S. Hrabar, I. Krois, and A. Kiricenko, "Towards active dispersionless ENZ metamaterial for cloaking applications," *Metamaterials*, vol. 4, nos. 2–3, pp. 89–97, Aug./Sep. 2010, doi: 10.1016/j.metmat.2010.07.001.
- [52] P.-Y. Chen, C. Argyropoulos, and A. Alù, "Broadening the cloaking bandwidth with non-Foster metasurfaces," *Phys. Rev. Lett.*, vol. 111, no. 23, Dec. 2013, Art. no. 233001, doi: 10.1103/PhysRevLett.111.233001.
- [53] J. C. Soric and A. Alù, "Wideband tunable and non-foster mantle cloaks," in *Proc. USA Nat. Committee URSI Nat. Radio Sci. Meeting (USNC-URSI NRSM)*, 2014, pp. 1–1, doi: 10.1109/USNC-URSI-NRSM.2014.6927975.
- [54] A. Chen and F. Monticone, "Active scattering-cancellation cloaking: Broadband invisibility and stability constraints," *IEEE Trans. Antennas Propag.*, vol. 68, no. 3, pp. 1655–1664, Mar. 2020, doi: 10.1109/TAP.2019.2948528.
- [55] M. M. Jacob and D. F. Sievenpiper, "Gain and noise analysis of non-Foster matched antennas," *IEEE Trans. Antennas Propag.*, vol. 64, no. 12, pp. 4993–5004, Dec. 2016, doi: 10.1109/TAP.2016.2617380.
- [56] E. Ugarte-Munoz, S. Hrabar, D. Segovia-Vargas, and A. Kiricenko, "Stability of non-Foster reactive elements for use in active metamaterials and antennas," *IEEE Trans. Antennas Propag.*, vol. 60, no. 7, pp. 3490–3494, Jul. 2012, doi: 10.1109/TAP.2012.2196957.
- [57] M. I. Abdelrahman, Z. Hayran, A. Chen, and F. Monticone, "Physical limitations on broadband invisibility based on fast-light media," *Nature Commun.*, vol. 12, no. 1, pp. 1–5, May 2021, doi: 10.1038/s41467-021-22972-w.

- [58] X. Wang, L. P. Katehi, and D. Peroulis, "Time-varying matching networks for signal-centric systems," *IEEE Trans. Microw. Theory Techn.*, vol. 55, no. 12, pp. 2599–2613, Dec. 2007, doi: 10.1109/TMTT.2007.910082.
- [59] A. Shlivinski and Y. Hadad, "Beyond the Bode-Fano bound: Wideband impedance matching for short pulses using temporal switching of transmission-line parameters," *Phys. Rev. Lett.*, vol. 121, no. 20, Nov. 2018, Art. no. 204301, doi: 10.1103/PhysRevLett.121.204301.
- [60] J. Mendonça and P. Shukla, "Time refraction and time reflection: Two basic concepts," *Physica Scripta*, vol. 65, no. 2, Jan. 2002, Art. no. 160, doi: 10.1238/Physica.Regular.065a00160.
- [61] Y. Hadad and A. Shlivinski, "Soft temporal switching of transmission line parameters: Wave-field, energy balance, and applications," *IEEE Trans. Antennas Propag.*, vol. 68, no. 3, pp. 1643–1654, Mar. 2020, doi: 10.1109/TAP.2020.2967302.
- [62] M. S. Mirmoosa, G. Ptitsyn, V. S. Asadchy, and S. A. Tretyakov, "Time-varying reactive elements for extreme accumulation of electromagnetic energy," *Phys. Rev. Appl.*, vol. 11, no. 1, Jan. 2019, Art. no. 014024, doi: 10.1103/PhysRevApplied.11.014024.
- [63] D. L. Sounas, "Virtual perfect absorption through modulation of the radiative decay rate," *Phys. Rev. B*, vol. 101, no. 10, Mar. 2020, Art. no. 104303, doi: 10.1103/PhysRevB.101.104303.
- [64] Z. Hayran and F. Monticone, "Capturing broadband light in a compact bound state in the continuum," *ACS Photon.*, vol. 8, no. 3, pp. 813–823, Mar. 2021, doi: 10.1021/acsphotonics.0c01696.
- [65] H. A. Wheeler, "Fundamental limitations of small antennas," *Proc. IRE*, vol. 35, no. 12, pp. 1479–1484, Dec. 1947, doi: 10.1109/JPROC.1947.226199.
- [66] L. J. Chu, "Physical limitations of omni-directional antennas," *J. Appl. Phys.*, vol. 19, no. 12, pp. 1163–1175, May 1948, doi: 10.1063/1.1715038.
- [67] R. F. Harrington, "Effect of antenna size on gain, bandwidth, and efficiency," *J. Res. Nat. Bureau Standards-D. Radio Propag.*, vol. 64D, no. 1, Jan./Feb. 1960, doi: 10.6028/jres.064D.003.
- [68] B. S. Yarman, *Design of Ultra Wideband Antenna Matching Networks: Via Simplified Real Frequency Technique*. New York, NY, USA: Springer Science & Business Media, 2008.
- [69] A. R. Lopez, "A historical note on impedance-matching limitations [Antenna Designer's Notebook]," *IEEE Antennas Propag. Mag.*, vol. 55, no. 4, pp. 163–164, Aug. 2013, doi: 10.1109/MAP.2013.6645159.
- [70] J. S. McLean, "A re-examination of the fundamental limits on the radiation Q of electrically small antennas," *IEEE Trans. Antennas Propag.*, vol. 44, no. 5, 1996, Art. no. 672, doi: 10.1109/8.496253.
- [71] M. Gustafsson, C. Sohl, and G. Kristensson, "Physical limitations on antennas of arbitrary shape," *Proc. Roy. Soc. A, Math., Phys. Eng. Sci.*, vol. 463, no. 2086, pp. 2589–2607, Oct. 2007, doi: 10.1098/rspa.2007.1893.
- [72] A. D. Yaghjian, "Overcoming the chu lower bound on antenna q with highly dispersive lossy material," *IET Microw., Antennas Propag.*, vol. 12, no. 4, pp. 459–466, Mar. 2018, doi: 10.1049/iet-map.2017.0648.
- [73] M. Jacob and H. Brauch, "Keying VLF transmitters at high speed," *Electronics*, vol. 27, no. 12, pp. 148–151, Jan. 1954.
- [74] H. Wolff, "High-speed frequency-shift keying of LF and VLF radio circuits," *IRE Trans. Commun. Syst.*, vol. 5, no. 3, pp. 29–42, Dec. 1957, doi: 10.1109/TCOM.1957.1097513.
- [75] J. Galejs, "Switching of reactive elements in high-Q antennas," *IEEE Trans. Commun. Syst.*, vol. 11, no. 2, pp. 254–255, Jun. 1963, doi: 10.1109/TCOM.1963.1088740.
- [76] W. Yao and Y. E. Wang, "Radiating beyond the bandwidth using direct antenna modulation," in *Proc. IEEE Antennas Propag. Soc. Symp.*, 2004, vol. 1, pp. 791–794, doi: 10.1109/APS.2004.1329789.
- [77] X. Wang, L. P. Katehi, and D. Peroulis, "Time-varying matching network for antennas in pulse-based systems," in *Proc. IEEE Antennas Propag. Soc. Int. Symp.*, 2007, pp. 89–92, doi: 10.1109/APS.2007.4395437.
- [78] X. Wang, L. P. Katehi, and D. Peroulis, "Analysis and measurement of a time-varying matching scheme for pulse-based receivers with high-Q sources," *IEEE Trans. Microw. Theory Techn.*, vol. 58, no. 8, pp. 2231–2243, Aug. 2010, doi: 10.1109/TMTT.2010.2052870.
- [79] M. Manteghi, "Antenna miniaturization beyond the fundamental limits using impedance modulation," in *Proc. IEEE Antennas Propag. Soc. Int. Symp.*, 2009, pp. 1–4, doi: 10.1109/APS.2009.5171747.
- [80] H. Li, A. Mekawy, and A. Alù, "Beyond Chu's limit with Floquet impedance matching," *Phys. Rev. Lett.*, vol. 123, no. 16, Oct. 2019, Art. no. 164102, doi: 10.1103/PhysRevLett.123.164102.
- [81] N. Zhu and R. W. Ziolkowski, "Broad-bandwidth, electrically small antenna augmented with an internal non-foster element," *IEEE Antennas Wireless Propag. Lett.*, vol. 11, pp. 1116–1120, Sep. 2012, doi: 10.1109/LAWP.2012.2219572.
- [82] J. Church, J.-C. S. Chieh, L. Xu, J. D. Rockway, and D. Arceo, "UHF electrically small box cage loop antenna with an embedded non-foster load," *IEEE Antennas Wireless Propag. Lett.*, vol. 13, pp. 1329–1332, Jul. 2014, doi: 10.1109/LAWP.2014.2337112.
- [83] T. Shi, M.-C. Tang, Z. Wu, H.-X. Xu, and R. W. Ziolkowski, "Improved signal-to-noise ratio, bandwidth-enhanced electrically small antenna augmented with internal non-foster elements," *IEEE Trans. Antennas Propag.*, vol. 67, no. 4, pp. 2763–2768, Apr. 2019, doi: 10.1109/TAP.2019.2894331.
- [84] A. Mekawy, H. Li, Y. Radi, and A. Alù, "Parametric enhancement of radiation from electrically small antennas," *Phys. Rev. Appl.*, vol. 15, no. 5, May 2021, Art. no. 054063, doi: 10.1103/PhysRevApplied.15.054063.
- [85] P. Loghmannia and M. Manteghi, "Low-noise impedance matching technique for small antennas based on a parametric amplifier," in *Proc. IEEE Int. Symp. Antennas Propag. North Amer. Radio Sci. Meeting*, 2020, pp. 1787–1788, doi: 10.1109/IEEECONF35879.2020.9329596.
- [86] P. Loghmannia and M. Manteghi, "Broadband parametric impedance matching for small antennas using the Bode-Fano limit: Improving on Chu's limit for loaded small antennas," *IEEE Antennas Propag. Mag.*, vol. 64, no. 5, pp. 55–68, Oct. 2022, doi: 10.1109/MAP.2021.3089997.
- [87] H. Li and A. Alù, "Temporal switching to extend the bandwidth of thin absorbers," *Optica*, vol. 8, no. 1, pp. 24–29, Jan. 2021, doi: 10.1364/OPTICA.408399.
- [88] X. He, S. Yan, G. Lu, Q. Zhang, F. Wu, and J. Jiang, "An ultra-broadband polarization-independent perfect absorber for the solar spectrum," *RSC Adv.*, vol. 5, no. 76, pp. 61,955–61,959, Jun. 2015, doi: 10.1039/C5RA09234E.
- [89] C. Yang et al., "Visible-infrared (0.4–20 μm) ultra-broadband absorber based on cascade film stacks," *Appl. Phys. Lett.*, vol. 118, no. 14, Apr. 2021, Art. no. 143501, doi: 10.1063/5.0042818.
- [90] Y. Cui et al., "Ultrabroadband light absorption by a sawtooth anisotropic metamaterial slab," *Nano Lett.*, vol. 12, no. 3, pp. 1443–1447, Mar. 2012, doi: 10.1021/nl204118h.
- [91] Q. Liang, T. Wang, Z. Lu, Q. Sun, Y. Fu, and W. Yu, "Metamaterial-based two dimensional plasmonic subwavelength structures offer the broadest waveband light harvesting," *Adv. Opt. Mater.*, vol. 1, no. 1, pp. 43–49, Jan. 2013, doi: 10.1002/adom.201200009.
- [92] Z. Hayran, M. Turduiev, H. Kurt, and K. Staliunas, "Stopped microwave rainbow in 3D chirped photonic crystals," in *Proc. Phys. Simul. Optoelectron. Devices XXV*, International Society for Optics and Photonics, 2017, vol. 10098, pp. 271–279, doi: 10.1117/12.2253899.
- [93] C. Firestein, A. Shlivinski, and Y. Hadad, "Absorption and scattering by a temporally switched lossy layer: Going beyond the Rozanov bound," *Phys. Rev. Appl.*, vol. 17, no. 1, Jan. 2022, Art. no. 014017, doi: 10.1103/PhysRevApplied.17.014017.
- [94] X. Yang, E. Wen, and D. F. Sievenpiper, "Broadband time-modulated absorber beyond the Bode-Fano limit for short pulses by energy trapping," *Phys. Rev. Appl.*, vol. 17, no. 4, Apr. 2022, Art. no. 044003, doi: 10.1103/PhysRevApplied.17.044003.
- [95] S. Suwunnarat, D. Halpern, H. Li, B. Shapiro, and T. Kottos, "Dynamically modulated perfect absorbers," *Phys. Rev. A*, vol. 99, no. 1, Jan. 2019, Art. no. 013834, doi: 10.1103/PhysRevA.99.013834.
- [96] R. Seconde, J. Khurgin, and N. Kinsey, "Absorptive loss and band non-parabolicity as a physical origin of large nonlinearity in epsilon-near-zero materials," *Opt. Mater. Exp.*, vol. 10, no. 7, pp. 1545–1560, Jul. 2020, doi: 10.1364/OME.394111.
- [97] P. Jayathurathmagne, F. Liu, M. S. Mirmoosa, X. Wang, R. Fleury, and S. A. Tretyakov, "Time-varying components for enhancing wireless transfer of power and information," *Phys. Rev. Appl.*, vol. 16, no. 1, Jul. 2021, Art. no. 014017, doi: 10.1103/PhysRevApplied.16.014017.
- [98] Z. Hayran, J. B. Khurgin, and F. Monticone, " $\hbar\omega$ versus $\hbar k$: Dispersion and energy constraints on time-varying photonic materials and time crystals," *Opt. Mater. Exp.*, vol. 12, no. 10, pp. 3904–3917, Aug. 2022, doi: 10.1364/OME.471672.
- [99] M. S. Mirmoosa, T. Koutserimpas, G. Ptitsyn, S. A. Tretyakov, and R. Fleury, "Dipole polarizability of time-varying particles," *New J. Phys.*, vol. 24, no. 6, Jun. 2022, Art. no. 063004, doi: 10.1088/1367-2630/ac6b4c.
- [100] D. M. Solit and N. Engheta, "Functional analysis of the polarization response in linear time-varying media: A generalization of the Kramers-Kronig relations," *Phys. Rev. B*, vol. 103, no. 14, Apr. 2021, Art. no. 144303, doi: 10.1103/PhysRevB.103.144303.
- [101] M. Bakunov, A. Shirokova, and A. Maslov, "Constitutive relations and adiabatic invariants for electromagnetic waves in a dynamic Lorentz medium," *Phys. Rev. B*, vol. 104, no. 3, Jul. 2021, Art. no. 035112, doi: 10.1103/PhysRevB.104.035112.





Victor Pacheco-Peña^{ID} and Nader Engheta^{ID}

Merging Effective Medium Concepts of Spatial and Temporal Media

Opening new avenues for manipulating wave-matter interaction in 4D.

While wave-matter interactions can be tailored in space via spatial inhomogeneities in material parameters, temporal and spacetime media are becoming increasingly popular as they may enable the full control of electromagnetic (EM) waves in four dimensions (4D). Here, expanding our previous work on the effective medium

concept of temporal media, we develop more general effective medium theories that combine spatial multilayered media with temporal multistep changes of the permittivity. This work represents a combination of spatial and temporal inhomogeneities in a single structure. As the temporal modulation is applied within certain spatial multilayers (not all the layers), our approach may relax the need for temporally modulating the *whole* medium where the wave travels while still achieving frequency conversion (a key feature of temporal multisteppe

Digital Object Identifier 10.1109/MAP.2023.3254480
Date of current version: 14 April 2023



IMAGE LICENSED BY INGRAM PUBLISHING

media). The theoretical formulation and closed-form expressions for the effective permittivity of such spacetime effective media are presented. The proposed structure is studied via numerical simulations, demonstrating the possibility of designing spacetime effective media using a combination of temporally and spatially modulated materials. The increased degrees of freedom provided by our approach may open new possibilities for manipulating wave-matter interaction in 4D.

INTRODUCTION

Controlling EM wave propagation at will has been of great interest within the scientific community for many years [1], [2]. The notion of metamaterials and metasurfaces can be considered an important paradigm in this context [3], [4], [5], [6], [7], [8]. This is due to the fact that they can enable an arbitrary manipulation of the EM properties of media, allowing the design of artificial materials with permittivity (ϵ) and/or permeability (μ) responses not easily available in nature, such as near-zero [9], [10], [11], [12], [13] and negative values [14], [15], [16], [17], [18], [19]. Importantly, the scenarios where metamaterials and metasurfaces can be implemented have increased over the years, enabling the scientific community to report their use in applications such as computing [20], [21], [22], [23], antennas [24], [25], [26], [27], [28], circuits [29], [30], [31], and invisibility cloaking devices [32], [33], [34], [35], among others, within frequency ranges spanning from microwaves to terahertz up to the optical regime [36], [37], [38], [39], [40], [41].

The applications of metamaterials and metasurfaces have been explored in the spatial domain (time-harmonic scenario) where the EM wave-matter interaction is achieved by means of introducing spatial (x , y , z) inhomogeneities along the path where EM waves propagate. In recent years, however, the extra degree of freedom of time (t) has been introduced, allowing the scientific community to increase the ability to manipulate EM waves from three dimensions (3D, space) to four dimensions (4D, spacetime) [42], [43]. Two of the early studies in the field of spacetime EM media date back to the last century, when Morgenstaler and Fante explored the propagation of a monochromatic EM wave within a medium where its relative value of ϵ_r was rapidly changed in time from ϵ_{r1} to ϵ_{r2} (all values larger than one $\epsilon_{r1}, \epsilon_{r2} \geq 1$) at $t = t_0$ [i.e., $\epsilon_r(t)$ modeled as a single-step function] [44], [45]. Such a rapid change of $\epsilon_r(t)$ (with a fall/rise time much shorter than the period T of the incident monochromatic EM wave) is now understood to be the temporal analog of a spatial boundary between two media with different values of ϵ_r . In these works, it was demonstrated theoretically how such a temporal boundary can produce a wave traveling forwards (FW wave) and a wave traveling backwards (BW wave). These initial studies have inspired the scientific community to further study the manipulation of EM wave propagation within spatiotemporal

This work represents a combination of spatial and temporal inhomogeneities in a single structure.

media, allowing their application in exciting and exotic scenarios, such as antireflection temporal coatings and filters [46], [47], [48]; non-Foster temporal media [49]; Fresnel drag [50]; phase conjugation [51]; temporal anisotropy for inverse prism [52] and temporal aiming [53]; generalization of the Kramers-Kroning relations [54] and causality considerations [55];

temporal meta-atoms [56], [57]; energy accumulation [58]; and amplification and lasing [59], among others [60]. In addition to these applications, as metamaterials and metasurfaces can be designed to emulate artificial media having effective EM responses (ϵ_{eff} and ϵ_{ref} ; i.e., effective media), recent studies have also shown how 4D metamaterials can be exploited to enable temporal [61] or spatiotemporal effective media [62], demonstrating the richness of spacetime media for an arbitrary and full control of EM waves.

Inspired by the different possibilities and opportunities enabled by the introduction of spacetime metamaterials and the importance of effective medium concepts in 4D, in this work, we present a study of a technique that provides effective medium theories for the combination of the spatial and temporal inhomogeneities. In our recent article, we showed how, in a spatially homogeneous unbounded medium, a rapid and periodic temporal change of $\epsilon_r(t)$ between ϵ_{r1} to ϵ_{r2} (a periodic change starting at $t = t_0$) can be modeled as an effective temporal permittivity $\epsilon_{\text{ref}}(t)$ that follows a single-step function, with a change of ϵ_r from ϵ_{r1} to ϵ_{ref} at $t = t_0$, which was the temporal equivalent of the effective medium theory for the spatial multilayered metamaterials [63]. Here, we build upon this work and explore how such a temporal multistep effective medium can be combined together with spatial multilayered effective media to achieve a combined effective medium concept for the design of spacetime effective metamaterials. To that end, we consider cases involving spatially subwavelength (horizontal and vertical) multilayers placed within a cavity in which the electric field of the mode is perpendicular to and parallel with these multilayers, respectively. The alternating spatial multilayers are considered to have either a constant or a time-dependent $\epsilon_r(t)$. Different scenarios are studied for the spatial layers having $\epsilon_r(t)$ values, including $\epsilon_r(t)$ modeled as a single step or a periodic function of time [where the ϵ_r of the medium is initially ϵ_{r1} and then is periodically alternated in time (with the temporal periodicity much shorter than the period of the EM signal) between ϵ_{r2} and ϵ_{r1} , starting at $t = t_0$]. It will be shown how these scenarios can be exploited to design combined effective media having an $\epsilon_r(t)$ modeled as single-step functions where $\epsilon_r(t)$ is rapidly changed from ϵ_{r1} to $\epsilon_{\text{ref_spacetime}}$ at $t = t_0$. The effect of the temporal and spatial filling fraction is also explored, showing how different values of $\epsilon_{\text{ref_spacetime}}$ can be obtained by modifying the time duration and/or spatial thickness of the temporal multisteps and/or the thickness of the spatial multilayers, respectively.

THEORETICAL APPROACH

The schematic representation of our spacetime effective medium concept is shown in Figure 1, where both temporal multistep media and spatial multilayers are considered. i.e., our technique combines *temporal effective* and *spatial effective medium* concepts. Before merging both configurations, let us first focus our attention on Figure 1(a), where the schematic representation of a temporal effective medium is presented. In this scenario, as we reported in [61], a monochromatic wave travels within a spatially homogeneous unbounded medium with a relative permittivity ϵ_{r1} for times $t < t_0$ (from now on, all values of ϵ_r are real, positive, and ≥ 1 ; note that the effective medium concept in temporal media is also applicable to temporal loss/gain functions [64]; here, however, without the loss of generality, we evaluate real-valued ϵ_r). At $t = t_0$, the ϵ_r of the whole medium is periodically alternated in time between ϵ_{r2} and ϵ_{r1} with a time period much shorter than the period of the incident signal (temporal multisteps $\ll T$). As shown in [61], such a temporal multistep function of $\epsilon_r(t)$ is the equivalent of having a temporally effective medium modeled as a single step where ϵ_r is ϵ_{r1} for times $t < t_0$, and it is changed to $\epsilon_{\text{eff_time}}$ at $t = t_0$ and kept to this value for $t > t_0$. Such a temporal effective value $\epsilon_{\text{eff_time}}$ can be theoretically calculated as [61]

$$\epsilon_{\text{eff_time}} = \frac{\epsilon_{r1} \epsilon_{r2}}{\epsilon_{r1} \overline{\Delta t}_2 + \epsilon_{r2} \overline{\Delta t}_1} \quad (1)$$

with $\overline{\Delta t}_1 = \Delta t_1 / (\Delta t_1 + \Delta t_2) = 1 - \overline{\Delta t}_2$ and $\overline{\Delta t}_2 = \Delta t_2 / (\Delta t_1 + \Delta t_2)$ as the temporal filling fractions for each periodic temporal step corresponding to the times where ϵ_r is either ϵ_{r1} or ϵ_{r2} , respectively. Based on this, the temporal effective medium indeed represents a single temporal boundary where the frequency of the wave inside the unbounded medium is modified from f_1 to $f_2 = f_1 \sqrt{\epsilon_{r1}/\epsilon_{\text{eff_time}}}$ (considering $\mu_{r1} = \mu_{r2} = \mu_r$) and the wavenumber \mathbf{k} is not modified [44], [45].

Now, with this review of our previous work on the concept of *temporal effective media*, we can now focus our attention on the spatial effective media shown on the right-hand side of Figure 1(c) (spatial multilayered media). Here, we consider a monochromatic Ey-polarized TEM mode within a 1D cavity of width $d = \lambda_1/2$ [$\lambda_1 = (c/\sqrt{\epsilon_{r1}})$, where c is the velocity of light in vacuum] filled with spatially subwavelength horizontal or vertical multilayers. (Note that we study an EM mode in a cavity instead of wave propagation in a multilayer medium in an unbounded region to better observe the field distribution with the structure, without complicating the problem with the presence of unequal forward and backward waves. However, the same approach here proposed for the spacetime effective media can be considered using spacetime multilayers placed outside of a cavity and being illuminated with a plane wave.) Now, as shown in Figure 1(c), the subwavelength spatial multilayers are periodically placed within the cavity with a spatial periodicity $\ll \lambda_1$. The spatially periodic arranged layers are filled with two different media

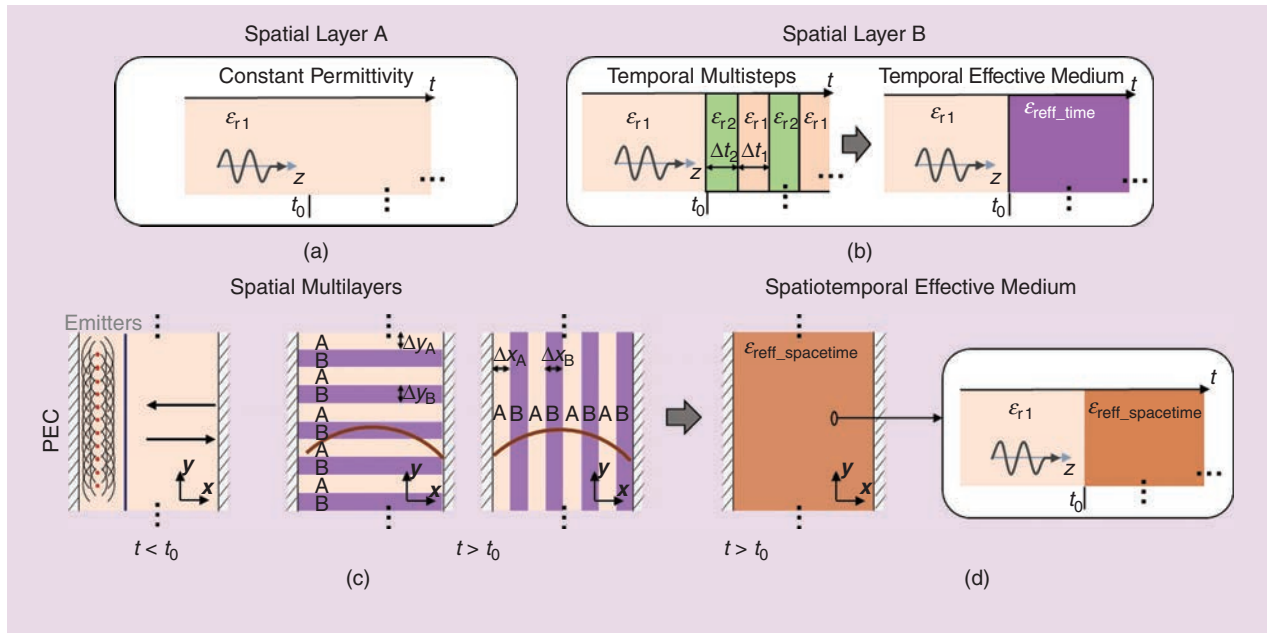


FIGURE 1. A schematic representation of the proposed spacetime effective media concept based on combined effective medium theories. For times $t < t_0$, the permittivity of the medium filling a cavity is constant $\epsilon_r = \epsilon_{r1} = \text{constant}$ [left panel in (c)]. At $t = t_0$, a spatial multilayered medium is created with some layers having a constant unchanged $\epsilon_r = \epsilon_{r1} = \text{constant}$ [see (a)], while others have a time-dependent permittivity $\epsilon_r(t)$ modeled either as a temporally periodic multistep medium (with periodicity much shorter than the period of the EM signal) or as a temporal effective medium using a single-step function of ϵ_r [left and right panels in (b), respectively]. In this setup, the EM signal is excited using an array of dipoles polarized along the y -axis, and they are switched off at $t = t_0$. With this configuration, the equivalent spacetime effective medium generated using the combination of temporal effective and spatial effective medium concepts is shown in (d). (a) Spatial layer A. (b) Spatial layer B. (c) Spatial multilayers. (d) Spatiotemporal effective medium.

having a relative permittivity of ϵ_{rA} and ϵ_{rB} with a filling fraction of $\Delta y_{A,B}$ or $\Delta x_{A,B}$, respectively, depending on the orientation of the spatial layers (horizontal or vertical, respectively). Now, as is known, for the E-field polarized parallel with the y -axis, such horizontal or vertical spatial multilayered media can be modeled as *spatial effective media* having an effective permittivity of, respectively [63]

$$\epsilon_{\text{reff_hor}} = \frac{\epsilon_{rA}\epsilon_{rB}}{\epsilon_{rA}\Delta y_B + \epsilon_{rB}\Delta y_A} \quad (2a)$$

$$\epsilon_{\text{reff_ver}} = \epsilon_{rA}\Delta x_A + \epsilon_{rB}\Delta x_B \quad (2b)$$

where $\Delta x_A = \Delta x_A / (\Delta x_A + \Delta x_B) = 1 - \Delta x_B$, $\Delta x_B = \Delta x_B / (\Delta x_A + \Delta x_B)$, $\Delta y_A = \Delta y_A / (\Delta y_A + \Delta y_B) = 1 - \Delta y_B$, and $\Delta y_B = \Delta y_B / (\Delta y_A + \Delta y_B)$ are the filling fractions for the subwavelength spatial layers considering vertical or horizontal multilayers.

Now, an interesting question can be asked: What would happen if one combined both the temporal effective and the spatial effective concepts within a single structure if both the spatial and temporal boundaries are merged in a single device? Such a spatiotemporal effective medium technique is the subject of this work, and the schematic representation is shown in full in Figure 1(c), where a monochromatic signal is considered to be present within this cavity. For times $t < t_0$, the relative permittivity ϵ_r of the whole medium filling the cavity is ϵ_{r1} [left panel of Figure 1(c)]. At $t = t_0$, the ϵ_r of part of the medium is changed in time such that a spatial multilayered structure is created. To do this, we consider that some of the deeply subwavelength spatial layers do not change their ϵ_r in time [$\epsilon_{rA} = \epsilon_{r1} = \text{constant}$, see Figure 1(a)], while other subwavelength spatial layers are made of materials with a time-dependent $\epsilon_r(t)$, as the one shown in Figure 1(b) (temporal effective medium), i.e., the spatial layers filled with $\epsilon_r(t)$ are those layers with $\epsilon_{rB}(t)$ where ϵ_{rB} is changed from ϵ_{r1} for $t < t_0$ to either a temporally periodic multistep function [left panel of Figure 1(b)] or an equivalent temporal effective medium [right panel of Figure 1(b)] with $\epsilon_{rB} = \epsilon_{\text{reff_time}}$ at $t = t_0$. In this context, the structure from Figure 1(c) can behave as a *spacetime effective medium* having a spacetime effective permittivity ($\epsilon_{\text{reff_spacetime}}$), which is a result of the combination of (1) and (2), i.e., the spacetime medium from Figure 1(c) corresponds to a *spacetime effective medium* modeled as a single-step function where its ϵ_r is ϵ_{r1} for $t < t_0$, and it is changed to $\epsilon_{\text{reff_spacetime}}$ at $t = t_0$ [see the schematic representation in Figure 1(d)], as follows:

$$\epsilon_{\text{reff_spacetime}} = \frac{\epsilon_{r1}\epsilon_{\text{reff_time}}}{\epsilon_{r1}\Delta y_2 + \epsilon_{\text{reff_time}}\Delta y_1} \quad (3a)$$

$$\epsilon_{\text{reff_spacetime}} = \epsilon_{r1}\Delta x_1 + \epsilon_{\text{reff_time}}\Delta x_2 \quad (3b)$$

for the horizontal and vertical configurations, respectively, for the y -polarized E-field. Finally, as such a single-step

The increased degrees of freedom provided by our approach may open new possibilities for manipulating wave-matter interaction in 4D.

function of ϵ_r is able to induce a temporal boundary, the frequency of the EM mode within the cavity will be changed from f_1 to $f_2 = f_1\sqrt{\epsilon_{r1}/\epsilon_{\text{reff_spacetime}}}$, as expected. In the following sections, we provide a detailed study of the proposed spacetime effective medium concept by exploring examples considering deeply subwavelength vertical and horizontal spatial multilayers filled with constant or time-dependent $\epsilon_r(t)$

modeled as temporal multistep or single-step temporal functions.

RESULTS AND DISCUSSION

Here, we study our proposed spacetime effective medium concept. The designs are studied numerically considering different configurations, including the combination of single temporal step functions of ϵ_r and spatial multilayers (horizontal or vertical setups), the combination of temporal multisteps with spatial multilayers, and the effect of the temporal and spatial filling fraction.

SIMULATION SETUP

All the designs are numerically studied using the time-domain solver of the software COMSOL Multiphysics® [65]. The cavity has a width of $d = \lambda_1/2$ along the x . Since we deal with a y -polarized TEM mode in the 1D cavity, for the 2D numerical simulation, we put the perfect electric conductor (PEC) walls on the top and bottom of this cavity to limit the computational domain. For the spatial multilayers, as shown in Figure 1(c), a periodicity of $0.05\lambda_1$ was implemented for both vertical and horizontal spatial configurations, using a total of 10 and 17 spatial periods along the x or y axis, respectively. The cavity was surrounded by PEC. To excite the structure, an array of 17 vertically polarized dipoles was placed $0.05\lambda_1$ away from the left PEC boundary. To better appreciate the effect of the proposed spacetime effective change of ϵ_r in the signal already present within the cavity, the dipoles are switched off once the ϵ_r within the cavity is changed at $t = t_0$. The structure was spatially meshed using a triangular mesh type with a maximum and minimum size of $7.5 \times 10^{-3}\lambda_1$ and $1.5 \times 10^{-4}\lambda_1$, respectively, with a curvature factor of 0.2 and a resolution of narrow regions of 3 to ensure accurate results. The rapid changes of ϵ_r in time were implemented using analytical functions having a rise/fall time of $1.5 \times 10^{-3} T$ with a smoothing of two continuous derivatives to ensure the convergence of the results.

COMBINING HORIZONTAL SPATIAL MULTILAYERS WITH A SINGLE TEMPORAL STEP OF ϵ_r

To begin with, let us first consider the case shown in Figure 2(a) using horizontal deeply subwavelength spatial multilayers combined with single temporal step functions of ϵ_r . For times $t < t_0$, the ϵ_r of the whole material filling the

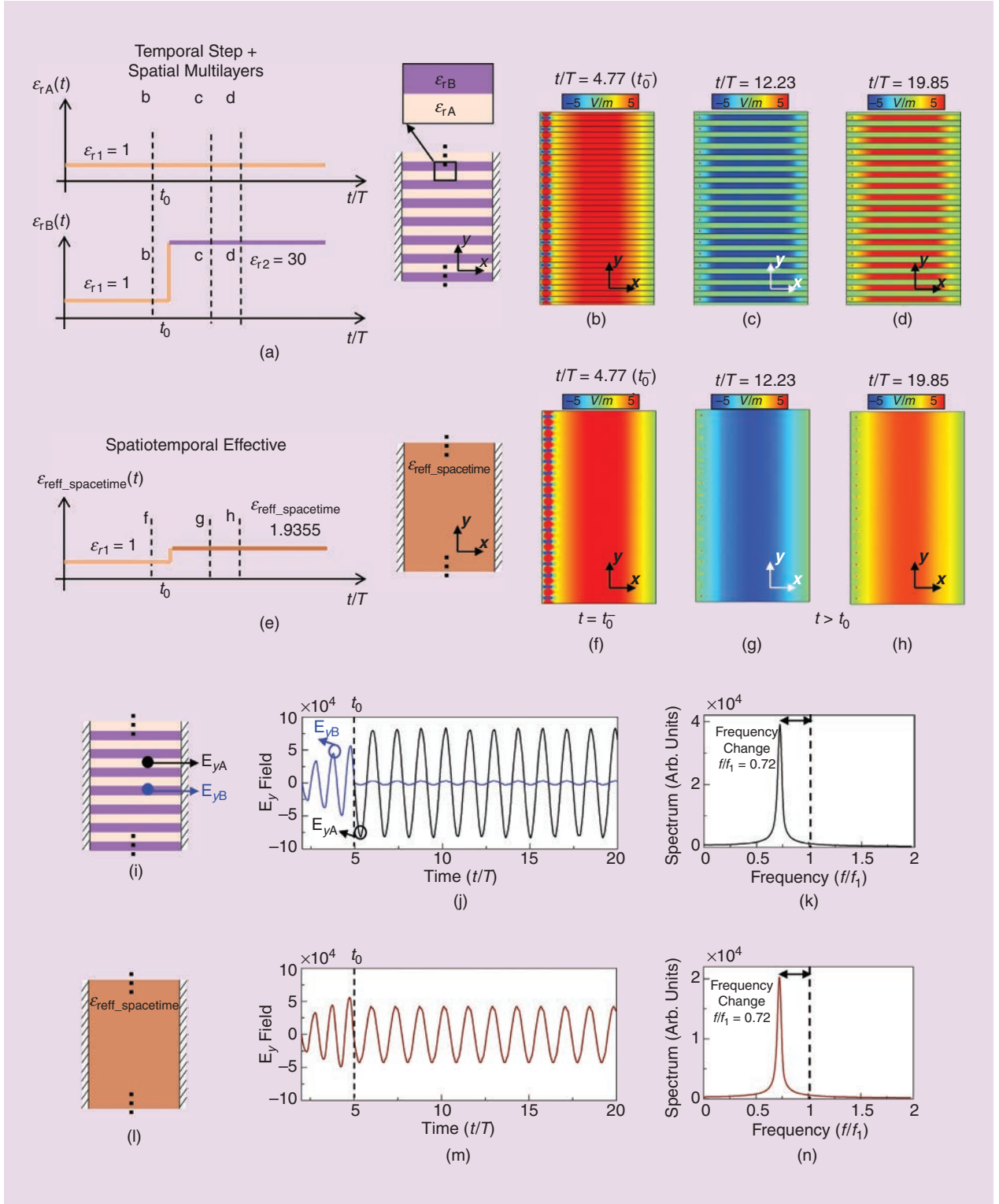


FIGURE 2. Combining horizontal spatial multilayers with a temporal step of ϵ_r . (a) The temporal functions of ϵ_r for the spatial regions with ϵ_{rA} and ϵ_{rB} are shown on the top and bottom panels, respectively. (e) The generated spacetime effective medium. The numerical results of the electric field (E_y) distribution at different times considering the spacetime structure from (a) and its spacetime effective medium from (e) are presented in (b)–(d) and (f)–(h), respectively. The numerical results of the recorded electric field distribution as a function of time within the spacetime structure from panels (a) and (i) and within the spacetime effective medium from (e) and (l) are shown in (j) and (m), respectively, along with the spectral content for $t > t_0$ inside the cavity in (k) and (n), respectively. For panel (k), the spectral content calculated within a spatial layer filled with $\epsilon_{rA}(t)$ is shown to better compare the results. The color bars from (b)–(d) and (f)–(h) have a scale of $\times 10^4$. All these results consider spatial filling fraction of 0.5, $\Delta y_A = \Delta y_B = 0.5$. Arb. units: arbitrary units.

cavity is $\epsilon_{r1} = 1$. Then, at $t = t_0$, a spatial multilayered medium is created within the cavity via alternating layers with a thickness of $0.025\lambda_1$ (i.e., a filling fraction of 0.5) and permittivity values of ϵ_{rA} and ϵ_{rB} . Here, ϵ_{rA} is constant in time (throughout this article, $\epsilon_{rA} = \epsilon_{r1} = \text{constant}$), while ϵ_{rB} is changed in time using a single step from 1 to $\epsilon_{rB} = \epsilon_{r2} = 30$. The schematic representations of the temporal functions for $\epsilon_{rA}(t)$ and $\epsilon_{rB}(t)$ are shown on the top and bottom panels in Figure 2(a) (left panels), respectively. By using (3a), such a spatiotemporal effective medium can be modeled as a single-step function where ϵ_r is $\epsilon_{r1} = 1$ for times $t < t_0$, and then, it is rapidly changed to $\epsilon_{\text{refr_spacetime}} = 1.9355$ at $t = t_0$ [see the schematic representation of $\epsilon_{\text{refr_spacetime}}(t)$ on the left panel of Figure 2(e)]. Note that as we are only modifying the $\epsilon_{rB}(t)$ using a single-step function, $\epsilon_{\text{refr_time}} = \epsilon_{r2} = 30$ in (3). With this setup, the numerical results of the electric field distribution (E_y) at different times considering the case using the single temporal step function of $\epsilon_{rB}(t)$ together with spatial multilayers along with the results for the case using a spacetime effective medium filling the cavity are shown in Figure 2(b)–(d) and Figure 2(f)–(h). As observed, an excellent agreement is obtained between the results, showing how both structures are indeed equivalent. To further corroborate these results, we recorded the E_y field distribution as a function of time within the multilayered structure (at a spatial location corresponding to a layer filled with ϵ_{rA} or ϵ_{rB}) and within the spacetime equivalent medium, and the results are shown in Figure 2(j) and (m), respectively. From these results, it is clear how the period of the E_y field distribution is the same after applying the temporal changes of ϵ_r in both configurations.

Finally, and to further compare the results, the spectral contents of these signals (for times $t > t_0$) are shown in Figure 2(k) and (n), considering again a spacetime medium and its spacetime effective counterpart, respectively. Note how the frequency in both configurations is changed from $f/f_1 = 1$ to $f/f_1 = 0.72$, in excellent agreement with the theoretical calculations, which predict a change of frequency to $f/f_1 = (1/1.9355)^{1/2} = 0.718 \sim 0.72$. For completeness, an animation showing the results presented in Figure 2(a)–(h) can be found in the supplementary material. Moreover, a case considering the same setup as in Figure 2 but when $\epsilon_{rB}(t)$ is changed from $\epsilon_{rB} = \epsilon_{r1} = 3$ to $\epsilon_{rB} = \epsilon_{r2} = 1$ at $t = t_0$ can be found as supplementary material.

COMBINING VERTICAL SPATIAL MULTILAYERS WITH A SINGLE TEMPORAL STEPS OF ϵ_r

For completeness, here we consider a similar configuration as in Figure 2 but now using vertical spatial multilayers. The schematic representation of the temporal functions of ϵ_r for the spatial regions filled with $\epsilon_{rA}(t)$ and $\epsilon_{rB}(t)$ are shown on the left-hand

In these works, it was demonstrated theoretically how such a temporal boundary can produce a wave traveling forwards (FW wave) and a wave traveling backwards (BW wave).

side of Figure 3(a). As in Figure 2, ϵ_{rA} is constant in time, while ϵ_{rB} is changed from $\epsilon_{rB} = \epsilon_{r1} = 1$ to $\epsilon_{rB} = \epsilon_{r2} = 30$ at $t = t_0$. By using (3b), the spacetime effective medium for times $t > t_0$ has a value of $\epsilon_{\text{refr_spacetime}} = 15.5$ [see the schematic representation in Figure 3(e)]. With this configuration, the numerical results of the E_y field distribution at different times considering the structure from Figure 3(a) and its spacetime effective counterpart [Figure 3(e)] are shown in Figure 3(b)–(d) and Figure 3(f)–(h), respectively. Again, a good agreement is observed. The numerically evaluated values for

E_y for both structures are also shown in Figure 3(j) and (m), respectively, along with the spectral content for times $t > t_0$ in Figure 3(k) and (n), respectively. As observed, the frequency of the signal within the cavity is changed from $f/f_1 = 1$ to $f/f_1 = 0.25$ in both structures from Figure 3(a) and (i) and Figure 3(e) and (l), in agreement with the theoretical calculations, $f/f_1 = (1/15.5)^{1/2} = 0.254 \sim 0.25$. Moreover, it is important to note how the temporal signals from Figure 3(j) present some high-frequency harmonics (seen as small ripples), which are due to the multiple reflections of the EM signals excited from each of the spatial layers where the permittivity is changed in time to ϵ_{rB} . In practical scenarios, if needed, low-pass filters could be implemented to eliminate such higher frequency harmonics. Finally, an animation showing the results presented in Figure 3(a)–(h) can be found in the supplementary material. As in the previous example, in the supplementary material, we have also considered the case with the same setup as in Figure 3 but when $\epsilon_{rB}(t)$ is changed from $\epsilon_{rB} = \epsilon_{r1} = 3$ to $\epsilon_{rB} = \epsilon_{r2} = 1$ at $t = t_0$.

COMBINING HORIZONTAL SPATIAL MULTILAYERS WITH PERIODIC TEMPORAL MULTISTEPS

Let us now consider the case shown in Figure 4(a), where we combine temporal multisteps of ϵ_r and spatial multilayers. As in the results discussed in Figures 2 and 3, the ϵ_r of the whole medium filling the cavity is $\epsilon_{r1} = 1$ for $t < t_0$. Then, at $t = t_0$, a spatial multilayered medium is created by alternating horizontal spatial layers with a thickness of $0.025\lambda_1$ (a filling fraction of $\widetilde{\Delta y_A} = \widetilde{\Delta y_B} = 0.5$) with ϵ_r values of ϵ_{rA} and ϵ_{rB} . As before, ϵ_{rA} is constant in time and remains $\epsilon_{rA} = \epsilon_{r1} = 1$. However, ϵ_{rB} is periodically changed in time (with a period much shorter than the period of the EM signal, 0.1 T in our case) between $\epsilon_{rB} = \epsilon_{r2} = 1.8$ and $\epsilon_{rB} = \epsilon_{r1} = 1$, starting at $t = t_0$, with a temporal duty cycle (DC) of 0.8 ($\widetilde{\Delta t}_2 = 0.8$ and $\widetilde{\Delta t}_1 = 0.2$). Note that here we chose a different temporal DC from 0.5 (1) to demonstrate that the DC can also be changed as in the temporal effective medium reported in [61] and 2) to enable the convergence of the numerical simulations. Now, by using (1), such a temporal multistep medium $\epsilon_{rB}(t)$ can be modeled

as a temporal effective medium using a single-step function of ϵ_r where ϵ_r is changed from $\epsilon_{r1} = 1$ to $\epsilon_{\text{refr_time}} = 1.55$ [see the purple line on the bottom panel of Figure 4(a)]. Then, we can simply use (3a) with a spatial filling fraction of 0.5 and calculate the spacetime effective value of $\epsilon_{\text{refr_spacetime}}$ for an effective medium modeled as in Figure 4(d), obtaining $\epsilon_{\text{refr_spacetime}} = 1.2162$ for times $t = t_0$.

With this configuration, the numerical results of the recorded electric field distribution as a function of time within a spatial layer filled with ϵ_{rB} and within the corresponding spacetime effective medium are shown in Figure 4(c) and (f), respectively. As observed, an excellent agreement between the results is obtained. Note how the amplitude of the electric field is increased/reduced periodically because of the effect

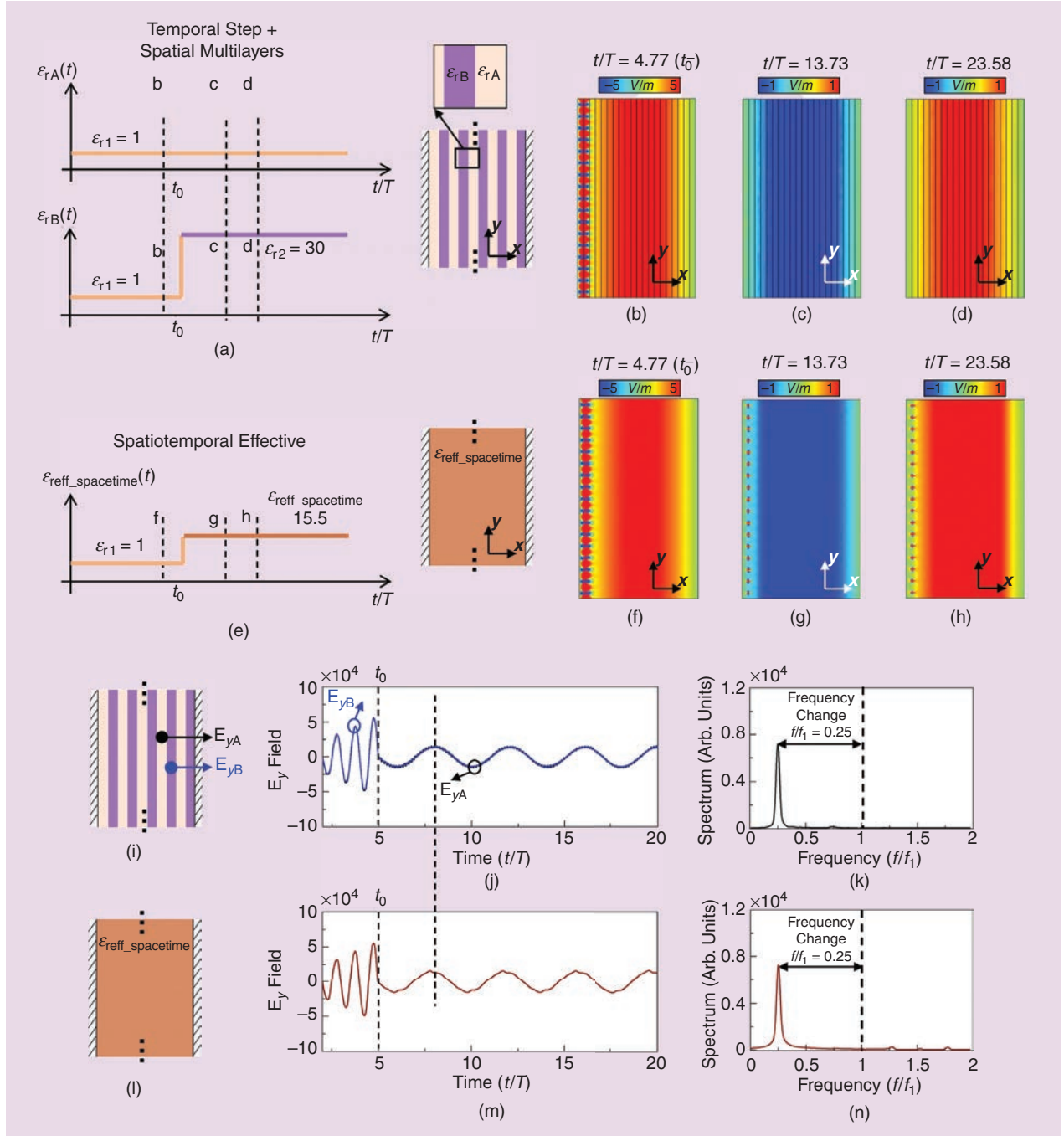


FIGURE 3. Combining vertical spatial multilayers with a temporal step of ϵ_r . All the panels from this figure are arranged following the same order as those shown in Figure 2. The schematic representations of the vertical spatial multilayers are shown in (a) and (i), and the schematic representations of the corresponding spacetime effective medium are shown in (e) and (l). The color bars from (b), (c), and (f)–(h) have a scale of $\times 10^4$. All these results consider a spatial filling fraction of 0.5, $\Delta x_A = \Delta x_B = 0.5$.

of the periodic temporal multisteps for $\epsilon_{rB}(t)$, as expected. Note that these “ripples” are of a different nature compared to those shown in Figure 3(j), where the “ripples” were due to the multiple spatial reflections after the $\epsilon_{rB}(t)$ of the multilayers is changed in time using a single-step function. Hence, the high-frequency harmonics from the results shown in Figure 4(c) are more pronounced than those shown in Figure 3(j) given the dependence of their amplitude with the periodic temporal modulation of $\epsilon_{rB}(t)$. These variations of amplitude translate into high-frequency harmonics, as shown in [61], which could be eliminated, if needed, using filters, as mentioned before. To guide the eye, vertical dashed green lines have been added to Figure 4(c) and (f), to demonstrate that the period of the signal is the same in both structures from Figure 4(b) and (e) with a period $t/T = 1.104$. This value is in agreement with the theoretical calculations that predict a frequency change from $f/f_1 = 1$ to $f/f_1 = (1/1.2162)^{1/2} = 0.906$, i.e., a theoretical period of the signal of $\sim t/T = 1.103$. An animation showing the results of Figure 4 can be found in the supplementary material.

As observed, an excellent agreement is obtained between the results, showing how both structures are indeed equivalent.

The corresponding case of vertical spatial multilayers with temporal multisteps is shown in the supplementary material, where it is shown how a combination of spatial multilayers and $\epsilon_{rB}(t)$ modulated using temporal multisteps also generates high-frequency harmonics but now due to both the spatial reflections within the multilayers [as shown and discussed in Figure 3(j)] and the temporal multistep modulation of $\epsilon_{rB}(t)$ [as discussed in the results of Figure 4(c)].

SINGLE TEMPORAL STEPS OF ϵ_r AND SPATIAL MULTILAYERS: CHANGING FILLING FRACTION

In the previous section, we have shown the case where the temporal multisteps have a DC different from 0.5. Here, as a final configuration, we carry out a similar study to the one shown in Figure 4 but considering a single-step function for $\epsilon_{rB}(t)$ while the spatial filling fraction of the spatial multilayer is changed. The schematic representations of the temporal functions for $\epsilon_{rA}(t)$ and $\epsilon_{rB}(t)$ are shown on the top and bottom panels of Figure 5(a), respectively. These functions are then implemented in the vertical spatial multilayer

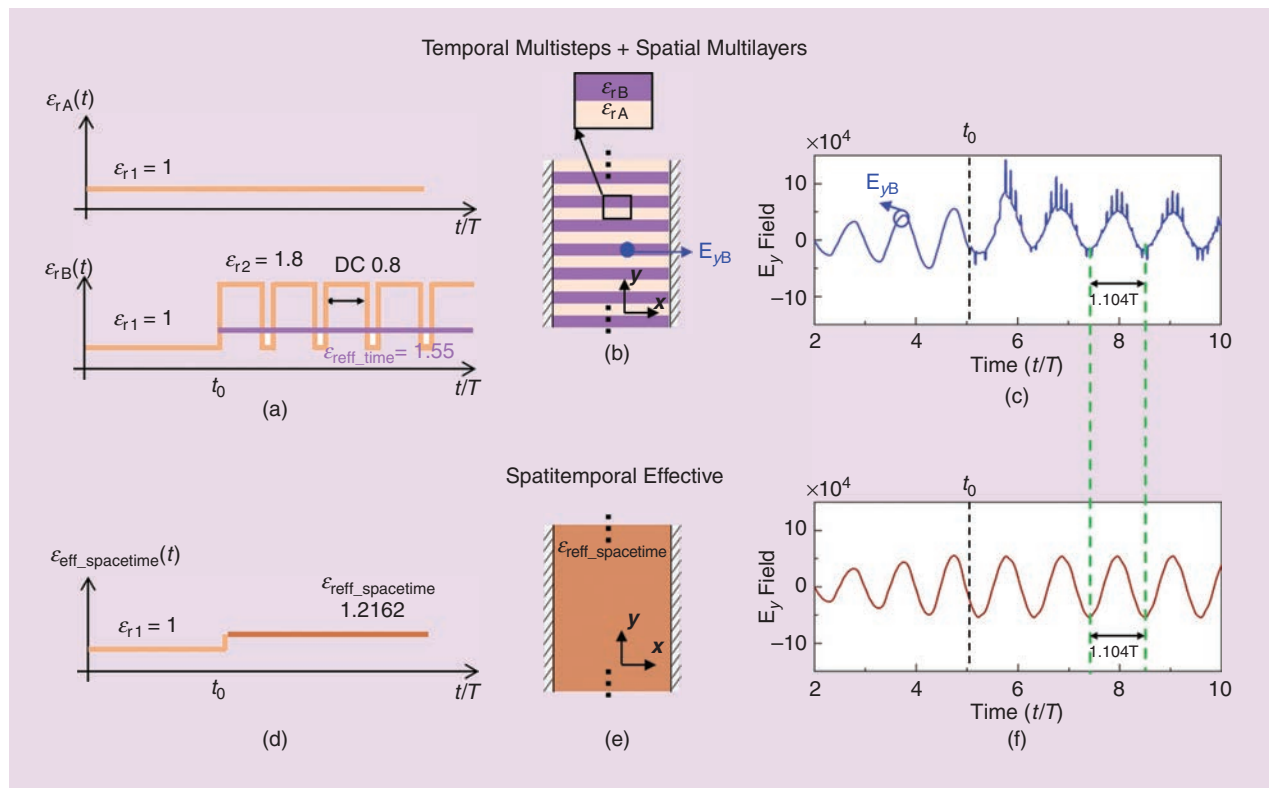


FIGURE 4. Combining horizontal spatial multilayers with temporal multisteps. The temporal functions of ϵ_r for the spatial regions filled with ϵ_{rA} and ϵ_{rB} are shown on the top and bottom panels in (a), respectively, and the schematic of the spatial multilayer is shown in (b). The spacetime effective medium is shown in (d) and (e). The numerical results for the recorded E_y as a function of time within the spacetime structure from (a) and (b) and within the spacetime effective medium from (d) and (e) are shown in (c) and (f), respectively. All these results consider a spatial filling fraction of 0.5 and a temporal duty cycle (DC) of 0.8.

shown in Figure 5(b) (note that we are showing only a section within the cavity, but this spatial multilayer medium is filling the whole cavity as in the previous sections). Finally, a filling fraction of $\Delta x_A = 0.8966$ ($\Delta x_B = 1 - \Delta x_A$) is implemented. With this configuration, we carried out numerical simulations, and the resulting spectral content of the EM signal for times $t > t_0$ within the cavity is shown on the right panel of Figure 5(b) as the black curve (calculated at a spatial location filled with ϵ_{rA}). As observed, the frequency is changed from $f/f_1 = 1$ to $f/f_1 = 0.5$, meaning that the numerically obtained spacetime value of $\epsilon_{\text{eff_spacetime}}$ is $\epsilon_{\text{eff_spacetime}} = 4$ for times $t > t_0$. These results are again in agreement with the theoretical calculations with a value of $\epsilon_{\text{eff_spacetime}} \sim 4$ [using (3b) with $\epsilon_{\text{eff_time}} = \epsilon_{r2} = 30$]. For completeness, the spectrum of the EM signal within the cavity for times $t > t_0$ considering the corresponding spacetime effective medium modeled with a single-step function of

Potential applications may include frequency modulation, temporal signal processing, and reconfigurable metamaterials and metasurfaces.

$\epsilon_r(\epsilon_{r1} = 1 \text{ for } t < t_0 \text{ and changed } \epsilon_{\text{eff_spacetime}} = 4 \text{ at } t = t_0)$ is also shown as the red dashed line on the right panel of Figure 5(b), demonstrating an agreement between the results. Finally, and to demonstrate the flexibility of the design using the proposed spacetime effective medium concept, we used the same functions for $\epsilon_{rA}(t)$ and $\epsilon_{rB}(t)$ as in Figure 5(a) but calculated the required filling fraction for an equivalent horizontal spatial multilayer that can generate the same spacetime effective medium as the one from Figure 5(b).

The resulting structure is shown in Figure 5(c) with a filling fraction of $\Delta y_A = 0.2241$ ($\Delta y_B = 1 - \Delta y_A$) (left panel) along with the spectral content of the EM signal within the cavity for time $t > t_0$ (right panel). From these results, it is clear how the same spacetime effective medium is obtained with an $\epsilon_{\text{eff_spacetime}} \sim 4$.

In terms of potential experimental demonstrations of the proposed spacetime effective medium concept, the structure

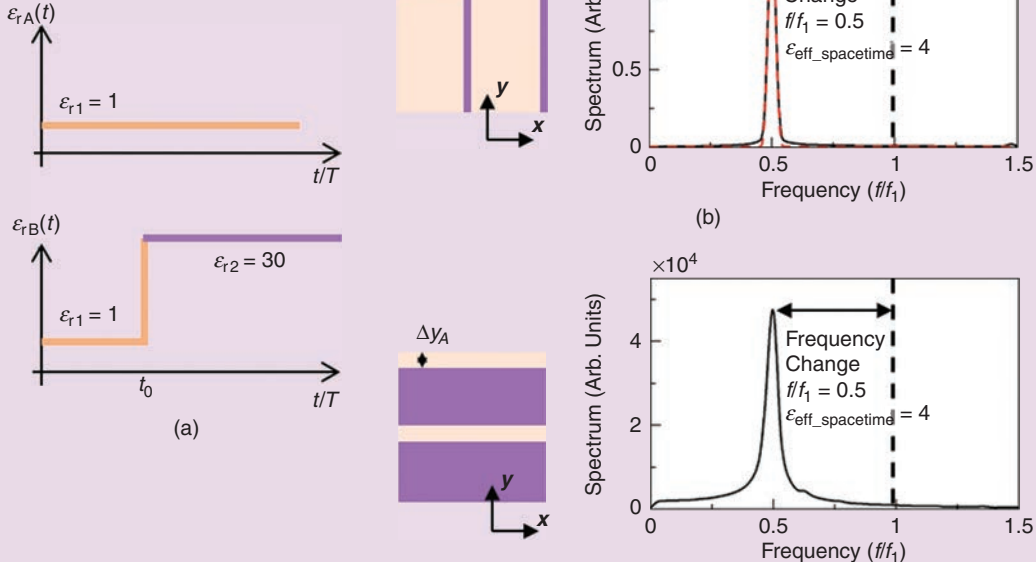


FIGURE 5. Combining spatial multilayers having different filling fractions with a single temporal step. (a) The temporal functions of ϵ_r for the spatial regions filled with ϵ_{rA} and ϵ_{rB} are shown on the top and bottom panels, respectively. (b) The schematic representation of the vertical spatial multilayer with $\Delta x_A = 0.8966$ ($\Delta x_A \sim 0.0448\lambda_1$) is shown on the left panel. The spectral content of the recorded E_y field distribution after $t > t_0$ (calculated within a region filled with ϵ_{rA}) for the vertical spatial multilayer is shown on the right panel of (b) as a black line along with the spectrum for the case using the spacetime effective medium concept (red dashed line). (c) A schematic of a horizontal spatial multilayer emulating the same response as the vertical spatial multilayer from (b) with $\Delta y_A = 0.2241$ ($\Delta y_A \sim 0.0112\lambda_1$), left panel, along with the spectrum of the recorded E_y field distribution (calculated within a region filled with ϵ_{rA}), right panel.

could be implemented by using transmission line techniques via loaded time-dependent circuit elements [66] where these elements could be added periodically in space to emulate the spatial multilayered regions where the ϵ_r is and is not changed in time (ϵ_{rB} and ϵ_{rA} , respectively). This could be more challenging at higher frequencies, such as in the optical domain; however, experimental studies of temporal and spacetime modulated media are an active research topic in various groups worldwide, reporting different configurations [67], [68], [69]. In this context, we are hopeful that our spacetime effective medium concept will be experimentally demonstrated within different frequency ranges in the near future. Potential applications may include frequency modulation, temporal signal processing, and reconfigurable metamaterials and metasurfaces.

CONCLUSIONS

In this work, we have studied the combined effective medium concepts by merging the temporal multistep changes of ϵ_r and spatial multilayers. The structure consisted of a 1D cavity filled with spatially periodic deeply subwavelength multilayers (either horizontal or vertically arranged) having either a constant permittivity or a temporally changing permittivity. Different scenarios were considered for the regions with a temporal permittivity, including single-step functions and temporally periodic multistep changes of ϵ_r . Moreover, studies of the effect of changing the spatial filling fraction as well as the temporal DC were presented. The physics behind the proposed spacetime effective medium concept was presented, and the designs were corroborated via numerical simulations, demonstrating an excellent agreement between the simulations and the theoretical designs. These results may open new avenues in the manipulation of wave propagation at will in 4D using spacetime effective media.

ACKNOWLEDGMENT

This research was sponsored in part by the Newcastle University (Newcastle University Research Fellowship) (to V. P.-P.), and in part by the Simons Foundation/Collaboration on Symmetry-Driven Extreme Wave Phenomena Grant 733684 (to N.E.). This article has supplementary downloadable material available at <https://doi.org/10.1109/MAP.2023.3254480>, provided by the authors.

AUTHOR INFORMATION

Victor Pacheco-Peña (victor.pacheco-peña@newcastle.ac.uk) is an associate professor (senior lecturer) at the School of Mathematics, Statistics and Physics, Newcastle University, NE1 7RU

These results may open new avenues in the manipulation of wave propagation at will in 4D using spacetime effective media.

Newcastle Upon Tyne, U.K. His research interests include light-based computing, metamaterials, space-time media, metasurfaces, plasmonics, and photonics.

Nader Engheta (engheta@seas.upenn.edu) is the H. Nedwill Ramsey Professor at the Department of Electrical and Systems Engineering, University of Pennsylvania, Philadelphia, PA 19104 USA. He received the 2023 Benjamin Franklin Medal in Electrical Engineering and 2020 Isaac Newton Medal and Prize from the Institute of Physics. He is a Life Fellow of IEEE.

REFERENCES

- [1] W. E. Kock, "Metallic delay lenses," *Bell Syst. Tech. J.*, vol. 27, no. 1, pp. 58–82, Jan. 1948, doi: 10.1002/j.1538-7305.1948.tb01331.x.
- [2] W. E. Kock, "Metal-lens antennas," *Proc. IRE*, vol. 34, pp. 828–836, Nov. 1946, doi: 10.1109/JRPROC.1946.232264.
- [3] V. G. Veselago, "The electrodynamics of substances with simultaneously negative values of ϵ and μ ," *Sov. Phys. Uspekhi*, vol. 10, no. 4, pp. 509–514, Apr. 1968, doi: 10.1070/PU1968v01n04ABEH003699.
- [4] N. Engheta and R. Ziolkowski, *Metamaterials: Physics and Engineering Explorations*, 1st ed. Hoboken, NJ, USA: Wiley, 2006.
- [5] L. Solymar and E. Shamonina, *Waves in Metamaterials*. New York, NY, USA: Oxford Univ. Press, 2009.
- [6] W. Cai and V. Shalaev, *Optical Metamaterials Fundamentals and Applications*, 1st ed. New York, NY, USA: Springer-Verlag, 2010.
- [7] C. Caloz and T. Itoh, *Electromagnetic Metamaterials: Transmission Line Theory and Microwave Applications*. Hoboken, NJ, USA: Wiley, 2005.
- [8] G. V. Eleftheriades and K. G. Balmain, *Negative-Refraction Metamaterials: Fundamental Principles and Applications*. Hoboken, NJ, USA: Wiley, 2005.
- [9] I. Liberal and N. Engheta, "Near-zero refractive index photonics," *Nature Photon.*, vol. 11, no. 3, pp. 149–158, Mar. 2017, doi: 10.1038/nphoton.2017.13.
- [10] V. Pacheco-Peña, N. Engheta, S. Kuznetsov, A. Gentsleev, and M. Beruete, "Experimental realization of an epsilon-near-zero graded-index metalens at terahertz frequencies," *Phys. Rev. Appl.*, vol. 8, no. 3, Sep. 2017, Art. no. 034036, doi: 10.1103/PhysRevApplied.8.034036.
- [11] V. Torres et al., "Terahertz epsilon-near-zero graded-index lens," *Opt. Exp.*, vol. 21, no. 7, pp. 9156–9166, Apr. 2013, doi: 10.1364/OE.21.009156.
- [12] B. Edwards, A. Ali, M. E. Young, M. Silveirinha, and N. Engheta, "Experimental verification of epsilon-near-zero metamaterial coupling and energy squeezing using a microwave waveguide," *Phys. Rev. Lett.*, vol. 100, no. 3, Jan. 2008, Art. no. 033903, doi: 10.1103/PhysRevLett.100.033903.
- [13] M. Silveirinha and N. Engheta, "Tunneling of electromagnetic energy through subwavelength channels and bends using ϵ -near-zero materials," *Phys. Rev. Lett.*, vol. 97, Oct. 2006, Art. no. 157403, doi: 10.1103/PhysRevLett.97.157403.
- [14] V. Pacheco-Peña, B. Orazbayev, V. Torres, M. Beruete, and M. Navarro-Cía, "Ultra-compact planoconcave zoned metallic lens based on the fishnet metamaterial," *Appl. Phys. Lett.*, vol. 103, Oct. 2013, Art. no. 183507, doi: 10.1063/1.4827876.
- [15] W. J. Padilla, D. N. Basov, and D. R. Smith, "Negative refractive index metamaterials," *Mater. Today*, vol. 9, nos. 7–8, pp. 28–35, Jul/Aug. 2006, doi: 10.1016/S1369-7021(06)71573-5.
- [16] R. A. Shelby, D. R. Smith, and S. Schultz, "Experimental verification of a negative index of refraction," *Science*, vol. 292, no. 5514, pp. 77–79, Apr. 2001, doi: 10.1126/science.1058847.
- [17] S. A. Tretyakov, "Meta-materials with wideband negative permittivity and permeability," *Microw. Opt. Technol. Lett.*, vol. 31, no. 3, pp. 163–165, Sep. 2001, doi: 10.1002/mop.1387.
- [18] J. B. Pendry, "Negative refraction makes a perfect lens," *Phys. Rev. Lett.*, vol. 85, no. 18, pp. 3966–3969, Oct. 2000, doi: 10.1103/PhysRevLett.85.3966.
- [19] D. R. Smith, W. J. Padilla, D. C. Vier, S. C. Nemat-Nasser, and S. Schultz, "Composite medium with simultaneously negative permeability and permittivity," *Phys. Rev. Lett.*, vol. 84, no. 18, pp. 4184–4187, May 2000.
- [20] N. Mohammadi Estakhri, B. Edwards, and N. Engheta, "Inverse-designed metastructures that solve equations," *Science*, vol. 363, no. 6433, pp. 1333–1338, Mar. 2019, doi: 10.1126/science.aaw2498.



- [21] F. Zangeneh-Nejad and R. Fleury, "Topological analog signal processing," *Nature Commun.*, vol. 10, no. 1, pp. 1–10, May 2019, doi: 10.1038/s41467-019-10086-3.
- [22] A. Cordaro, H. Kwon, D. Sounas, A. F. Koenderink, A. Alù, and A. Polman, "High-index dielectric metasurfaces performing mathematical operations," *Nano Lett.*, vol. 19, no. 12, pp. 8418–8423, Dec. 2019, doi: 10.1021/acs.nanolett.9b02477.
- [23] T. Knightley, A. Yakovlev, and V. Pacheco-Peña, "Neural network design of multilayer metamaterial for temporal differentiation," *Adv. Opt. Mater.*, vol. 11, no. 5, Mar. 2023, Art. no. 2202351, doi: 10.1002/adom.202202351.
- [24] E. Lier, D. H. Werner, C. P. Scarborough, Q. Wu, and J. A. Bossard, "An octave-bandwidth negligible-loss radiofrequency metamaterial," *Nature Mater.*, vol. 10, no. 3, pp. 216–222, Mar. 2011, doi: 10.1038/nmat2950.
- [25] S. Legaria, J. Teniente, S. Kuznetsov, V. Pacheco-Peña, and M. Beruete, "Highly efficient focusing of terahertz waves with an ultrathin superoscillatory metascreen: Experimental demonstration," *Adv. Photon. Res.*, vol. 2, no. 9, Sep. 2021, Art. no. 2000165, doi: 10.1002/adpr.202000165.
- [26] Y. Wang et al., "Electrical tuning of phase-change antennas and metasurfaces," *Nature Nanotechnol.*, vol. 16, no. 6, pp. 667–672, Jun. 2021, doi: 10.1038/s41565-021-00882-8.
- [27] X. G. Zhang et al., "Polarization-controlled dual-programmable metasurfaces," *Adv. Sci.*, vol. 7, no. 11, pp. 1–10, Apr. 2020, doi: 10.1002/advs.201903382.
- [28] G. V. Eleftheriades, M. Kim, V. G. Ataloglu, and A. H. Dorrah, "Prospects of Huygens' metasurfaces for antenna applications," *Engineering*, vol. 11, pp. 21–26, Apr. 2022, doi: 10.1016/j.eng.2021.05.011.
- [29] M. Mischiglio et al., "Approximate analog computing with metatronic circuits," *Commun. Phys.*, vol. 4, no. 1, Dec. 2021, Art. no. 196, doi: 10.1038/s42005-021-00683-4.
- [30] Y. Li, I. Liberal, and N. Engheta, "Dispersion synthesis with multi-ordered metatronic filters," *Opt. Exp.*, vol. 25, no. 3, pp. 1937–1948, Feb. 2017, doi: 10.1364/OE.25.001937.
- [31] S. Jiang et al., "Flexible metamaterial electronics," *Adv. Mater.*, vol. 34, no. 52, Jul. 2022, Art. no. e2200070, doi: 10.1002/adma.202200070.
- [32] B. Orazbayev, N. Mohammadi Estakhri, M. Beruete, and A. Alù, "Terahertz carpet cloak based on a ring resonator metasurface," *Phys. Rev. B*, vol. 91, no. 19, May 2015, Art. no. 195444, doi: 10.1103/PhysRevB.91.195444.
- [33] A. Alù and N. Engheta, "Achieving transparency with plasmonic and metamaterial coatings," *Phys. Rev. E*, vol. 72, no. 1, Jul. 2005, Art. no. 016623, doi: 10.1103/PhysRevE.72.016623.
- [34] B. Orazbayev, M. Beruete, A. Martínez, and C. García-Meca, "Diffusive-light invisibility cloak for transient illumination," *Phys. Rev. A*, vol. 94, no. 6, Dec. 2016, Art. no. 063850, doi: 10.1103/PhysRevA.94.063850.
- [35] J. B. Pendry, D. Schurig, and D. R. Smith, "Controlling electromagnetic fields," *Science*, vol. 312, no. 5781, pp. 1780–1782, Jun. 2006, doi: 10.1126/science.1125907.
- [36] E. J. R. Vesseur, T. Coenen, H. Caglayan, N. Engheta, and A. Polman, "Experimental verification of n=0 structures for visible light," *Phys. Rev. Lett.*, vol. 110, no. 1, Jan. 2013, Art. no. 013902, doi: 10.1103/PhysRevLett.110.013902.
- [37] H. Jung et al., "Electrically controllable molecularization of terahertz meta-atoms," *Adv. Mater.*, vol. 30, no. 31, Jun. 2018, Art. no. 1802760, doi: 10.1002/adma.201802760.
- [38] M. Beruete, N. Engheta, and V. Pacheco-Peña, "Experimental demonstration of deeply subwavelength dielectric sensing with epsilon-near-zero (ENZ) waveguides," *Appl. Phys. Lett.*, vol. 120, no. 8, Feb. 2022, Art. no. 081106, doi: 10.1063/5.0079665.
- [39] M. Nicolussi, J. A. Riley, and V. Pacheco-Peña, "Unidirectional transparency in epsilon-near-zero based rectangular waveguides induced by parity-time symmetry," *Appl. Phys. Lett.*, vol. 119, no. 26, Dec. 2021, Art. no. 263507, doi: 10.1063/5.0076236.
- [40] J. Shi et al., "THz photonics in two dimensional materials and metamaterials: Properties, devices and prospects," *J. Mater. Chem. C*, vol. 6, no. 6, pp. 1291–1306, Jan. 2018, doi: 10.1039/C7TC05460B.
- [41] L. H. Nicholls et al., "Ultrafast synthesis and switching of light polarization in nonlinear anisotropic metamaterials," *Nature Photon.*, vol. 11, no. 10, pp. 628–633, Sep. 2017, doi: 10.1038/s41566-017-0002-6.
- [42] C. Caloz and Z.-L. Deck-Léger, "Spacetime metamaterials—Part I: General concepts," *IEEE Trans. Antennas Propag.*, vol. 68, no. 3, pp. 1569–1582, Mar. 2020, doi: 10.1109/TAP.2019.2944225.
- [43] C. Caloz and Z.-L. Deck-Léger, "Spacetime metamaterials—Part II: Theory and applications," *IEEE Trans. Antennas Propag.*, vol. 68, no. 3, pp. 1583–1598, Mar. 2020, doi: 10.1109/TAP.2019.2944216.
- [44] F. Morgenthaler, "Velocity modulation of electromagnetic waves," *IEEE Trans. Microw. Theory Techn.*, vol. 6, no. 2, pp. 167–172, Apr. 1958, doi: 10.1109/TMTT.1958.1124533.
- [45] R. Fante, "Transmission of electromagnetic waves into time-varying media," *IEEE Trans. Antennas Propag.*, vol. 19, no. 3, pp. 417–424, May 1971, doi: 10.1109/TAP.1971.1139931.
- [46] V. Pacheco-Peña and N. Engheta, "Antireflection temporal coatings," *Optica*, vol. 7, no. 4, Apr. 2020, Art. no. 323, doi: 10.1364/OPTICA.381175.
- [47] D. Ramaccia, A. Alù, A. Toscano, and F. Bilotti, "Temporal multilayer structures for designing higher-order transfer functions using time-varying metamaterials," *Appl. Phys. Lett.*, vol. 118, no. 10, Mar. 2021, Art. no. 101901, doi: 10.1063/5.0042567.
- [48] G. Castaldi, V. Pacheco-Peña, M. Moccia, N. Engheta, and V. Galdi, "Exploiting space-time duality in the synthesis of impedance transformers via temporal metamaterials," *Nanophotonics*, vol. 10, no. 14, pp. 3687–3699, Aug. 2021, doi: 10.1515/nanoph-2021-0231.
- [49] V. Pacheco-Peña, Y. Kiasat, B. Edwards, and N. Engheta, "Salient features of temporal and spatio-temporal metamaterials," in *Proc. Int. Conf. Electromagn. Adv. Appl. (ICEAA)*, 2018, pp. 524–526, doi: 10.1109/ICEAA.2018.8520356.
- [50] P. A. Huidobro, E. Galiffi, S. Guenneau, R. V. Craster, and J. B. Pendry, "Fresnel drag in space-time-modulated metamaterials," *Proc. Natl. Acad. Sci.*, vol. 116, no. 50, pp. 24,943–24,948, Dec. 2019, doi: 10.1073/pnas.1915027116.
- [51] S. Yin and A. Alù, "Efficient phase conjugation in a space-time leaky waveguide," *ACS Photon.*, vol. 9, no. 3, pp. 5–10, Feb. 2022, doi: 10.1021/acspophotonics.1c01836.
- [52] A. Akbarzadeh, N. Chamanara, and C. Caloz, "Inverse prism based on temporal discontinuity and spatial dispersion," *Opt. Lett.*, vol. 43, no. 14, pp. 3297–3300, 2018, doi: 10.1364/OL.43.003297.
- [53] V. Pacheco-Peña and N. Engheta, "Temporal aiming," *Light Sci. Appl.*, vol. 9, no. 129, pp. 1–12, Dec. 2020, doi: 10.1038/s41377-020-00360-1.
- [54] D. M. Solís and N. Engheta, "Functional analysis of the polarization response in linear time-varying media: A generalization of the Kramers-Kronig relations," *Phys. Rev. B*, vol. 103, no. 14, Apr. 2021, Art. no. 144303, doi: 10.1103/PhysRevB.103.144303.
- [55] Z. Hayran, A. Chen, and F. Monticone, "Spectral causality and the scattering of waves," *Optica*, vol. 8, no. 8, Jun. 2021, Art. no. 1040, doi: 10.1364/OPTICA.423089.
- [56] V. Pacheco-Peña and N. Engheta, "Spatiotemporal isotropic-to-anisotropic meta-atoms," *New J. Phys.*, vol. 23, no. 9, Sep. 2021, Art. no. 095006, doi: 10.1088/1367-2630/ac21df.
- [57] G. Ptitsyn, M. S. Mirmoosa, and S. A. Tretyakov, "Time-modulated meta-atoms," *Phys. Rev. Res.*, vol. 1, no. 2, pp. 1–11, Sep. 2019, doi: 10.1103/PhysRevResearch.1.023014.
- [58] M. S. Mirmoosa, G. A. Ptitsyn, V. S. Asadchy, and S. A. Tretyakov, "Time-varying reactive elements for extreme accumulation of electromagnetic energy," *Phys. Rev. Appl.*, vol. 11, no. 1, Jan. 2019, Art. no. 014024, doi: 10.1103/PhysRevApplied.11.014024.
- [59] M. Lyubarov, Y. Lumer, A. Dikopoltsev, E. Lustig, Y. Sharabi, and M. Segev, "Amplified emission and lasing in photonic time crystals," *Science*, vol. 377, no. 6604, pp. 425–428, Jun. 2022, doi: 10.1126/science.abo3324.
- [60] E. Galiffi et al., "Photonics of time-varying media," *Adv. Photon.*, vol. 4, no. 1, pp. 1–32, Feb. 2022.
- [61] V. Pacheco-Peña and N. Engheta, "Effective medium concept in temporal metamaterials," *Nanophotonics*, vol. 9, no. 2, pp. 379–391, Dec. 2020, doi: 10.1515/nanoph-2019-0305.
- [62] P. A. Huidobro, M. G. Silveirinha, E. Galiffi, and J. B. Pendry, "Homogenization theory of space-time metamaterials," *Phys. Rev. Appl.*, vol. 16, no. 1, Jul. 2021, Art. no. 014044, doi: 10.1103/PhysRevApplied.16.014044.
- [63] A. Silhola, *Electromagnetic Mixing Formulas and Applications*, 1st ed. London, U.K.: Inst. Elect. Eng., 1999.
- [64] V. Pacheco-Peña and N. Engheta, "Temporal metamaterials with gain and loss," Aug. 2021, arXiv:2108.01007.
- [65] COMSOL Multiphysics. COMSOL. [Online]. Available: <https://www.comsol.com/>
- [66] S. Qin, Q. Xu, and Y. E. Wang, "Nonreciprocal components with distributedly modulated capacitors," *IEEE Trans. Microw. Theory Techn.*, vol. 62, no. 10, pp. 2260–2272, Oct. 2014, doi: 10.1109/TMTT.2014.2347935.
- [67] J. P. Turpin, J. A. Bossard, K. L. Morgan, D. H. Werner, and P. L. Werner, "Reconfigurable and tunable metamaterials: A review of the theory and applications," *Int. J. Antennas Propag.*, vol. 2014, pp. 1–18, May 2014, doi: 10.1155/2014/429837.
- [68] K. Lee et al., "Linear frequency conversion via sudden merging of meta-atoms in time-variant metasurfaces," *Nature Photon.*, vol. 12, no. 12, pp. 765–773, Dec. 2018, doi: 10.1038/s41566-018-0259-4.
- [69] S. F. Preble, Q. Xu, and M. Lipson, "Changing the colour of light in a silicon resonator," *Nature Photon.*, vol. 1, no. 5, pp. 293–296, May 2007, doi: 10.1038/nphoton.2007.72.

Generalized Space-Time Engineered Modulation (GSTEM) Metamaterials

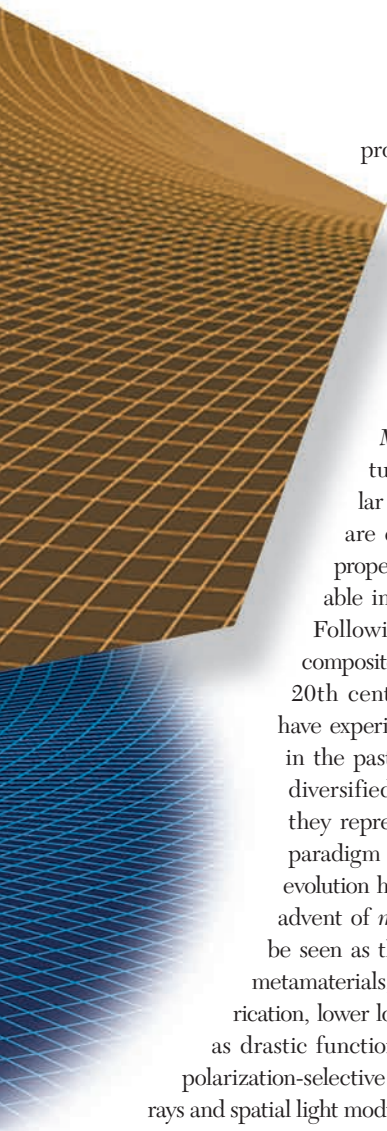
IMAGE LICENSED BY INGRAM PUBLISHING

A global and extended perspective.

This article presents a global and extended perspective of electrodynamic metamaterials formed by space and time engineered modulations, which we name *generalized space-time engineered modulation (GSTEM) metamaterials*, or *GSTEMs*. This perspective describes metamaterials from a unified *spacetime viewpoint* and introduces *accelerated metamaterials* as an extra type of dynamic metamaterials. First, it positions GSTEMs in the even broader context of electrodynamic systems that include (nonmodulated) moving sources in vacuum and moving bodies, explains the difference between

the moving-matter nature of the latter and the moving-perturbation nature of GSTEMs, and enumerates the different types of GSTEMs considered, namely space EMs (SEMs), time EMs (TEMs), uniform space-time EMs (USTEMs), and accelerated space-time EMs (ASTEMs). Next, it establishes the physics of the related interfaces, which includes direct-spacetime scattering and inverse-spacetime transition transformations. Then, it exposes the physics of the GSTEMs formed by stacking these interfaces and homogenizing the resulting crystals; this includes an original explanation of light deflection by USTEMs as being a *spacetime weighted averaging phenomenon* and the demonstration of ASTEM light curving and black hole light attraction. Finally, it discusses some future

Digital Object Identifier 10.1109/MAP.2022.3216773
Date of current version: 16 December 2022



prospects. Useful complementary information and animations are provided in the downloadable supplementary materials available at <http://doi.org/10.1109/MAP.2022.3216773>.

INTRODUCTION

Metamaterials are artificial structures consisting of supramolecular but subwavelength particles that are engineered to provide medium properties beyond (*μετά*) those available in conventional materials [1]–[3]. Following rudimentary ancient nanocomposites, medieval stained glasses, and 20th century artificial dielectrics, they have experienced spectacular developments in the past two decades, where they have diversified and expanded to a point that they represent nowadays a powerful new paradigm in science and technology. This evolution has been largely facilitated by the advent of *metasurfaces* [4], [5], which may be seen as the 2D counterpart of voluminal metamaterials, with the benefits of easier fabrication, lower loss, and greater flexibility as well as drastic functional extensions of frequency- or polarization-selective surfaces, reflect- or transmittarays and spatial light modulators.

Most of the metamaterials and metasurfaces investigated until recently have been *static*, i.e., modulated only in space; we shall therefore refer to them as *SEMs*. A major advance in the field has been realized by making metamaterials *dynamic*, either by replacing the space modulation by a time modulation or by adding a time modulation to the space modulation. This introduction of the *dimension of time* as a new structural medium parameter has resulted in the metamaterial classes of *TEM metamaterials*, or *TEMs* [6]–[18], and *STEM metamaterials*, or *STEMs* [19]–[40]. [Note: The terminology “time-modulated metamaterials” and “space-time modulated metamaterials” applies to metamaterials that already have a spatial modulation *before* being temporally modulated, but *not to*—equally relevant!—metamaterials whose dynamic structure is really *formed* (and *engineered*) by a time or space-time modulation. Hence our introduction of the *general* terms *TEMs* and *STEMs*, and related terminology in Table 1.] Specifically, *TEMs* and *STEMs* are metamaterials that are formed by the variation (modulation) of a medium parameter in time and in both space and time, respectively, induced by an external drive. In the case of electromagnetic metamaterials, on which this article focuses, the modulated parameter may be the refractive index, the permittivity, the permeability, or any of the bianisotropic and higher order spatial-dispersion constitutive parameters and combination thereof, while the modulation drive may be acoustic (e.g.,

surface/bulk acoustic waves in a piezoelectric crystal), electronic (e.g., electric voltage variations in varactor chips), optical (e.g., laser pulses in semiconductor slabs), etc. [41], [42]. *TEMs* and *STEMs* may thus be seen as *medium—generally 3 + 1D, or 4D—extensions* of electronic and optical active lumped element and circuit systems, such as parametric amplifiers [43], [44] and acoustoelectric/optic modulators [45], [46].

This article presents a global and extended perspective of dynamic metamaterials. The *global aspect* consists of describing all metamaterials, including *SEMs* and *TEMs*, in terms of *space-time*—or *spacetime*—modulations, with various degrees of complexity and in connection with the physics of moving bodies, while the extended aspect concerns the generalization of *STEMs* with *uniform* (constant in both space and time) modulation velocity, i.e., *USTEM metamaterials*, or *USTEMs*, to *STEMs* with accelerated modulation, i.e., *ASTEM metamaterials*, or *ASTEMs*. [Note: The two spellings (with and without a hyphen) of the word *spacetime* are found in the literature on dynamic systems, whether for the noun or for the adjective. The one-word spelling is the universal standard when referring to the mathematical model that describes the merged nature of the space and time dimensions into a four-dimensional manifold in relativity physics (e.g., curved spacetime), while the spelling with a hyphen is preferable in reference to modulated structures, where the spatial and temporal features of the modulation are distinct and may exist independently of each other (e.g., space-time modulated metasurface). The present article follows this convention.] We shall refer to these diverse possible types of metamaterials as *GSTEMs*, where it is noted that *ASTEMs* may feature different orders (derivatives) of acceleration and, hence, subdivide in further classes. Table 1 summarizes the terminology.

RELATED ELECTRODYNAMIC SYSTEMS

Electromagnetic *GSTEMs* are not the only *electrodynamic systems*. They represent only the category of *moving-perturbation* (or moving-modulation) electrodynamic systems. Two other fundamental types of electrodynamic systems should be considered here, *vacuum moving-source* systems and *moving-matter* (or moving-body) systems [47], because *GSTEMs* support physical effects that are inherited from them, although, as we shall see, in distinct embodiments. We shall next describe and compare the three categories, with the help of the illustrations provided in Figure 1.

Vacuum moving-source systems, illustrated in Figure 1(a), are systems involving objects (e.g., star or car) that emit or reflect light while moving in *vacuum* relatively to the observer (e.g., Earth or road), with *vacuum* being defined as a portion of space that is essentially devoid of matter. [Note: We use here the term “light”, as commonly done in the optics community, to designate electromagnetic waves and photons of any frequency or wavelength, for brevity, but a broader spectrum, including radio and terahertz waves, is implicitly assumed.] The earliest reported related effect is the *Bradley aberration* [Figure 1(a), top panel], whereby a terrestrial observer sees a star in a direction that is tilted toward the direction of the motion of Earth in

its orbit around the sun [48]. Another effect, which commonly manifests itself in daily life with sound sources, is the *Doppler shift* [Figure 1(a), bottom panel], whereby an observer of a moving source sees the frequency of the wave emitted or reflected by that source as depending on its velocity, with larger and lower frequency for approaching and receding motion, respectively [49]. Vacuum moving-source systems are the simplest electrodynamic systems since they are restricted to light propagation without light-matter interaction.

Moving-matter/body systems, illustrated in Figure 1(b), are systems involving *matter* (e.g., water or dielectric) that moves relatively to the observer (e.g., a laboratory experimenter) and that supports the propagation of light emitted from the reference frame of the observer, with matter motion defined as a collective translation or/and rotation of atoms and molecules over

distances that are much larger than the molecular scale; these systems involve thus typically moving solids, fluids or gases. A related effect is the *Fresnel-Fizeau drag* [Figure 1(b), top panel], whereby the speed of light is reduced or increased for downstream or upstream propagation in a moving fluid [50], [51]. Another effect that is of major importance in electrodynamics is *Röntgen magnetoelectric coupling* [Figure 1(b), bottom panel], whereby the motion (here, the rotation) of a solid submitted to an electric field induces a magnetic field in the frame of a rest observer due to the creation of surface polarization currents [52], [53]. Moving-matter/body systems are more complex than vacuum moving-source systems because of the addition of their matter drag and magnetoelectric-coupling effects on top of the aberration and Doppler shift effects occurring in vacuum moving-source systems.

Finally, *moving-perturbation/modulation systems*, illustrated in Figure 1(c), are systems involving a *perturbation* (e.g., an acoustic wave in a piezoelectric crystal) that moves relatively to the observer (e.g., a frame of an optical or microwave device) and that scatters light emitted from the reference frame of the observer, with perturbation motion defined as a traveling-wave (or standing-wave) *modulation* of some electromagnetic medium parameter, *without any net transfer of matter*, i.e., with motion restricted to oscillations of bound charges over submolecular distances (dielectric or magnetic polarization). [Note: Thermodynamics provides an insightful analogy to distinguish moving perturbation and moving matter in associating the former with heat conduction and the latter with heat convection.] A common example of such a system is the *acousto-optic modulator (AOM)*

TABLE 1. TERMINOLOGY AND ACRONYMS.

EM	Engineered Modulation (metamaterial)
SEM	Space EM
TEM	Time EM
STEM	Space-Time EM
USTEM	Uniform (-velocity) Space-Time EM
ASTEM	Accelerated Space-Time EM
GSTEM	Generalized Space-Time EM

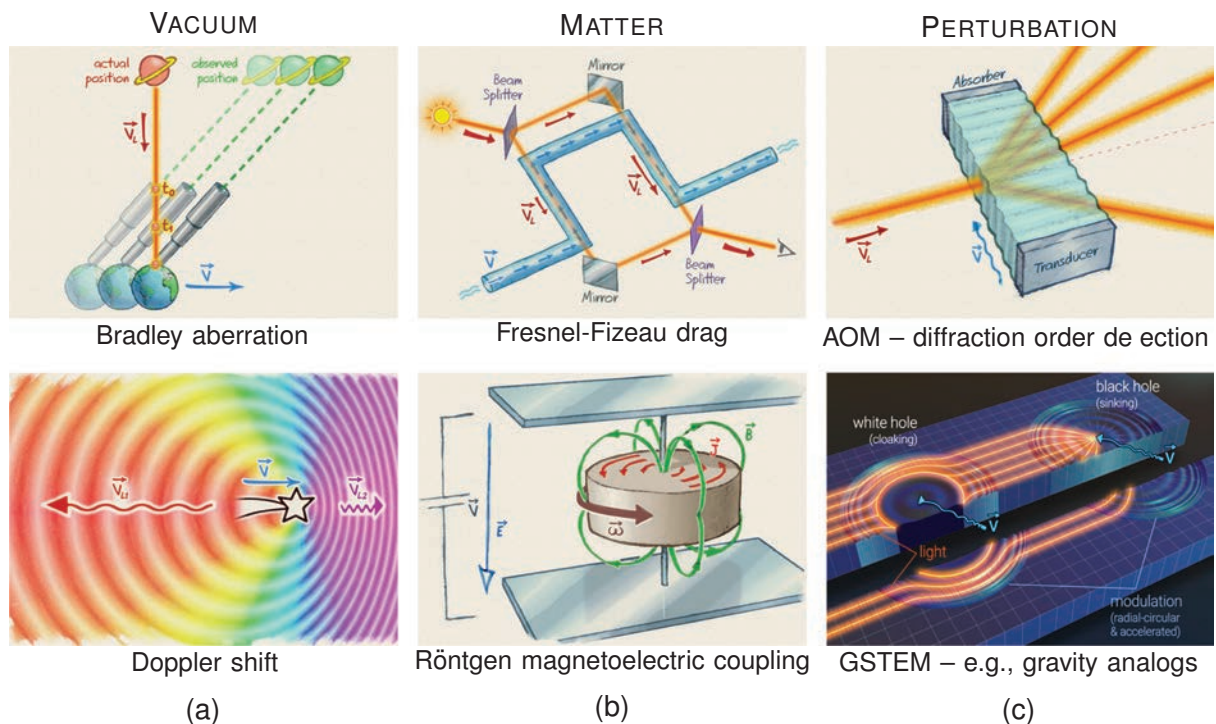


FIGURE 1. Different types of electrodynamic systems and related physical effects. (a) Moving sources in vacuum. (b) Moving matter or bodies. (c) Moving perturbation or modulation. AOM: acousto-optic modulator.

[Figure 1(c), top panel], whereby a periodic propagating perturbation (“spacetime modulation grating”), induced by variations of the molecular density of the medium from an electric signal (piezoelectricity), *deflects the diffraction* orders of the incident light in the direction of the perturbation via Bragg-Brillouin scattering [45], [46]. GSTEMs [Figure 1(c), bottom panel], particularly USTEMs and ASTEMs, belong to this category of electrodynamic systems, where they generalize AOM-type systems to multidimensional ($2 + 1\text{D} = 3\text{D}$ and $3 + 1\text{D} = 4\text{D}$), multivelocity (uniform or nonuniform) [54], homogenized [38] and “new-physics” [36], [37] electrodynamic systems.

MOVING PERTURBATION VERSUS MOVING MATTER

Figure 2 compares the electrodynamic structures of the moving-matter/body systems [Figure 1(b)] on the one hand and the moving-perturbation/modulation systems [Figure 1(c)], which include GSTEMs, on the other hand. Figure 2(a) shows a moving-matter system (e.g., a sliding curling stone), where the atoms and molecules (matter) move together with the body, along with the comoving frame, K' , at a velocity v with respect to the (fixed) laboratory frame, K . Figure 2(b) shows a moving-perturbation system (e.g., a dielectric slab excited by a laser-pump pulse or piezoelectric slab excited by a voltage source). In this case, the atoms and molecules oscillate about their bound position within the (solid) body, under the polarizing effect of the drive excitation, but do not experience any net motion in K . Only the related two perturbation interfaces move, inducing a STEM *pulse modulation* of the form $n(z, t) = n_0 + \Delta n \cdot \Pi[(z - v_m t)/D_m]$, where n_0 is the average refractive index, Δn is the modulation depth, $\Pi(\cdot)$ is the pulse

function, D_m is the spatial extent of the pulse and $v_m = v$ is the velocity of the corresponding perturbation. Note that the atoms and molecules, while stationary in K , move with respect to K , in the opposite direction, with velocity $v'_{\text{atom}} = -v$.

Figure 2(c) shows a continuous (periodic) version of the pulse structure in Figure 2(b) (e.g., using a periodically pulsed laser-pump or electroacoustic drive), with the STEM medium function $n(z, t) = n_0 + \Delta n \cdot \text{sgn}[(\cos(k_m z - \omega_m t) + 1)/2]$, where $\text{sgn}(\cdot)$ is the sign function, and k_m and ω_m , with $v_m = \omega_m/k_m$, are the spatial and temporal frequencies, respectively, of the modulation. Finally, Figure 2(d) shows a variant of Figure 2(c), where the drive excites the system from the top of the structure (e.g., an oblique laser pump illumination or electroacoustic source), under an angle θ with respect to the propagation axis, which provides *superluminal* modulation with velocity $v_m = v_{mz} = c/\sin \theta$ [36], reducing to instantaneous (pure time) modulation for $\theta = 0$.

Moving perturbation/modulation systems [Figure 2(b)–(d)], and particularly GSTEMs, are more promising than their moving-matter/body counterparts [Figure 2(a)] toward real-life applications because 1) they do not require cumbersome moving parts; 2) they easily attain relativistic velocities and accelerations; and 3) they possess richer functionality potential, resulting both from their dimensional extension of previous modulated systems and from their capability to mimic and transcend cosmological systems (e.g., equivalent horizons and black holes; superluminality and negative mass equivalent) [55], [56]. These are the reasons why GSTEMs are so attractive at this point of research in the field of metamaterials. We shall hereafter restrict our attention to GSTEMs and refer to the

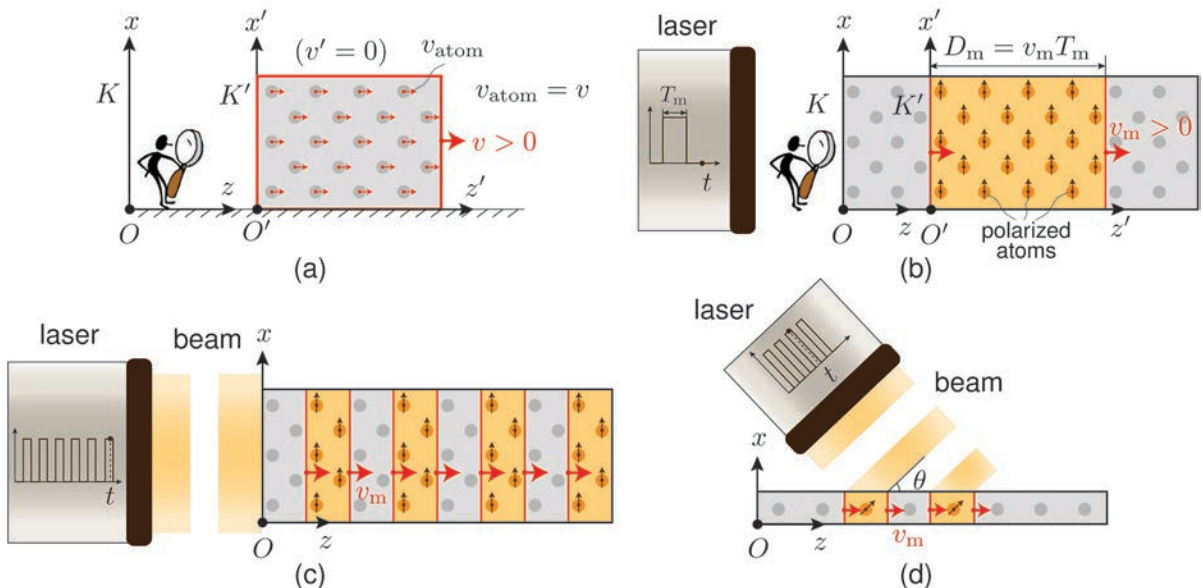


FIGURE 2. Comparison of the electrodynamic structures of the media involved in Figure 1(b) and (c). (a) Moving (matter) body. (b) Moving (perturbation) modulation. (c) Periodic version of (b). (d) Oblique excitation version of (c), where $v_m = v_{mz} = c/\sin \theta$, with even greater diversity attainable with a SEM or STEM mask at the output of the laser. Although the figures consider the specific example of laser-driven modulations, the principle holds for any type of modulation (optical, electronic, acoustic, mechanical, chemical, etc.) [41], [42].

moving-matter/body dynamic systems only for the purpose of structural or property comparison.

PERSPECTIVE AND GENERALIZATION

Figure 3 depicts the proposed *global and extended perspective* of GSTEMs. The central part of the figure lists the related metamaterials—SEMs, TEMs, USTEMs, and ASTEMs (Table 1)—in the order of increasing dynamics generality from the bottom up. The periphery of the figure shows the spacetime (or Minkowski) diagrams [57] corresponding to the four main types of GSTEMs considered in this article, with suggestive artistic illustrations (supplementary material section A). Such a global perspective offers multiple benefits, including 1) an elegant *classification*, based on the natural concept of spacetime structuration; 2) a powerful *unification*, suggesting insightful comparisons and cross-fertilization concepts (e.g., time duals of space systems [15], [58], [59] or space-time extensions of pure space/time systems [35], [60]); and 3) a *connection* to the physics of special relativity [61], [62], [63] and general relativity [62], [64], [65] (supplementary material section B.1), which rather involves sources [Figure 1(a)] or bodies [Figure 1(b)] moving in vacuum.

The concept of a *continuous medium* [66] is an idealization. In reality, all materials are formed by a more or less (crystal or amorphous) periodic collection of particles—atoms and molecules in the case of conventional materials and resonant scatterers in the case of metamaterials—which subtend the macroscopic response of the medium in terms of dipolar/

multipolar responses at the microscopic scale. All materials can therefore be represented as periodically alternating regions of vacuum and particles, as suggested by the alternating gray-golden bands in the spacetime diagrams of Figure 3. This is true even when the medium exhibits a gradual variation, such as a GSTEM with the common sinusoidal modulation $n(z, t) = n_0 + \Delta n \cos(k_m z - \omega_m t)$, with $\lambda_m = 2\pi/k_m$ and $T_m = 2\pi/\omega_m$, which may be considered as a gradual version of the structure in Figure 3 and which is common in practice. In the *metamaterial—subwavelength and subperiod regime*, corresponding to the twofold condition $\lambda_m \ll \lambda$ and $T_m \ll T$, where λ and T are the smallest wavelength and period of the wave, respectively, the wave propagating in the medium is myopic to such fine detail of the sinusoidal modulation; it probes only the index extrema, with blurred transitions between them, and the modulation can therefore be safely approximated by the discrete *bilayer function* $n(z, t) = n_0 + \Delta n \cdot \text{sgn}[\cos(k_m z - \omega_m t) + 1]/2$ [“Moving Perturbation Versus Moving Matter” section and Figure 2(c)]. [Note: Although this article focuses on the metamaterial (i.e., homogeneous) regime, the concepts of GSTEMs naturally extend to the Bragg regime, where the GSTEM structures, better called then GSTEM *crystals*, exhibit interesting oblique bandgap configurations and physical properties [19], [30], [35].] Thus, the spacetime diagrams of GSTEMs can *generally* be represented by the periodic bilayer spacetime patterns shown in Figure 3.

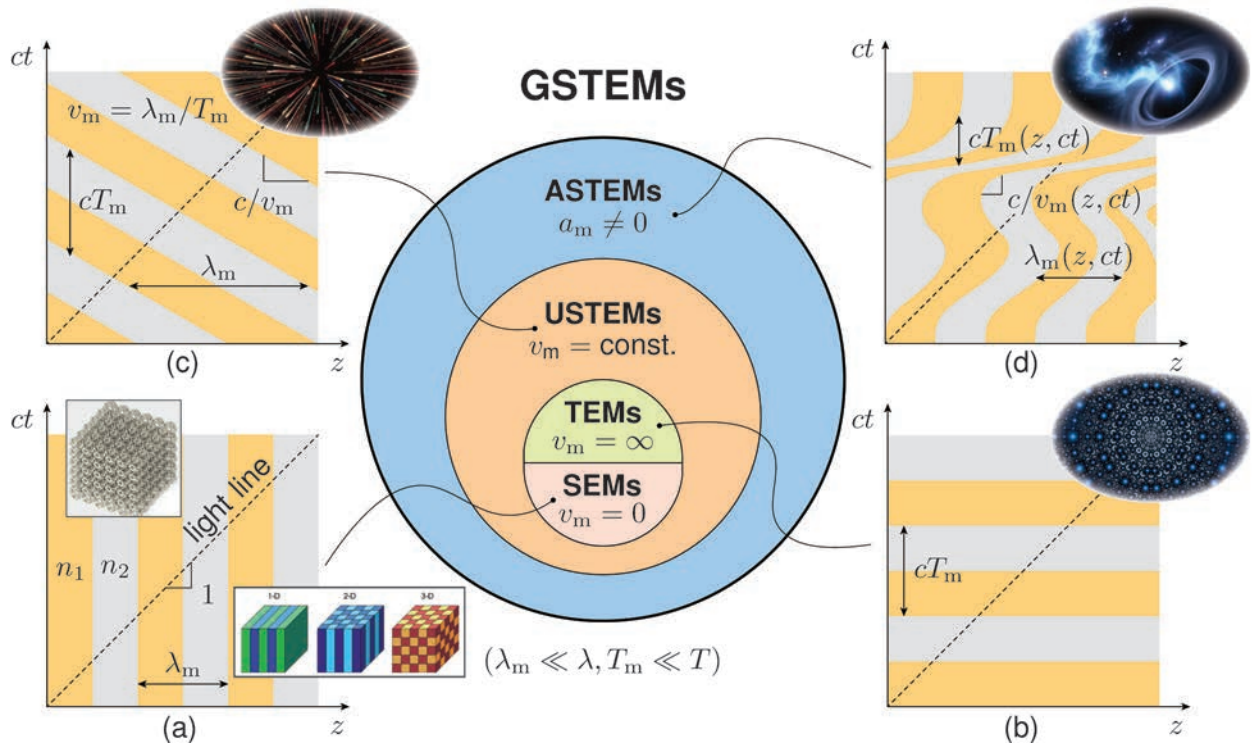


FIGURE 3. GSTEMs. (a) SEMs. (b) TEMs. (c) USTEMs. (d) ASTEMs. The subscript “m” refers to “modulation”, n_1 and n_2 are the refractive indices of the constituent media, which are assumed to be isotropic and nondispersive, and z represents the spacetime hyperspace, which may include up to three spatial dimensions (x, y, z). Const.: constant.

SEMs [Figure 3(a)] are GSTEMs whose parameters vary only in space. They represent the particular static limit case of GSTEMS with zero modulation velocity, $v_m = 0$, and include conventional metamaterials [1]–[3] as well as photonic crystals in the long-wavelength regime [67]. The TEMs in Figure 3(b) are GSTEMs whose features do not vary in space but in time, as with some parametric amplifiers [43] and solid-state time crystals [68], [69]. They represent the particular *instantaneous* limit case of GSTEMS with infinite modulation velocity, $v_m = \infty$ [6]–[18]. We have next actual STEMs, with modulation occurring both in space and in time. USTEMs [Figure 3(c)] are characterized by a constant modulation velocity, $v_m = \text{const.}$, as typical acousto-optical modulators [top panel of Figure 1(c)] [19]–[40], while ASTEMs [Figure 3(d)], introduced only recently [54], are characterized by an accelerated modulation, $a_m \neq 0$, which may be constant in the moving frame (constant proper acceleration), or have nonzero temporal derivatives—jerk ($\partial a_m / \partial t \neq 0$), snap ($\partial^2 a_m / \partial t^2 \neq 0$), crackle ($\partial^3 a_m / \partial t^3 \neq 0$), pop ($\partial^4 a_m / \partial t^4 \neq 0$), etc. [70].

INTERFACE PHYSICS

As discussed in the “Perspective and Generalization” section and illustrated by the spacetime diagrams in Figure 3, GSTEMs can be modeled by alternating isotropic medium layers. The *interfaces* delimiting these layers are therefore the main discontinuities or nonuniformities of the structure and represent hence the entities that underpin the light-matter interaction of the metamaterial. For this reason, this section is dedicated to GSTEM interfaces, while the “Metamaterial Physics” section will reveal how the related principles extend to complete GSTEM media.

Let us start with the simplest cases of SEM and TEM interfaces. The electrodynamics of these interfaces is described in Figure 4, with Figure 4(a) and (b) representing the SEM and TEM cases, respectively [37]. When a wave hits a simple interface, or *SEM interface*, it splits into a reflected wave and a transmitted wave, which propagate in opposite directions over time, with well-known scattering (Fresnel) coefficients γ and τ , as shown in the left panel of Figure 4(a). These coefficients are found by enforcing the conservation of the tangential \mathbf{E} and \mathbf{H} fields at the (spatial) interface discontinuity, which is required to avoid making the \mathbf{B} and \mathbf{D} fields singular (at the interface) through the spatial derivative ($\nabla \times$) in Maxwell equations [37]. On the other hand, the transmitted wavelength is compressed (or the wavenumber increases) if the second medium is denser, as shown in the right panel of Figure 4(a). Note that this transformation does not involve any change of temporal frequency ($\Delta\omega = 0$, energy conservation) since the discontinuity is purely spatial.

The problem of a simple instantaneous interface, or *TEM interface*, is the perfect dual of that of the SEM interface. Now, the incident wave splits into a later backward wave and a later forward wave, which also propagate in opposite directions, but in the same (later) medium and with different scattering coefficients [6], ζ and ξ , as shown in the left panel of Figure 4(b). These coefficients are found by enforcing the conservation

of \mathbf{B} and \mathbf{D} at the (temporal) interface discontinuity, which is required to avoid making \mathbf{E} and \mathbf{H} singular (at the interface) through the temporal derivative ($\partial/\partial t$) in Maxwell equations [37]. The two scattered waves are red-shifted (or their frequency decreases) if the second medium is denser, as shown in the right panel of Figure 4(b). It is thus the temporal frequency that changes in this transformation, while the spatial frequency remains unchanged ($\Delta k_z = 0$, momentum conservation) since the discontinuity is purely temporal. This space-to-time duality has several applications, including the *inverse prism*, a device that, instead of decomposing colors into angles as the Newton prism, maps angles into colors [58].

STEM interfaces may be considered as spacetime extensions of their SEM and TEM counterparts. The electrodynamics of USTEM interfaces is described in Figure 5, with Figure 5(a) and (b) representing the *subluminal* regime [$v_{mz} < c/\max(n_1, n_2)$, e.g., as in Figure 2(c)] and the *superluminal* regime [$v_{mz} > c/\min(n_1, n_2)$, e.g., as in Figure 2(d)], respectively [37]. [Note: We avoid here the *interluminal* regime, corresponding to $c/\max(n_1, n_2) < v_{mz} < c/\min(n_1, n_2)$, which involves complex physics that has not been fully investigated so far [20], [71], [72].] Now, the modulation occurs simultaneously in space and time, as in all the electrodynamics systems represented in Figure 1. Scattering is space like—with reflected and transmitted waves—for the subluminal case and time-like—with later backward and later forward waves—in the superluminal case [37]. The corresponding scattering coefficients are found by enforcing the continuity of $(\mathbf{E}', \mathbf{H}')$ in the subluminal comoving frame (K' , where $\Delta\omega' = 0$) and of $(\mathbf{D}', \mathbf{B}')$ in the superluminal simultaneity frame (K' , where $\Delta k'_z = 0$) [60], which reveals, upon inverse-Lorentz transformation [63], [73],

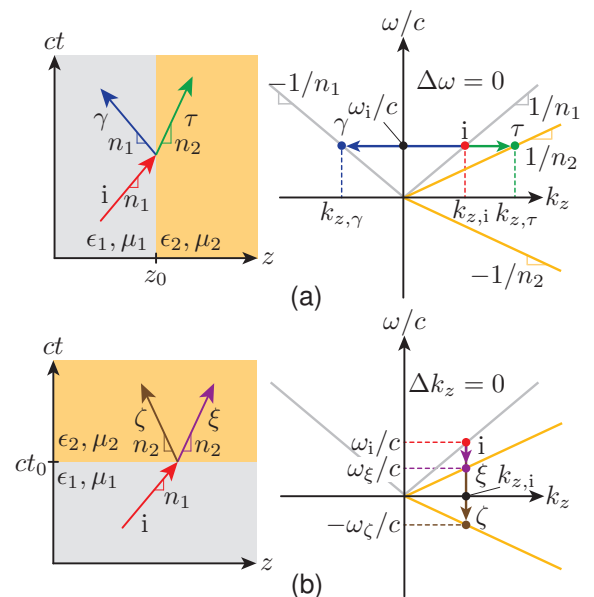


FIGURE 4. Electrodynamics of the simplest GSTEM interfaces, represented in terms of direct (left) and inverse (right) spacetime diagrams, for the case of normal incidence. (a) SEM interface [Figure 3(a)]. (b) TEM interface [Figure 3(b)].

[74] (supplementary material section B.2), the conservation of the quantities $E_x - v_m B_y$ and $B_y - v_m E_x/c^2$ for the plane wave with components (E_x, B_y, k_z) and of $E_y + v_m B_x$ and $B_x + v_m E_y/c^2$ for $(E_y, -B_x, k_z)$ [37], [74]–[76]. On the other hand, the spectral transitions, whose reflective and transmissive parts are manifestations of the *Doppler effect* and of an *index contrast effect*, respectively, are oblique since the discontinuity is both spatial and temporal, leading to simultaneous spatial and temporal frequency transformations [77]. In the case of *oblique incidence*, the dispersion curves, between which the oblique transitions occur, are altered by the change of the incident momentum on the interface, and the scattered angles are deflected toward/against the direction of motion in the sub-/superluminal cases [60] (supplementary material section C).

Finally, an ASTEM interface may be seen as a generalization of a USTEM interface, where both the direct-spacetime interfaces and the normal-incidence dispersion lines change from straight to curved, as illustrated in Figure 3(d) for the case of an ASTEM metamaterial with a complex acceleration profile, including direction reversal, and, hence, jerk ($\partial a_m/\partial t \neq 0$). While an accelerated system is *locally* uniform, so that special relativity and Lorentz transformation apply *locally*, it globally requires a much more complex treatment that belongs to the realm of general relativity and, hence, differential geometry [65], [78], [79]. In this case, the (linear) Lorentz transformations must be replaced by nonlinear transformations corresponding to the type of acceleration at hand [56], [65], the simplest being the K' -constant and rectilinear (or proper) acceleration, which is associated with Rindler transformations (supplementary material section B.3). Physically, the USTEM space-time

transformation (diffraction-Doppler) effect is promoted to a *space-time chirping effect* [80]–[83], with still little explored physics and application potential. A first application is the recently reported ASTEM waveform generator, whose properly designed acceleration trajectory allows virtually arbitrary pulse shaping [54].

METAMATERIAL PHYSICS

Stacking the different GSTEM bilayer unit cells introduced in the “Perspective and Generalization” section, which involve the interfaces analyzed in the “Interface Physics” section, leads to the formation of the corresponding GSTEM structures in Figure 3 [Figure 4(a) → Figure 3(a), Figure 4(b) → Figure 3(b), Figure 5 → Figure 3(c), curved version of Figure 5 → Figure 3(d)]. Before homogenization, these structures are generally periodic spacetime structures (or, possibly, only locally quasi-periodic with a period gradient for the case of ASTEMs) or *GSTEM crystals*, and they involve the same direct (scattering) and inverse (transition) spacetime transformations as their interface counterparts. However, these crystals represent *spacetime-distributed structures*, as opposed to spacetime-localized discontinuities, and support therefore in addition multiple spacetime scattering and multiple spacetime transitions, leading to specific spacetime crystal properties [35].

The GSTEM crystal can be *spatially* 1D, 2D, or 3D, as shown in the bottom right inset of Figure 3(a). If the wave of interest propagates in a space of a dimension that is larger than the spatial dimension of the crystal [specifically, oblique incidence in a 1D crystal and off-plane incidence in a 2D crystal], the crystal is seen by the wave as anisotropic, with different tangential field components for different (e.g., p and s) wave polarizations. Since this represents the most general and most common configuration in early GSTEMs, let us consider henceforth this case of an *anisotropic crystal*, noting in passing that anisotropy, with an anisotropic medium being defined as a medium that exhibits different properties in different directions, is a purely spatial concept since time is monodimensional.

In moving-matter dynamic systems [e.g., Figure 2(a)], the problems are ideally solved in the comoving frame (K'), where everything is stationary, and hence, the boundary conditions and the constitutive relations are both trivial. The situation is more complicated in moving-perturbation systems [e.g., Figure 2(b)] because they involve motion in *both* frames [e.g., moving interfaces in K and (backward) moving atoms and molecules in K']! Let us still choose the K' frame on the grounds that moving matter with stationary boundaries is a known problem [84], whereas moving boundaries is a more difficult problem. To enter the metamaterial regime, we homogenize the GSTEM by prescribing subwavelength [$\max(\lambda_m) \ll \min(\lambda)$] and sub-period [$\max(T_m) \ll \min(T)$] operation. This operation leads to GSTEM-metamaterial anisotropic constitutive parameters with the same tensorial structure as that of their crystal parent [38], [85]. However, another effect is present in K' : the contradirectional motion of polarized atoms and molecules [e.g., focus on the moving K' frame with K -stationary atoms and molecules in Figure 2(b)] ($v'_{\text{atom}} = -v$); the problem is thus a *moving-matter*

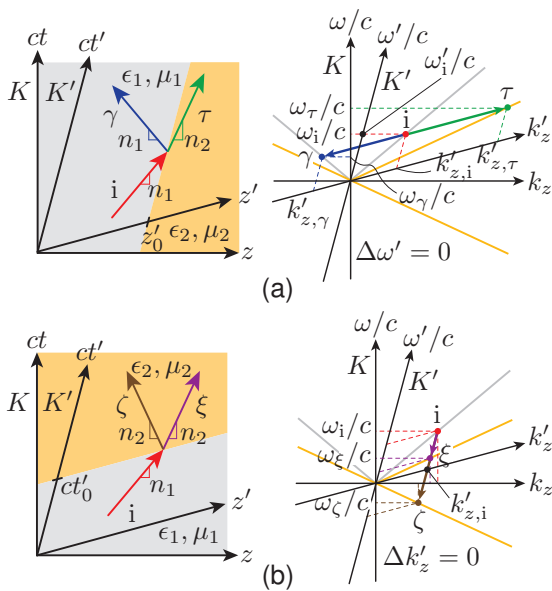


FIGURE 5. Electrodynamics of USTEM interfaces [Figure 3(c)], represented in terms of direct (left) and inverse (right) spacetime diagrams, for the case of normal incidence. (a) Subluminal (space-like) regime. (b) Superluminal (time-like) regime.

problem in K' , with the usual *Fresnel-Fizeau* drag and related *motion bianisotropy* [i.e., Röntgen magnetoelectric coupling, bottom panel of Figure 1(b)] (supplementary material sections D.1 and E.1), due to the magnetic part of the Lorentz force, $\mathbf{F} = q\mathbf{E} + q\mathbf{v} \times \mathbf{B}$ [74], [75] that is associated with the magnetic part of the Lorentz force (supplementary material section D.2). GSTEMs are thus generally *bianisotropic* in K' [75], [76], [86], [87] (supplementary material section E.1).

The fundamental properties of a GSTEM metamaterial, in the frame of interest (K), may be inferred from these preliminary considerations with the help of the spectral graphs provided in Figure 6, with Figure 6(a) representing the problem from the K' viewpoint and Figure 6(b) representing the problem from the K viewpoint. Since the Fresnel-Fizeau drag occurs in the $-z'$ ($= -z$) direction in K' , as suggested in the panel at the extreme right bottom of the figure, the wave velocity, $v'_{gz} = v'_{pz} = c/n'$ (nondispersive medium assumption), is increased in the $-k'_z$ (or $-z'$) direction and decreased in the $+k'_z$ direction, i.e., $1/n' > 1/n^+$, so that the spectral cone is tilted toward the positive k'_z direction [top panel of Figure 6(a)]. As a result, the isofrequency curve at $\omega' = \omega'_0$ is a right-shifted ellipse [bottom panel of Figure 6(a)], located between the $n'_1(\mathbf{k}')$ and $n'_2(\mathbf{k}')$, also right-shifted ellipses, which is a manifestation of the expected bianisotropy (off-centered ellipse \rightarrow bianisotropy, centered ellipse \rightarrow anisotropy, centered circle \rightarrow isotropy) (supplementary material section E.2) and associated *nonreciprocity* [88]. The counterclockwise rotation, by the angle φ' , of the group velocity, $\mathbf{v}'_g(\mathbf{k}') = \nabla'_k \omega'(\mathbf{k}')$, with respect to the phase velocity, $\mathbf{v}'_p = (\omega'/k')\hat{\mathbf{k}}'$, corresponds to the addition of a $-z'$ directed component to the velocity and, thus, clearly shows the backward effect of the Fresnel-Fizeau drag.

We finally need to perform the required (Lorentz, Rindler, etc.) inverse transformation from K' to K to complete the resolution of the electrodynamics problem at hand. Obviously, the elimination of the motion of the atoms and molecules in the transition from K' to K eliminates motion-related bianisotropy since $v_{\text{atom}} = 0$. In contrast, the exact nature (bianisotropic, anisotropic, biisotropic, homoisotropic) of the K solution is difficult to predict and can be precisely found only by performing the exact K' -to- K inverse transformation (inverse-Lorentz transformation, \mathcal{L}^{-1} , in the USTEM case of Figure 6) (supplementary material section E.3). Figure 6(b) shows a typical result. Note that the $n'_1(\mathbf{k}')$ and $n'_2(\mathbf{k}')$ isofrequency ellipses have transformed to simple centered circles, corresponding to the expected curves for the assumed isotropic constituent media with (scalar) refractive indices n_1 and n_2 .

Interestingly, the USTEM curve is still a right-shifted ellipse, with a deflection of the group velocity by an angle of φ , still in the counterclockwise direction with respect to the phase velocity; this deflection is necessarily an effect of the moving-modulation *interfaces* since matter motion does not exist anymore. We have here $\varphi < \varphi'$, indicating that the deflection due to the modulation (K frame) is smaller than that due to the matter (K frame), but the effect is greater and can reach $\varphi > \varphi'$ if the constitutive media have less-than-one indices ($n_1, n_2 < 1$) (plasma-type media). Most importantly, the observed *light deflection* is contradirectional to the modulation ($+z$) and, hence, *opposite to the direction of the drag for a moving body*, consistently with the finding in [89].

This GSTEM deflection effect is quite distinct from the Fresnel-Fizeau drag. Indeed, it does not involve any motion of matter that would “push” or “pull”—i.e., *drag*—light. It is rather an effect of *spacetime weighted averaging*, as first suggested in [35]. This effect is illustrated Figure 7. In the SEM problem, represented in Figure 7(a), light spends on average the same amount of time in medium 1 and in medium 2 in the forward and backward directions so that the corresponding effective metamaterial indices are equal, i.e., $n^+ = n^-$. In the K' -USTEM problem, represented in Figure 7(b), light is subjected to the conventional Fresnel-Fizeau drag and propagates therefore faster in the backward (downstream) direction than in the forward (upstream) direction so that $n^+ > n^-$. In the K -USTEM problem, represented in Figure 7(c), the spacetime slopes are the same as in the SEM problem since no matter motion occurs, but the medium is spacetime-wise oblique, here tilting in the forward direction, and the following—rather subtle—effect occurs due to this tilting. Consider,

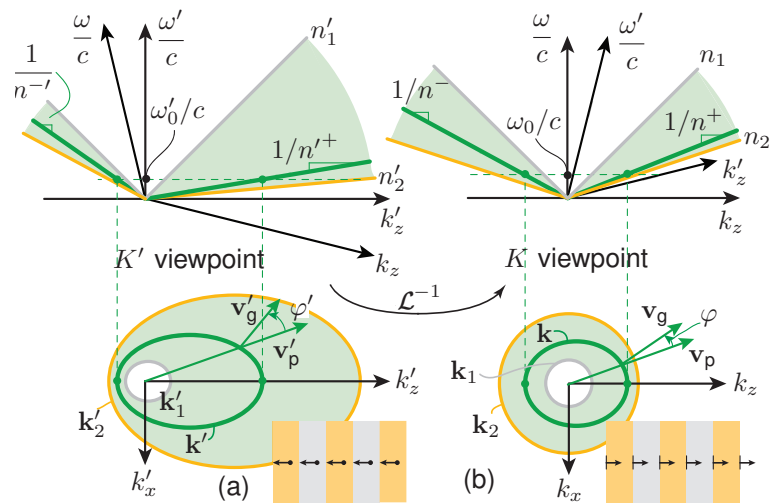


FIGURE 6. Spectral analysis for a 1+1D-(z ; t) USTEM metamaterial under oblique $[(k_z, k_x)]$ incidence with modulation traveling in the $+z$ direction, including the $(\omega, k_z)^{(i)}$ -cuts at $k_x^{(i)} = 0$ of the $(\omega, k_z, k_x)^{(i)}$ cones (top panels) and $(\omega_0, k_z, k_x)^{(i)}$ isofrequency projections (bottom panels), compared with the cases of the bulk constituent media, with refractive indices $n'_1(\mathbf{k}')$ and $n'_2(\mathbf{k}')$ or n_1 and n_2 . (a) K' viewpoint, with Fizeau-Fresnel drag, due to the motion of matter, in the $-z$ direction. (b) K viewpoint, with “inverse drag,” due to the motion of the interfaces.

for simplicity, that $n_2 \gg n_1$, as in Figure 7 [where the vertical axes have been denormalized to ensure a restricted graphical aspect ratio without introducing (unphysical) superluminal light curves]. Then, light spends much more time (see dashed lines) in medium 2, the slower medium, in the forward direction, where it propagates almost parallel to the medium trajectory, than in the backward direction, where the propagation is

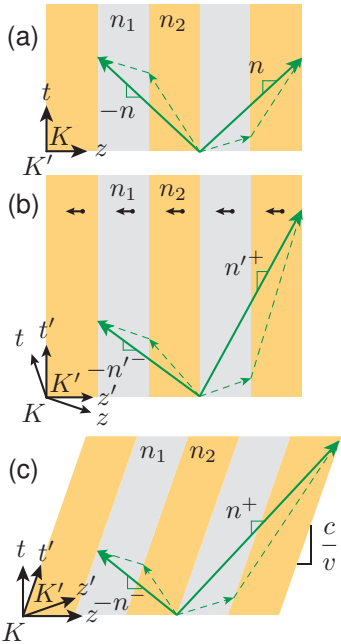


FIGURE 7. GSTEM weighted averaging deflection. (a) SEM. (b) USTEM, K' viewpoint. (c) USTEM, K viewpoint.

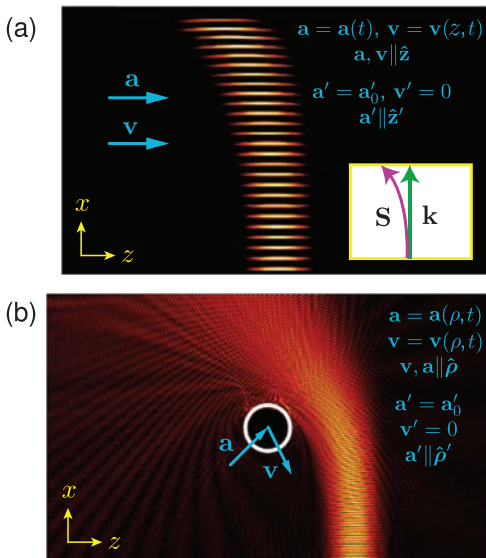


FIGURE 8. Examples of ASTEM metamaterials and related transformations of a light beam (injected from the bottom). (a) Rectilinear (Rindler metric [91], [92]) ASTEM, inducing curved light deflection. (b) Black hole (Schwarzschild metric [56], [93]) ASTEM, attracting and partly absorbing light.

relatively more perpendicular to the medium trajectory, while the ratio of the forward to backward traveled distances increases in a much smaller ratio, as clearly apparent in the figure. As a result, $n^+ > n^-$, and, hence, $v^+ < v^-$, consistently with the observation in Figure 6. This is really, as announced, a space-time weighted averaging phenomenon; an exact mathematical formula for this phenomenon is provided in [35] (supplementary material section E.4), and a related animation is provided in the file *GSTEM_Space-Time_Weighted_Averaging_phenomenon.mp4* of the supplementary material.

As ASTEM interfaces are the curved-spacetime generalization of USTEM interfaces (“Interface Physics” section), ASTEM metamaterials are the curved-spacetime generalization of USTEM metamaterials. Therefore, the principles exposed in conjunction with the USTEM graphs in Figures 6 and 7 largely extend to ASTEMs metamaterials, although their rigorous treatment requires a quantum jump from the *theory of special relativity* [61], [63], routinely applied to USTEMs, to the *theory of general relativity* [56], [64]. Figure 8 presents two illustrative examples of ASTEM metamaterials [85]. Figure 8(a) shows a rectilinear ASTEM metamaterial, which exhibits the modulation-contradirectional group velocity deflection [$\mathbf{v}_g(\mathbf{r}) \parallel \mathbf{S} = \mathbf{E} \times \mathbf{H}$] and straight phase velocity [$\mathbf{v}_p(\mathbf{r}) \parallel \mathbf{k}$] propagation predicted in Figure 6; the beam curvature can be here qualitatively inferred from piecewise (straight) USTEM deflection. Figure 8(b) shows a Schwarzschild ASTEM black hole, which attracts and absorbs light like a cosmic black hole, an effect that is unattainable in simple graded-index lenses [90].

FUTURE PROSPECTS

Given their very fundamental nature and virtually unlimited diversity, GSTEMs have a formidable *potential for scientific and technological innovation*. The *scientific prospects* include

- 1) the study of the properties of higher dimensional ($2 + 1D = 3D$ and $3 + 1D = 4D$) GSTEM (unbounded) structures.
- 2) the analysis of the scattering and diffraction at the interfaces and wedges of *spacetime-truncated* [35] GSTEMs.
- 3) the exploration of new *GSTEM geometries* (e.g., Rindler, Schwarzschild, Kerr, jerk, snap, crackle, etc.) in both the homogeneous and Bragg regimes.
- 4) the extension of *gravity analogs*, currently restricted to interface horizons [94], such as white hole or Bose-Einstein condensate analogs.
- 5) the elaboration of new electrodynamic computational tools for spacetime nonuniformities, using, for instance, foliation decomposition [95], and for modulation-related multiphysics,
- 6) the investigation of novel GSTEM physics (e.g., superluminal and interluminal scattering; spacetime reversal; generalized spacetime metrics; spacetime quantum; and subcycle phenomena).

The *technological prospects* include, on the one hand, the development of efficient modulation platforms and techniques (e.g., acoustic, electronic, and optical) for the experimental implementation of the new GSTEM phenomena, and on the other hand, the identification and demonstration of novel related applications. Many potential USTEM-related applications have

been identified in [37]; we expect that these applications will generalize to ASTEM-type systems, with extra opportunities offered by various spacetime curvatures and generalized spacetime “chirping”.

ACKNOWLEDGMENT

Useful complementary information and animations are provided in the supplementary materials available at <http://doi.org/10.1109/MAP.2022.3216773>.



AUTHOR INFORMATION

Christophe Caloz (christophe.caloz@kuleuven.be) is a professor at KU Leuven, Leuven 3001, Belgium. His research interests include classical and quantum electrodynamics (microwave, terahertz, and optical) science and technology. He is a Fellow of IEEE.

Zoé-Lise Deck-Léger (zoe-lise.deck-leger@polymtl.ca) is a Ph.D. student at Polytechnique Montréal, Montréal H3T 1J4, Canada.

Amir Bahrami (amirbahrami@kuleuven.be) is a Ph.D. student at KU Leuven, Leuven 3001, Belgium.

Oscar Céspedes Vicente (oscar.cespedes-vicente@polymtl.ca) received the B.Eng. degree from Polytechnique Montréal, Montréal H3T 1J4, Canada.

Zhiyu Li (lizhiyu@stu.xjtu.edu.cn) is a Ph.D. student at Xi'an Jiaotong University, Xi'an 710049, China.

REFERENCES

- [1] C. Caloz and T. Itoh, *Electromagnetic Metamaterials: Transmission Line Theory and Microwave Applications*. Hoboken, NJ, USA: Wiley, 2005.
- [2] N. Engheta and R. W. Ziolkowski, Eds. *Metamaterials: Physics and Engineering Explorations*. Hoboken, NJ, USA: Wiley, 2006.
- [3] F. Capolino, Ed. *Metamaterials Handbook*, vol. 2. Boca Raton, FL, USA: CRC Press, 2009.
- [4] S. I. Bozhevolnyi, P. Genevet, and F. Ding, Eds. *Metasurfaces: Physics and Applications*. Basel, Switzerland: MDPI, 2018.
- [5] K. Achouri and C. Caloz, *Electromagnetic Metasurfaces: Theory and Applications*. Hoboken, NJ, USA: Wiley, 2021.
- [6] F. R. Morgensthaler, “Velocity modulation of electromagnetic waves,” *IRE Trans. Microw. Theory Techn.*, vol. 6, no. 2, pp. 167–172, Apr. 1958, doi: 10.1109/TMTT.1958.1124533.
- [7] D. Holberg and K. Kunz, “Parametric properties of fields in a slab of time-varying permittivity,” *IEEE Trans. Antennas Propag.*, vol. 14, no. 2, pp. 183–194, Mar. 1966, doi: 10.1109/TAP.1966.1138637.
- [8] J. A. Richards, *Analysis of Periodically Time-Varying Systems*. Berlin, Germany: Springer-Verlag, 1983.
- [9] D. K. Kalluri, *Electromagnetic of Time Varying Complex Media: Frequency and Polarization Transformer*. Boca Raton, FL, USA: CRC Press, 2018.
- [10] A. Shlivinski and Y. Hadad, “Beyond the Bode-Fano bound: Wideband impedance matching for short pulses using temporal switching of transmission-line parameters,” *Phys. Rev. Lett.*, vol. 121, no. 20, Nov. 2018, Art. no. 204301, doi: 10.1103/PhysRevLett.121.204301.
- [11] M. Mirmoosa, G. Ptitsyn, V. Asadchy, and S. Tretyakov, “Time-varying reactive elements for extreme accumulation of electromagnetic energy,” *Phys. Rev. Appl.*, vol. 11, no. 1, Jan. 2019, Art. no. 014024, doi: 10.1103/PhysRevApplied.11.014024.
- [12] G. Ptitsyn, M. S. Mirmoosa, and S. A. Tretyakov, “Time-modulated meta-atoms,” *Phys. Rev. Res.*, vol. 1, no. 2, Sep. 2019, Art. no. 023014, doi: 10.1103/PhysRevResearch.1.023014.
- [13] D. Ramaccia, D. L. Sounas, A. V. Marini, A. Toscano, and F. Bilotti, “Electromagnetic isolation induced by time-varying metasurfaces: Nonreciprocal Bragg grating,” *IEEE Antennas Wireless Propag. Lett.*, vol. 19, no. 11, pp. 1886–1890, Nov. 2020, doi: 10.1109/LAWP.2020.2996275.
- [14] Y. Mazor and A. Alù, “One-way hyperbolic metasurfaces based on synthetic motion,” *IEEE Trans. Antennas Propag.*, vol. 68, no. 3, pp. 1739–1747, Mar. 2020, doi: 10.1109/TAP.2019.2949134.
- [15] V. Pacheco-Peña and N. Engheta, “Antireflection temporal coatings,” *Optica*, vol. 7, no. 4, pp. 323–331, Apr. 2020, doi: 10.1364/OPTICA.381175.
- [16] Y. Mazor, M. Cotrufo, and A. Alù, “Unitary excitation transfer between coupled cavities using temporal switching,” *Phys. Rev. Lett.*, vol. 127, no. 1, Jul. 2021, Art. no. 013902, doi: 10.1103/PhysRevLett.127.013902.
- [17] D. Ramaccia, A. Alù, A. Toscano, and F. Bilotti, “Temporal multilayer structures for designing higher-order transfer functions using time-varying metamaterials,” *Appl. Phys. Lett.*, vol. 118, no. 10, Mar. 2021, Art. no. 101901, doi: 10.1063/5.0042567.
- [18] E. Galiffi et al., “Photonics of time-varying media,” *Adv. Photon.*, vol. 4, no. 1, Jan. 2022, Art. no. 014002, doi: 10.1117/1.AP.4.1.014002.
- [19] E. S. Cassidy and A. A. Oliner, “Dispersion relations in time-space periodic media: Part I—stable interactions,” *Proc. IEEE*, vol. 51, no. 10, pp. 1342–1359, Oct. 1963, doi: 10.1109/PROC.1963.2566.
- [20] E. S. Cassidy, “Dispersion relations in time-space periodic media: Part II—unstable interactions,” *Proc. IEEE*, vol. 55, no. 7, pp. 1154–1168, Jul. 1967, doi: 10.1109/PROC.1967.5775.
- [21] J. T. Mendonça, *Theory of Photon Acceleration*. Bristol, U.K.: Institute of Physics Publishing, 2007.
- [22] A. B. Shvartsburg, “Optics of nonstationary media,” *Phys. Uspekhi*, vol. 48, no. 8, pp. 797–823, Aug. 2005, doi: 10.1070/PU2005v04n08ABEH002119.
- [23] K. A. Lurie, *An Introduction to the Mathematical Theory of Dynamic Materials*. Cham, Switzerland: Springer-Verlag, 2007.
- [24] F. Biancalana, A. Amann, A. V. Uskov, and E. O'Reilly, “Dynamics of light propagation in spatiotemporal dielectric structures,” *Phys. Rev. E*, vol. 75, no. 4, Apr. 2007, Art. no. 046607, doi: 10.1103/PhysRevE.75.046607.
- [25] Z. Yu and S. Fan, “Optical isolation based on nonreciprocal phase shift induced by interband photonic transitions,” *Appl. Phys. Lett.*, vol. 94, no. 17, p. 171116, Apr. 2009, doi: 10.1063/1.3127531.
- [26] A. Bahabad, M. M. Murnane, and H. C. Kapteyn, “Quasi-phase-matching of momentum and energy in nonlinear optical processes,” *Nat. Photonics*, vol. 4, pp. 570–575, Aug. 2010, doi: 10.1038/nphoton.2010.122.
- [27] A. M. Shalhout, A. Kildishev, and V. M. Shalaev, “Time-varying metasurfaces and Lorentz non-reciprocity,” *Opt. Mater. Exp.*, vol. 5, no. 11, pp. 2459–2467, Nov. 2015, doi: 10.1364/OME.5.002459.
- [28] N. A. Estep, D. L. Sounas, J. Soric, and A. Alù, “Magnetic-free non-reciprocity and isolation based on parametrically modulated coupled-resonator loops,” *Nat. Phys.*, vol. 10, no. 12, pp. 923–927, Dec. 2014, doi: 10.1038/nphys3134.
- [29] Y. Hadad, D. L. Sounas, and A. Alù, “Space-time gradient metasurfaces,” *Phys. Rev. B*, vol. 92, no. 10, Sep. 2015, Art. no. 100304, doi: 10.1103/PhysRevB.92.100304.
- [30] N. Chamanara, S. Taravati, Z.-L. Deck-Léger, and C. Caloz, “Optical isolation based on space-time engineered asymmetric photonic band gaps,” *Phys. Rev. B*, vol. 96, no. 15, Oct. 2017, Art. no. 155409, doi: 10.1103/PhysRevB.96.155409.
- [31] J. Vila, R. K. Pal, M. Ruzzene, and G. Trainiti, “A Bloch-based procedure for dispersion analysis of lattices with periodic time-varying properties,” *J. Sound Vib.*, vol. 406, pp. 363–377, Oct. 2017, doi: 10.1016/j.jsv.2017.06.011.
- [32] S. Taravati, “Giant linear nonreciprocity, zero reflection, and zero band gap in equilibrated space-time varying media,” *Phys. Rev. A*, vol. 9, no. 6, Jun. 2018, Art. no. 064012, doi: 10.1103/PhysRevApplied.9.064012.
- [33] S. Taravati, “Aperiodic space-time modulation for pure frequency mixing,” *Phys. Rev. B*, vol. 97, no. 11, Jun. 2018, Art. no. 115131, doi: 10.1103/PhysRevB.97.115131.
- [34] N. Chamanara, Z.-L. Deck-Léger, C. Caloz, and D. Kalluri, “Unusual electromagnetic modes in space-time modulated dispersion-engineered media,” *Phys. Rev. A*, vol. 97, no. 6, Oct. 2018, Art. no. 063829, doi: 10.1103/PhysRevA.97.063829.
- [35] Z.-L. Deck-Léger, N. Chamanara, M. Skorobogaty, M. G. Silveirinha, and C. Caloz, “Uniform-velocity spacetime crystals,” *Adv. Photon.*, vol. 1, no. 5, Oct. 2019, Art. no. 056002, doi: 10.1117/1.AP.1.056002.
- [36] C. Caloz and Z.-L. Deck-Léger, “Spacetime metamaterials, part I: General concepts,” *IEEE Trans. Antennas Propag.*, vol. 68, no. 3, pp. 1569–1582, Mar. 2019, doi: 10.1109/TAP.2019.2944225.
- [37] C. Caloz and Z.-L. Deck-Léger, “Spacetime metamaterials, part II: Theory and applications,” *IEEE Trans. Antennas Propag.*, vol. 68, no. 3, pp. 1583–1598, Mar. 2020, doi: 10.1109/TAP.2019.2944216.
- [38] P. A. Huidobro, M. G. Silveirinha, E. Galiffi, and J. B. Pendry, “Homogenization theory of space-time metamaterials,” *Phys. Rev. Appl.*, vol. 16, no. 1, Jul. 2021, Art. no. 014044, doi: 10.1103/PhysRevApplied.16.014044.
- [39] X. Wang, V. S. Asadchy, S. Fan, and S. Tretyakov, “Space-time metasurfaces for power combining of waves,” *ACS Photon.*, vol. 8, no. 10, pp. 3034–3041, Sep. 2021, doi: 10.1021/acsphtronics.1c00981.

- [40] G. Milton and O. Mattei, "Field patterns: A new mathematical object," *Proc. Roy. Soc. A Math. Phys. Eng. Sci.*, vol. 473, no. 2198, Feb. 2017, Art. no. 20160819, doi: 10.1098/rspa.2016.0819.
- [41] M. A. Gaafar, T. Baba, M. Eich, and A. Y. Petrov, "Front-induced transitions," *Nat. Photonics*, vol. 13, no. 11, pp. 737–748, Sep. 2019, doi: 10.1038/s41566-019-0511-6.
- [42] A. M. Shaltout, V. M. Shalaev, and M. L. Brongersma, "Spatiotemporal light control with active metasurfaces," *Science*, vol. 364, no. 6441, pp. 1–10, May 2019, doi: 10.1126/science.aat3100.
- [43] P. K. Tien, "Parametric amplification and frequency mixing in propagating circuits," *J. Appl. Phys.*, vol. 29, no. 9, pp. 1347–1357, Sep. 1958, doi: 10.1063/1.1723440.
- [44] A. Cullen, "Theory of the travelling-wave parametric amplifier," *Proc. Inst. Electr. Eng. B, Electron. Commun. Eng.*, vol. 107, no. 32, pp. 101–107, Apr. 1960, doi: 10.1049/pi-b-2.1960.0085.
- [45] W. Rhodes, "Acousto-optic signal processing: Convolution and correlation," *Proc. IEEE*, vol. 69, no. 1, pp. 65–79, Jan. 1981, doi: 10.1109/PROC.1981.11921.
- [46] B. E. A. Saleh and M. C. Teich, *Fundamentals of Photonics*, vol. 2. Hoboken, NJ, USA: Wiley, 2019, ch. 20.
- [47] J. D. Jackson, *Classical Electrodynamics*, 3rd ed. Hoboken, NJ, USA: Wiley, 1998.
- [48] J. Bradley, "IV. A letter from the Reverend Mr. James Bradley Savilian Professor of Astronomy at Oxford, and F. R. S. to Dr. Edmond Halley Astronom. Reg. &c. giving an account of a new discovered motion of the fix'd stars," *Philos. Trans. Roy. Soc.*, vol. 35, no. 406, pp. 637–661, Dec. 1728, doi: 10.1098/rstl.1727.0064.
- [49] C. Doppler, *Ueber Das Farbige Licht Der Doppelsterne Und Einiger Anderer Gestirne Des Himmels: Versuch Einer Das Bradley'sche Aberrations-Theorem Als Integrirenden Theil in Sich Schliessenden Allgemeineren Theorie*. London, U.K.: Forgotten Books, 1903 (from a treatise written in 1842).
- [50] A. Fresnel, "Lettre d'Augustin Fresnel à François Arago sur l'influence du mouvement terrestre dans quelques phénomènes d'optiques," *Ann. Chem. Phys.*, vol. 9, pp. 57–66, Sep. 1818.
- [51] H. Fizeau, "Sur les hypothèses relatives à l'éther lumineux, et sur une expérience qui paraît démontrer que le mouvement des corps change la vitesse avec laquelle la lumière se propage dans leur intérieur," *Comptes Rendus Hebdomadaires Séances Acad. Sci.*, vol. 33, pp. 349–355, 1851.
- [52] W. C. Röntgen, "Ueber die durch Bewegung eines im homogenen elektrischen Felde befindlichen Dielectricums hervorgerufene electrodynamische Kraft," *Ann. Phys.*, vol. 271, no. 10, pp. 264–270, 1888, doi: 10.1002/andp.18882711003.
- [53] A. Sommerfeld, *Electrodynamics: Lectures on Theoretical Physics*, vol. 3. New York, NY, USA: Academic, 1952.
- [54] A. Bahrami and C. Caloz, "Cloaking using spacetime curvature induced by perturbation," in *Proc. 15th Int. Congr. Artif. Mater. Novel Wave Phenomena (Metamaterials)*, 2021, pp. 29–31, doi: 10.1109/Metamaterials52332.2021.9577130.
- [55] S. Weinberg, *Gravitation and Cosmology: Principles and Applications of the General Theory of Relativity*. New York, NY, USA: Wiley, 1972.
- [56] C. W. Misner, K. S. Thorne, and J. A. Wheeler, *Gravitation*. Princeton, NJ, USA: Princeton Univ. Press, 2017.
- [57] H. Minkowski, "Raum und Zeit," *Phys. Z.*, vol. 10, pp. 104–111, 1909.
- [58] A. Akbarzadeh, N. Chamanara, and C. Caloz, "Inverse prism based on temporal discontinuity and spatial dispersion," *Opt. Lett.*, vol. 43, no. 14, pp. 3297–3300, Jul. 2018, doi: 10.1364/OL.43.003297.
- [59] V. Pacheco-Peña and N. Engheta, "Temporal equivalent of the Brewster angle," *Phys. Rev. B*, vol. 104, no. 21, Dec. 2021, Art. no. 214308, doi: 10.1103/PhysRevB.104.214308.
- [60] Z.-L. Deck-Léger, A. Akbarzadeh, and C. Caloz, "Wave deflection and shifted refocusing in a medium modulated by a superluminal rectangular pulse," *Phys. Rev. B*, vol. 97, no. 10, Mar. 2018, Art. no. 104305, doi: 10.1103/PhysRevB.97.104305.
- [61] A. Einstein, "Zur elektrodynamik bewegter Körper," *Ann. Phys.*, vol. 322, no. 10, pp. 891–921, Jun. 1905, doi: 10.1002/andp.19053221004.
- [62] W. Pauli, *Theory of Relativity*. London, U.K.: Pergamon, 1958.
- [63] A. P. French, *Special Relativity*. New York, NY, USA: Norton, 1968.
- [64] A. Einstein, *Zur Allgemeinen Relativitätstheorie*. Akademie der Wissenschaften. New York, NY, USA: Wiley, 1915.
- [65] S. M. Carroll, *Spacetime and Geometry*. Cambridge, U.K.: Cambridge Univ. Press, 2019.
- [66] L. D. Landau, J. Bell, M. Kearsley, L. Pitaevskii, E. Lifshitz, and J. Sykes, *Electrodynamics of Continuous Media*, vol. 8. Amsterdam, The Netherlands: Elsevier, 2013.
- [67] J. D. Joannopoulos, S. G. Johnson, J. N. Winn, and R. D. Meade, *Photonic Crystals: Molding the Flow of Light*, 2nd ed. Princeton, NJ, USA: Princeton Univ. Press, 2008.
- [68] A. Shapere and F. Wilczek, "Classical time crystals," *Phys. Rev. Lett.*, vol. 109, no. 16, Oct. 2012, Art. no. 160402, doi: 10.1103/PhysRevLett.109.160402.
- [69] F. Wilczek, "Quantum time crystals," *Phys. Rev. Lett.*, vol. 109, no. 16, Oct. 2012, Art. no. 160401, doi: 10.1103/PhysRevLett.109.160401.
- [70] C. M. Harris and A. G. Piersol, *Harris' Shock and Vibration Handbook*, vol. 5. New York, NY, USA: McGraw-Hill, 2002.
- [71] L. A. Ostrovskii, "Some 'moving boundaries paradoxes' in electrodynamics," *Sov. Phys. Uspekhi*, vol. 18, no. 6, pp. 452–458, Jun. 1975, doi: 10.1070/PUP1975v01n06ABEH001967.
- [72] Z.-L. Deck-Léger and C. Caloz, "Scattering at interluminal interface," in *Proc. IEEE Int. Symp. Antennas Propag. USNC-USRI Radio Sci. Meeting*, Atlanta, GA, USA, Jul. 2019, pp. 367–368, doi: 10.1109/APUSNCURSINRSM.2019.8889224.
- [73] H. A. Lorentz, "Electromagnetic phenomena in a system moving with any velocity smaller than that of light," in *Proc. Roy. Netherlands Acad. Arts Sci. (KNAW)*, 1904, vol. 6, pp. 809–831.
- [74] J. V. Bladel, *Relativity and Engineering*. Berlin, Germany: Springer-Verlag, 1984.
- [75] J. A. Kong, "Theorems of bianisotropic media," *Proc. IEEE*, vol. 60, no. 9, pp. 1036–1046, Sep. 1972, doi: 10.1109/PROC.1972.8851.
- [76] J. A. Kong, *Electromagnetic Wave Theory*. Cambridge, MA, USA: EMW Publishing, 2008.
- [77] N. Chamanara, Y. Vahabzadeh, and C. Caloz, "Simultaneous control of the spatial and temporal spectra of light with space-time varying metasurfaces," *IEEE Trans. Antennas Propag.*, vol. 67, no. 4, pp. 2430–2441, Apr. 2019, doi: 10.1109/TAP.2019.2891706.
- [78] R. B. Sher and R. J. Daverman, *Handbook of Geometric Topology*. New York, NY, USA: Elsevier, 2001.
- [79] L. W. Tu, *An Introduction to Manifolds*, 2nd ed. New York, NY, USA: Springer-Verlag, 2011.
- [80] J. Anderson and J. Ryon, "Electromagnetic radiation in accelerated systems," *Phys. Rev.*, vol. 181, no. 5, May 1969, Art. no. 1765, doi: 10.1103/PhysRev.181.1765.
- [81] K. Tanaka, "Relativistic study of electromagnetic waves in the accelerated dielectric medium," *J. Appl. Phys.*, vol. 49, no. 8, pp. 4311–4319, Aug. 1978, doi: 10.1063/1.325483.
- [82] K. Tanaka, "Reflection and transmission of electromagnetic waves by a linearly accelerated dielectric slab," *Phys. Rev. A*, vol. 25, no. 1, pp. 385–390, Jan. 1982, doi: 10.1103/PhysRevA.25.385.
- [83] U. Leonhardt and P. Piwnicki, "Optics of nonuniformly moving media," *Phys. Rev. A*, vol. 60, no. 6, pp. 4301–4312, Dec. 1999, doi: 10.1103/PhysRevA.60.4301.
- [84] Z.-L. Deck-Léger, X. Zheng, and C. Caloz, "Electromagnetic wave scattering from a moving medium with stationary interface across the interluminal regime," *Photonics*, vol. 8, no. 6, pp. 1–15, Jun. 2021, doi: 10.3390/photonics8060202.
- [85] A. Bahrami, Z.-L. Deck-Léger, and C. Caloz, "Electrodynamics of metamaterials formed by accelerated modulation," Jul. 2022, *arXiv:2208.11506*.
- [86] C. Caloz and A. Sihvola, "Electromagnetic chirality, part I: The microscopic perspective," *IEEE Antennas Propag. Mag.*, vol. 62, no. 1, pp. 58–71, Feb. 2020, doi: 10.1109/MAP.2019.2955698.
- [87] C. Caloz and A. Sihvola, "Electromagnetic chirality, part II: The macroscopic perspective," *IEEE Antennas Propag. Mag.*, vol. 62, no. 2, pp. 82–98, Apr. 2020, doi: 10.1109/MAP.2020.2969265.
- [88] C. Caloz, A. Alù, S. Tretyakov, D. Sounas, K. Achouri, and Z.-L. Deck-Léger, "Electromagnetic nonreciprocity," *Phys. Rev. Appl.*, vol. 10, no. 4, Oct. 2018, Art. no. 047001, doi: 10.1103/PhysRevApplied.10.047001.
- [89] P. A. Huidobro, E. Galiffi, S. Guenneau, R. V. Craster, and J. B. Pendry, "Fresnel drag in space-time-modulated metamaterials," *Proc. Nat. Acad. Sci. USA*, vol. 116, no. 50, pp. 24,943–24,948, Dec. 2019, doi: 10.1073/pnas.1915027116.
- [90] U. Leonhardt and T. Philbin, *Geometry and Light: The Science of Invisibility*. New York, NY, USA: Dover, 2010.
- [91] C. Moller, *The Theory of Relativity*. Oxford, U.K.: Clarendon, 1952.
- [92] W. Rindler, "Hyperbolic motion in curved space time," *Phys. Rev.*, vol. 119, no. 6, pp. 2082–2089, Sep. 1960, doi: 10.1103/PhysRev.119.2082.
- [93] K. Schwarzschild, "Über das Gravitationsfeld eines Massenpunktes nach der Einsteinschen Theorie," *Sitzungsberichte Koeniglich Preussischen Akademie Wissenschaften Berlin*, vol. 18, pp. 189–196, Jan. 1916.
- [94] D. Faccio, F. Belgiorno, S. Cacciatori, V. Gorini, S. Liberati, and U. Moschella, Eds. *Analogue Gravity Phenomenology: Analogue Spacetimes and Horizons, from Theory to Experiment*. Berlin, Germany: Springer-Verlag, 2013.
- [95] E. Gourgoulhon, *3+1 Formalism in General Relativity: Bases of Numerical Relativity*, vol. 846. Berlin, Germany: Springer-Verlag, 2012.
- [96] J. A. Kong, "Time-harmonic fields in source-free bianisotropic media," *J. Appl. Phys.*, vol. 39, no. 12, pp. 5792–5796, Nov. 1968, doi: 10.1063/1.1656050.
- [97] J. Van Bladel, "Electromagnetic fields in the presence of rotating bodies," *Proc. IEEE*, vol. 64, no. 3, pp. 301–318, Mar. 1976, doi: 10.1109/PROC.1976.10111.





Sajjad Taravati  and George V. Eleftheriades 

4D Wave Transformations Enabled by Space–Time Metasurfaces

Foundations and illustrative examples.

Static metasurfaces have been shown to be prominent compact structures for reciprocal and frequency-invariant transformations of electromagnetic waves in space. However, incorporating temporal variation to static

metasurfaces enables dynamic apparatuses that are capable of 4D tailoring of both the spatial and temporal characteristics of electromagnetic waves, leading to functionalities that are far beyond the capabilities of conventional static metasurfaces. This includes nonreciprocal full-duplex wave transmission, pure frequency conversion, parametric wave amplification, space–time (ST) decomposition, and ST wave diffraction. This article

Digital Object Identifier 10.1109/MAP2022.3201195
Date of current version: 12 September 2022



IMAGES LICENSED BY INGRAM PUBLISHING

overviews our recent progress on the analysis and functionalities of ST metasurfaces and slabs to break reciprocity. We study different operation regimes of ST metasurfaces, such as scattering and diffraction at ST interfaces, ST sinusoidally varying surfaces and slabs, and transmissive and reflective ST metasurfaces. Additionally, corresponding applications are outlined.

INTRODUCTION

Controlled transformation of electromagnetic fields has advanced drastically in recent years, thanks to the advent and evolution of metamaterials and metasurfaces [1], [2], [3], [4]. Static metamaterials and metasurfaces have allowed for substantial progress in wave engineering applications [5], [6]. Recently, there has been a growing interest in ST periodic (STP) metasurfaces for 4D wave engineering, where adding the temporal variation to static metasurfaces leads to functionalities that are far beyond the capabilities of conventional static metasurfaces. For instance, asymmetric wave transmission can be achieved by spatially asymmetric structures when multiple modes are involved at different ports. On the other hand, nonreciprocal wave transmission is a far more challenging task that requires an external bias field for breaking the time invariance of the structure [7], [8], [9], unilateral-transistor-loaded cells [3], or nonlinear materials. Among these nonreciprocity approaches, ST modulation is of high interest because of its immense capability for affecting the spectrum of electromagnetic waves while breaking the time-reversal symmetry.

ST metasurfaces provide huge degrees of freedom for arbitrary alteration of the wave vector and temporal frequency of electromagnetic waves, leading to advanced 4D wave processing in fields from acoustics and microwaves [8], [10], [11], [12], [13], [14], [15], [16], [17] to terahertz and optics [18], [19], [20], [21], [22]. They represent a class of compact dynamic wave processors that have been recently proposed for extraordinary manipulation of electromagnetic waves. Such 4D compact apparatuses are endowed with unique properties not readily seen in conventional static metamaterials and metasurfaces. ST metasurfaces may take advantage of ST modulation capabilities, including nonreciprocal frequency generation [14], [23], [24], parametric wave amplification [11], [25], [26], and asymmetric dispersion [27], [28], [29]. Frequency generation and nonreciprocity are of particular interest in STP slabs [22], [23], [27], [29], [30], [31], [32], which are endowed by asymmetric periodic electromagnetic transitions in their dispersion diagrams [15], [27], [28], [33]. In practice, the ST modulation is achieved by pumping external energy into the medium [8], [13], [14], [23], [27].

Some of the recently proposed applications of STP metamaterials and metasurfaces include mixer-duplexer-antennas [34], unidirectional beam splitters [13], nonreciprocal filters [35], signal coding metasurfaces [17], ST metasurfaces for advanced wave engineering and extraordinary control over electromagnetic waves [8], [10], [14], [15], [16], [18], [20], [36], [37], [38], [39], [40], [41], [42], [43], [44], nonreciprocal platforms [27], [29], [42], [45], [46], [47], [48], [49], frequency converters [14], [23], [24], [50], time-modulated antennas [51], [52], spectral camouflage metasurfaces [53], [54], antenna-mixer-amplifiers [55], and enhanced-resolution imaging

photonic crystals [56]. This diverse and significant capability of ST-modulated (STM) media is due to their unique interactions with the incident field [27], [57], [58], [59].

This article provides a review on the properties, analysis, and dispersion diagrams of ST metasurfaces and their 4D wave-transformation characteristics. We provide a few examples on how such a peculiar 4D wave guidance in ST metasurfaces can lead to new extraordinary electromagnetic apparatuses. As a complementary article, we have provided a review on experimental implementations of ST metasurfaces and their applications and functionalities in [4]. We first present key properties of ST interfaces, including spatial interfaces, temporal interfaces, and ST interfaces. Then, we show that a nonreciprocal metasurface acts as a very thin ST slab, i.e., a moving metasurface. Next, the analysis of general STM metasurfaces is outlined, including the derivation of scattered electromagnetic fields, 4D dispersion diagrams, boundary conditions, and ST decomposition. Then, full-wave finite difference time domain (FDTD) simulations of ST metasurfaces are presented. Finally, illustrative examples are provided to show the peculiar and unique functionalities of ST metasurfaces.

ELECTROMAGNETIC WAVES IN ST STRUCTURES

Figure 1 shows the Minkowski ST diagram and its Fourier-transformed pair known as the *dispersion diagram*. The Minkowski diagram is the most well-known class of ST diagrams and was developed by Hermann Minkowski in 1908. This diagram is generally a 2D graph that depicts events as happening in a universe consisting of one time dimension and one space dimension. In contrast to regular distance-time graphs, here the distance is demonstrated on the horizontal axis and time on the vertical axis. Furthermore, the time and space units are chosen such that an object moving at the speed of light in the background medium follows a 45° angle to the diagram's axes. The Minkowski ST diagram in Figure 1 is constituted of two light cones, representing propagation of light in the past and future. The two cones have their apexes at the present, where the 3D (x , y , and z) hyperspace exists. Any discontinuity in the 4D ST diagram results in forward and backward waves in space. The analysis and design of ST media and metasurfaces can be substantially eased by understanding the Fourier pair of the Minkowski diagram. ST metasurfaces and slabs can be analyzed as two interfaces sandwiched between two semi-infinite regions in space. Therefore, to best investigate the wave diffraction by an STM grating, we first study the interaction of the electromagnetic wave with space and time interfaces, separately [60], [61], [62]. In general, three different ST discontinuities may be studied as follows.

SPACE INTERFACE

Figure 2(a) sketches the ST diagram of a spatial interface at $z = z_0$ in the plane $(z, v_b t)$ between two media of refractive indexes n_1 and n_2 , intrinsic impedances η_1 and η_2 , and phase velocities $v_1 = v_b/n_1$ and $v_2 = v_b/n_2$, respectively. Here, v_b represents the velocity of the wave in the background medium. This figure shows scattering of forward and backward fields and

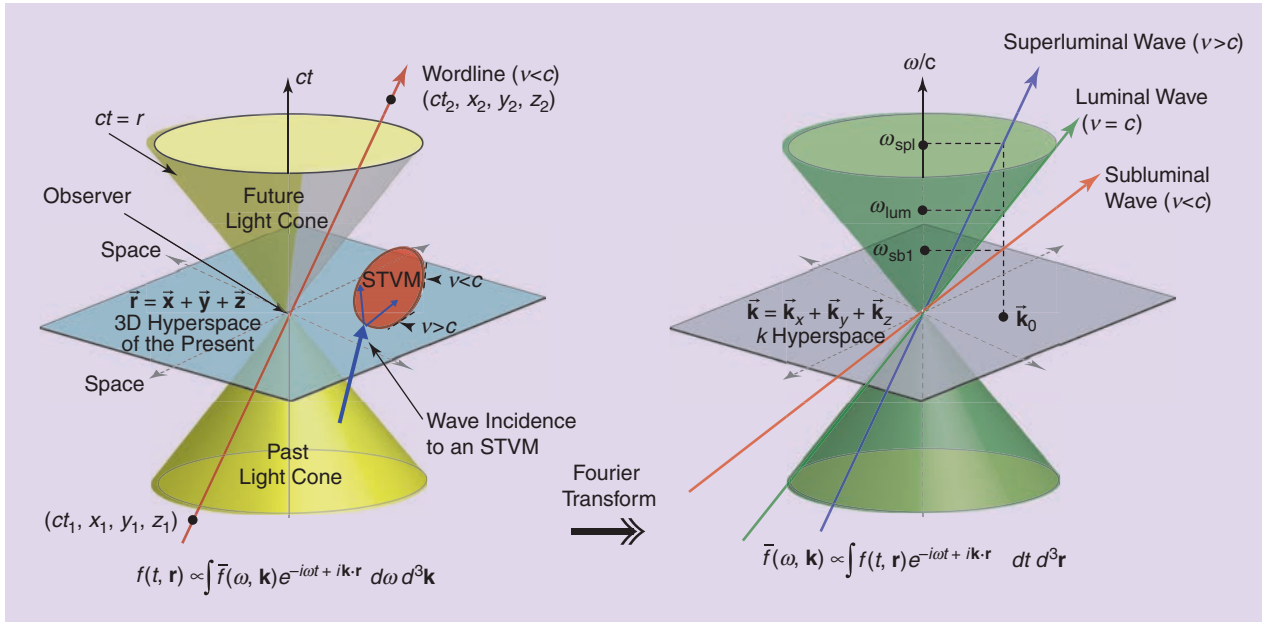


FIGURE 1. ST Fourier pair diagrams. STVM: space-time-varying medium.

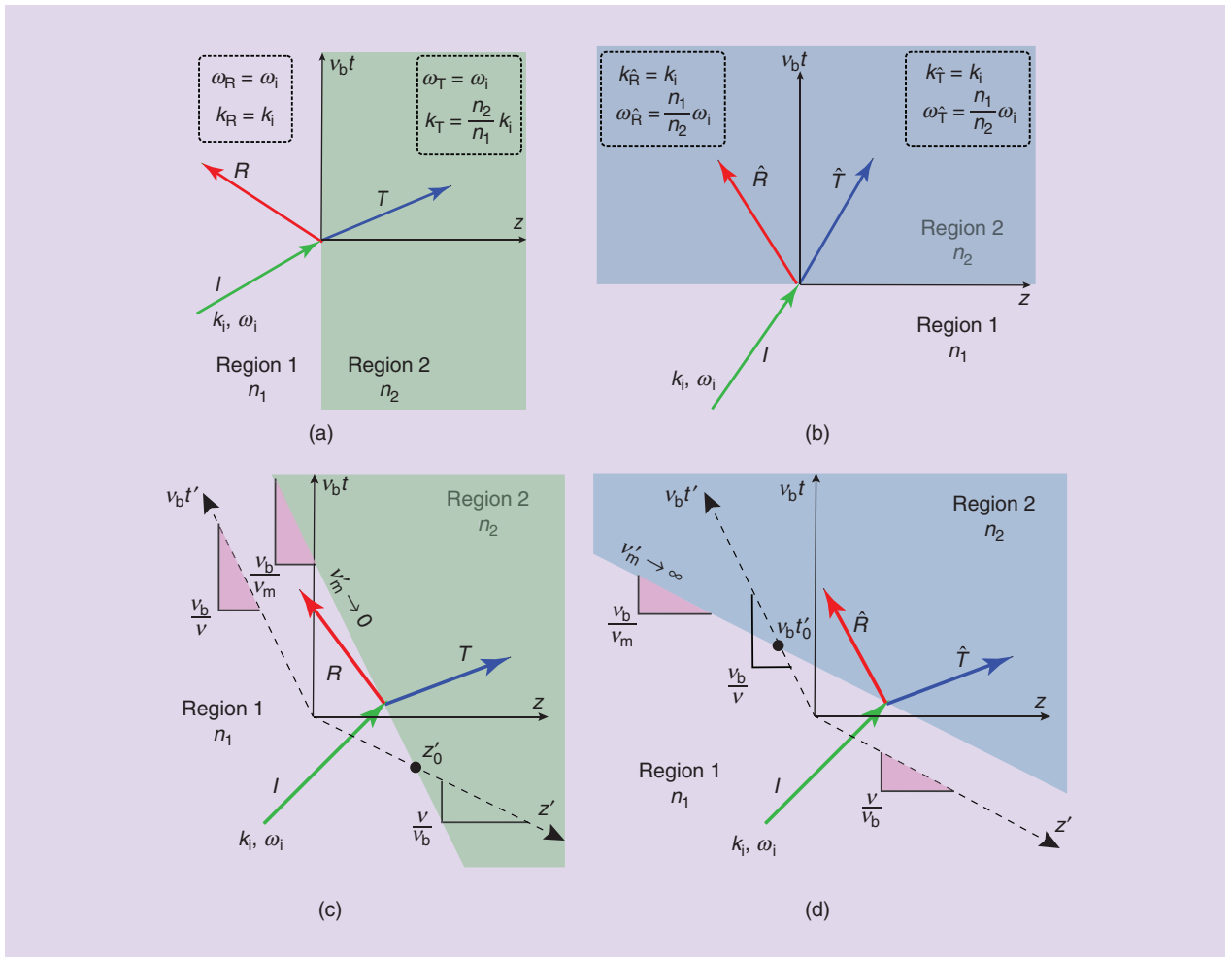


FIGURE 2. ST diagrams showing scattering of forward and backward fields and conservation of energy and momentum for different scenarios. (a) Spatial interface, i.e., $n(z < 0) = n_1$ and $n(z > 0) = n_2$. (b) Temporal interface, i.e., $n(t < 0) = n_1$ and $n(t > 0) = n_2$. (c) Subluminal ST interface ($v_m < v_b$), where $v = v_m$. (d) Superluminal ST interface ($v_m > v_b$), where $v = v_b^2/v_m$.

conservation of energy and momentum for different scenarios. The temporal axis of the Minkowski ST diagram is scaled with the speed of light and is labeled with v_{bt} for changing the dimension of the addressed physical quantity from time to length, in accordance to the dimension associated to the spatial axes labeled z .

This problem represents the textbook case of electromagnetic wave incidence and scattering from a spatial (static) interface, where $n(z < 0) = n_1$ and $n(z > 0) = n_2$. The boundary conditions are

derived by applying the fundamental physical fact that all physical quantities must remain bounded everywhere and at every time to the space and time derivatives in the sourceless Maxwell equations $\nabla \times \mathbf{E} = -\partial \mathbf{B} / \partial t$ and $\nabla \times \mathbf{H} = \partial \mathbf{D} / \partial t$. The discontinuity of the tangential components of electric and magnetic fields at $z = z_0$ would result in unbounded and singular electromagnetic fields at the interface, which is not physically possible. Therefore, the tangential components of the electric and magnetic fields must be continuous at a space discontinuity; i.e., $\hat{z} \times (\mathbf{E}_2 - \mathbf{E}_1)|_{z=z_0} = 0$ and $\hat{z} \times (\mathbf{H}_2 - \mathbf{H}_1)|_{z=z_0} = 0$. As a result, the wavenumber k changes; i.e., energy is preserved but momentum changes, such that the wavenumbers of the backward reflected wave in region 1 and the forward transmitted wave in region 2 correspond to $k_R = -k_i$ and $k_T = k_i n_2 / n_1$, respectively, whereas the temporal frequencies of the backward reflected and forward transmitted waves are equal to that of the incident wave, i.e., $\omega_R = \omega_i$ and $\omega_T = \omega_i$.

Throughout the article, we use the wave's time dependence of $\exp(-i\omega t)$ such that with $\omega > 0$ the wave travels from left to right if the wavenumber is positive ($k > 0$) and from right to left if the wavenumber is negative ($k < 0$). We consider the incident field in region 1 (traveling toward the $+z$ direction) as $\mathbf{E}_i = \exp[i(k_i z - \omega_i t)]$, the reflection field in region 1 (traveling toward the $-z$ direction) as $\mathbf{E}_R = R \exp[i(-k_i z - \omega_i t)]$, and the transmitted field in region 2 (traveling toward the $+z$ direction) as $\mathbf{E}_T = T \exp[i(k_i z - \omega_i t)]$, where R and T represent the spatial reflection and transmission coefficients, respectively. The total field in region 1 reads $\mathbf{E}_1 = \mathbf{E}_i + \mathbf{E}_R$, and the field in region 2 reads $\mathbf{E}_2 = \mathbf{E}_T$. We next apply the spatial boundary condition at $z = z_0$ (i.e., $\mathbf{E}_1|_{z=z_0} = \mathbf{E}_2|_{z=z_0}$ and $\mathbf{H}_1|_{z=z_0} = \mathbf{H}_2|_{z=z_0}$) to determine R and T as $R = (\eta_2 - \eta_1) / (\eta_1 + \eta_2)$ and $T = 2\eta_2 / (\eta_1 + \eta_2)$ where $\eta_1 = \sqrt{\mu_1 / \epsilon_1}$ and $\eta_2 = \sqrt{\mu_2 / \epsilon_2}$. More details can be found in the supplementary materials available at <http://doi.org/10.1109/MAP.2022.3201195>.

TIME INTERFACE

Figure 2(b) shows the ST diagram of a time interface between two media of refractive indices n_1 and n_2 , which is the dual case of the spatial metasurface in Figure 2(a). Here, the refractive index suddenly changes from one value (n_1) to another

ST modulation is of high interest because of its immense capability for affecting the spectrum of electromagnetic waves while breaking the time-reversal symmetry.

(n_2) at a given time throughout all space; i.e., $n(t < 0) = n_1$ and $n(t > 0) = n_2$. The temporal change of the refractive index produces both reflected (backward) and transmitted (forward) waves, which are analogous to the reflected and transmitted waves produced at the spatial interface between two different media in Figure 2(a). The discontinuity of \mathbf{D} and \mathbf{B} at $v_{bt} = v_{bt0}$ would result in unbounded and singular \mathbf{E} and \mathbf{H} at the interface, which is not physically possible. Therefore, \mathbf{D} and \mathbf{B} must be continuous at a time inter-

face; that is, $(\mathbf{D}_2 - \mathbf{D}_1)|_{v_{bt} = v_{bt0}} = 0$ and $(\mathbf{B}_2 - \mathbf{B}_1)|_{v_{bt} = v_{bt0}} = 0$. The total charge Q and the total flux ψ must remain constant at the moment of the jump from n_1 to n_2 , implying that both the transversal and normal components of \mathbf{D} and \mathbf{B} do not change instantaneously, which is different than the static case [shown in Figure 2(a)], where only the normal components of the magnetic field \mathbf{B} and electric field displacement \mathbf{D} are conserved. Specifically, at a time interface, the magnetic field \mathbf{B} , the electric field displacement \mathbf{D} , and the wavenumber k are preserved. This yields a change in the temporal frequency of the incident wave so that the frequency of the reflected wave in region 2 and the forward transmitted wave in region 2 correspond to $\omega_R = \omega_i n_1 / n_2$, $\omega_T = \omega_i n_1 / n_2$, respectively. However, the spatial frequencies of the backward reflected and forward transmitted waves are equal to that of the incident wave, i.e., $k_R = k_T = k_i$, where momentum is preserved but energy changes. More details can be found in the supplementary materials available at <http://doi.org/10.1109/MAP.2022.3201195>. We consider $D_1 = a_0 \exp[i(k_i z - \omega_i t)]$ and $D_2 = a_0 \exp(ik_i z)(\hat{T} \exp(-i\omega_i t) + \hat{R} \exp(i\omega_i t))$, where \hat{R} and \hat{T} represent the temporal reflection and transmission coefficients, respectively. These two coefficients are determined by applying the boundary conditions $\mathbf{D}_1|_{v_{bt} = v_{bt0}} = \mathbf{D}_2|_{v_{bt} = v_{bt0}}$ and $\mathbf{B}_1|_{v_{bt} = v_{bt0}} = \mathbf{B}_2|_{v_{bt} = v_{bt0}}$, as $\hat{R} = n_1(\eta_2 - \eta_1) / (2n_2\eta_1)$ and $\hat{T} = n_1(\eta_1 + \eta_2) / (2n_2\eta_1)$. More details can be found in the supplementary materials available at <http://doi.org/10.1109/MAP.2022.3201195>.

SPACE-TIME INTERFACES

Figure 2(c) and (d) depicts the ST diagram of subluminal ($v_m < v_b$) and superluminal ($v_m > v_b$) ST interfaces, where $n(z/v_b + t < 0) = n_1$ and $n(z/v_b + t > 0) = n_2$, as the combination of the space and time interfaces in Figure 2(a) and (b), respectively. Here, v_m represents the velocity of the interface, and the slope of the ST interface is v_b/v_m . It may be seen that the ST interface resembles the spatial interface configuration in Figure 2(a) in the region $n = n_1$ and the temporal interface configuration in Figure 2(b) for $n = n_2$.

To derive boundary conditions for subluminal and superluminal ST interfaces, we apply the following Lorentz

transformations [63], which transform the coordinates of an event from the laboratory (unprimed) frame (x, y, z, t) to the primed frame (x', y', z', t'), comoving with the medium at a constant velocity $\mathbf{v} = \mathbf{a}_z v$ (where $v < v_b$) relative to the laboratory (unprimed) frame, in special relativity, as

$$x' = x, \quad y' = y, \quad z' = \gamma(z - vt) \quad \text{and} \quad t' = \gamma\left(t - \frac{v}{v_b^2}z\right), \quad (1)$$

where $\gamma = 1/\sqrt{1 - (v/v_b)^2}$. Then, by applying the chain rule, that is, $\partial/\partial z = (\partial/\partial z')(\partial z'/\partial z) + (\partial/\partial t')(\partial t'/\partial z)$, and $\partial/\partial t = (\partial/\partial t')(\partial t'/\partial t) + (\partial/\partial z')(\partial z'/\partial t)$, we derive Maxwell's equations in the primed frame as (more details can be found in the supplementary materials available at <http://doi.org/10.1109/MAP.2022.3201195>)

$$\frac{\partial}{\partial z'}(\gamma[E_x(z) - vB_y(z)]) = -\frac{\partial}{\partial t'}\left(\gamma\left[B_y(z) - \frac{v}{v_b^2}E_x(z)\right]\right) \quad (2a)$$

$$-\frac{\partial}{\partial z'}(\gamma[H_y(z) - vD_x(z)]) = \frac{\partial}{\partial t'}\left(\gamma\left[D_x(z) + \frac{v}{v_b^2}H_y(z)\right]\right). \quad (2b)$$

SUBLUMINAL ST INTERFACE

Consider a medium moving at a constant velocity $\mathbf{v}_m = \mathbf{a}_z v_m$ (where $v_m < v_b$) relative to the laboratory (unprimed) frame, as shown in Figure 2(c). Hence, the slopes of the primed frame v_b/v and the slope of the interface v_b/v_m are equal, which results in $v = v_m$ such that the primed frame is comoving with the interface, i.e., $v'_m = 0$ where v'_m is the velocity of the interface in the primed frame. Maxwell's equations in the primed frame in (2) provide the following boundary conditions for the subluminal (space-like) ST interface:

$$(E_1 - v\mu_1 H_1)|_{z'=z_0} = (E_2 - v\mu_2 H_2)|_{z'=z_0} \quad \text{and} \\ (H_1 - v\epsilon_1 E_1)|_{z'=z_0} = (H_2 - v\epsilon_2 E_2)|_{z'=z_0}. \quad (3a)$$

The reflection and transmission coefficients at a subluminal ST interface read (more details can be found in the supplementary materials available at <http://doi.org/10.1109/MAP.2022.3201195>)

$$R = \frac{\eta_2 - \eta_1}{\eta_1 + \eta_2} \frac{v_1 - v_m}{v_1 + v_m} \quad \text{and} \quad T = \frac{2\eta_2}{\eta_1 + \eta_2} \frac{1 - \frac{v_m}{v_1}}{1 - \frac{v_m}{v_2}}, \quad (3b)$$

and the temporal and spatial frequencies of the reflected and transmitted waves read (more details can be found in the supplementary materials available at <http://doi.org/10.1109/MAP.2022.3201195>)

$$\omega_R = \omega_i \frac{v_1 - v_m}{v_1 + v_m}, \quad \omega_T = \omega_i \frac{1 - \frac{v_m}{v_1}}{1 - \frac{v_m}{v_2}}, \\ k_R = k_i \frac{v_1 - v_m}{v_1 + v_m}, \quad k_T = k_i \frac{1 - \frac{v_m}{v_1}}{1 - \frac{v_m}{v_2}}, \quad (3c)$$

where $v_1 = v_b/n_1$ and $v_2 = v_b/n_2$. The pure-space interface is the $v_m = 0$ limit of a subluminal ST interface.

SUPERLUMINAL ST INTERFACE

Consider a medium moving at a constant velocity $\mathbf{v}_m > v_b$ relative to the laboratory (unprimed) frame, as shown in Figure 2(d). The proper use of the Lorentz transformation in the superluminal regime ($v_m > v_b$), e.g., to avoid the imaginary Lorentz factor γ , requires setting the primed frame as one where the medium is purely temporal instead of purely spatial. Therefore, as shown in Figure 2(d), the two slopes v/v_b and v_b/v_m are equal, which results in $v = v_b^2/v_m$, such that the frame is costanding with the interface in time. Maxwell's equations in the primed frame in (2) provide the following boundary conditions for the superluminal (time-like) ST interface:

$$\left(D_1 - \frac{v}{v_b^2}H_1\right)|_{v_bt'=v_bt'_0} = \left(D_2 - \frac{v}{v_b^2}H_2\right)|_{v_bt'=v_bt'_0} \quad \text{and} \\ \left(B_1 - \frac{v}{v_b^2}E_1\right)|_{v_bt'=v_bt'_0} = \left(B_2 - \frac{v}{v_b^2}E_2\right)|_{v_bt'=v_bt'_0}, \quad (4a)$$

and the reflection and transmission coefficients at a superluminal ST interface read (more details can be found in the supplementary materials available at <http://doi.org/10.1109/MAP.2022.3201195>)

$$\hat{R} = \frac{n_1}{n_2} \frac{(\eta_2 - \eta_1)}{2\eta_1} \left(\frac{1 - \frac{v_1}{v_m}}{1 + \frac{v_2}{v_m}} \right), \quad \text{and} \quad \hat{T} = \frac{n_1}{n_2} \left(\frac{\eta_1 + \eta_2}{2\eta_1} \right) \left(\frac{1 - \frac{v_1}{v_m}}{1 - \frac{v_2}{v_m}} \right), \quad (4b)$$

where the temporal and spatial frequencies of the reflected and transmitted waves read (more details can be found in the supplementary materials available at <http://doi.org/10.1109/MAP.2022.3201195>)

$$k_R = k_i \frac{1 - \frac{v_1}{v_m}}{1 + \frac{v_2}{v_m}}, \quad k_T = k_i \frac{1 - \frac{v_1}{v_m}}{1 - \frac{v_2}{v_m}}. \\ \omega_R = \omega_i \frac{1 - \frac{v_m}{v_1}}{1 + \frac{v_m}{v_2}}, \quad \omega_T = \omega_i \frac{1 - \frac{v_m}{v_1}}{1 - \frac{v_m}{v_2}}. \quad (4c)$$

The pure-time interface is the $v_m = \infty$ limit of a superluminal ST interface.

DIFFERENCE BETWEEN NONRECIPROCAL AND ASYMMETRIC WAVE TRANSMISSIONS

The difference between the excitation and response for validation of the symmetry and reciprocity of electromagnetic systems is clarified in Figure 3(a) and (b) [7], [17]. Here, we consider the general case of new frequency generation that occurs in ST metasurfaces. However, the symmetry and reciprocity properties of media are not related to frequency generation such that a symmetric/reciprocal metasurface can either produce new frequencies or not. Figure 3(a) shows the forward and backward problems for the symmetry test of a particular symmetric

electromagnetic system, where the backward problem is represented by the spatial inversion of the forward problem; that is, the applied excitation wave (input) of the backward problem must be the spatial inversion of the excitation wave (input) of the forward problem. As a result, for a symmetric system, the output of the backward problem would be exactly the spatial inversion of the output of the forward problem. Otherwise, the system is asymmetric. Figure 3(b) shows the

forward and backward problems for the reciprocity test of a particular reciprocal electromagnetic system, where the backward problem is the spatial inversion of the *time-reversed* forward problem; that is, the applied excitation wave (input) of the backward problem must be the spatial inversion of the output of the forward problem. As a result, for a reciprocal system, the output of the backward problem would be exactly the spatial inversion of the input of the forward problem. Otherwise, the system is nonreciprocal.

EXPERIMENTAL DEMONSTRATION OF ST INTERFACE

Transistor-loaded metasurfaces can represent an ST interface [2], [3], [11]. Figure 4(a) depicts the operation principle of a nonreciprocal nongyrotropic metasurface. For $t < 0$, the

For a reciprocal system, the output of the backward problem would be exactly the spatial inversion of the input of the forward problem.

metasurface operates as a reflector where the incident wave, traveling along the $+z$ direction, is reflected by the metasurface and travels back along the $-z$ direction. For $t > 0$, the metasurface operates as a nonreciprocal sheet, where a $+z$ -directed traveling wave passes through the metasurface with gain and without polarization alteration, whereas a wave traveling along the opposite direction is being reflected by the metasurface.

The transmission scattering parameters of the metasurface are not equal, i.e., $S_{21} > S_{12}$, where

$S_{21} = \psi_{\text{out}}^{\text{F}} / \psi_{\text{in}}^{\text{F}} > 1$ and $S_{12} = \psi_{\text{out}}^{\text{B}} / \psi_{\text{in}}^{\text{B}} < 1$. It can be shown that such a nonreciprocal nongyrotropic metasurface is equivalent to a moving metasurface [11], as depicted in Figure 4(b).

Figure 5(a) shows the full-wave simulation results, where the transmission of waves from left to right is allowed and accompanied by power amplification, but the transmission of waves from right to left is prohibited. Figure 5(b) shows a photo of the fabricated metasurface [11]. The metasurface is formed by an array of unit cells. These unit cells are constituted of two microstrip patch elements interconnected through a unilateral transistor, introducing transmission gain in one direction and transmission loss in the other direction. Figure 5(c) shows the measured transmission levels for both directions and for $t < 0$

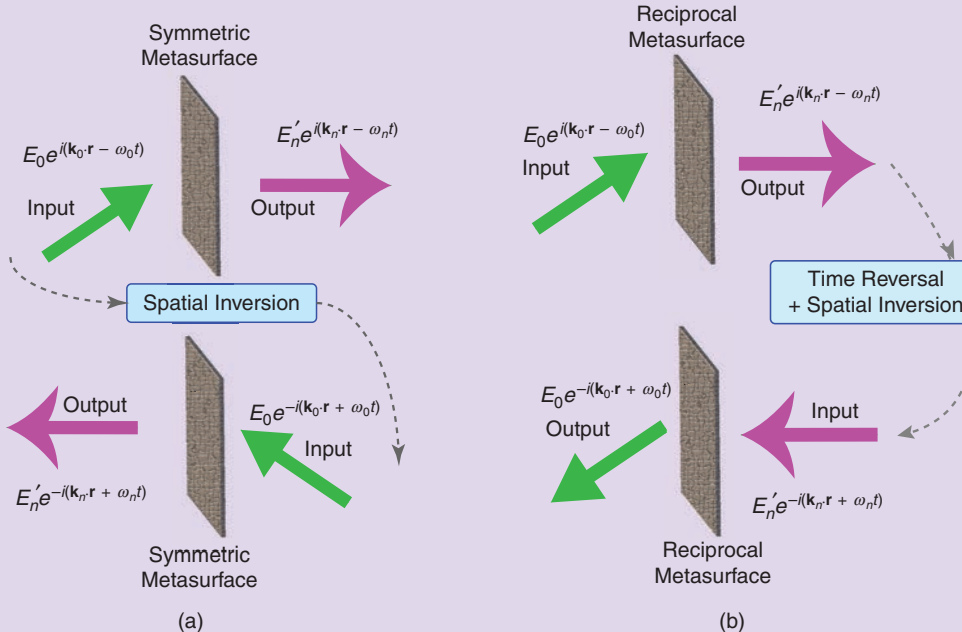


FIGURE 3. A schematic of the experimental setup configurations for validation of the symmetric and reciprocal response of electromagnetic systems. (a) The electromagnetic symmetry of the system is validated, in which the backward problem is the *spatial inversion* of the forward problem. (b) The electromagnetic reciprocity of the system is validated, in which the backward problem is the *spatial inversion* of the *time-reversed* forward problem.

and $t > 0$. The general case of a bianisotropic medium reads [11] $\mathbf{D} = \bar{\epsilon} \cdot \mathbf{E} + \bar{\xi} \cdot \mathbf{H}$ and $\mathbf{B} = \bar{\zeta} \cdot \mathbf{E} + \bar{\mu} \cdot \mathbf{H}$.

The continuity equations of a metasurface may be expressed as

$$\hat{z} \times \Delta \mathbf{H} = j\omega\epsilon_0 \bar{\chi}_{ee} \cdot \mathbf{E}_{av} + jk_0 \bar{\chi}_{em} \cdot \mathbf{H}_{av}, \quad (5a)$$

$$\Delta \mathbf{E} \times \hat{z} = j\omega\mu_0 \bar{\chi}_{mm} \cdot \mathbf{H}_{av} + jk_0 \bar{\chi}_{me} \cdot \mathbf{E}_{av}, \quad (5b)$$

where Δ and the subscript “av” represent, respectively, the difference of the fields and the average of the fields between the two sides of the metasurface. Equation (5) provides a relation between the electromagnetic fields on the two sides of a metasurface and its susceptibilities in the absence of normal susceptibility components. The constitutive parameters of the metasurface may be represented according to the susceptibilities in (5) as $\bar{\epsilon} = \epsilon_0(\bar{I} + \bar{\chi}_{ee})$, $\bar{\mu} = \mu_0(\bar{I} + \bar{\chi}_{mm})$, $\bar{\xi} = \bar{\chi}_{em}/c_0$, $\bar{\zeta} = \bar{\chi}_{me}/c_0$.

We then seek the susceptibilities that provide the nonreciprocal nongyrotropic response of the metasurface by substituting the electromagnetic fields of the corresponding transformation into (5). Such a transformation includes

passing a $+z$ -propagating plane wave through the metasurface and complete absorption of a $-z$ -propagating plane incident wave, yielding $\bar{\chi}_{ee} = -j/k_0[10; 01]$, $\bar{\chi}_{mm} = -j/k_0[10; 01]$, $\bar{\chi}_{em} = j/k_0[01; -10]$, $\bar{\chi}_{me} = j/k_0[0-1; 10]$. This shows that elements $\bar{\chi}_{em}$ and $\bar{\chi}_{me}$ are the ones that contribute to the nonreciprocity of the metasurface. This form of the susceptibility tensors is identical to that of a moving uniaxial medium [11].

BLOCH-FLOQUET ANALYSIS OF STP METASURFACES

Space, time, and ST interfaces are fundamental parts of electromagnetic structures. In practice, ST sinusoidally periodic structures are substantially more common than ST interfaces as they introduce peculiar and interesting features and physical phenomena, and they are significantly easier to experimentally realize. Such spatiotemporally periodic structures (usually in sinusoidal form) can be theoretically represented as an infinite cascade of ST interfaces [29]. This section provides an analysis on wave propagation in ST metasurfaces. Electromagnetic scattering from an STP slab is depicted in Figure 6(a) [15]. Such a scattering is composed of the reflection and transmission of ST harmonics (STHs). The ST slab is characterized with the

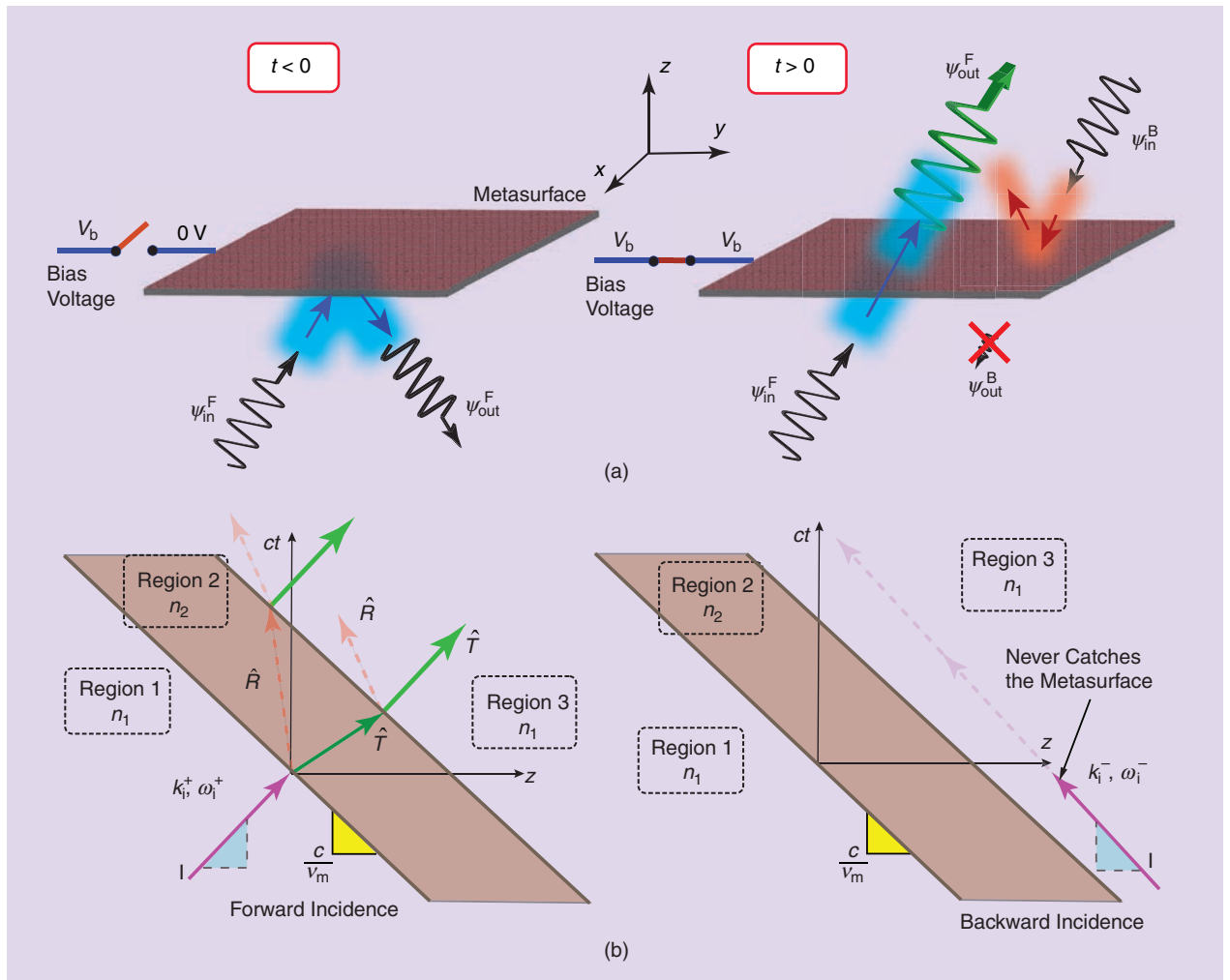


FIGURE 4. A nonreciprocal nongyrotropic metasurface. (a) For $t < 0$ it operates as a reflective sheet, whereas for $t > 0$ it operates as a nonreciprocal transmissive sheet. (b) The ST representation of the nonreciprocal nongyrotropic metasurface.

wavenumber k_0 and possesses the ST-varying electric permittivity $\epsilon(z, t)$ and ST-varying magnetic permeability $\mu(z, t)$. The ST-varying slab is sandwiched between two semi-infinite unmodulated media; that is, region 1 is characterized with the wavenumber $k_0 = \omega_0 \sqrt{\epsilon_{r,1} \mu_{r,1}} / c = \sqrt{k_x^2 + k_z^2}$ and region 3 with the wavenumber $k'_0 = \omega_0 \sqrt{\epsilon_{r,3} \mu_{r,3}} / c = \sqrt{k'_x^2 + k'_z^2}$. We assume the STM structure is infinite in the y direction; that is, $k_y = k'_y = k''_y = 0$. Here, ω_0 is the temporal frequency of the incident wave, $\epsilon_{r,1}$ and $\epsilon_{r,3}$ are the electrical permittivities of regions 1 and 3, respectively, and $\mu_{r,1}$ and $\mu_{r,3}$ are the magnetic permeabilities of regions 1 and 3, respectively.

A general analysis assumes a metasurface with *temporally periodic* electric permittivity and magnetic permeability and a general *aperiodic/periodic* spatial variation [15]. Given the temporal periodicity of the structure, we may decompose these constitutive parameters into time-Floquet waves, as $\epsilon(z, t) = \sum_{s=-\infty}^{\infty} \epsilon_{k, \text{aper}}(z) \exp(is\Omega t)$ and $\mu(z, t) = \sum_{s=-\infty}^{\infty} \mu_{k, \text{aper}}(z) \exp(is\Omega t)$, where Ω is the temporal frequency of the modulation, and $\epsilon_{k, \text{aper}}(z)$ and $\mu_{k, \text{aper}}(z)$ are coefficients of the permittivity and permeability that are computed according to the spatial variation of the structure. The incident electric field is considered as a y -polarized plane wave, expressed as $\mathbf{E}_I(x, z, t) = \hat{\mathbf{y}} E_0 \exp[i(k_x x + k_z z - \omega_0 t)]$ that impinges on the structure in region 1 under the angle of incidence θ , where E_0 is the electric incident wave magnitude. We then express

the electric field inside the metasurface as time-Floquet waves; that is,

$$\mathbf{E}_M(x, z, t) = \hat{\mathbf{y}} \sum_{n,p} \mathbf{E}_{np} (A_{0p} e^{i\beta_{np}^+ z} + B_{0p} e^{-i\beta_{np}^- z}) e^{i(k_x x - \omega_n t)}. \quad (6)$$

Here, $\omega_n = \omega_0 + n\Omega$ is the temporal frequency of the n th temporal harmonic, and A_{0p} and B_{0p} are unknown field coefficients to be found by solving Maxwell's equations and applying boundary conditions [29]. Next, we apply the ST boundary conditions for electric and magnetic fields at $z = 0$ and $z = L$; that is, $\mathbf{E}_I(x, 0, t) + \mathbf{E}_R(x, 0, t) = \mathbf{E}_M(x, 0, t)$ and $\mathbf{E}_M(x, L, t) = \mathbf{E}_T(x, L, t)$. The scattered electric fields in regions 1 and 3 read

$$\mathbf{E}_R = \hat{\mathbf{y}} \sum_{n,p} [E_{np} (A_{0p} + B_{0p}) - E_0 \delta_{n0}] e^{i[k_x x - k_z z - \omega_n t]}, \quad (7a)$$

$$\mathbf{E}_T = \hat{\mathbf{y}} \sum_{n,p} E_{np} (A_{0p} e^{i\beta_{np} L} + B_{0p} e^{-i\beta_{np} L}) e^{i[k'_x x - k'_z z - \omega_n t]}, \quad (7b)$$

where δ_{n0} represents the Kronecker delta and is equal to one if $n = 0$ and zero otherwise.

ST DECOMPOSITION

The most common and practical form of periodic ST modulation is the sinusoidal form as $\epsilon(z, t) = \epsilon_0 \epsilon_r [1 + \delta_\epsilon \sin(qz - \Omega t)]$ and $\mu(z, t) = \mu_0 \mu_r [1 + \delta_\mu \sin(qz - \Omega t)]$, where δ_ϵ and δ_μ

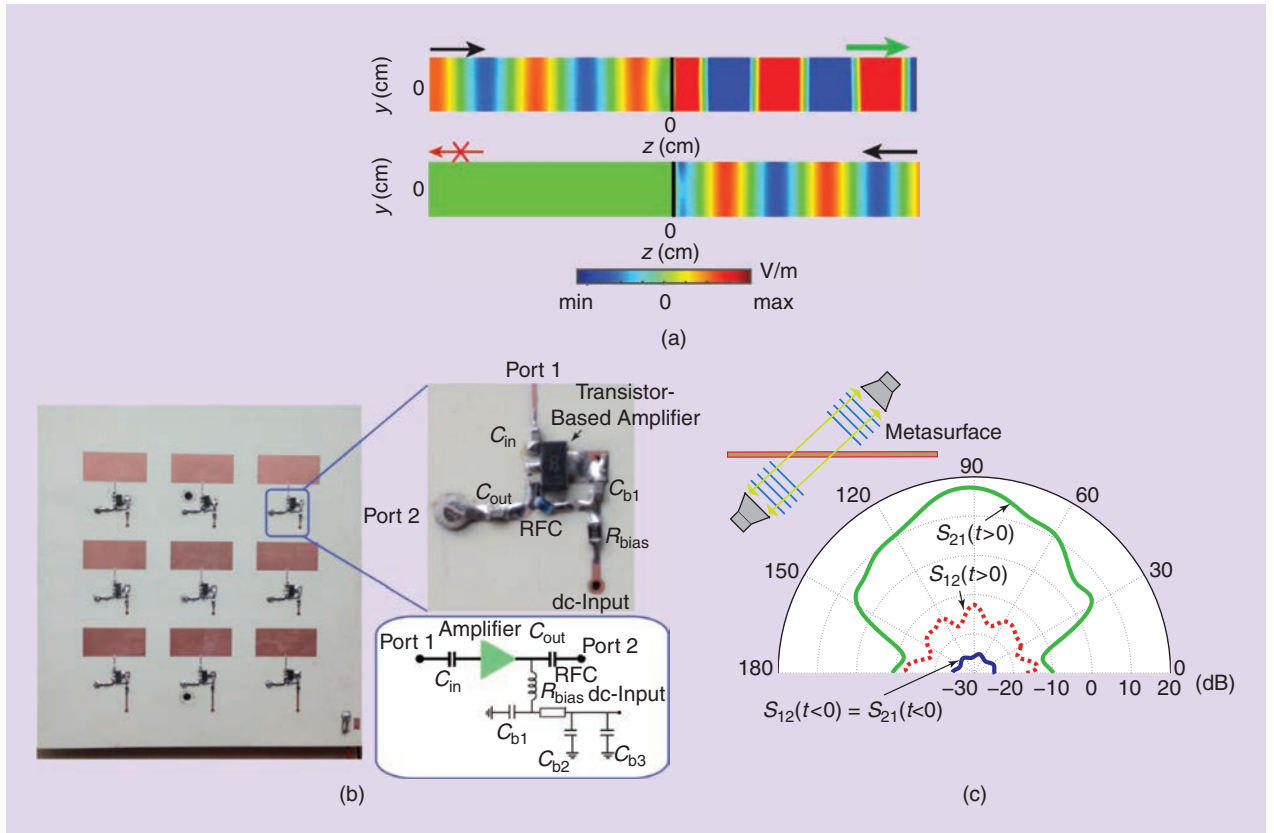


FIGURE 5. Nonreciprocal metasurface. (a) Full-wave (FDTD) electric field distribution for excitations from the left and right (bottom) [11]. (b) An image of the fabricated metasurface [11]. (c) Experimental scattering parameters versus angle at $f = 5.9$ GHz for transmission in a straight line under an oblique angle [11].

represent, respectively, the permittivity and permeability modulation strengths. The ST-varying intrinsic impedance of the structure may be represented as [29] $\eta(z, t) = \sqrt{\mu(z, t)/\epsilon(z, t)}$. Considering an equilibrated ST modulation, where $\delta_\mu = \delta_\epsilon$, the structure acquires an ST-invariant intrinsic impedance $\eta(z, t) = \eta_0 \eta_t$ that is immune to space and time local reflections. The ST decomposition of the reflected and transmitted STHs is illustrated in Figure 6(a). The reflection and transmission angles of the STHs can be derived by satisfying the Helmholtz relations; that is, $k^2 \sin^2(\theta_1) + k_n^2 \cos^2(\theta_{Rn}) = k_n^2$ and $k''^2 \sin^2(\theta_1) + k_n''^2 \cos^2(\theta_{Tn}) = k_n''^2$. Here, θ_{Rn} and θ_{Tn} denote the angles of reflection and transmission for the n th STH, which read

$$\theta_m = \theta_{t,n} = \sin^{-1} \left(\frac{\sin(\theta_1)}{1 + \frac{n\Omega}{\omega_0}} \right), \quad (8)$$

which demonstrates spectral decomposition of the scattered STHs. Considering $k' = k'' = k_0$, the reflection and transmission angles of the n th harmonic are equal for equal tangential wavenumbers $k_x = k_0 \sin(\theta_1)$ in all of the regions. The STHs ranging from $\omega_0(\sin(\theta_1) - 1)/\Omega$ to $+\infty$ are reflected and transmitted at angles ranging from 0 to $\pi/2$ through θ_1 for $n = 0$, while the rest of the STHs are imaginary k'_{znp} and propagate as surface waves along the boundary of the metasurface. The scattering angle of the p th mode of the n th STH inside the modulated region is given by $\theta_{np}^\pm = \tan^{-1}(k'_x/k'_{\text{znp}}) = \tan^{-1}(k'_0 \sin(\theta_1)/(k'_{0p} \pm nq))$.

NUMERICAL COMPUTATION SCHEME

To best gain insight into the wave propagation in ST metasurfaces and support the analytical solution, we study ST

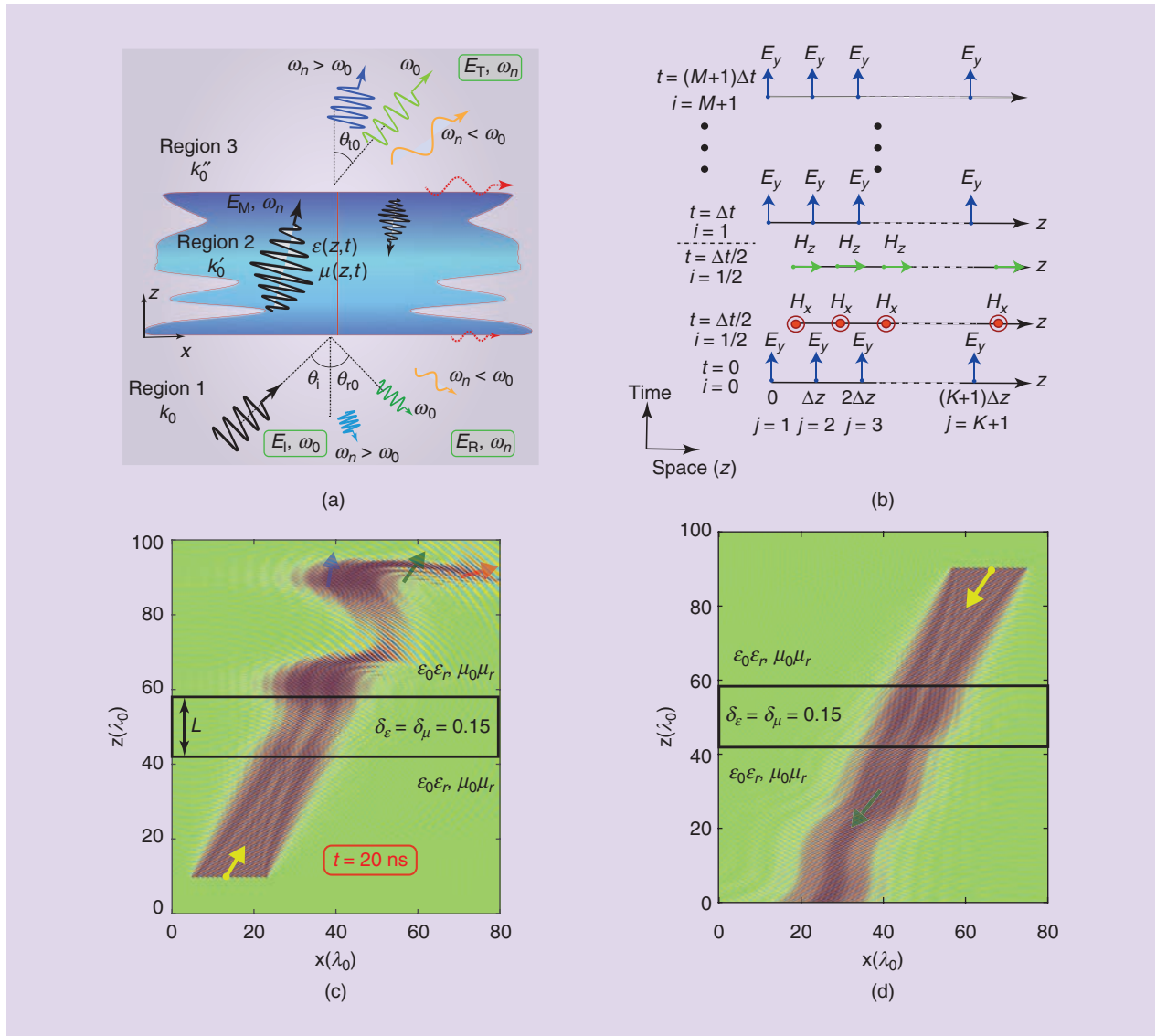


FIGURE 6. Wave scattering from an ST slab. (a) ST decomposition resulting from oblique incidence to an STM metasurface [15]. (b) FDTD scheme for numerical computation of the wave propagation and scattering in STP metasurfaces and slabs [13]. (c) E_y at $t = 20$ ns for forward wave incidence (from the bottom) and transmission [15]. (d) E_y at $t = 20$ ns for backward wave incidence (from the top) and transmission [15].

electromagnetic field propagation and scattering through FDTD numerical computation of Maxwell's equations. The FDTD scheme for oblique incidence to a general ST permittivity- and permeability-modulated metasurface is depicted in Figure 6(b), where the structure is discretized to $K + 1$ and $M + 1$ spatial and temporal samples, respectively, considering the spatial steps Δz and temporal steps Δt . Considering $\epsilon' = \partial\epsilon(z, t)/\partial t$ and $\mu' = \partial\mu(z, t)/\partial t$, we obtain

$$H_x|_{j+1/2}^{i+1/2} = \left(1 - \Delta t \frac{\mu'|_{j+1/2}^{i-1/2}}{\mu|_{j+1/2}^i}\right) H_x|_{j+1/2}^{i-1/2} + \frac{\Delta t}{\mu|_{j+1/2}^i \Delta z} (E_y|_{j+1}^i - E_y|_j^i), \quad (9a)$$

$$H_z|_{j+1/2}^{i+1/2} = \left(1 - \Delta t \frac{\mu'|_{j+1/2}^{i-1/2}}{\mu|_{j+1/2}^i}\right) H_z|_{j+1/2}^{i-1/2} - \frac{\Delta t}{\mu|_{j+1/2}^i \Delta z} (E_y|_{j+1}^i - E_y|_j^i), \quad (9b)$$

$$E_y|_j^{i+1} = \left(1 - \frac{\Delta t \epsilon'|_j^i}{\epsilon|_j^{i+1/2}}\right) E_y|_j^i + \frac{\Delta t / \Delta z}{\epsilon|_j^{i+1/2}} \cdot [(H_x|_{j+1/2}^{i+1/2} - H_x|_{j-1/2}^{i+1/2}) - (H_z|_{j+1/2}^{i+1/2} - H_z|_{j-1/2}^{i+1/2})]. \quad (9c)$$

Figure 6(c) and (d) plots FDTD computation results for nonreciprocal electric field scattering from a sinusoidally STP metasurface for forward and backward wave incidences, respectively. Such an equilibrated STP metasurface exhibits strong frequency generation, ST decomposition, and nonreciprocal wave transmission. In [29], it is shown that an equilibrated STM metasurface with $\delta_\mu = \delta_\epsilon > 0$ can be created using the same amount of pumping energy that is required for the creation of a permittivity-modulated metasurface, where $\delta_\epsilon > 0$ and $\delta_\mu = 0$. Additionally, such an equilibrated STP metasurface exhibits a matched intrinsic impedance and, therefore, is immune to local space and time reflections.

DIFFRACTION REGIME OF ST METASURFACES

The analysis provided in the previous section is applicable for ST metasurfaces operating outside the diffraction regime and is not directly applicable to the diffraction regime of ST metasurfaces. We shall stress that the FDTD numerical simulation scheme provided in the section "Numerical Computation Scheme" is applicable to all operation regimes of ST media, including the diffraction regime that will be discussed in this section. This section analyzes ST metasurfaces that provide spatial diffractions, where each spatial diffraction order denoted by m comprises temporal diffractions denoted by n [17]. The wave vector diagram in Figure 7(a) represents a powerful tool for studying ST diffractions from STP diffraction gratings. This diagram is constituted based on the phase matching of ST diffractions inside and outside the grating. The parameters of the STP grating are the temporal frequency Ω and the spatial frequency K , with $\Lambda = 2\pi/K$ being the spatial periodicity of the grating. Here, regions 1 to 3 present the phase velocities $v_r = c/n_1$, $v'_r = c/n_{av}$, and $v''_r = c/n_3$, and the wave vectors $\mathbf{k}_{mn} = k_{x,mn}\hat{\mathbf{x}} + k_{z,mn}\hat{\mathbf{z}}$, $\mathbf{k}_{pmn} = k'_{x,pmn}\hat{\mathbf{x}} + k'_{z,pmn}\hat{\mathbf{z}}$, and $\mathbf{k}_{mn}'' = k''_{x,mn}\hat{\mathbf{x}} + k''_{z,mn}\hat{\mathbf{z}}$, respectively. Here, p is the number of the mode inside the grating (these modes only exist inside the

grating), m denotes the number of the spatial harmonic, and n represents the number of the temporal harmonic.

The diffraction condition for ST diffraction gratings can be found by considering $|\sin(\theta_{mn})| \leq 1$. Hence, the m th propagating diffraction order should satisfy the condition [4]

$$\left| \frac{\sin(\theta_l) + m\Delta k}{1 + n\Delta\omega} \right|_{n=m} \leq 1 \quad (10)$$

to be diffracted as a propagating ST diffraction order. Here, $\Delta k = K/k_0$ and $\Delta\omega = \Omega/\omega_0$. The condition $n = m$ in (10) is due to the fact that in the m th spatial diffraction order the $n = m$ th temporal diffraction order represents the dominant ST diffraction order and possesses the largest amplitude [17]. Figure 7(b) presents the FDTD numerical computation of ST diffraction from an STP diffraction metasurface for a y -polarized electric field incident wave. Here, $k''_{x,mn} = k_n \sin(\theta_{mn})$ and $k''_{z,mn} = \sqrt{(k''_{mn})^2 - (k''_{x,mn})^2} = k_n \cos(\theta_{mn})$ are the x and z components of the wave vectors in region 3, respectively, where $k_n'' = k_0'' + n\Omega/v_r''$ and $k_0'' = \omega_0/v_r''$. By applying the momentum and energy conservation laws, we obtain $k_{x,diff} = k''_{x,mn} = k_x + mK$ and $\omega_{diff} = \omega_0 + n\Omega$, where $k_{x,diff}$ and ω_{diff} denote the x component wave vector and temporal frequency of the diffracted field, respectively. Then, the diffraction angle of the forward and backward ST diffracted orders is obtained as [17]

$$\sin(\theta_{mn}'') = \frac{\sin(\theta_l) + mK/k_0}{1 + n\Omega/\omega_0}. \quad (11)$$

We next calculate the electromagnetic fields inside the STP diffractive metasurface as the superposition of ST modes, denoted by p , such that the electromagnetic field of each mode is represented by ST Bloch–Floquet plane waves, denoted by m and n . The operation regime of diffractive metasurfaces may be categorized in two classes, Bragg regime diffraction of thick STP diffractive metasurfaces and Raman–Nath regime diffraction of thin STP diffractive metasurfaces [17]. Such ST diffractive metasurfaces that are modulated unidirectionally introduce nonreciprocal and angle-asymmetric ST diffractions, as shown in Figure 8(a)–(d) for a reflective STP metasurface.

ILLUSTRATIVE EXAMPLES

SUPERLUMINAL ST MODULATION: UNIDIRECTIONAL BEAM SPLITTING

Beam splitters are essential parts of optical and microwave systems. Conventional beam splitters are passive bulky structures that present a reciprocal response and introduce considerable transmission loss. In [13], it was shown that periodic ST modulation can create a unidirectional active beam splitter and amplifier based on coherent electromagnetic transitions emerging from oblique illumination of STP metasurfaces. The proposed one-way beam splitter and amplifier and its functionality are illustrated in Figure 9(a). The operation of this apparatus is based on a unidirectional energy and momentum transition between the incident wave with temporal frequency ω_0 and

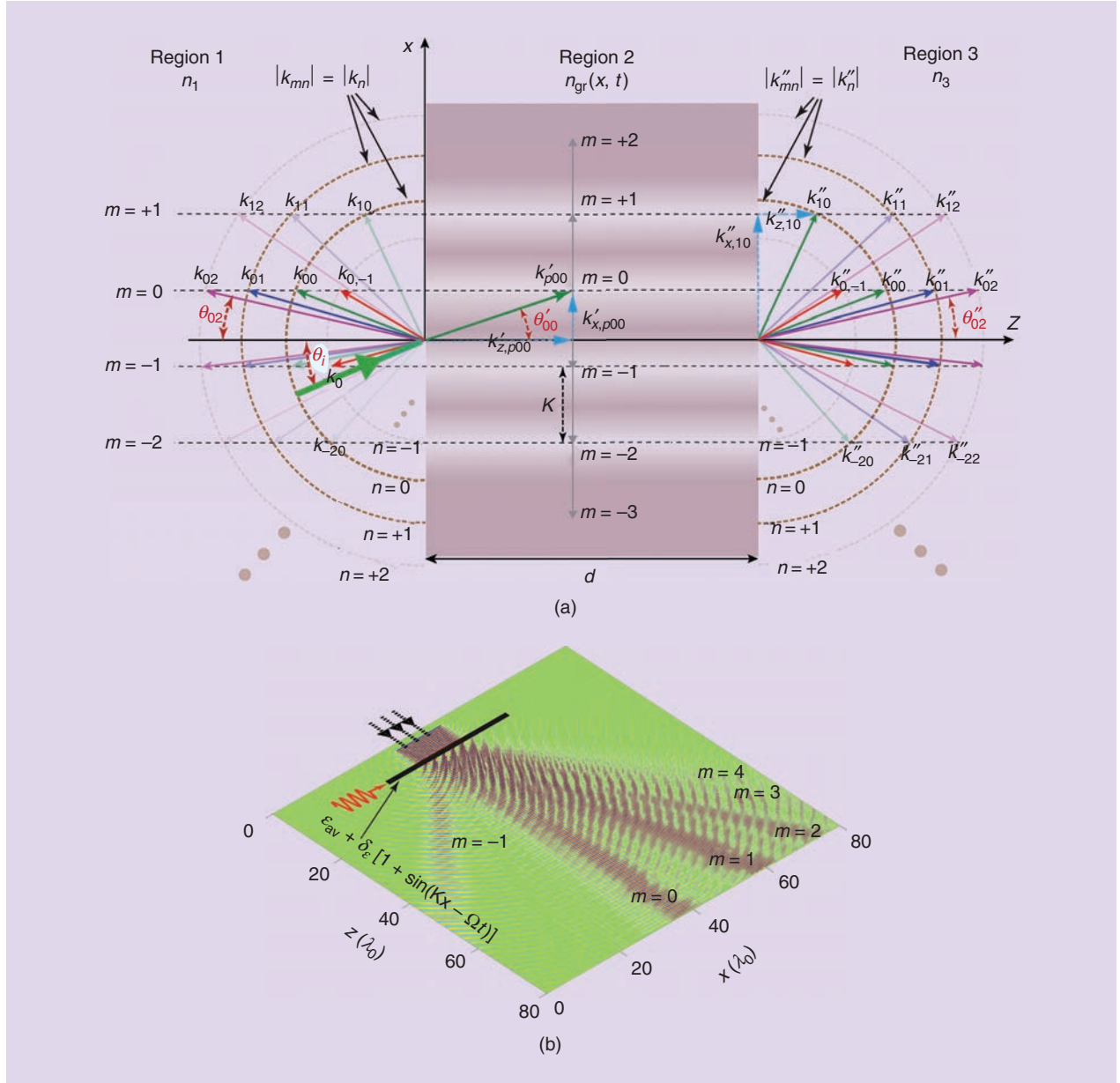


FIGURE 7. A transmissive STP diffractive metasurface. (a) The wave vector diagram for analysis of the ST diffraction based on phase matching of ST diffractions inside and outside the modulated metasurface [17]. (b) FDTD numerical computation of Raman–Nath diffraction from a thin sinusoidal STP metasurface [17].

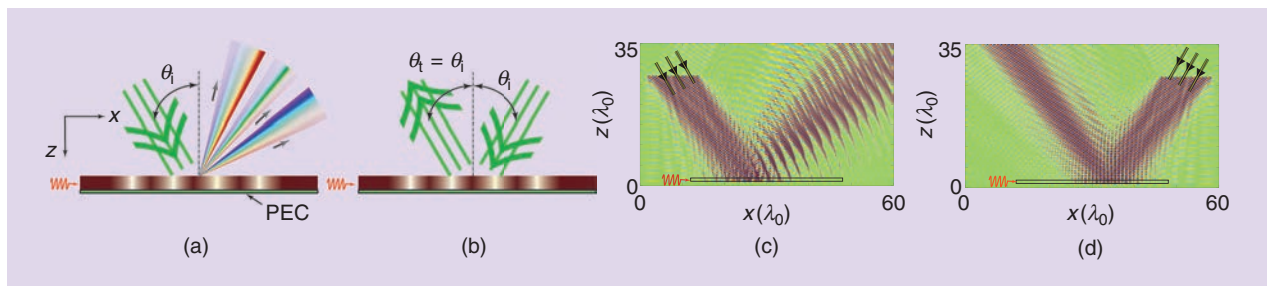


FIGURE 8. A reflective STP diffractive metasurface introducing angle-asymmetric and nonreciprocal ST diffractions. (a) and (c) Wave incidence from the left side (forward problem) [17]. (b) and (d) Wave incidence from the right side (backward problem) for angle-asymmetric and nonreciprocal diffraction demonstration [17]. PEC: perfect electric conductor.

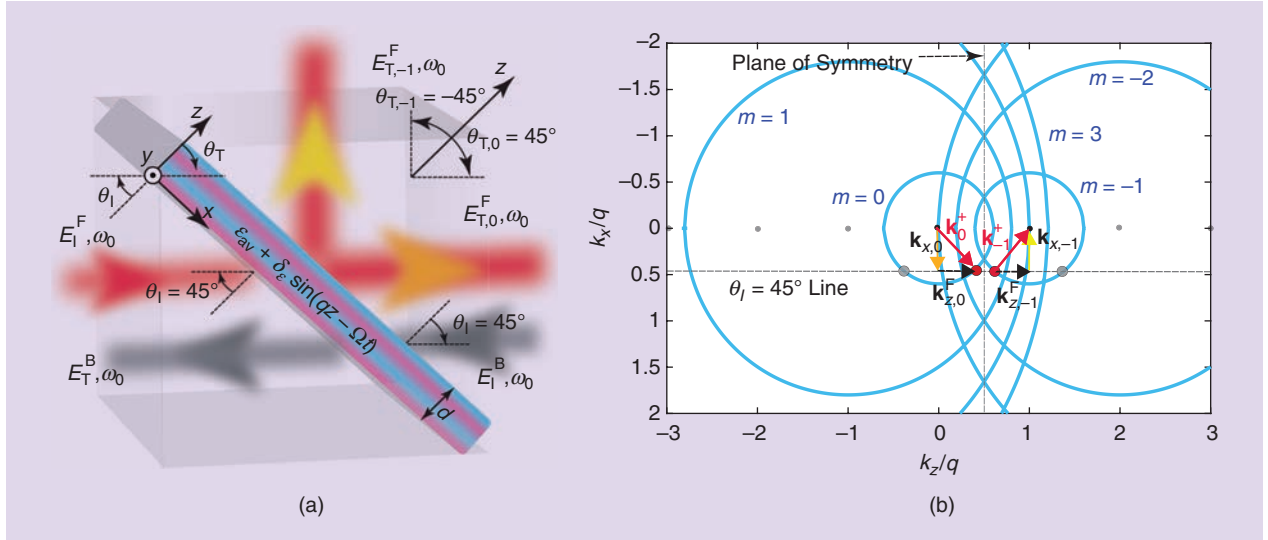


FIGURE 9. One-way beam splitting by an STP metasurface, where the two forward transmitted beams, $E_{T,0}^F$ and $E_{T,-1}^F$, are amplified. (a) The schematic [13]. (b) The isofrequency dispersion diagram at $\omega = \omega_0$ [13].

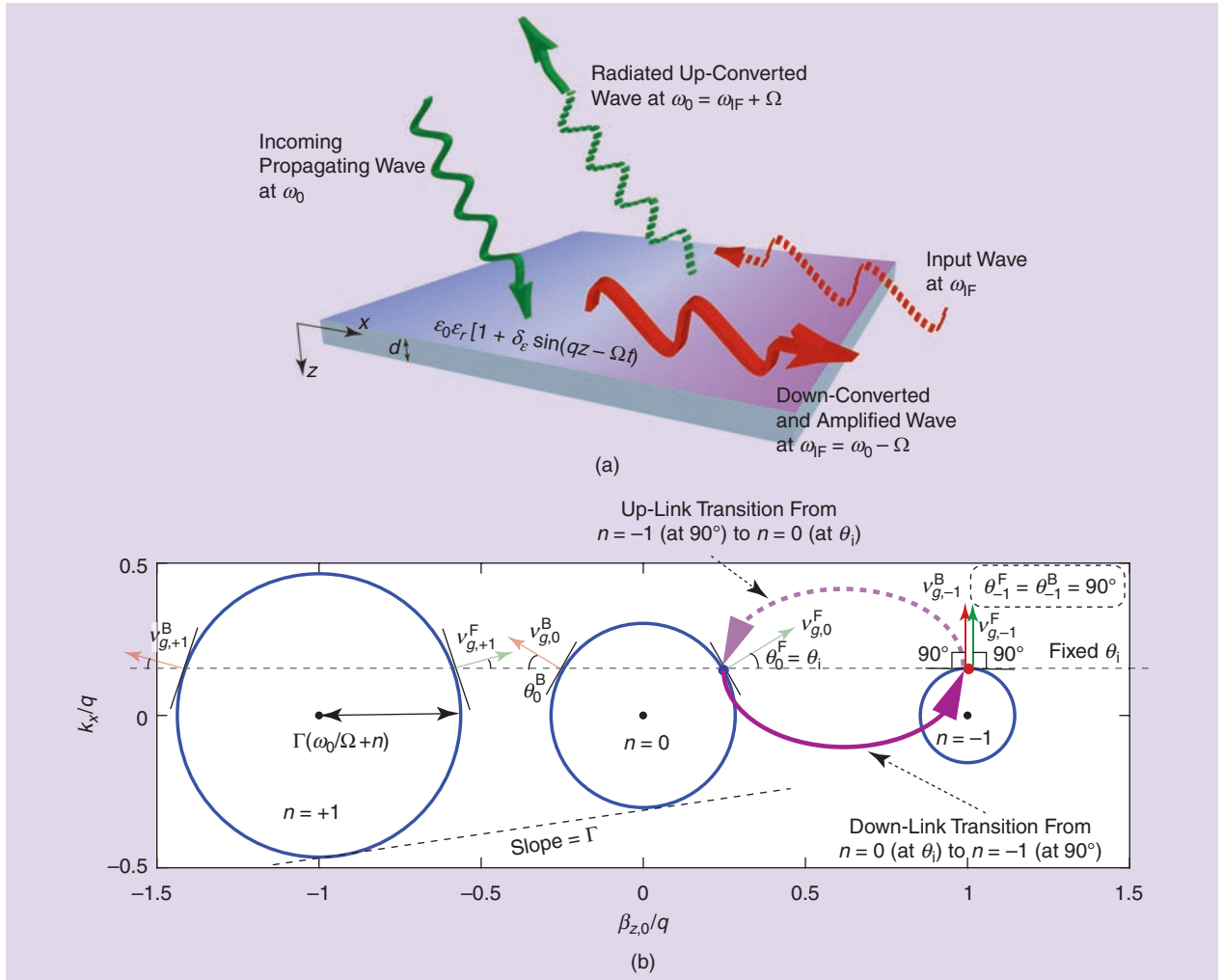


FIGURE 10. Antenna–mixer–amplifier metasurface. (a) Schematic representation showing the down-link and up-link wave transformations [55]. (b) Isofrequency diagram depicting, for $\epsilon_m \rightarrow 0$ and $\Gamma = 0.2$, the down-link electromagnetic transition from an incoming space wave to an ST surface wave and the up-link electromagnetic transition from a surface wave to an ST radiating space wave [55].

the ST modulation with temporal frequency $2\omega_0$. Then, by setting the angle of incidence of $\theta_i = 45^\circ$, the fundamental ($n = 0$) and first lower ($n = -1$) STHs are transmitted under angles of transmissions $\theta_{T,0} = 45^\circ$ and $\theta_{T,-1} = -45^\circ$, respectively. Additionally, the two transmitted STHs with a 45° -angle difference acquire the same temporal frequency as the incident wave ω_0 , which leads to a perfect unidirectional beam splitter and amplifier. The analytical isofrequency dispersion diagram in Figure 9(b) plots the one-way ST coherency between the $n = 0$ and $n = -1$ STHs.

The beam splitter is created by an STP slab with spatial modulation $q = 2k_0/\Gamma$ and temporal modulation frequency $\Omega = 2\omega_0$, where $\Gamma = v_m/v_b = 1.2$. The temporal modulation frequency $\Omega = 2\omega_0$ is chosen to achieve a constructive ST coherency and beam splitting as follows. The transmission angle of the STHs can be determined by satisfying the Helmholtz relation as $\theta_{T,n} = \sin^{-1}(k_x/k_n) = \sin^{-1}(\sin(\theta_i)/(1+2n))$, which reveals that the $n = 0$ and $n = -1$ STHs possessing temporal frequency ω_0 acquire a 90° -angle difference; that is, $\theta_{T,0} = \theta_i = 45^\circ$ and $\theta_{T,-1} = -\theta_i = -45^\circ$.

SUBLUMINAL ST MODULATION: ANTENNA–MIXER–AMPLIFIER FUNCTIONALITY

Consider the metasurface in Figure 10(a) characterized with a sinusoidal STP electric permittivity and thickness d . In the down-link reception state, the space wave with temporal frequency ω_0 makes a transition to an ST surface wave with temporal frequency $\omega_{IF} = \omega_0 - \Omega$. In the up-link transmission state, the ST surface wave at ω_{IF} makes a transition to a space wave at $\omega_0 = \omega_{IF} + \Omega$. Because of the ST periodicity of the metasurface, the complex spatial frequency of the STHs is given by $K_{z,n} = k_z + nq + i\alpha_{z,n}$, and the temporal frequency of the STHs is $\omega_n = \omega_0 + n\Omega$. Additionally, the incident angle is set to $\theta_i = \sin^{-1}(1 - \Omega/\omega_0)$. Figure 10(b) shows that a strong electromagnetic transition from the $n = 0$ STH to the $n = -1$ STH can be achieved by designing the dispersion band of the structure in such a way that the scattered $n = -1$ STH propagates in parallel to the two ST surface waves along the boundaries at $z = 0$ and $z = d$ ($\theta_{n=-1} = 90^\circ$). This engineering of the ST modulation leads to $\beta_{z,-1} = 0$. This results in a purely imaginary z -component wave vector, that is, $K_{z,-1} = i\alpha_{z,-1}$, while the incident space wave possess a real wave vector.

CONCLUSIONS

We presented a comprehensive review of the theory and analysis of wave propagation in ST metasurfaces and examples of extraordinary 4D wave transformations in such media. It is shown that ST metasurfaces are capable of 4D electromagnetic wave transformations, which are significantly more versatile and useful than the 3D wave transformations of conventional spatially variant static metamaterials and metasurfaces. Recent progress on ST metasurfaces for breaking time-reversal symmetry and reciprocity reveals a great potential for applications of these metasurfaces in low-energy and energy-harvesting telecommunication systems and compact and integrated nonreciprocal devices and subsystems.

ACKNOWLEDGMENT

This research was sponsored by the Natural Sciences and Engineering Research Council of Canada. This article has supplementary downloadable material available at <http://doi.org/10.1109/MAP.2022.3201195>.



AUTHOR INFORMATION

Sajjad Taravati (sajjad.taravati@utoronto.ca) is with the Edward S. Rogers Sr. Department of Electrical and Computer Engineering, University of Toronto, Toronto, ON M5S 2E4, Canada. His research interests include applied physics, electromagnetics, nonreciprocal magnetless systems, space-time-modulated structures, circuits, and metamaterials and metasurfaces. He is a Senior Member of IEEE.

George V. Eleftheriades (gelefh@ece.utoronto.ca) is a professor in the Edward S. Rogers Sr. Department of Electrical and Computer Engineering, University of Toronto, Toronto, ON M5S 2E4, Canada, where he holds the Velma M. Rogers Graham Endowed Chair in Engineering. He is a Fellow of IEEE.

REFERENCES

- [1] T. W. Ebbesen, H. J. Lezec, H. Ghaemi, T. Thio, and P. Wolff, "Extraordinary optical transmission through sub-wavelength hole arrays," *Nature*, vol. 391, no. 6668, p. 667, Feb. 1998, doi: 10.1038/35570.
- [2] S. Taravati and G. V. Eleftheriades, "Programmable nonreciprocal metaprism," *Sci. Rep.*, vol. 11, no. 1, pp. 1–12, Apr. 2021.
- [3] S. Taravati and G. V. Eleftheriades, "Full-duplex reflective beamsteering metasurface featuring magnetless nonreciprocal amplification," *Nature Commun.*, vol. 14, p. 4414, Jul. 2021, doi: 10.1038/s41467-021-24749-7.
- [4] S. Taravati and G. V. Eleftheriades, "Microwave space-time-modulated metasurfaces," *ACS Photon.*, vol. 9, no. 2, pp. 305–318, 2022, doi: 10.1021/acspophotonics.1c01041.
- [5] V. G. Atalagou, M. Chen, M. Kim, and G. V. Eleftheriades, "Microwave Huygens' metasurfaces: Fundamentals and applications," *IEEE J. Microw.*, vol. 1, no. 1, pp. 374–388, Jan. 2021, doi: 10.1109/JMW.2020.3034578.
- [6] R. A. Shelby, D. R. Smith, and S. Schultz, "Experimental verification of a negative index of refraction," *Science*, vol. 292, no. 5514, pp. 77–79, Apr. 2001, doi: 10.1126/science.1058847.
- [7] C. Caloz, A. Alù, S. Tretyakov, D. Sounas, K. Achouri, and Z.-L. Deck-Léger, "Electromagnetic nonreciprocity," *Phys. Rev. Appl.*, vol. 10, no. 4, p. 047001, Oct. 2018.
- [8] S. Taravati and G. V. Eleftheriades, "Full-duplex nonreciprocal beam steering by time-modulated phase-gradient metasurfaces," *Phys. Rev. Appl.*, vol. 14, no. 1, p. 014027, Jul. 2020.
- [9] A. Kord, D. L. Sounas, and A. Alù, "Microwave nonreciprocity," *Proc. IEEE*, vol. 108, no. 10, pp. 1728–1758, Oct. 2020, doi: 10.1109/JPROC.2020.3006041.
- [10] Y. Hadad, D. L. Sounas, and A. Alù, "Space-time gradient metasurfaces," *Phys. Rev. B*, vol. 92, no. 10, p. 100304, Sep. 2015, doi: 10.1103/PhysRevB.92.100304.
- [11] S. Taravati, B. A. Khan, S. Gupta, K. Achouri, and C. Caloz, "Nonreciprocal nongyrotropic magnetless metasurface," *IEEE Trans. Antennas Propag.*, vol. 65, no. 7, pp. 3589–3597, Jul. 2017, doi: 10.1109/TAP.2017.2702712.
- [12] L. Zhang et al., "Space-time-coding digital metasurfaces," *Nature Commun.*, vol. 9, no. 1, p. 4334, May 2018, doi: 10.1038/s41467-018-06802-0.
- [13] S. Taravati and A. A. Kishk, "Dynamic modulation yields one-way beam splitting," *Phys. Rev. B*, vol. 99, no. 7, p. 075101, Jan. 2019, doi: 10.1103/PhysRevB.99.075101.
- [14] Z. Wu and A. Grbic, "Serrodyne frequency translation using time-modulated metasurfaces," *IEEE Trans. Antennas Propag.*, vol. 68, no. 3, pp. 1599–1606, Mar. 2019, doi: 10.1109/TAP.2019.2943712.
- [15] S. Taravati and A. A. Kishk, "Advanced wave engineering via obliquely illuminated space-time-modulated slab," *IEEE Trans. Antennas Propag.*, vol. 67, no. 1, pp. 270–281, Jan. 2019, doi: 10.1109/TAP.2018.2877394.
- [16] J. W. Zang, D. Correas-Serrano, J. T. S. Do, X. Liu, A. Alvarez-Melcon, and J. S. Gómez-Díaz, "Nonreciprocal waveform engineering with time-modulated gradient metasurfaces," *Phys. Rev. Appl.*, vol. 11, no. 5, p. 054054, 2019, doi: 10.1103/PhysRevApplied.11.054054.

- [17] S. Taravati and G. V. Eleftheriades, "Generalized space-time periodic diffraction gratings: Theory and applications," *Phys. Rev. Appl.*, vol. 12, no. 2, p. 024026, Aug. 2019.
- [18] M. M. Salary, S. Jafar-Zanjani, and H. Mosallaei, "Electrically tunable harmonics in time-modulated metasurfaces for waveform engineering," *New J. Phys.*, vol. 20, no. 12, p. 123,023, Dec. 2018, doi: 10.1088/1367-2630/aa4f7a.
- [19] X. Guo, Y. Ding, Y. Duan, and X. Ni, "Nonreciprocal metasurface with space-time phase modulation," *Light Sci. Appl.*, vol. 8, no. 123, pp. 1–9, May 2019.
- [20] M. M. Salary, S. Farazi, and H. Mosallaei, "A dynamically modulated all-dielectric metasurface doublet for directional harmonic generation and manipulation in transmission," *Adv. Opt. Mater.*, vol. 7, no. 23, p. 1,900,843, Sep. 2019, doi: 10.1002/adom.201900843.
- [21] M. M. Salary and H. Mosallaei, "Time-modulated conducting oxide metasurfaces for adaptive multiple access optical communication," *IEEE Trans. Antennas Propag.*, vol. 68, no. 3, pp. 1628–1642, Mar. 2020, doi: 10.1109/TAP.2019.2938613.
- [22] H. B. Sedeh, M. M. Salary, and H. Mosallaei, "Time-varying optical vortices enabled by time-modulated metasurfaces," *Nanophotonics*, vol. 9, no. 9, pp. 2957–2976, Jul. 2020, doi: 10.1515/nanoph-2020-0202.
- [23] S. Taravati, "Aperiodic space-time modulation for pure frequency mixing," *Phys. Rev. B*, vol. 97, no. 11, p. 115,131, Mar. 2018, doi: 10.1103/PhysRevB.97.115131.
- [24] P. Chu, J. Chen, Z. Xiong, and Z. Yi, "Controllable frequency conversion in the coupled time-modulated cavities with phase delay," *Opt. Commun.*, vol. 476, p. 126,338, Dec. 2020, doi: 10.1016/j.optcom.2020.126338.
- [25] A. L. Cullen, "A travelling-wave parametric amplifier," *Nature*, vol. 181, no. 4605, p. 332, Feb. 1958, doi: 10.1038/181332a0.
- [26] X. Zhu, J. Li, C. Shen, G. Zhang, S. A. Cummer, and L. Li, "Tunable unidirectional compact acoustic amplifier via space-time modulated membranes," *Phys. Rev. B*, vol. 102, no. 2, p. 024309, Jul. 2020, doi: 10.1103/PhysRevB.102.024309.
- [27] S. Taravati, N. Chamanara, and C. Caloz, "Nonreciprocal electromagnetic scattering from a periodically space-time modulated slab and application to a quasisonic isolator," *Phys. Rev. B*, vol. 96, no. 16, p. 165,144, Oct. 2017, doi: 10.1103/PhysRevB.96.165144.
- [28] S. Y. Elnaggar and G. N. Milford, "Controlling nonreciprocity using enhanced Brillouin scattering," *IEEE Trans. Antennas Propag.*, vol. 66, no. 7, pp. 3500–3511, Jul. 2018, doi: 10.1109/TAP.2018.2835305.
- [29] S. Taravati, "Giant linear nonreciprocity, zero reflection, and zero band gap in equilibrated space-time-varying media," *Phys. Rev. Appl.*, vol. 9, no. 6, p. 064012, Jun. 2018.
- [30] D. Ramaccia, D. L. Soumas, A. Alù, A. Toscano, and F. Bilotti, "Phase-induced frequency conversion and doppler effect with time-modulated metasurfaces," *IEEE Trans. Antennas Propag.*, vol. 68, no. 3, pp. 1607–1617, Mar. 2020, doi: 10.1109/TAP.2019.2952469.
- [31] H. Barati Sedeh, M. M. Salary, and H. Mosallaei, "Topological space-time photonic transitions in angular-momentum-biased metasurfaces," *Adv. Opt. Mater.*, vol. 8, no. 11, p. 2,000,075, Mar. 2020, doi: 10.1002/adom.202000075.
- [32] P. A. Huidobro, E. Galiffi, S. Guenneau, R. V. Craster, and J. Pendry, "Fresnel drag in space-time-modulated metamaterials," *Proc. Nat. Acad. Sci. USA*, vol. 116, no. 50, pp. 24,943–24,948, Nov. 2019, doi: 10.1073/pnas.1915027116.
- [33] S. Taravati and G. V. Eleftheriades, "Lightweight low-noise linear isolator integrating phase- and amplitude-engineered temporal loops," *Adv. Mater. Technol.*, vol. 7, no. 6, p. 2,100,674, Dec. 2021, doi: 10.1002/admt.202100674.
- [34] S. Taravati and C. Caloz, "Mixer-duplexer-antenna leaky-wave system based on periodic space-time modulation," *IEEE Trans. Antennas Propag.*, vol. 65, no. 2, pp. 442–452, Feb. 2017, doi: 10.1109/TAP.2016.2632735.
- [35] X. Wu, X. Liu, M. D. Hickle, D. Peroulis, J. S. Gómez-Díaz, and A. Á. Melcón, "Isolating bandpass filters using time-modulated resonators," *IEEE Trans. Microw. Theory Techn.*, vol. 67, no. 6, pp. 2331–2345, Jun. 2019, doi: 10.1109/TMTT.2019.2908863.
- [36] V. Bacot, M. Labousse, A. Eddi, M. Fink, and E. Fort, "Time reversal and holography with spacetime transformations," *Nature Phys.*, vol. 12, no. 10, p. 972, 2016, doi: 10.1038/nphys3810.
- [37] S. A. Stewart, T. J. Smy, and S. Gupta, "Finite-difference time-domain modeling of space-time-modulated metasurfaces," *IEEE Trans. Antennas Propag.*, vol. 66, no. 1, pp. 281–292, Jan. 2018, doi: 10.1109/TAP.2017.2772045.
- [38] N. Wang, Z.-Q. Zhang, and C. Chan, "Photonic Floquet media with a complex time-periodic permittivity," *Phys. Rev. B*, vol. 98, no. 8, p. 085142, Aug. 2018, doi: 10.1103/PhysRevB.98.085142.
- [39] S. Taravati and A. A. Kishk, "Space-time modulation: Principles and applications," *IEEE Microw. Mag.*, vol. 21, no. 4, pp. 30–56, Apr. 2020, doi: 10.1109/MMM.2019.2963606.
- [40] G. A. Ptitsyn, M. S. Mirmoosa, and S. A. Tretyakov, "Time-modulated meta-atoms," *Phys. Rev. Res.*, vol. 1, no. 2, p. 023014, Sep. 2019, doi: 10.1103/PhysRevResearch.1.023014.
- [41] V. Tuukkaara, T. J. Smy, and S. Gupta, "Floquet analysis of space-time modulated metasurfaces with Lorentz dispersion," *IEEE Trans. Antennas Propag.*, vol. 69, no. 11, pp. 7667–7678, Nov. 2021, doi: 10.1109/TAP.2021.3070718.
- [42] A. Li, Y. Li, J. Long, E. Forati, Z. Du, and D. Sievenpiper, "Time-modulated nonreciprocal metasurface absorber for surface waves," *Opt. Lett.*, vol. 45, no. 5, pp. 1212–1215, Mar. 2020, doi: 10.1364/OL.382865.
- [43] R. Sabri, M. M. Salary, and H. Mosallaei, "Broadband continuous beamsteering with time-modulated metasurfaces in the near-infrared spectral regime," *APL Photon.*, vol. 6, no. 8, p. 086109, Aug. 2021, doi: 10.1063/5.0051815.
- [44] X. Wang, V. S. Asadchy, S. Fan, and S. A. Tretyakov, "Space-time metasurfaces for power combining of waves," *ACS Photon.*, vol. 8, no. 10, pp. 3034–3041, Sep. 2021, doi: 10.1021/acspolit.1c00981.
- [45] J. L. Wentz, "A nonreciprocal electrooptic device," *Proc. IEEE*, vol. 54, no. 1, pp. 97–98, Jan. 1966, doi: 10.1109/PROC.1966.4617.
- [46] S. Taravati, "Self-biased broadband magnet-free linear isolator based on one-way space-time coherency," *Phys. Rev. B*, vol. 96, no. 23, p. 235,150, Dec. 2017, doi: 10.1103/PhysRevB.96.235150.
- [47] M. Oudich, Y. Deng, M. Tao, and Y. Jing, "Space-time phononic crystals with anomalous topological edge states," *Phys. Rev. Res.*, vol. 1, no. 3, p. 033069, Nov. 2019.
- [48] M. Chegnizadeh, M. Memarian, and K. Mehrany, "Non-reciprocity using quadrature-phase time-varying slab resonators," *J. Opt. Soc. Am. B*, vol. 37, no. 1, pp. 88–97, 2020, doi: 10.1364/JOSAB.37.000088.
- [49] S. Wan, L. Cao, Y. Zhu, M. Oudich, and B. Assouar, "Nonreciprocal sound propagation via cascaded time-modulated slab resonators," *Phys. Rev. Appl.*, vol. 16, no. 6, p. 064061, Dec. 2021.
- [50] S. Taravati and G. V. Eleftheriades, "Pure and linear frequency-conversion temporal metasurface," *Phys. Rev. Appl.*, vol. 15, no. 6, p. 064011, Jun. 2021.
- [51] S. Taravati and A. A. Kishk, "Space-time-varying surface-wave antenna," in *Proc. 2018 IEEE 18th Int. Symp. Antennas Technol. Appl. Electromagn. (ANTEM)*, pp. 1–2, doi: 10.1109/ANTEM.2018.8573041.
- [52] J. Zang, X. Wang, A. Alvarez-Melcon, and J. S. Gómez-Díaz, "Nonreciprocal Yagi-Uda filtering antennas," *IEEE Antennas Wireless Propag. Lett.*, vol. 18, no. 12, pp. 2661–2665, Dec. 2019, doi: 10.1109/LAWP.2019.2947847.
- [53] M. Liu, A. B. Kozyrev, and I. V. Shadrivov, "Time-varying metasurfaces for broadband spectral camouflage," *Phys. Rev. Appl.*, vol. 12, no. 5, p. 054052, Nov. 2019.
- [54] X. Wang and C. Caloz, "Spread-spectrum selective camouflaging based on time-modulated metasurface," *IEEE Trans. Antennas Propag.*, vol. 69, no. 1, pp. 286–295, Jan. 2020, doi: 10.1109/TAP.2020.3008621.
- [55] S. Taravati and G. V. Eleftheriades, "Space-time medium functions as a perfect antenna-mixer-amplifier transceiver," *Phys. Rev. Appl.*, vol. 14, no. 5, p. 054017, Nov. 2020.
- [56] Z. Manzoor and S. Taravati, "Enhanced resolution imaging by aperiodically perturbed photonic time crystals," in *Proc. 2020 IEEE Conf. Lasers Electro-Opt. (CLEO)*, pp. 1–2.
- [57] J. Li, C. Shen, X. Zhu, Y. Xie, and S. A. Cummer, "Nonreciprocal sound propagation in space-time modulated media," *Phys. Rev. B*, vol. 99, no. 14, p. 144,311, Apr. 2019, doi: 10.1103/PhysRevB.99.144311.
- [58] M. Liu, D. A. Powell, Y. Zarate, and I. V. Shadrivov, "Huygens' metadevices parametric waves," *Phys. Rev. X*, vol. 8, no. 3, p. 031077, 2018, doi: 10.1103/PhysRevX.8.031077.
- [59] S. Y. Elnaggar and G. N. Milford, "Modeling space-time periodic structures with arbitrary unit cells using time periodic circuit theory," *IEEE Trans. Antennas Propag.*, vol. 68, no. 9, pp. 6636–6645, Sep. 2020, doi: 10.1109/TAP.2020.2985712.
- [60] C. Caloz and Z.-L. Deck-Leger, "Spacetime metamaterials—Part II: Theory and applications," *IEEE Trans. Antennas Propag.*, vol. 68, no. 3, pp. 1583–1598, Mar. 2019, doi: 10.1109/TAP.2019.2944216.
- [61] J. G. Gaxiola-Luna and P. Halevi, "Temporal photonic (time) crystal with a square profile of both permittivity $\epsilon(t)$ and permeability $\mu(t)$," *Phys. Rev. B*, vol. 103, no. 14, p. 144,306, Apr. 2021, doi: 10.1103/PhysRevB.103.144306.
- [62] D. M. Solís and N. Engheta, "Functional analysis of the polarization response in linear time-varying media: A generalization of the Kramers-Kronig relations," *Phys. Rev. B*, vol. 103, no. 14, p. 144,303, Apr. 2021, doi: 10.1103/PhysRevB.103.144303.
- [63] H. A. Lorentz, "Electromagnetic phenomena in a system moving with any velocity smaller than that of light," in *Collected Papers*. Dordrecht, The Netherlands: Springer Science & Business Media, 1937, pp. 172–197.



Call for Papers



2024 International Workshop on Antenna Technology

Small Antennas, Novel Metamaterials and Their Applications

April 15–18, 2024, Tohoku University, Sendai, Japan

<https://attend.ieee.org/iwat-2024/>

General Co-Chairs

Qiang Chen
Tohoku Univ.

Nozomu Ishii
Niigata Univ.

International Advisory Committee Co-Chairs
Zhi Ning Chen
National Univ. of Singapore

Raj Mittra
Univ. of Central Florida

Koichi Ito
Chiba Univ.

TPC Chair
Naoki Honma
Iwate Univ.

TPC Vice Chairs
Takuji Arima
Tokyo Univ. of Agri. & Tech,

Naobumi Michishita
National Defense Academy,

Qiaowei Yuan
Tohoku Inst. of Tech.

Finance Chair
Yukiko Kishiki
Kozo Keikaku Engineering, Inc.

Local Organization Chair
Hiroyasu Sato
Tohoku Univ.

Local Organization Vice Chairs
Jerdvisanop Chakarothai
NICT

Yumiko Ito
Tohoku Univ.

Publicity Chairs
Jiro Hirokawa
Tokyo Inst. of Tech.

Takeshi Fukusako
Kumamoto Univ.

Conference Secretaries
Keisuke Konno
Tohoku Univ.

Nozomi Haga
Toyohashi Univ. of Tech.

The International Workshop on Antenna Technology (iWAT) is an annual forum for the exchange of information on the progress of research and development in innovative antenna technology. It especially focuses on small antennas and applications of advanced and artificial materials to the antenna design. At iWAT, all the oral presentations are delivered by invited prominent researchers and professors. iWAT has a particular focus on posters by which authors have the opportunity to interact with leading researchers in their fields. iWAT is a series of annual international antenna workshops which has been held in various countries all over the world. Student Paper Awards and Student Encouragement Awards will be presented to the students with high-quality works at iWAT2024. These awards will be presented at the banquet. iWAT 2024 commemorates 100 years anniversary of Yagi-Uda antenna developed by Prof. Hidetsugu Yagi and Shintaro Uda at Tohoku University, Sendai, Japan.



Photograph of Yagi-Uda antenna used as a UHF receiver for a communication experiment from Sendai to Otakamori in 1929 (Citation from web page of RIEC, Tohoku Univ., <https://www.riecl.tohoku.ac.jp/ja/about-riecl/antenna/>).

Topics include but are not limited to the following:

Small Antennas

- Adaptive (smart) arrays
- Antenna design and analysis based on characteristic or eigen modes
- Antenna measurements
- Antennas on/in IC packages
- Body-centric antennas
- Broadband antennas
- Conformal antennas
- Magnetic nanoparticles, graphene or carbon-nanotubes in Antennas
- Measurements for SAR of handheld devices

- MEMS/nanotechnology for antennas
- Terahertz nano and optical antennas
- Modeling and simulations
- Non-Foster/active elements
- On-chip antennas
- Reconfigurable antennas
- Reflectarrays
- Ultra-wideband (UWB) antennas
- Wearable, implanted, and encapsulated antennas
- 3D-printed antennas and structures

Novel Metamaterials

- Analysis and design of EM materials
- Artificial magnetic conductors (AMC)
- Electromagnetic anisotropy
- Intelligent materials
- Electromagnetic bandgap (EBG) structures

- Frequency-selective surfaces (FSS)
- Single and double negative metamaterials
- Electromagnetic skins: epidermal, flexible, and stretchable antennas, sensing substrates
- Reconfigurable intelligent surfaces

Applications

- Automotive systems
- Antennas for cube satellites
- Biomedical and healthcare applications
- Bluetooth/WLAN (PDAs, laptops)
- Energy harvesting
- Hyperthermia and RF Ablation
- GPS systems
- Medical diagnostic and therapeutic applications
- Millimeter-wave/terahertz communications and imaging
- MIMO systems

- RFID antennas and wireless sensing systems
- Software-defined/cognitive radio
- Satellite communications
- UWB communications
- WBAN systems
- Wireless communication systems (handheld devices, base stations)
- Wireless power transmission and harvesting for implanted systems
- Smart radio environment for 6G communication systems

Important Dates

Deadline of paper submission: December 8, 2023

Notification of acceptance: January 19, 2024

Paper Submission Guidelines

Authors **MUST** submit camera-ready papers that are **2 to 4 pages** including figures by December 8, 2023 via the workshop website. All papers must be formatted in two-column IEEE format including figures and electronic submissions must meet all IEEEExplore specifications. See the workshop website for templates and more information on creating acceptable electronic files.



IEEE Antennas and Propagation Society

Sendai Tourism,
Convention and
International Association



IEICE
Communications
Society



Raymond P. Wasky^{ID}

EDITOR'S NOTE

The worldwide coronavirus (COVID-19) pandemic may have resulted in the cancellation or delay of some of the meetings and symposia listed below. Please check all meeting websites for the latest information prior to making plans for registration or travel.

The number of submissions for meetings and symposia has fallen off drastically in the past 1–2 years. To help keep this column current, please e-mail any notices or calls for papers of upcoming conferences to raymond.wasky@jhuapl.edu.

35TH URSI GENERAL ASSEMBLY AND SCIENTIFIC SYMPOSIUM (URSI GASS 2023)

19–26 August 2023, Sapporo, Hokkaido, Japan. Contacts: Kazuya Kobayashi, URSI GASS 2023 general chair, e-mail: kazuya@tamacc.chuo-u.ac.jp; Satoshi Yagitani, URSI GASS 2023 general co-chair, e-mail: yagitani@is.t.kanazawa-u.ac.jp; URSI GASS 2023 secretariat, e-mail: gass2023_secretariat@c-linkage.co.jp. <https://www.ursi-gass2023.jp>.

45TH ANNUAL MEETING AND SYMPOSIUM OF THE ANTENNA MEASUREMENT TECHNIQUES ASSOCIATION (AMTA 2023)

8–13 October 2023, Seattle, WA, USA. Contacts: Dennis Lewis, AMTA 2023 chair, e-mail: amta2023@amta.org; Janet O'Neil, AMTA 2023 vice-chair, e-mail: amta2023@amta.org. <http://www.2023.amta.org>.

INTERNATIONAL CONFERENCE ON ELECTROMAGNETICS IN ADVANCED APPLICATIONS (ICEAA 2023)—IEEE-APS TOPICAL CONFERENCE ON ANTENNAS AND PROPAGATION IN WIRELESS COMMUNICATIONS (IEEE APWC 2023)

9–13 October 2023, Venice, Italy. Contacts: Roberto D. Graglia, chair of organizing committee, Dipartimento di Elettronica e TLC, Politecnico di Torino, Corso Duca degli Abruzzi, 24,

10129 Torino, Italy, e-mail: roberto.graglia@polito.it; Piergiorgio L.E. Uslenghi, chair of scientific committee, Department of ECE (MC 154), University of Illinois at Chicago, 851 South Morgan Street, Chicago, IL 60607-7053 USA, e-mail: uslenghi@uic.edu. <http://www.iceaa.net/>; Guido Lombardi, paper submission and technical program, Politecnico di Torino; e-mail: iceaa23@polito.it; Manuela Trinchero, organizing secretariat-treasurer/administration, SELENE FSrl-Eventi e Congressi, Via Medici 23 10143 Torino, Italy. +39-011-7499601, fax: +39-011-7499576, e-mail: iceaa@seleneweb.com. <http://www.iceaa.net/>.

IEEE GLOBAL COMMUNICATIONS CONFERENCE

(IEEE GLOBECOM 2023)

4–8 December 2023, Kuala Lumpur, Malaysia. <http://globecom2023.ieee-globecom.org>.

60TH ANNUAL AOC INTERNATIONAL SYMPOSIUM AND CONVENTION

11–13 December 2023, National Harbor, MD, USA. Amy Belicev, Association of Old Crows, 1555 King Street, Suite 500, Alexandria, VA 22314 USA. +1 703 549 1600, e-mail: belicev@crows.org. <https://www.crows.org/page/annualsymposium>.

2024 USNC-URSI NATIONAL RADIO SCIENCE MEETING (NRSM 2023) "50TH ANNIVERSARY EVENT"

9–13 January 2024, Boulder, CO, USA. (Papers and abstracts including papers for Student Paper Competition: 13 September 2023.) Contacts: Technical Program: Sembiam R. Rengarajan, Department of Electrical and Computer Engineering, California State University, Northridge, CA 91330-8346 USA. +1 818 677 3571, e-mail: srengarajan@csun.edu. Michael H. Newkirk, Johns Hopkins University Applied Physics Laboratory, Laurel, MD 20723 USA. +1 240 228 6976, e-mail: michael.newkirk@jhuapl.edu. Conference Logistics: Christina Patarino, CCEP, CU Conference Services, University of Colorado Boulder, 454 UCB, Boulder, CO 80309, USA. +1 303 492 5151, fax: +1 303 492 5959, e-mail: christina.patarino@colorado.edu. <http://www.nrsmboulder.org>.

CALL FOR PAPERS



IEEE International Symposium on Phased Array Systems and Technology



15 - 18 October 2024
Hynes Convention Center
Boston, Massachusetts, USA
www.ieee-array.org

Sponsors and Exhibitors

Contact:

[sponsorships@
ieee-array.org](mailto:sponsorships@ieee-array.org)

Technical Co-Sponsors



Media Sponsor



About the Symposium

Phased array systems continue to be a rapidly evolving technology with steady advances motivated by the challenges presented to modern military and commercial applications. This symposium will present the most recent advances in phased array technology and offer a unique opportunity for members of the international community to interact with colleagues in the field of phased array systems and technology.

The committee is thrilled to announce two major changes to the symposium to better reflect the interest and pace of technology development: (1) moving to the larger [Hynes Convention Center](#) in the Back-Bay neighborhood of Boston; and (2) increasing the symposium frequency to a two-year cadence.

Be a Symposium Sponsor or Exhibitor

For sponsorship and exhibit opportunities please reach out to Mark McClure and Marc Angelucci at: sponsorships@ieee-array.org.

Suggested Topics

- 5G Arrays
- Array Design
- Array Measurements
- Array Signal Processing
- Automotive Arrays
- Beamforming & Calibration
- Digital Array Architectures
- Dual Polarized Arrays
- Low Cost Commercial Arrays
- MIMO Arrays
- Medical Applications
- Metamaterial Phased Arrays
- mmWave and Terahertz
- T/R Modules
- Low Frequency Arrays
- SATCOM Arrays
- Weather Arrays
- Wideband Arrays

Paper Template and Submission Procedures

Template and submission procedures are available at:
<https://ieee-array.org/call-for-papers>.

Important Dates

- Full paper submission (2-8 pages including figures): 13 May 2024
- Author notification: 22 July 2024
- Author registration deadline: 01 Sept 2024

We are looking forward to seeing you at this next gathering.

Committee

Symposium Chairs

Sean Duffy (C), MIT LL
Wajih Elsallal (VC), MITRE

Technical Program Chairs

David Mooradd (C), MIT LL
Glenn Hopkins (VC), GTRI

Special Sessions Chairs

Matt Faccine, NGC
Kenneth E. Kolodziej, MIT LL

Plenary Session Chair

Will Moulder, MIT LL

Student Program

Matilda Livadaru, Raytheon Tech
Justin Kasemodel, Raytheon Tech

Tutorials

Cara Kataria, MIT LL
Frank Vliet, TNO

Sponsorship and Exhibits

Marc Angelucci, LMC
Mark McClure, STR

Digital Platforms Chairs

Pierre Dufilie, Raytheon Tech
Jacob Houck, GTRI
Mark Fosberry, MITRE
Shireen Warnock, MIT LL

Publications/Publicity

Philip Zurek, MIT LL
Jack Logan, NRL
Elizabeth Kowalski, MIT LL

Poster Sessions Chair

Honglei Chen, MathWorks

Advisors

Daniel Culkin, NGC
Alan J. Fenn, MIT LL
Jeffery S. Herd, MIT LL
Bradley Perry, MIT LL
William Weedon, Applied Radar

Arrangements/Administration

Robert Alongi, IEEE Boston
Kathleen Ballos, Ballos Assoc.



Raymond P. Wasky

EDITOR'S NOTE

The worldwide coronavirus (COVID-19) pandemic may have resulted in the cancellation or delay of some of the short courses listed below. Please check all course websites for the latest information prior to making plans for registration or travel. Please e-mail notices of upcoming short courses to raymond.wasky@jhuapl.edu.

956-8805 or +1 888 501-2100, fax: +1 410 956-5785, e-mail: ati@ATIcourses.com. <http://www.ATIcourses.com>.

ELECTROMAGNETIC MATERIALS AND MEASUREMENTS:

RAM, RADOME AND RAS

19–21 September 2023, Atlanta, GA, USA.

BASIC ELECTROMAGNETIC WARFARE MODELING

19–22 September 2023. ONLINE.

FUNDAMENTALS OF RADAR SIGNAL PROCESSING

25–28 September 2023, Atlanta, GA, USA.

RADOMES

26–29 September 2023, Atlanta, GA, USA. Georgia Institute of Technology, Professional Education, P.O. Box 93686, Atlanta, GA 30377-0686 USA. +1 404 385-3500, fax: +1 404 894-8925. <http://www.pe.gatech.edu>.

BASIC ANTENNA CONCEPTS

3–5 October 2023, Lake Buena Vista, FL, USA.

MODELING AND SIMULATION OF PHASED-ARRAY ANTENNAS

17–19 October 2023. ONLINE.

PRINCIPLES OF MODERN RADAR

23–27 October 2023, Atlanta, GA, USA.

RADAR WARNING RECEIVER SYSTEM DESIGN AND ANALYSIS

24–26 October 2023, Atlanta, GA, USA.

RADAR CROSS SECTION REDUCTION

30 October–1 November 2023, Atlanta, GA, USA.

MODELING AND SIMULATION OF ANTENNAS

30 October–2 November 2023, Atlanta, GA, USA.

SHORT COURSES

SPACE-BASED RADAR

14–18 August 2023, Las Vegas, NV, USA.

AIRBORNE AESA RADAR

15–17 August 2023, Las Vegas, NV, USA.

BASIC ANTENNA CONCEPTS

15–17 August 2023, Las Vegas, NV, USA.

BASIC RF ELECTROMAGNETIC WARFARE CONCEPTS

29–31 August 2023, Shalimar, FL, USA. Georgia Institute of Technology, Professional Education, P.O. Box 93686, Atlanta, GA 30377-0686 USA. +1 404 385-3500, fax: +1 404 894-8925. <http://www.pe.gatech.edu>.

SONAR PRINCIPLES AND ASW ANALYSIS

22–24 August 2023, ONLINE.

SONAR & TARGET MOTION ANALYSIS—FUNDAMENTALS

12–14 September 2023, ONLINE.

SONAR SIGNAL PROCESSING

19–21 September 2023. ONLINE. Applied Technology Institute, 349 Berkshire Drive, Riva, MD 21140-1433 USA. +1 410

Body Feature Intercomparison of Specific Absorption Rate Induced by High-Power, Portable, and Broadband Electromagnetic Sources

Eliana Canicattì^{ID}, Danilo Brizi^{ID}, Angelica Masi^{ID}, Nunzia Fontana^{ID}, and Agostino Monorchio^{ID}

This work presents an electromagnetic exposure intercomparison among representative human models with different body features (i.e., height, weight, and age) and genders when exposed to near-field, high-power, and broadband devices. Such devices are commonly used in the military field for communication and jamming purposes. With the aim of obtaining accurate and detailed whole-body-averaged (WBA) specific absorption rate (SAR) and 10-g SAR evaluations, a realistic scenario is numerically simulated. Three different antenna configurations are adopted, faithfully reproducing the radiative characteristics and operative frequency bands of similar devices (40–2,700 MHz). Then, we equally expose in the working band three different human body models (Hugo, Duke, and Ella). The obtained results show that the WBA-SAR is mainly related to the total body weight, as expected from its definition. Conversely, the 10-g SAR varies along with the frequency range, and different results are observed for each human model. Guidelines for exposure reduction and physical considerations are also presented. This study can be a useful reference for conducting com-

EDITOR'S NOTE

This article for the “Bioelectromagnetics” column provides a comparative dosimetry study for high-power broadband devices with wireless functionality. The study considers three different antenna configurations in the 40- to 2,700-MHz frequency range as well as three different anatomical human body models (male and female), with a focus in the near-field region. The results provide informative insights on the formation and location of hot spots with respect to intersubject variability.

This column welcomes articles on biomedical applications of electromagnetics, antennas, and propagation in terms of research, education, outreach, and more. If you are interested in contributing, please e-mail me at kiourti.1@osu.edu.



Asimina Kiourtzi

plete and accurate radio-frequency (RF) dosimetry analysis for such particular and high-risk devices, differentiating the study for different genders and body shapes of human body models.

INTRODUCTION

The problem of the exponentially rising exposure of the general population to electromagnetic fields (EMFs) has raised the attention of the scientific community regarding the possible risks for human health [1]. Accordingly, the evaluation of the electromagnetic energy deposition on biological tissues is fundamental to assess whether a radiative source can be safely used near or in contact with the human body. As a metric, the SAR (watts

per kilogram) has been defined, and it is generally adopted. Hence, to protect the population from massive exposure to EMFs, the International Commission on Non-Ionizing Radiation Protection (ICNIRP) and IEEE have developed safety guidelines [2] and standards [3], respectively. These guidelines provide both methods for measuring the SAR and limit thresholds to effectively assess when a device becomes potentially hazardous for human health.

Experimental evidence has shown that a SAR value greater than 4 W/kg, averaged over the total body volume (i.e., the WBA-SAR), can lead to irreversible biological effects; this is due to the fact that such energy deposition can

easily produce an overall body temperature increase of about 1 °C when the exposure exceeds 30 min [4], [5]. Therefore, this value has been adopted in the international standards as a reference safety margin. In particular, the whole-body exposure (WBA-SAR) limits have been cautiously set at 0.4 W/kg (10 times lower than the aforementioned threshold value) for workers and 0.08 W/kg (50 times lower than the aforementioned threshold value) for the general public [2], [3], respectively. In addition to the whole-body exposure, another fundamental aspect is the localized near-field exposure assessment by means of the local SAR distribution. Since the use of radiating devices closely placed or direct in contact to the human body is dramatically increasing, an accurate estimation of localized heating is needed. To this end, limits on the averaged peak SAR value on 10 g of tissue in international standards have also been introduced. These local SAR limits have been obtained by increasing the basic WBA margin by a factor of 25. Hence, the local SAR limit was set at 10 W/kg for workers and 2 W/kg for the public [2], [3].

In the light of the preceding considerations, it is evident that a correct SAR level estimation is required for a careful safety assessment of a radiating device. Currently, some works in the literature have explored the exposure level quantification for mobile devices, tablets, and smartwatches [6], [7], [8], [9], [10], [11]; moreover, the SAR rating for wearable systems have been investigated, such as for devices monitoring biological parameters or prosthetic implants [12], [13], [14], [15], [16]. Generally, the common feature of all these devices is their operative modality; they work in the near-field region but in a very narrow frequency band or even a single frequency, as in the case of biomedical monitoring systems.

Nevertheless, there are commercially available high-power portable electromagnetic devices that act both in the near-field region and in a wider frequency band. These types of devices are usually employed for military applications in the form of wearable backpack systems for communications, jamming, or situational awareness [17].

In [18], the effect of the aforementioned radiative sources on a specific human body voxel model has been evaluated, and guidelines for the reduction of exposure levels have been defined. However, it is acknowledged that the human population has strongly variable anatomical characteristics in terms of height and weight; furthermore, it is well known that body composition differs among males and females, especially in terms of adipose content [19] and as a function of age. As a consequence, different bodies can be subjected to different levels of exposure in the presence of the same radiative source [20], [21]. Several works in the literature have carried out the SAR evaluation for different body models and genders in the far-field region by using a vertically polarized impinging plane wave [22], [23], [24], [25]. Nonetheless, the use of similar radiative sources does not provide a realistic SAR assessment since plane waves never occur in reality, and often, the human body is illuminated within the near-field region.

To overcome these limitations, we performed a broadband SAR analysis in the near-field region, using realistic high-power (60-W) radiating sources operating on a wider frequency band (40–2,700 MHz). Three different standard voxel phantom models (Hugo [26], Duke, and Ella [27]) have been adopted; they represent two men of different ages and body conformations and a woman. By considering the dispersive dielectric properties of the tissues in the entire frequency band, the exposure levels and localization of SAR hot spots were accurately assessed. In [28], some preliminary results related to the WBA-SAR have already been presented. Since these results have shown a significantly higher SAR level for the female model, we have carried out a more in-depth and accurate analysis. Important information can be inferred from this study by determining how hot spot locations vary with gender and body conformation. To the best of our knowledge, such an analysis has not yet been performed in the literature. The present work is organized as follows. The “Problem Statement” section presents the problem statement and purpose of the study. The “Method” section deals

with the description of human body voxel models that have been adopted and the settings of the numerical scenario. In the “Numerical Results” section, numerical results are presented and discussed. Finally, conclusions are described.

PROBLEM STATEMENT

The aim of this study is the intercomparison of the electromagnetic energy absorption among human models, differing in gender and body features (i.e., height, weight, and age), when they are exposed to portable, high-range, and broadband electromagnetic devices. As mentioned, similar systems are extremely common in military applications, where they are used in tactical communication or situational awareness. In the context of the ICNIRP and IEEE international norms [2], [3], the EMF exposure of workers represents a significant health risk; hence, it is necessary to assess whether such equipment can be safely used [29] without causing adverse biological effects.

To evaluate this problem in an accurate way, a realistic near-field scenario has been set up. We have considered three standard voxel human models (Hugo, Duke, and Ella; Figure 1) representing adult people of a different sex, age, and body conformation. Each model was equipped with a portable backpack system that simulates a typical device used in military communication. A similar methodology has already been developed in [18] for a single human body model; herein, it has been extended to the young male (Duke) and female (Ella) models.

As depicted in Figure 2, the system is characterized by a backpack closely placed to the body. To simulate a realistic communication or jamming application, the device operates on a wide bandwidth (40–2,700 MHz); in fact, these systems are equipped with an arrangement of several monopole and dipole antennas switched on according to the transmission radio communication band. In addition, since this type of system transmits high-intensity signals, its input power has been set at 60 W.

To summarize, this study is aimed at providing a general safety assessment of

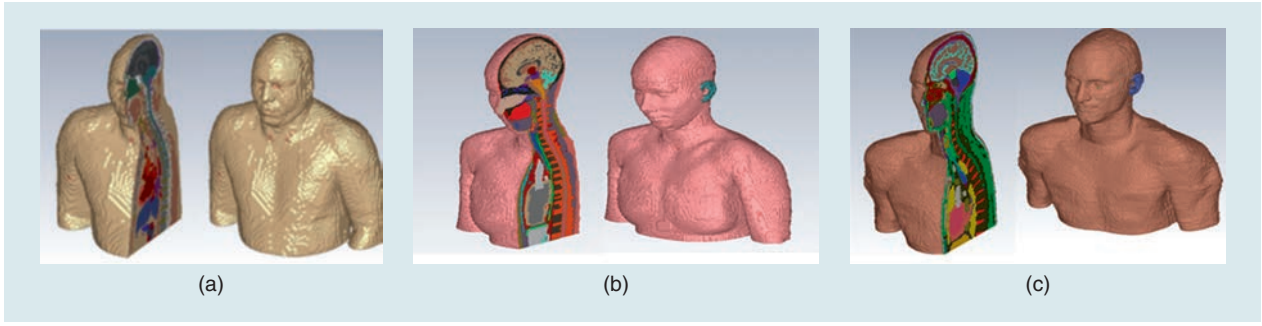


FIGURE 1. The sectional and half-bust voxel-based human models: (a) Hugo, (b) Ella, and (c) Duke.

high-power broadband devices for different categories of users, exploring how different genders and ages may affect the SAR deposition.

METHOD

VOXEL ANATOMICAL BODY MODEL

The SAR evaluation and related dosimetry studies cannot be experimentally conducted on actual human bodies since this assessment is practically unfeasible. Besides, realizing biological phantoms able to actually replicate the inhomogeneities of human tissues is still a challenge. Therefore, to overcome these limitations, extremely accurate anthropomorphic numerical phantoms have been developed, starting from tomography data, to be used in SAR assessment.

As stated, three human body models representative of gender and body conformation diversity have been employed to obtain results as accurate as possible in terms of the exposure level quantification of portable device antennas. As shown in Figure 1, such voxel models are Hugo, Duke, and Ella, respectively [28].

As described in [18], Hugo is probably the most popular and adopted voxel model [26]. It is characterized by high-fidelity anatomical detail acquired on a real human body by using high-resolution magnetic resonance imaging (MRI) data. This activity was carried out as part of the Visible Human Project [31] developed by the U.S. National Institute of Health. This phantom represents a 38-year-old man; his digitalized body model presents 32 different tissues with a voxel resolution that can range from approximately $8 \times 8 \times 8 \text{ mm}^3$ to $1 \times 1 \times 1 \text{ mm}^3$.

The other two models, Duke and Ella, represent a 34-year-old man and a

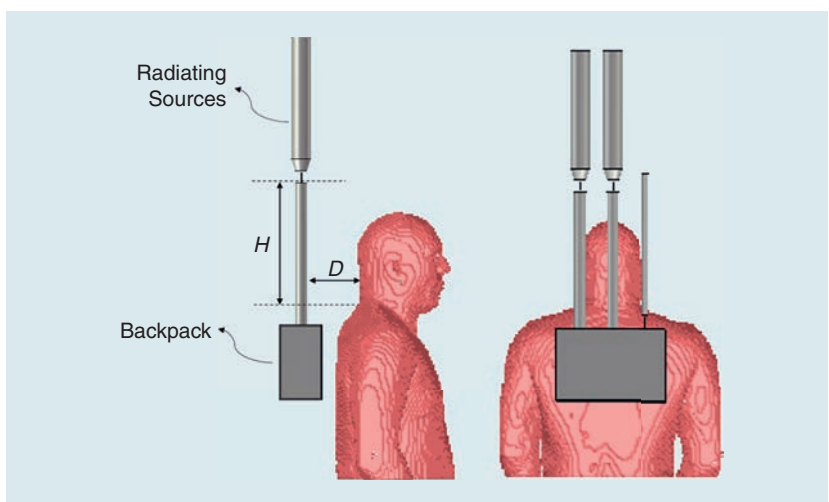


FIGURE 2. Typical portable military equipment.

26-year-old woman, respectively. They are part of the Virtual Family, a project carried out in collaboration with the U.S. Food and Drug Administration, the Foundation for Research on Information Technologies in Society, and other academic and industrial partners [32]. Also, in this case, the numerical models have been obtained by referring to high-resolution MRI data acquired on healthy volunteers; their inner organs and tissues are featured by highly detailed 3D CAD objects with a voxel resolution ranging from $5 \times 5 \times 5 \text{ mm}^3$ to $0.5 \times 0.5 \times 0.5 \text{ mm}^3$. Their features are listed in Table 1.

As already highlighted for the Hugo model [18], these standard phantoms exhibit tissue dielectric properties evaluated only for a discrete number of frequencies. To perform an accurate broadband SAR assessment, the

dielectric properties dataset has been customized. In more detail, by implementing the most widely used dispersive model in the literature, that is, the Gabriel and Gabriel model [33], we have calculated the dielectric parameters in the entire frequency range for each tissue. Consequently, the voxel model became broadband, allowing much greater SAR estimation accuracy.

To further optimize the numerical setup, it is necessary to evaluate the optimal voxel resolution for full-wave

TABLE 1. THE CHARACTERISTICS OF THE THREE ANATOMICAL HUMAN BODY MODELS.

Characteristic	Hugo	Ella	Duke
Sex	Male	Female	Male
Number of tissues	32	74	77
Body conformation	Fat	Slim	Slim
Height (m)	1.87	1.6	1.74
Weight (kg)	113	58	70

simulations. Although a finer voxel resolution naturally brings more accurate results, computational resources and simulation time can be prohibitive. Thus, in [18], a final voxel resolution of $4 \times 4 \times 4$ mm has been chosen for the Hugo model as a good compromise between the accuracy of the SAR calculation and the simulation computational burden. This choice has been suggested by [34] and [35], in which the authors stated that the variation of the voxel size had a negligible effect on the SAR estimation and that the use of a finer resolution is necessary only to calculate small body structures and organs (e.g., eyes and the thyroid).

Finally, we have also implemented this choice for the Duke and Ella models by adopting a voxel resolution of $5 \times 5 \times 5$ mm [28], based on the previous considerations and in accordance with [36].

RADIATING SOURCE MODEL

In a typical arrangement, military backpack devices include a set of antennas, mainly monopoles and dipoles, operating on different frequency ranges to cover the entire radio communications band. In [18], three different antennas have been specifically designed to faithfully represent the behavior of such radiative systems.

The first type is a quarter-wavelength monopole working in the 40–530-MHz band. It consists of an upright cylindrical-shaped conductor

mounted perpendicularly on a perfectly conductive metal box used as a ground plane [Figure 3(a)]. The monopole has been tuned and matched to be operative in the entire 40–530-MHz band by gradually changing its electrical length.

The second type [Figure 3(b)] consists of an ultrawideband (UWB) dipole. In particular, two cylindrical rods with tapered ends are employed to obtain broadband impedance matching. From this general conception, two antennas have been designed by simply rescaling their dimensions: the dipoles were appropriately designed to accomplish frequency tuning and adequate impedance matching by maintaining their electrical length in the desired frequency band by exhibiting a minimum –10-dB matching level in both free space and in the presence of a biological load. Thus, we reproduced, with high precision, the typical performance of backpack devices, which often include electronic circuitry that matches the antenna impedance to work correctly with different operators. Hence, we ensured that the various antenna designs were functioning correctly and that over 90% of the amplifier's input power was supplied to the radiating system. Therefore, the two designed UWB dipoles work in the band between 530 and 1,800 MHz and 1,800–2,700 MHz, respectively.

We carried out the antenna design by using CST Studio Suite (Dassault Systems, France) electromagnetic software.

In [18], we have shown the antennas' performance and radiative characteristics both in free space and in the presence of the numerical model Hugo. Herein, we have simulated the antennas in the presence of the other two voxel-based models, showing almost unaltered radiation patterns and good matching in terms of the reflection coefficient, under the threshold of –10 dB (Figure 4).

As illustrated in Figure 4, the degree of electromagnetic coupling varies according to the scenario. This phenomenon occurs because a biological load affects the antennas' input impedance. If an antenna is designed to transmit in free space, the unavoidable mismatch induced by loading will result in a decrease in transmitted power and, consequently, an increase in the reflection coefficient. Part of the reflected energy couples to the generator load through the antenna port, altering the input impedance and antenna matching. Hence, based on the latter considerations, it is also possible to conclude that, since the three voxel-based human models differ in height and body features, the incident wave that is partially absorbed and partially reflected also differs, determining a different reflection coefficient.

COMPLETE NEAR-FIELD NUMERICAL SCENARIO

To perform the full-wave simulations, a time-domain numerical electromagnetic algorithm has been employed, namely, the Finite Integration Technique (FIT). This choice was motivated by the memory-efficient capability and flexibility with respect to different materials and complex geometries of the FIT technique. The WBA-SAR value in the solver is obtained by dividing the total power absorbed in the human body by the full body weight. Conversely, local SAR values are averaged in a tissue mass of 10 g, as specified in the international ICNIRP norms [37].

To simulate real exposure conditions and the use of such backpack devices in military fields, we have chosen three different exposure scenarios for the three voxel-based human models. As in [18] and [28], the position of the radiative sources with respect to the human

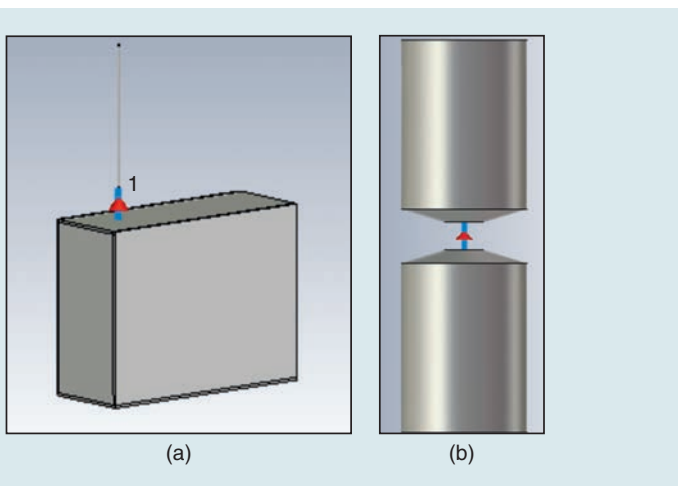


FIGURE 3. The radiating broadband device. (a) A quarter-wavelength monopole operating in the 40–530-MHz frequency range. (b) The general configuration of the ultrawideband dipole antenna.

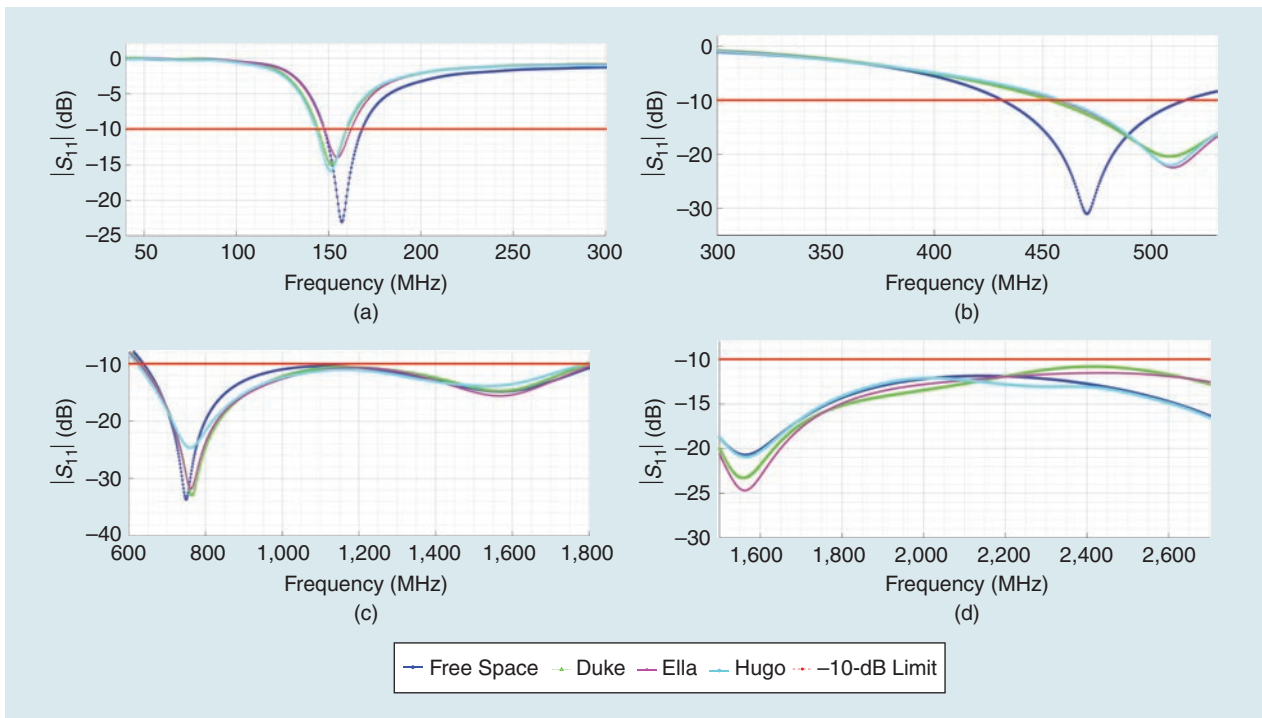


FIGURE 4. The S_{11} parameter of the previously described antennas in free space and the presence of the voxel-based human bodies (Hugo, Duke, and Ella): the (a) S_{11} of the monopole tuned at 150 MHz, (b) S_{11} of the monopole tuned at 500 MHz, and (c) S_{11} of the UWB dipole antenna operating in the range of 600–1,800 MHz and (d) 1,800–2,700 MHz.

models has been fixed at 13 cm from the neck and 3 cm from the shoulders.

In the first configuration, each voxel phantom is illuminated by the tuned monopole antenna, operating in the frequency band of 40–530 MHz, as depicted in Figure 5(a)–(c). Each model is chosen and assumed to be standing in free space and considered barefoot. Although in [23] and [38] it is reported that the maximum SAR is achieved when the incident electric field is vertically polarized and the model is barefoot on a ground plane, simulations with the radiative source placed in the near field were carried out in [18], observing that no significant variation in the results comes from the ground plane presence or absence.

On the other hand, in the second and third configurations, the three voxel-based models are in the presence of the UWB dipole antennas, operating in their proper frequency band. In this case, according to the considerations reported in [18], we have adopted the three models in the form of a half bust [Figure 6(a)–(c)] since the higher operative frequencies minimally influence the SAR deposition in the lower part of the body.

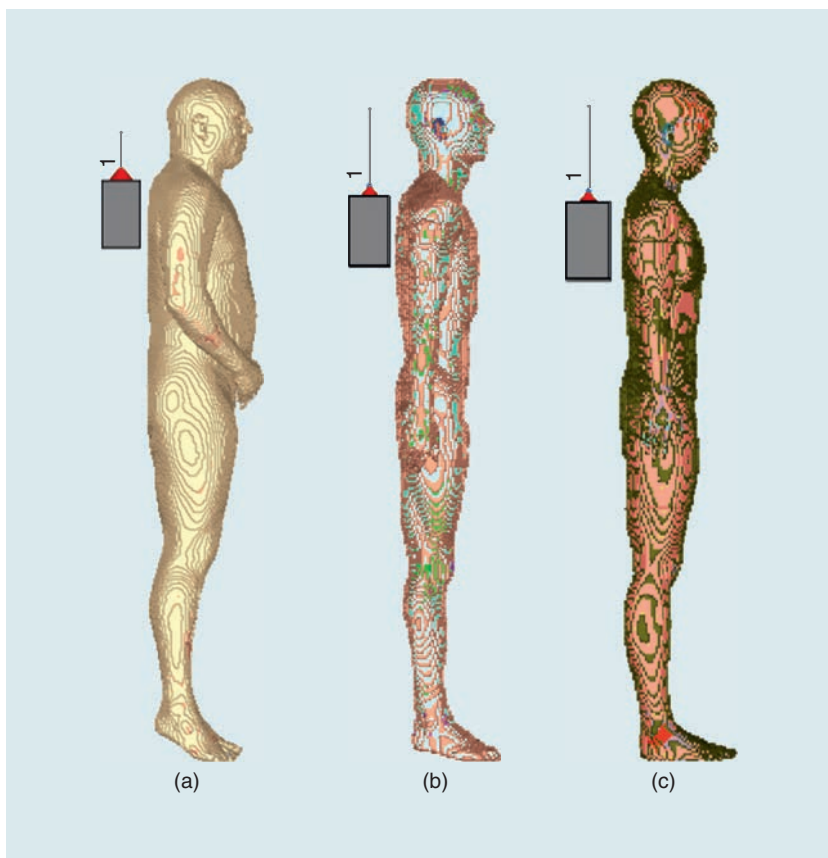


FIGURE 5. The first exposure configuration: the tuned monopole antenna operating in frequency range of 40–530 MHz. The (a) Hugo full-body model, (b) Duke full-body model, and (c) Ella full-body model.

All simulations were performed in the continuous wave condition since this is the worst exposure condition, as derived from the results of the multiphysics analysis carried out in [18] and [37].

NUMERICAL RESULTS

In this section, we present the WBA-SAR and 10-g SAR numerical results related to the three scenarios presented in Figures 5 and 6, respectively.

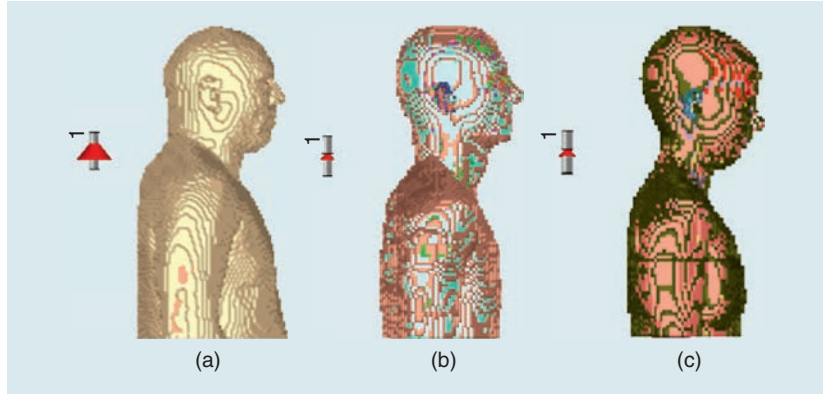


FIGURE 6. The second and third exposure configurations: the UWB dipole antenna operating in frequency ranges of 600–1,800 MHz and 1,500–2,700 MHz. The (a) Hugo half-bust model, (b) Duke half-bust model, and (c) Ella half-bust model.

Such results refer to a peak input power equal to 1 W. Notably, by setting the peak input power to 1 W, we aimed to make our study generalizable and a useful resource for doing comprehensive and precise RF dosimetry analyses on similar devices with different peak input power. Since such backpack military devices usually work at input powers levels equal to 60 W and an assumed system linearity characteristic, we implemented the following scaling formula [18] in the postprocessing procedure:

$$\text{SAR}_{10g,\text{new}} = \text{SAR}_{10g,1W} \frac{P_{\text{new}}}{P_{1W}}. \quad (1)$$

WBA-SAR AND 10-G SAR ANALYSIS

The simulations have been executed by adopting a frequency sampling equal to

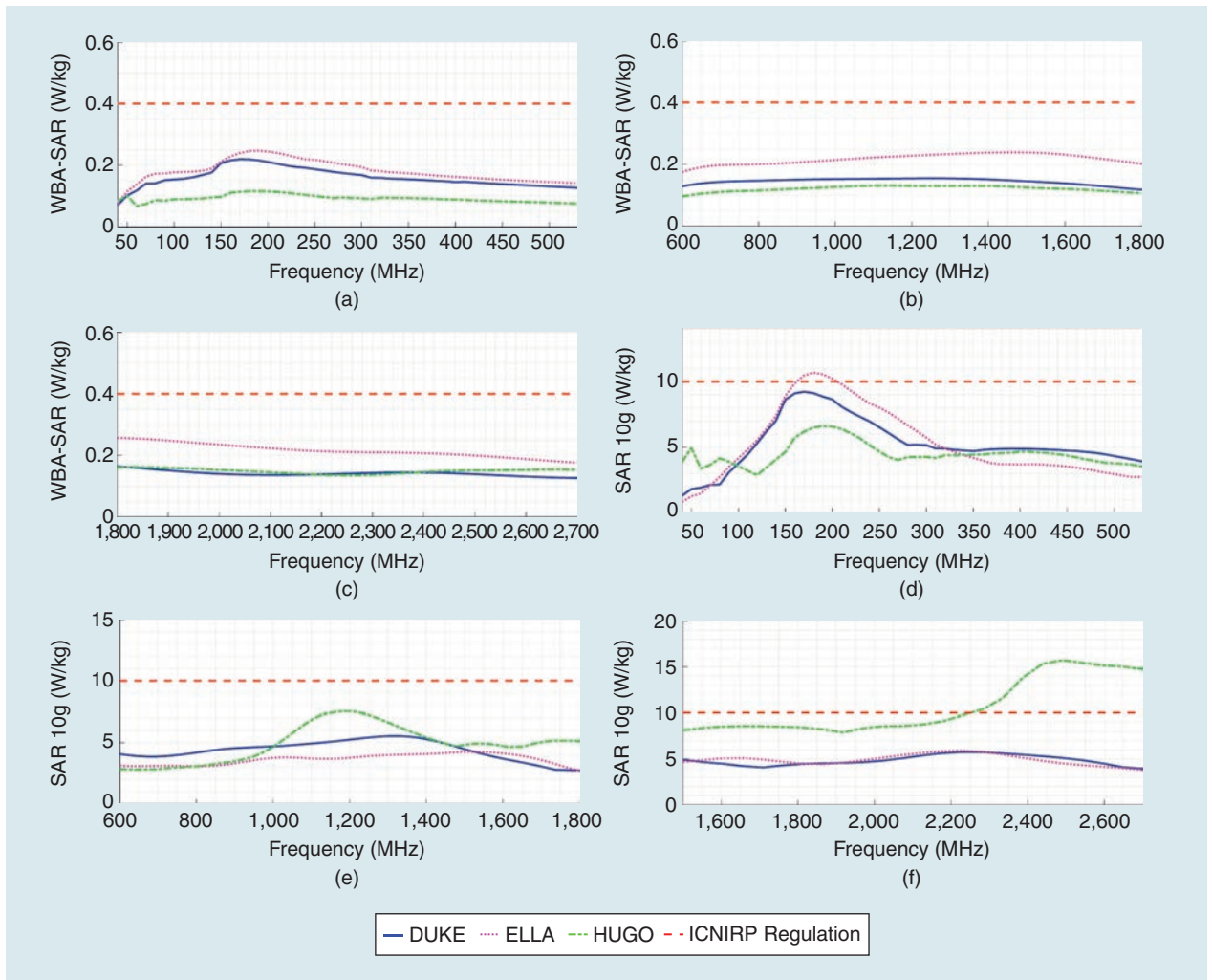


FIGURE 7. The WBA-SAR trend for a peak input power equal to 60 W: (a) 40–530 MHz, (b) 600–1,800 MHz, and (c) 1,500–2,700 MHz. The 10-g SAR trend for a peak input power equal to 60 W: (d) 40–530 MHz, (e) 600–1,800 MHz, and (f) 1,500–2,700 MHz.

10 MHz in the frequency range up to 1,800 MHz, whereas a coarser sampling of 50 MHz in the frequency range of 1,500–2,700 MHz has been chosen. The last choice is related to the SAR dependence with respect to the dispersive tissue characteristics, whose trend becomes stable at higher frequencies [33].

Then, we processed the collected data through an in-house postprocessing algorithm. Figure 7(a)–(c) represents the WBA-SAR results on the three subbands for each numerical voxel model. In agreement with [39], the results have general behavior that is similar in each case despite the substantial differences among the phantom models.

The last obtained result proves that electromagnetic energy absorption does not depend on body shape but on the considered radiative source. Nonetheless, it must be noticed that the WBA-SAR values' amplitude is greater in the female model than in the male ones; however, the last result is due to the WBA-SAR definition itself: the total power absorbed by the whole body over the total body weight, which is lower in the female model [40].

Generally, the WBA-SAR is a parameter used to evaluate the effect of far-field sources (i.e., plane waves and radar [41]); since such radiative sources are localized and placed close to the human body, the local 10-g SAR evaluation is more appropriate for near-field applications (e.g., as usually adopted for mobile terminals too).

By adopting the same postprocessing algorithm, the results in terms of the 10-g SAR have been provided in Figure 7(d)–(f). In the first subband, the results are in good agreement among the models. In fact, there is a 10-g SAR peak for each voxel model at a frequency around 170 MHz. The reason is to be ascribed to the antenna length (1.7 m), which is comparable to the heights of the voxel numerical models at this frequency. Thus, a resonance phenomenon that amplifies the fields and absorbed power is present [36]. However, a substantial difference in absorption between the female model and the male counterparts can be appreciated.

These results are in line with those described in [23] and [25] since the fat

tissue percentage in women (i.e., subcutaneous adipose tissue and breast mammary tissue [42]) is higher than in men. Due to its dielectric properties, fat is a

good propagation medium inside the human body at lower frequencies [43], [44]. So, the exposure levels may exceed the limits imposed by [2] for female

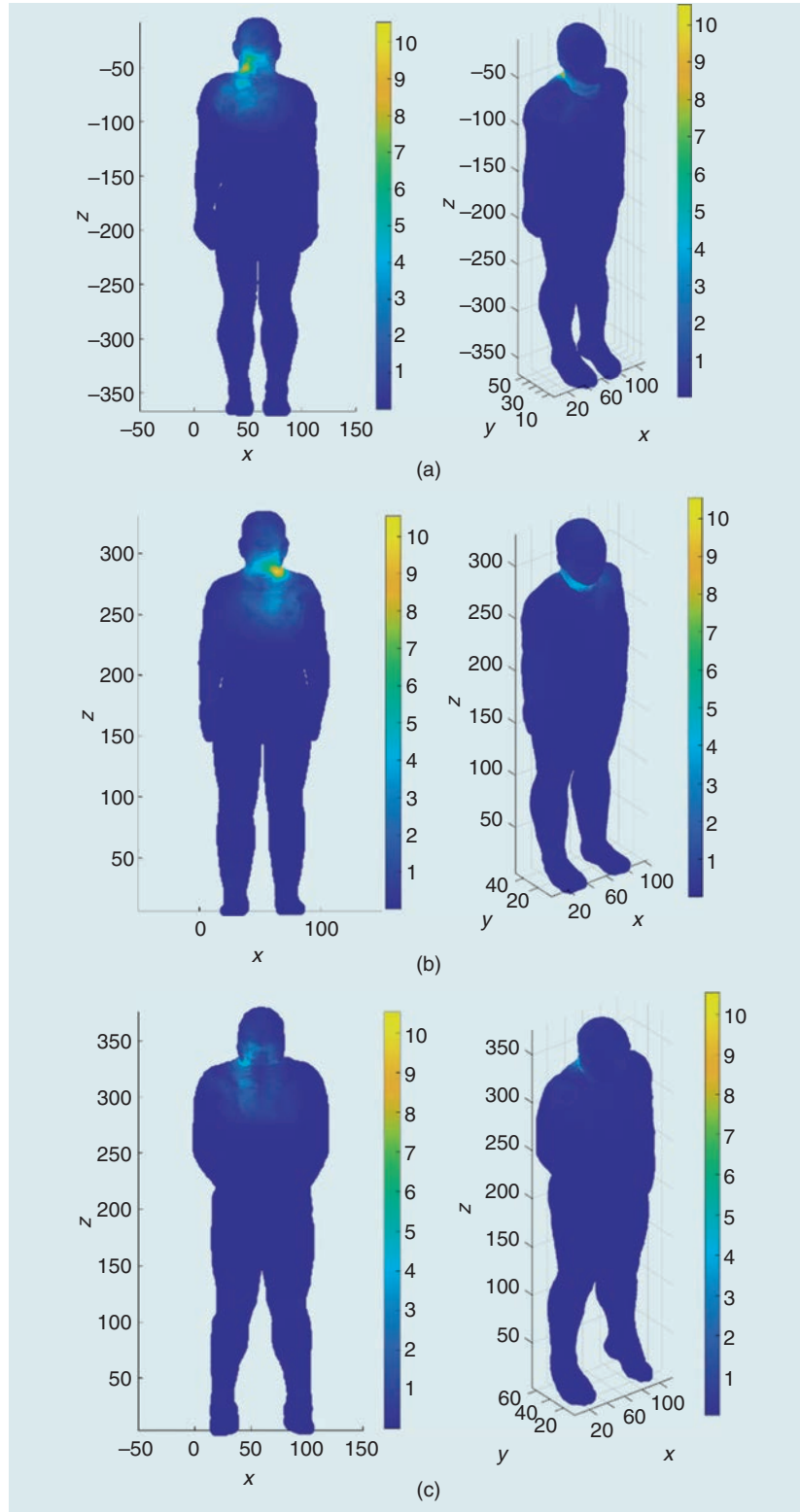


FIGURE 8. The maximum 10-g SAR hot spot localization for a peak input power equal to 60 W in the frequency range of 40–530 MHz: (a) Duke, (b) Ella, and (c) Hugo.

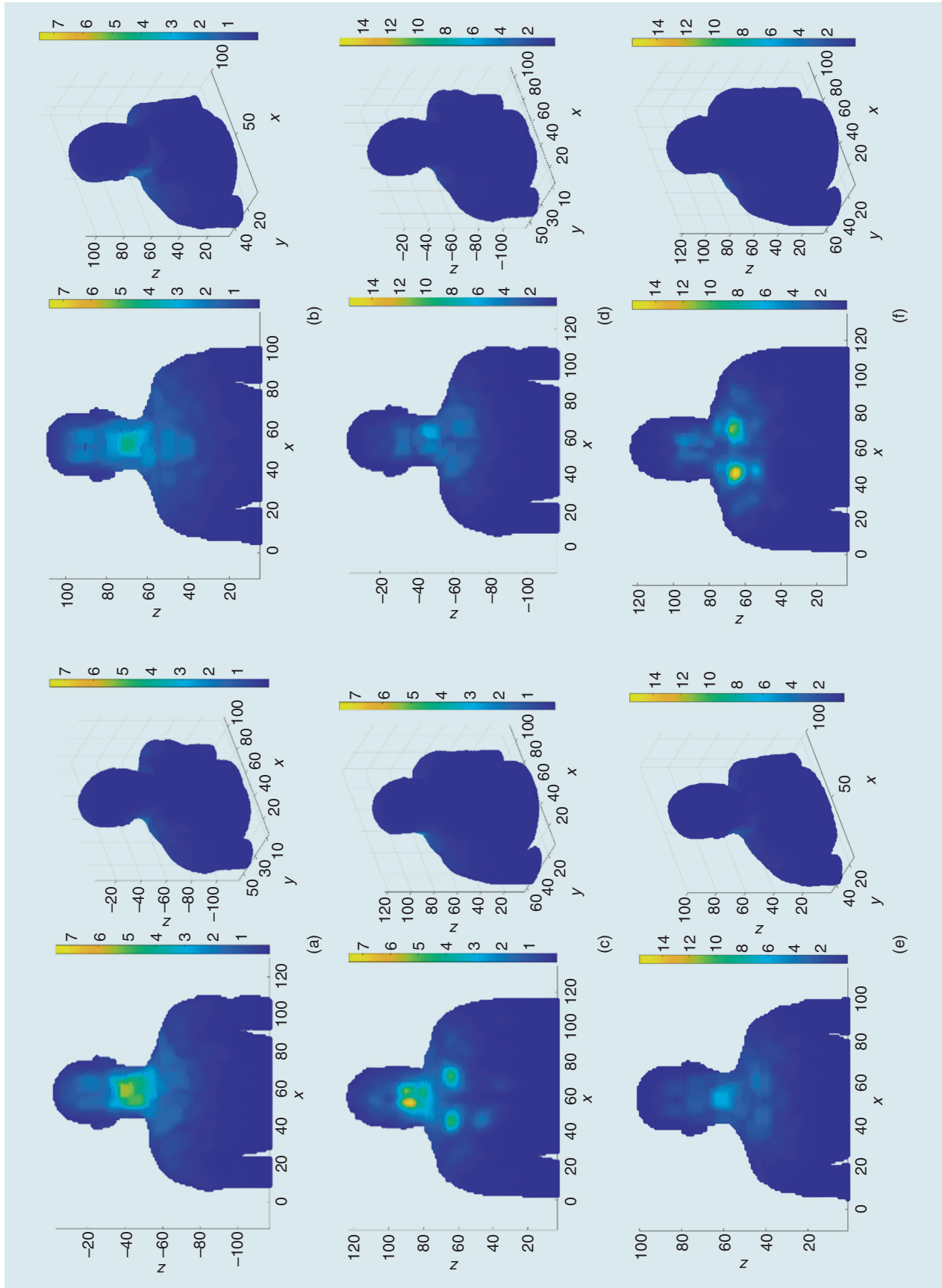


FIGURE 9. The maximum 10-g SAR hot spot localization for a peak input power equal to 60 W in the frequency range of 600–1,800 MHz: (a) Duke, (b) Ella, and (c) Hugo. The maximum 10-g SAR hot spot localization for a peak input power equal to 60 W in the frequency range of 1,500–2,700 MHz: (d) Duke, (e) Ella, and (f) Hugo.

models; therefore, guidelines for SAR exposure reduction must be adopted, as reported in [18].

Regarding the subbands in 600–1,800 MHz and 1,500–2,700 MHz, lower 10-g SAR values are found in the Duke and Ella models, compared to the Hugo one. However, these are due to the intrinsic conformation of the Hugo model, which has an outer layer mainly consisting of fat, without the skin layer (differing from Duke and Ella). It is possible to conclude that the presence of skin increases the reflection at higher frequencies and generally reduces SAR levels below the norm limitations [25].

To conclude the exposure risk assessment, we evaluated the localization and identification of the hot spots within the three voxel human body models. Specifically, we have elaborated the 2D and 3D SAR maps for each sampled frequency and visualized them for different geometric planes.

In this study, we report the SAR maps for each voxel model, corresponding to the maximum 10-g SAR peaks identified on each respective subband. To understand the position of the hot spots within the body, we have depicted the maps both in the coronal plane and a 3D view (Figures 8 and 9). Furthermore, in Figure 10, the maximum values and positions of the hot spots for each model on each respective subband are summarized.

The hot spot distributions were scaled to the maximum SAR 10-g value among the three models to highlight qualitative and quantitative variation between SAR distributions for the three human voxel models. From the 2D maps, it is possible to observe how hot spots change their position according to the frequency band. In addition, it is interesting to note how exposure levels vary from model to model. In general, it can be inferred that hot spots tend to cluster near the shoulders and neck, i.e., near radiative sources, as expected.

ASSESSMENT OF THE SKIN EFFECT ON THE VOXEL-BASED MODELS

When the human body is excited by the antennas, part of the signal is scattered away, and part is absorbed. The reflec-

tion level mainly depends on the air-tissue interface, which can determine higher exposure levels and, consequently, higher SAR values. In particular, this phenomenon has been observed at higher frequencies (1,500–2,700 MHz) since the SAR trend [Figure 7(f)] is in good agreement between the Duke and Ella models but significantly higher in Hugo.

Therefore, we have carried out further investigations; by analyzing the three voxel models in detail, we have observed that Duke and Ella have skin outer layers, while a skin outer layer is not present in the Hugo numerical model.

Therefore, it was inferred that the presence of skin can affect the EMF reflection and, consequently, the electromagnetic energy absorption in the

human body. In [45] and [46], the absorption and reflection levels of a plane wave referred to a layered model with and without skin were evaluated. The authors found that the reflection coefficients among the two models are different, and this phenomenon is explained by the presence of skin. Furthermore, when the skin layer is removed, the reflection coefficient is close to the model without it.

Based on these considerations, we simulated two stratified cylinders [Figure 11(a) and (b)] equal to Hugo's torso size (60 cm in height, 38 cm in diameter), consisting of an inner muscle layer and an intermediate 7-mm fat layer [47]. Only one cylinder has the outer 2-mm skin layer [30], [48] [Figure 11(b)]. The

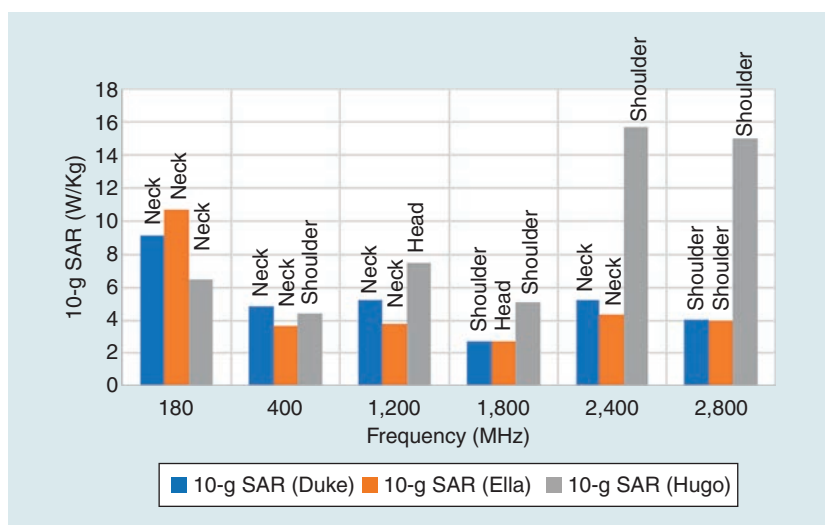


FIGURE 10. The maximum 10-g SAR values and body localization for each model on the three subbands.

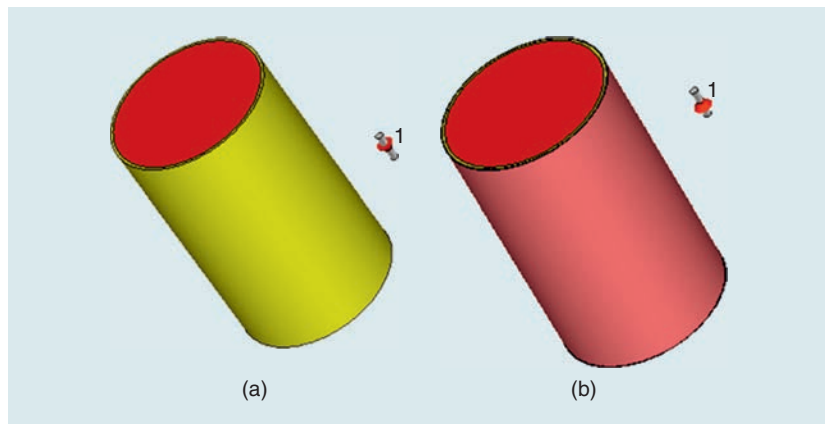


FIGURE 11. The layered cylinders equal to the Hugo torso size, illuminated by the UWB dipole (1,500–2,700 MHz): (a) two layers of muscle and fat and (b) three layers of muscle, fat, and skin.

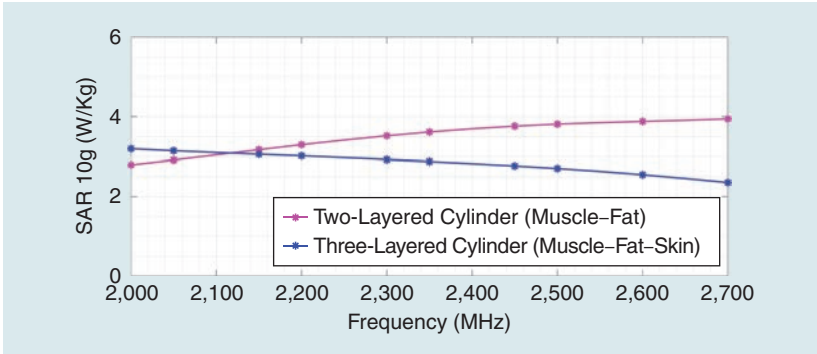


FIGURE 12. The 10-g SAR estimation trend for a peak input power equal to 60 W, evaluated for the two-layer (muscle–fat) and three-layer (muscle–fat–skin) cylinders. It can be noticed that the skin presence drastically reduces the SAR level for the same input power.

assumption is that the cylinders were irradiated by the UWB dipole (1,500–2,700 MHz), placed 13 cm from their surface, to simulate the same realistic scenario represented in Figure 6.

The results in terms of the 10-g SAR are given in Figure 12. The results explain what was observed among the three models in terms of SAR differences at this frequency range. Indeed, due to the high permittivity values, the skin prevents antenna signal propagation, shielding the body and minimizing SAR deposition. Indeed, skin acts as a barrier between the antenna and body, especially at higher frequencies, in which the penetration depth is reduced.

In the cylinder without skin, the antenna impedance matching is maximized; the propagation loss is lower, so higher exposure levels result. Although Hugo is one of the most employed voxel models in the literature, the problem of skin absence must be carefully considered when employing this model for exposure assessment.

CONCLUSIONS

In this work, we proposed a systematic electromagnetic energy absorption assessment for human body models of different sexes and body conformations, when exposed to high-intensity, portable, and broadband signal devices. Starting from our previous works, we have modeled radiative sources as realistic backpack devices, generally used for communication or situational awareness purposes in the military field. Three antennas have been specifically designed to faithfully represent the behavior of

such broadband radiative systems (40–2,700 MHz) to cover the entire radio communication band. To obtain detailed and accurate exposure levels results, we adopted three realistic human models representative of shape and gender variability (Hugo, Duke, and Ella).

To the best of our knowledge, this is the first systematic literature study where different voxel phantoms exposed to broadband high-power near-field sources are investigated in terms of electromagnetic exposure. We estimated both the WBA-SAR and local 10-g SAR. Regarding the WBA-SAR, significantly higher exposure levels were observed for the female model, due to reduced body weight compared to the male counterparts.

Due to the peculiar application, i.e., where the radiating systems are placed very close to the body, particular attention was focused on the evaluation of the 10-g SAR, as it is significant for localized tissue heating. It was found that at lower frequencies, the presence of a greater percentage of fat in the female model led to increased energy absorption. In addition, the presence of the skin layer increases reflection at higher frequencies, with a consequent reduction in exposure levels.

The results showed that the WBA-SAR is closely related to total body weight. Conversely, the 10-g SAR varies according to the frequency range and with each voxel model. Only in the case of female exposure were the limits imposed by the ICNIRP exceeded for a radiating power of 60 W. The proposed study can be used as a general methodology to infer the risk levels of other

critical and high-exposure test cases by performing accurate numerical studies.

AUTHOR INFORMATION

Eliana Canicatti (eliana.canicatti@phd.unipi.it) is with the Department of Information Engineering, University of Pisa, 56122 Pisa, Italy. She is a Student Member of IEEE.

Danilo Brizi (danilo.brizi@unipi.it) is with the Department of Information Engineering, University of Pisa, 56122 Pisa, Italy. He is a Member of IEEE.

Angelica Masi (angelica.masi@phd.unipi.it) is with the Department of Information Engineering, University of Pisa, 56122 Pisa, Italy. She is a Student Member of IEEE.

Nunzia Fontana (nunzia.fontana@unipi.it) is an associate professor with the Department of Energy, Systems, Territory, and Construction Engineering, University of Pisa, 56122 Pisa, Italy. She is a Senior Member of IEEE.

Agostino Monorchio (agostino.monorchio@unipi.it) is with the Department of Information Engineering, University of Pisa, 56122 Pisa, Italy. He is a Fellow of IEEE.

REFERENCES

- [1] “The international EMF project,” World Health Organization, Geneva, Switzerland, 1994–1995. [Online]. Available: <https://www.who.int/initiatives/the-international-emf-project>
- [2] International Commission on Non-Ionizing Radiation Protection, “Guidelines for limiting exposure to time-varying electric, magnetic, and electromagnetic fields (up to 300 GHz). International commission on non-ionizing radiation protection,” *Health Phys.*, vol. 74, no. 4, pp. 494–522, Apr. 1998.
- [3] IEEE Standard for Safety Levels with Respect to Human Exposure to Radio Frequency Electromagnetic Fields, 3 kHz to 300 GHz, IEEE Standard C95.1-2005 (Revision of IEEE Std C95.1-1991), Institute of Electrical and Electronics Engineers, New York, NY, USA, Apr. 2006.
- [4] F. G. Shellock and J. V. Crues, “Temperature, heart rate, and blood pressure changes associated with clinical MR imaging at 1.5 T,” *Radiology*, vol. 163, no. 1, pp. 259–262, Apr. 1987, doi: 10.1148/radiology.163.1.3823445.
- [5] R. L. Magin, R. P. Liburdy, and B. Persson, *Biological Effects and Safety Aspects of Nuclear Magnetic Resonance Imaging and Spectroscopy*. New York, NY, USA: New York Academy of Sciences, 1992.
- [6] P. Bernardi, M. Cavagnaro, S. Pisa, and E. Puzzi, “Specific absorption rate and temperature increases in the head of a cellular-phone user,” *IEEE Trans. Microw. Theory Techn.*, vol. 48, no. 7, pp. 1118–1126, Jul. 2000, doi: 10.1109/22.848494.
- [7] J. B. Ferreira, A. A. Almeida de Salles, and C. E. Fernandez-Rodriguez, “SAR simulations of

- EMF exposure due to tablet operation close to the user's body," in *Proc. SBMO/IEEE MTT-S Int. Microw. Optoelectronics Conf. (IMOC)*, Porto de Galinhas, Brazil, Nov. 2015, pp. 1–5, doi: 10.1109/IMOC.2015.7369205.
- [8] H. Wang, "Analysis of electromagnetic energy absorption in the human body for mobile terminals," *IEEE Open J. Antennas Propag.*, vol. 1, pp. 113–117, Mar. 2020, doi: 10.1109/OJAP2020.2982507.
- [9] S. Kim, Y. Sharif, and I. Nasim, "Human electromagnetic field exposure in wearable communications: A review," 2019. [Online]. Available: <http://arxiv.org/abs/1912.05282>
- [10] P. Bernardi, M. Cavagnaro, S. Pisa, and E. Piuza, "SAR distribution and temperature increase in an anatomical model of the human eye exposed to the field radiated by the user antenna in a wireless LAN," *IEEE Trans. Microw. Theory Techn.*, vol. 46, no. 12, pp. 2074–2082, Dec. 1998, doi: 10.1109/22.739285.
- [11] M. S. Morelli, S. Gallucci, B. Siervo, and V. Hartwig, "Numerical analysis of electromagnetic field exposure from 5G mobile communications at 28 GHz in adults and children users for real-world exposure scenarios," *Int. J. Environ. Res. Public. Health*, vol. 18, no. 3, Feb. 2021, Art. no. 1073, doi: 10.3390/ijerph18031073.
- [12] K. H. Kuther, I. H. Ali, and R. K. Ahmed, "Radiation effect of fractal sierpinski square patch antenna," *Int. J. Electr. Comput. Eng.*, vol. 10, no. 5, pp. 5329–5334, Oct. 2020, doi: 10.11591/ijece.v10i5.pp5329-5334.
- [13] M. Smondrk, M. Benova, and Z. Psenakova, "Specific absorption rate evaluation in human body model comprising of metallic implant," in *Proc. 19th Int. Conf. Comput. Problems Electr. Eng.*, Banska Stiavnica, Slovakia, 2018, pp. 1–4, doi: 10.1109/CPEE.2018.8507101.
- [14] F. Kaburcuk and A. Z. Elsherbeni, "SAR and temperature rise distributions in a human head due to a multi-frequency antenna source," in *Proc. Int. Appl. Comput. Electromagn. Soc. Symp. (ACES)*, Denver, CO, USA, Mar. 2018, pp. 1–2, doi: 10.23919/ROPACES.2018.8364205.
- [15] S. il Kwak, D.-U. Sim, J. H. Kwon, and Y. J. Yoon, "Design of PIFA with metamaterials for body-SAR reduction in wearable applications," *IEEE Trans. Electromagn. Compat.*, vol. 59, no. 1, pp. 297–300, Feb. 2017, doi: 10.1109/TEMC.2016.2593493.
- [16] A. Shah and P. Patel, "E-textile slot antenna with spurious mode suppression and low SAR for medical wearable applications," *J. Electromagn. Waves Appl.*, vol. 35, no. 16, pp. 2224–2238, Nov. 2021, doi: 10.1080/09205071.2021.1934905.
- [17] IEEE Standard for Military Workplaces—Force Health Protection Regarding Personnel Exposure to Electric, Magnetic, and Electromagnetic Fields, 0 Hz to 300 GHz, IEEE Standard C95.1-2345-2014, May 2014.
- [18] E. Canicattì, E. Giampietri, D. Brizi, N. Fontana, and A. Monorchio, "A numerical exposure assessment of portable self-protection, high-range, and broadband electromagnetic devices," *IEEE Open J. Antennas Propag.*, vol. 2, pp. 555–563, Apr. 2021, doi: 10.1109/OJAP2021.3072548.
- [19] M. A. Bredella, "Sex differences in body composition," in *Sex and Gender Factors Affecting Metabolic Homeostasis, Diabetes and Obesity*, vol. 1043, F. Mauvais-Jarvis, Ed. Cham, Switzerland: Springer International Publishing, 2017, pp. 9–27.
- [20] H. Homann, P. Börnert, H. Eggers, K. Nehrke, O. Dössel, and I. Graesslin, "Toward individualized SAR models and in vivo validation: Individualized SAR models," *Magn. Reson. Med.*, vol. 66, no. 6, pp. 1767–1776, Dec. 2011, doi: 10.1002/mrm.22948.
- [21] H. Homann et al., "Local SAR management by RF Shimming: A simulation study with multiple human body models," *Magn. Reson. Mater. Phys., Biol. Med.*, vol. 25, no. 3, pp. 193–204, Jun. 2012, doi: 10.1007/s10334-011-0281-8.
- [22] A. Hirata, I. Laakso, T. Oizumi, R. Hamanishi, K. H. Chan, and J. Wiart, "The relationship between specific absorption rate and temperature elevation in anatomically based human body models for plane wave exposure from 30 MHz to 6 GHz," *Phys. Med. Biol.*, vol. 58, no. 4, pp. 903–921, Jan. 2013, doi: 10.1088/0031-9155/58/4/903.
- [23] L. Sandrini, A. Vaccari, C. Malacarne, L. Cristoforetti, and R. Pontalti, "RF dosimetry: A comparison between power absorption of female and male numerical models from 0.1 to 4 GHz," *Phys. Med. Biol.*, vol. 49, no. 22, pp. 5185–5201, Oct. 2004, doi: 10.1088/0031-9155/49/22/012.
- [24] P. J. Dimbylow, A. Hirata, and T. Nagaoka, "Intercomparison of whole-body averaged SAR in European and Japanese voxel phantoms," *Phys. Med. Biol.*, vol. 53, no. 20, pp. 5883–5897, Sep. 2008, doi: 10.1088/0031-9155/53/20/022.
- [25] P. Dimbylow, "Resonance behaviour of whole-body averaged specific energy absorption rate (SAR) in the female voxel model, NAOMI," *Phys. Med. Biol.*, vol. 50, no. 17, pp. 4053–4063, Aug. 2005, doi: 10.1088/0031-9155/50/17/009.
- [26] DiPP GmbH, Apr. 2013, "Anatomical volume data sets," DiPP GmbH. [Online]. Available: <http://www.r-laboratory.com>
- [27] "Human models," ITIS Foundation, Zurich, Switzerland. [Online]. Available: <https://itis.swiss/virtual-population/virtual-population/overview/>
- [28] E. Canicattì, E. Giampietri, D. Brizi, N. Fontana, and A. Monorchio, "SAR evaluation from high-intensity and broadband sources for different human body models," in *Proc. IEEE Int. Symp. Antennas Propag. USNC-USRI Radio Sci. Meeting (APS/URSI)*, Singapore, 2021, pp. 359–360, doi: 10.1109/APS/URSI47566.2021.9703715.
- [29] N. Fontana, E. Giampietri, E. Canicattì, D. Brizi, and A. Monorchio, "Broadband numerical evaluation of SAR distribution due to high-intensity radiated fields by portable systems," in *Proc. IEEE Int. Symp. Antennas Propag. North Amer. Radio Sci. Meeting*, Montreal, QC, Canada, 2020, pp. 307–308, doi: 10.1109/IEEECONF35879.2020.9329849.
- [30] R. Y. Ha, K. Nojima, W. P. Adams, and S. A. Brown, "Analysis of facial skin thickness: Defining the relative thickness index," *Plastic Reconstructive Surgery*, vol. 115, no. 6, pp. 1769–1773, May 2005, doi: 10.1097/01.PRS.0000161682.63535.9B.
- [31] "Visible human project," The National Library of Medicine, Bethesda, MD, USA. [Online]. Available: http://www.nlm.nih.gov/research/visible/visible_human.html
- [32] A. Christ et al., "The virtual family—Development of surface-based anatomical models of two adults and two children for dosimetric simulations," *Phys. Med. Biol.*, vol. 55, no. 2, pp. N23–N38, Dec. 2010, doi: 10.1088/0031-9155/55/2/N01.
- [33] S. Gabriel, R. W. Lau, and C. Gabriel, "The dielectric properties of biological tissues: III. Parametric models for the dielectric spectrum of tissues," *Phys. Med. Biol.*, vol. 41, no. 11, pp. 2271–2293, Nov. 1996, doi: 10.1088/0031-9155/41/11/003.
- [34] A. D. Timinswood, C. M. Furse, and O. P. Gandhi, "Power deposition in the head and neck of an anatomically based human body model for plane wave exposures," *Phys. Med. Biol.*, vol. 43, no. 8, pp. 2361–2378, Aug. 1998, doi: 10.1088/0031-9155/43/8/026.
- [35] J. M. Ziriax et al., "Effects of frequency, permittivity, and voxel size on predicted specific absorption rate values in biological tissue during electromagnetic-field exposure," *IEEE Trans. Microw. Theory Techn.*, vol. 48, no. 11, pp. 2050–2058, Nov. 2000, doi: 10.1109/22.884194.
- [36] A. Ijeh, M. Cueille, J.-L. Dubard, and M. Ney, "Modeling finite-radius VHF and HF wire-antennas for numerical dosimetry applications in near-field interaction scenarios," in *Proc. 15th Eur. Conf. Antennas Propag. (EuCAP)*, Düsseldorf, Germany, Mar. 2021, pp. 1–5, doi: 10.23919/EuCAP51087.2021.9411288.
- [37] IEC/IEEE International Standard -- Determining the Peak Spatial-Average Specific Absorption Rate (SAR) in the Human Body from Wireless Communications Devices, 30 MHz to 6 GHz – Part 1: General Requirements for Using the Finite-Difference Time-Domain (FDTD) Method for SAR Calculations, IEC/IEEE International Standard 62704-1:2017, 2017.
- [38] "Assessing the compliance of emissions from HF broadcast transmitters," European Broadcasting Union, Geneva, Switzerland, Tech. Rev. 306, Apr. 2006. [Online]. Available: https://tech.ebu.ch/publications/trev_306-emf_hf
- [39] Institute of Electrical and Electronics Engineers, 2013 International Symposium on Electromagnetic Compatibility (EMC Europe 2013). Piscataway, NJ, USA: IEEE, 2013.
- [40] E. Conil, A. Hadjem, F. Lacroux, M. F. Wong, and J. Wiart, "Variability analysis of SAR from 20 MHz to 2.4 GHz for different adult and child models using finite-difference time-domain," *Phys. Med. Biol.*, vol. 53, no. 6, pp. 1511–1525, Mar. 2008, doi: 10.1088/0031-9155/53/6/001.
- [41] Y. Guo, J. Wang, H.-K. Ma, L.-D. Wang, and W.-Y. Yin, "Specific absorption rate (SAR) evaluation of human body model in the presence of radar wave radiation on a warship deck," in *Proc. IEEE Int. Symp. Electromagn. Compat. (EMC)*, Dresden, Germany, 2015, pp. 541–545, doi: 10.1109/ISEM.2015.7256220.
- [42] I. VilasBoas-Ribeiro, G. C. van Rhoon, T. Drizdal, M. Franckena, and M. M. Paulides, "Impact of number of segmented tissues on SAR prediction accuracy in deep pelvic hyperthermia treatment planning," *Cancers*, vol. 12, no. 9, Sep. 2020, Art. no. 2646, doi: 10.3390/cancers12092646.
- [43] N. B. Asan et al., "Intra-body microwave communication through adipose tissue," *Healthcare Technol. Lett.*, vol. 4, no. 4, pp. 115–121, May 2017, doi: 10.1049/htl.2016.0104.
- [44] M. Saretoniemi, C. Pomalaza-Raez, C. Kissi, M. Berg, M. Hamalainen, and J. Innati, "WBAN channel characteristics between capsule endoscope and receiving directive UWB on-body antennas," *IEEE Access*, vol. 8, pp. 55,953–55,968, Mar. 2020, doi: 10.1109/ACCESS.2020.2982247.
- [45] E. M. Staderini, "UWB radars in medicine," *IEEE Aerosp. Electron. Syst. Mag.*, vol. 17, no. 1, pp. 13–18, Jan. 2002, doi: 10.1109/62.978359.
- [46] M. Cavagnaro, S. Pisa, and E. Pittella, "Safety aspects of human exposure to ultra wideband radar fields," in *Proc. Int. Symp. Electromagn. Compat. – EMC EUROPE*, Rome, Italy, 2012, pp. 1–5, doi: 10.1109/EMCEurope.2012.6396885.
- [47] P. Störchle, W. Müller, M. Sengeis, S. Lackner, S. Holasek, and A. Fürhapter-Rieger, "Measurement of mean subcutaneous fat thickness: Eight standardised ultrasound sites compared to 216 randomly selected sites," *Sci. Rep.*, vol. 8, no. 1, Nov. 2018, Art. no. 16268, doi: 10.1038/s41598-018-34213-0.
- [48] Y. Lee and K. Hwang, "Skin thickness of Korean adults," *Surgical Radiologic Anatomy*, vol. 24, nos. 3–4, pp. 183–189, Aug./Sep. 2002, doi: 10.1007/s00276-002-0034-5.

Call for Nominations of IEEE AP-S

Distinguished Lecturers

Nomination Deadline: August 31, 2023

The Call for nominations of IEEE Antennas and Propagation Society Distinguished Lecturers for the period 2024–2026 is now open.

Self-nominations are welcome and encouraged. In addition to the conventional Distinguished Lecturer (DL) positions, one DL position will be awarded to a person who has demonstrated successful entrepreneurship or exceptional contributions towards commercialization in an antenna or propagation-related field and has given related presentations to engage with others. Nominees who wish to be considered under this category should indicate their corresponding experience in the nomination documents. Decisions will normally be made on or before the end of the year.

All nominees must state in the nomination documents that they agree to give at least three distinguished lectures in developing countries during the tenure of three years if selected. As a guideline, any country or area that is not recognized by the United Nations as a Developed Economy is considered “developing” for this program. Please read Table A. Developed Economies, “Country classification” in this [link](#). The Chair of the DL Committee can consider and approve exceptions.

In addition to the specialized lectures, each nominee must propose and give one lecture suitable for the general audience – a lecture that all AP Society members can appreciate.

The entire nomination package should be e-mailed to the Chair of the Committee, with the subject: “AP-S Distinguished Lecturer Nomination 2022” on or before the deadline for the consideration of the three-year term to be started in 2023. The mandatory video clip can be submitted through sharing the link to online storages such as Dropbox, Google Drive or OneDrive.

The nomination package should include the following six pdf files. Please be reminded that all six files are mandatory and any additional material, including those exceed the page limit, will not be considered.

1. A letter of recommendation from the nominator, or a statement of purpose in the case of self-nomination (Page limit: 1 page; Filename: NomineeLastName_Letter): This should indicate the feedback received by the nominee after previous external, preferably international, presentations, and his/her willingness to travel to chapters around the world as part of the service.
2. A curriculum vitae or resume of the nominee (Page limit: 5 pages; Filename: NomineeLastName_Resume): It includes the complete or partial list of presentations given by the nominee since 2016. In the list, identify those presentations which are more general / tutorial/workshop nature with an asterisk.
3. A set of abstracts for the proposed lectures that the nominee plans on offering (Page limit: 3 pages; Filename: NomineeLastName_Abstracts): The abstracts from current DLs are available on the Distinguished Lecturer Program [webpage](#) for the nominees' reference. The number of lectures offered by each DL varies; 3 to 4 lectures are suggested which include the lecture for the general audience.
4. A sample set of slides (Page limit: 40 slides; Filename: NomineeLastName_Slides): It can be from one or several recent presentations given by the nominee.
5. Ten slides on the lecture proposed for the general audience (Page limit: 10 slides; Filename: NomineeLastName_SlidesGeneral): This lecture does not need to be completed at this stage.
6. A 10-minute video (with voice) of one of the proposed lectures (Length: 10 minutes, size: < 1 GB; Filename: NomineeLastName_Video): This lecture does not need to be completed at this stage.

Nominees will be evaluated by the Committee based on the following selection criteria:

- Outstanding communication and presentation skills (30%)
- Quality and relevance of proposed lectures that are of current or tutorial interest to both specialized and general audiences (30%)
- An outstanding record of accomplishment in the field of Antennas and Propagation (40%)
- Demonstrated entrepreneurship and/or exceptional contributions towards commercialization in an antenna- or propagation-related field (only applicable to nominees in the entrepreneurship category)

Professor Kwai Man Luk

IEEE AP-S Distinguished Lecturer Program Committee Chair

Department of Electrical Engineering, City University of Hong Kong

E-mail: eekmluk@cityu.edu.hk

May 31, 2023



Rajeev Bansal

Don't Leave Home Without It

Readers of a certain age may remember a classic American Express advertising campaign from the 1970s. As reported in [1], the line “Don’t leave home without it” got its start “in a series of ads where a fedora wearing Karl Malden warned about the dangers of carrying cash instead of American Express Travelers Cheques.” Well, those traveler’s checks have gone the way of VHS players, but one product “introduced” in the 1970s has conquered the world in the last 50 years.

According to a report on CNN [2], it was on 3 April 1973 that “Martin Cooper stood on a sidewalk on Sixth Avenue in Manhattan with a device the size of a brick and made the first public call from a cell phone to one of the men he’d been competing with to develop the device. ‘I’m calling you on a cell phone, but a real cell phone, a personal, handheld, portable cell phone,’ Cooper, then an engineer at Motorola, said on the phone to Joel Engel, head of AT&T-owned Bell Labs.” Manufacturing issues and federal regulatory processes had delayed the availability of cell phones to the public for a decade, when a version of that DynaTAC (Dynamic Adaptive Total Area Coverage) phone, which weighed 2.5 lb and

was about a foot tall, hit the market for a hefty US\$3,900. It took another decade before cell phones became really practical in terms of size and weight, but since then the technology has seen a phenomenal growth, with some 97% of Americans owning a cell phone of some kind [2].

If you asked millennials about the one product they would not leave home without, it would undoubtedly be their cell phones [3]. In any restaurant, it is a common sight these days to see a group of young people sitting around a table, not looking at their menus or talking to one another, but scrolling through their smartphones and dispatching a flurry of emojis. How did young people of earlier generations communicate with one other without these gadgets? As the 18 April 2023 entry in my daily Forgotten English calendar [4] reminded me, “more than a hundred messages could be telegraphed by women [in 18th century England] based on the movement of her fan, body position and actions. For instance, covering the left ear with an open fan said, ‘Please keep this a secret,’ while striking anything with a fan indicated that the woman was becoming impatient” [4].

Martin Cooper, the inventor of the first portable cell phone, told CNN [2] that “too many engineers are wrapped up in what they call technology and

the gadgets, the hardware, and they forget that the whole purpose of technology is to make peoples’ lives better. People forget that, and I have to keep reminding them. We are trying to improve the human experience. That’s what technology is all about.” So from fans to cell phones, what has not changed is the fundamental human need to communicate. Any guesses on how we will be meeting that need 50 years from now?

ACKNOWLEDGMENT

I would like to thank my Committee on Man and Radiation (COMAR) colleague Ken Foster for posting a link to the CNN story on the COMAR listserve.

REFERENCES

- [1] F. Ulrich, “Don’t launch a global brand campaign without it,” *Media Logic*, Jun. 2018. Accessed: May 9, 2023. [Online]. Available: <https://www.medialogic.com/blog/financial-services-marketing/american-express-brand-campaign/>
- [2] J. Korn, “50 years ago, he made the first cell phone call.” *CNN*, Apr. 2023. Accessed: May 9, 2023. [Online]. Available: <https://www.cnn.com/2023/04/03/tech/cell-phone-turns-50/index.html>
- [3] M. Casciano, “Millennials can’t live without these 10 relatable life essentials, TBH,” *Elite Daily*, May 2019. [Online]. Available: <https://www.elitedaily.com/p/10-things-millennials-can-t-live-without-because-theyre-essential-to-living-your-bestlife-17869861>
- [4] J. Kacirk, *Forgotten English (a Daily Calendar)*. South Portland, ME, USA: Sellers Publishing, 2023.



Vikass Monebhurrun^{ID}

Why Every Member of the AP-S Should Own a Copy of the Antenna Measurement Standard IEEE Standard 149

Jeff Fordham, Lars J. Foged^{ID}, Vicente Rodriguez^{ID},
Justin Dobbins^{ID}, and Vikass Monebhurrun^{ID}

The revised version of IEEE Standard 149 is finally available as IEEE Standard 149-2021, approved by the IEEE Standards Association Standards Board (SASB) in September 2021 and effectively published in February 2022. This is the first in-depth revision of the standard since 1979. Rewritten as a recommended practice, the standard is an essential desk reference for anyone involved in antenna measurements. While most instructions on antenna engineering are centered on the designs, types, and numerical methods applied to antennas, the standard focuses on the art of measuring antennas and understanding the best approach for measuring different parameters of antennas. With almost 200 bibliographical references, the standard provides guidance on the methods and approaches to measure realistic implementations of antennas or points the reader to relevant sources of information. No antenna engineer is completely prepared without an understanding of the proper approach to perform antenna measurements and how to estimate the uncertainty of an antenna measurement.

INTRODUCTION

Over the years, the authors, who have been involved in aspects of antenna engineering ranging across areas such as the design of antennas, measurements of complex active antennas, and the design of antenna measurement facilities and systems, have noticed that instruction at the university level is lacking in the antenna measurement area. This is understandable, given the cost associated with constructing a proper laboratory to perform antenna measurements. In addition, common textbooks on antennas dedicate only a minor part to the topic of antenna measurements. Kraus, out of 890 pages, has a 40-page chapter on antenna measurements [1], that is, 4.5% of the book. Balanis dedicates a 44-page chapter of the 925 pages of his book, or 4.7% [2]. Both Kraus and Balanis locate the measurements chapter as the last chapter of their books. Stutzman and Thiele place the chapter that covers measurements before the chapters on numerical methods [3]. Their chapter, which also covers antennas in systems, consists of 31 pages out of the total 643 pages of the book, or 4.8%. The authors regularly observe a lack of understanding on how to perform accurate antenna measurements among a vast majority of antenna engineers graduating from dif-

ferent universities. It is very common to see papers at IEEE Antennas and Propagation Society (AP-S)-sponsored symposia where the presenter essentially compares numerical results to measurements and de facto dismisses the eventual deviations as “manufacturing tolerances” without providing clear information about important measurement details. For example: How was the antenna mounted? How were the cables handled? What was the reflectivity of the range, and how did the stray energy affect the measured pattern features? What was the test distance? How was the gain measured?

IEEE Standard 149-2021 can help technicians and engineers as well as students and Young Professionals understand how to perform low-uncertainty antenna measurements. The members of the IEEE Std 149 Working Group (WG) spent more than eight years revising the previous document—updating the existing content and adding new material. The WG comprised 63 experts on antenna metrology. They dedicated their volunteer time and expertise to produce a document that, while not perfect and potentially not complete, is a repository of knowledge and references related to antenna measurements. In this article, the authors provide a clause-by-clause

summary of the contents of the standard, showing the reader why it is a must-have anyone involved with antenna measurements.

REVISION OF CLAUSES

In the SASB nomenclature the documents prepared (whether mandatory standards, recommended practices, or guides) follow *clauses*, as opposed to *chapters*. In the present section, the authors describe the clauses of the standard and provide information to the reader as to what information the clauses contain and their importance. The changes to the document compared to the original 1979 [4] version have been described in several papers presented at conferences that provided updates on the progress by the WG [5], [6]. In these works, it was mentioned that the main and most significant change to IEEE Standard 149 is the conversion of the standard to a recommended practice. Following discussions within the WG, and to account for the wide range of existing antenna measurement facilities, it was more appropriate to provide recommendations (i.e., the use of “should”) for good measurement practices and describe the variety of available techniques and technologies, rather than to impose mandatory requirements (i.e., the use of “shall”). The document is very useful, both for those designing and evaluating antenna test facilities and for those performing antenna measurements. The revised document retains the IEEE Standard 149 identifier but is now titled *IEEE Recommended Practice for Antenna Measurements* [7], as shown in Figure 1.

CLAUSES 1 THROUGH 3

These clauses can be described as housekeeping clauses. They are mandated by the SASB procedures; e.g., they provide information, such as the scope of the standard. One important point is that the standard is centered on passive reciprocal linear devices. However, the techniques described can be used in the testing of additional devices, e.g., active phased arrays, in many cases. Indeed, the standard has an informative annex (Annex D) that describes

The document is very useful, both for those designing and evaluating antenna test facilities and for those performing antenna measurements.

the over-the-air (OTA) measurement of integrated devices, such as mobile phones. These first clauses also provide definitions for some relevant terms and provide a list of other normative references that are indispensable for the document, such as the *IEEE Standard for Definition of Terms for Antennas* [8]. Common acronyms are also listed in these clauses. An important point mentioned in Clause 1 is the usage of the time convention. While the standard uses the IEEE-compliant $e^{(+j\omega t)}$ time convention, many of the references provided use the physics preference of $e^{(-i\omega t)}$. Guidance is given on how to avoid potential errors from using equations derived using the physics convention instead of the IEEE convention.

CLAUSE 4

Clause 4 deals with the antenna range design, including the selection of the best antenna measurement range for different types of antennas. The WG members considered it important to point out that there is not a single antenna

measurement solution that fits all problems. Antennas come in such a variety of designs that not every antenna range is suitable to measure a given antenna. It is desirable to be in the far field of an antenna when measuring its radiation performance. However, a mobile phone-sized antenna having a maximum aperture

dimension of about 17 cm, but operating at 22 GHz, requires a test distance in excess of 4.24 m as per the well-known equation for the lower limit distance, R , of the far field given by

$$R \geq \frac{2D^2}{\lambda} \quad (1)$$

where D is the maximum dimension of the antenna and λ is the wavelength.

The clause starts by giving general guidance on what an antenna range should provide, e.g., type of illumination, levels of amplitude taper and ripple, and common errors due to phase variation across the aperture. The clause then provides guidelines for designing outdoor ranges, both elevated and ground reflection ranges. The discussion on ground reflection ranges should be of interest to antenna engineers working in the automobile industry, where some of the antenna systems work at frequencies such that the vehicle must be measured outdoors with the vehicle placed on a metallic turntable. One of the additions to the document compared to the 1979 edition is the discussion on the design of indoor ranges (see Figure 2). Both rectangular far-field anechoic chambers and tapered anechoic chambers are described. It should be noted that ranges for near-to-far-field transformation measurements are not discussed here but in the companion document IEEE Standard 1720-2012 [9], which addresses near-field antenna measurement and is currently under revision. The guidelines for a reflector-based compact range anechoic room are also given in this clause [see Figure 4(a)].

Reverberation chambers are introduced in Clause 4 as an alternative methodology for measuring the efficiency of



FIGURE 1. IEEE Standard 149 front cover.

antennas. An equation is provided for the minimum volume of the chamber to satisfy the criteria of supporting at least 60 resonant modes at the lowest frequency of operation.

CLAUSE 5: INSTRUMENTATION

Clause 5 discusses all instrumentation in antenna measurements, to include the radio-frequency subsystem as well as the positioning subsystem, which employs electronic control of mechanical positioners to capture spatial radiation patterns. The clause provides guidance and recommendation on the following topics: range antennas, the transmit subsystem, the receive subsystem, the positioning subsystem, and the workstation/software. Topics such as frequency multipliers, the use of remote mixers, dynamic range, amplifiers, and choice of cables are discussed. A discussion of the typical antenna positioning geometries, such as azimuth over elevation, elevation over azimuth, and roll over azimuth, is provided in this clause. The main software functions used on the workstation to control the test are also discussed.

CLAUSE 6: ANTENNA RANGE EVALUATION

Clause 6 closes the trio of clauses related to the environment and equipment used to measure an antenna under test (AUT). Clause 6 provides recommendations for the evaluation of the range used to perform the measurement. The concept of a quiet zone (QZ) is revisited, and techniques to assess the purity of the QZ are discussed. Methods for measuring the quality of the plane wave incident onto the AUT are provided. An updated discussion of the well-known free space voltage standing-wave ratio method for evaluating the reflectivity in the QZ is also provided. This is probably the first detailed discussion of the method in a standards document since its first description in 1963 [10]. A new addition to the standard is the use of Fourier analysis of QZ performance for chamber validation and diagnostics. In this technique, a plane in the QZ is scanned while sampling the magnitude and phase of the field, a common practice for QZ evaluation. But in this case,

Guidance is given on how to avoid potential errors from using equations derived using the physics convention instead of the IEEE convention.

a Fourier transform of the data is performed to decompose the measurement into a series of plane waves arriving from different directions. This alternative analysis method can be used to diagnose problems in the range by pinpointing the origin of reflected energy from the lateral surfaces or other features in the range.

MEASUREMENT CLAUSES

While Clauses 4 through 6 comprise a trio related to the tools to perform measurements, Clauses 7 through 11 provide information on measuring specific parameters of an AUT.

CLAUSE 7: MEASUREMENT OF RADIATION PATTERN

This clause provides a series of definitions and guidelines. Among other things, it provides a more precise defi-

nition of the far-field condition and the lower limit of the far field depending on the antenna electrical size (see Figure 3). While most people are familiar with (1), it is not recommended that this equation be applied for AUTs that are less than four or five wavelengths in any cross-sectional dimension of the aperture.

The clause discusses configurations for measuring the amplitude pattern as well as the approach for measuring the phase pattern and the phase center of an AUT.

CLAUSE 8: MEASUREMENT OF GAIN AND DIRECTIVITY

Clause 8 is probably the most broadly applicable section of the standard, providing information on the measurement of directivity, gain (as defined by the IEEE), and realized gain (as it is often measured) of an AUT. The clause also discusses the *antenna factor*, a parameter used in electromagnetic compatibility measurements but rarely mentioned in antenna textbooks. Direct methods for measuring the AUT gain, such as the three-antenna method and the extrapolation range method, are covered. These techniques are especially applicable to

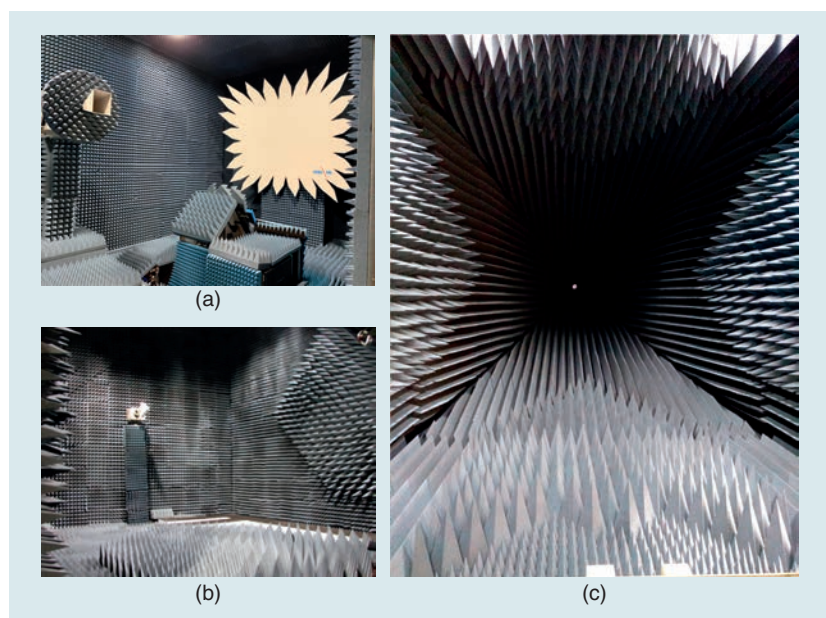


FIGURE 2. (a) A compact range, (b) a rectangular far-field chamber, and (c) a tapered chamber.

calibrating gain standards since several measurement methods use gain standards to assess the gain of an AUT. A discussion on potential sources of error on antenna calibrations is provided in the clause.

CLAUSE 9: MEASUREMENT OF POLARIZATION

Clause 9 deals with measurements of the polarization of antennas. After a series of definitions of different parameters related to antenna polarization, the standard provides descriptions and guidance on how to measure and calculate the polarization of antennas. This is one type of measurement where it is important to pay attention to the time convention used in deriving the equations used to obtain the different parameters. Using the wrong time convention will change the sense of the reported polarization.

CLAUSE 10: MEASUREMENT OF EFFICIENCY

Clause 10 describes methods for measuring radiation efficiency. In addition to the well-known Wheeler cap technique, the standard introduces the use of rever-

beration chambers to measure efficiency. Two approaches are provided: one that uses a reference to perform the efficiency measurements and one that incorporates a rotation of three antennas to evaluate the efficiency of each antenna. The pattern integration method is also discussed in the clause.

CLAUSE 11: MEASUREMENT OF IMPEDANCE

Clause 11 deals with the measurement of impedance of antennas. To support this clause, there is an informative annex in the standard (Annex F) with additional theory and detail. The clause also describes sources of error and uncertainty. Clause 11 concludes the set of clauses related to measurements of specific antenna parameters.

CLAUSE 12: SPECIAL MEASUREMENT TECHNIQUES

Clause 12, while not specific to antenna parameters, provides information on specific strategies related to antenna measurements. These strategies include the use of scaled models as well as techniques to generate localized plane waves to measure antennas at shorter

distances (including, but not limited to, the compact range reflector). Clause 12 briefly describes the concept of near-to-far-field measurements, which are the topic of [9]. The clause also discusses methods for measuring angle-tracking antennas and gain over temperature for receiving antenna systems that include active electronics. This last topic is a slight deviation from the stated scope of the standard, but the WG agreed that it was important to add the discussion because of the prevalence of active antenna systems.

CLAUSE 13: UNCERTAINTY

Clause 13 has been described as the most important addition in the standard [5], [6]. Indeed, a measurement is meaningless without an uncertainty associated with it (and the specification of its units). The clause follows the ISO/IEC *Guide to the Expression of Uncertainty in Measurement* [11] as directed by the SASB. The standard provides guidance on how to set up an uncertainty analysis. The clause uses the compact range as an example of how to perform an uncertainty analysis. Uncertainty is one of the topics of antenna measurements that are not mentioned in [1], [2], or [3] and yet are of the utmost importance. This makes IEEE Standard 149-2021 a must-have document for all members of the AP-S.

CLAUSES 14 THROUGH 16

The three final clauses of the standard relate to the daily operation of an antenna range. Clause 14 provides guidance on how to manage a test range, covering topics such as record keeping, periodic calibrations, technician training, and scheduling of testing. Related to the use of the range and its operation, Clause 15 reminds the reader about exposure to electromagnetic fields. While the IEEE document related to this topic is IEEE Standard C95.1-2019 [12], Clause 15 presents two plots that can be easily referenced to check the exposure limits for test personnel. The final clause, Clause 16, reminds the reader about radome effects and the effects of temperature and moisture on antenna measurements and includes considerations

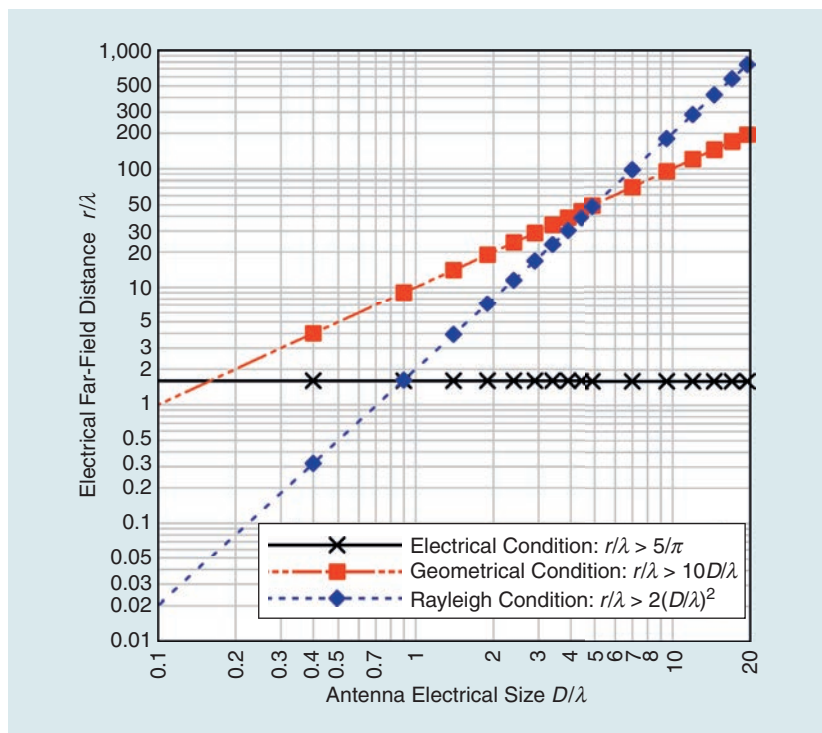


FIGURE 3. The lower limit of the far field depending on the antenna electrical size.

for testing antennas that will operate in extreme environments.

ANNEXES

As mentioned previously, the standard is an invaluable desk reference for the antenna engineer. It contains a large amount of information that is concentrated in a single, organized document. The included annexes supplement the main document with information to help readers explore further.

An important annex is Annex A, which contains the bibliography. A total of 193 references is provided to direct readers to more depth into some of the topics covered by the standard. For example, [1], [2], and [3] are listed in the bibliography as sources for some of the included topics in the standard.

Annex B discusses the different field regions, that is, the reactive near field, the radiated near field, and the far field. Annex C provides an informative background on the topic of reciprocity. Annex D, as mentioned previously, touches on OTA testing, an area of importance in the mobile phone industry but also now in a wide variety of areas, given the spread of wireless communications.

Annex E provides guidance on boresighting antennas and finding the peak of the pattern, which may not coincide with the mechanical boresight.

The last informative annex, Annex F, provides additional information about impedance measurements as a supplement to Clause 11.

USING THE STANDARD

The standard is a repository of knowledge from recognized industry leaders. Armed with it, the antenna engineer can assess different facilities available to perform antenna measurements and ensure that the measurements will have an acceptable level of uncertainty. The authors performed an Internet search of companies that provide antenna pattern measurement services. It was interesting to observe that none of the companies found provide information regarding the reflectivity of the QZ or the test distance. Typically, they mention the frequency range and the largest antenna

that can be tested. Most of these facilities have earned an accreditation from one of the laboratory certification agencies, such as the American Association for Laboratory Accreditation (A2LA) or the National Voluntary Laboratory Accreditation Program (NVLAP), signifying compliance with ISO 17025 [13]. Achieving this compliance requires a documented uncertainty analysis. While the companies may be willing to share their uncertainty analyses, an antenna engineer who has read the standard would recognize that many of the uncertainty terms are dependent on the AUT and must be assessed individually.

As an example, consider an antenna engineer who needs to measure the radiation patterns of an antenna with a 20-cm by 20-cm aperture operating at 18 GHz. One available facility claims a frequency range from 300 MHz to 40 GHz for antennas up to 61 cm by 61 cm in a fully anechoic rectangular chamber. Since the antenna is 12λ by 12λ , the diagonal length is about 17λ . Clause 7 indicates that, for this example scenario, the test distance should be at least 9.62 m. The antenna engineer could make a simple inquiry to the provider to determine whether the facility meets this requirement and, regardless of the answer, use the information in Clause 4 to estimate the effects of both amplitude and phase taper at finite measurement distances.

As mentioned previously, antenna pattern measurement service providers do not typically mention the reflectivity level of their ranges. This is a critical term in the uncertainty assessment since the level of reflected energy in the QZ induces an error in the pattern measurement. Clause 6 provides metrics and methods for qualifying an antenna pattern measurement range, and Clause 4 provides guidance for estimating the reflectivity based on the chamber dimensions and absorber treatment. Clause 4 also provides a convenient method to bound the pattern measurement uncertainty due to reflections. To continue our example, let us assume that the range has a QZ reflectivity level of -40 dB. If the AUT has sidelobe levels of -15 dB,

then potentially the ratio between the reflected signal observed by the AUT main beam and the -15-dB sidelobe of interest will be -25 dB. Clause 4 shows that the error bound in this scenario is ± 0.5 dB. A -25-dB feature in the pattern can potentially result in an error bound of approximately ± 1.5 dB. Figure 4, found in Clause 4, shows the error for in-phase and out-of-phase interference between the reflected and direct signals, with our two example scenarios highlighted with green arrows.

It should be noted that we have only discussed two sources of uncertainty in this article: finite range length and multipath. Clause 13 provides a list of 15 potential error terms to consider along with a specific example of a 15-term uncertainty budget for a compact range. All members of our community, including the engineers and the service providers, now have an updated source of information for assessing uncertainties (Clause 13) and qualifying a range (Clause 6).

CONCLUSIONS

IEEE Standard 149-2021 has been published as of 18 February 2022 [7]. This document is a recommended practice with the title *IEEE Recommended Practice for Antenna Measurements*. This document, while not intended to be a textbook on antenna measurements, fills a gap in the available bibliography for antenna measurements. It provides an overview of antenna measurements that makes this standard a must-have document for any antenna engineer who must oversee the creation of a new antenna design, from concept and model in a software package to final deliverable product. The standard has been significantly revised to reflect modern measurement practices and provide general guidance for improving measurement quality while considering associated uncertainties. The changes make the document an essential reference for anyone involved, not only in antenna measurements, but in antenna engineering in general. Any member of the AP-S should own or have access to a copy of this standard document.

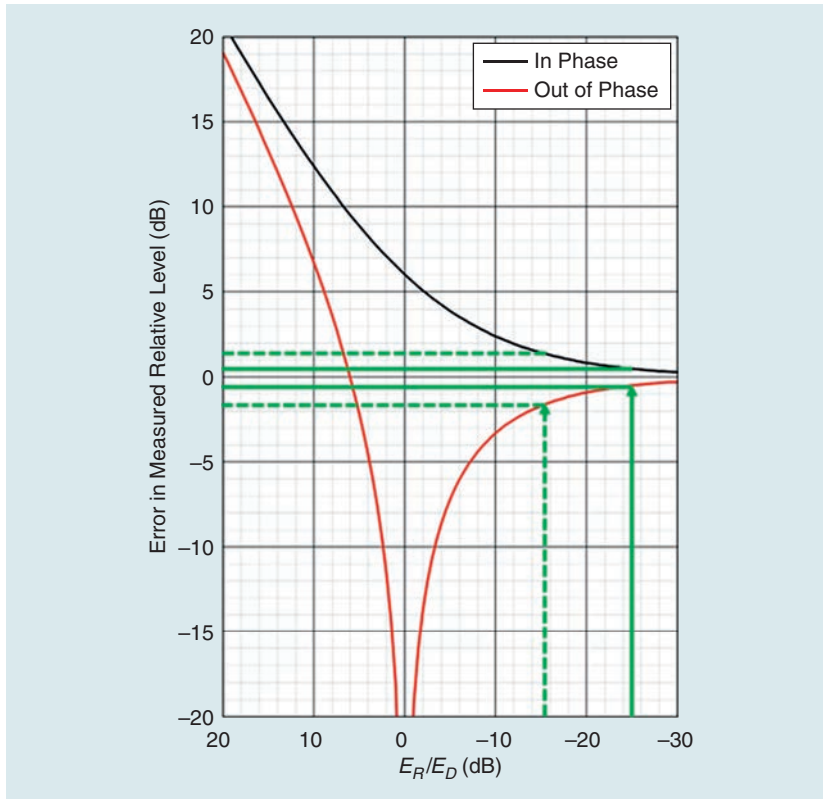


FIGURE 4. In-phase and out-of-phase errors for different reflected-to-direct signal ratios in the antenna range. The solid green lines show the error range for -25 dB and the dashed green lines show the error for -15 dB .

AUTHOR INFORMATION

Jeff Fordham (jeff.fordham@ametek.com) is with NSI-MI Technologies, Suwanee, GA 30024 USA. He is a Member of IEEE.

Lars J. Foged (lars.foged@mvg-world.com) is with MVG, Microwave Vision Italy, 00071 Pomezia, Italy. He is a Member of IEEE.

Vicente Rodriguez (vince.rodriguez@ametek.com) is with NSI-MI Technolo-

gies, Suwanee, GA 30024 USA. He is a Senior Member of IEEE.

Justin Dobbins (justin.dobbins@rtx.com) is with Raytheon Technologies, Tucson, AZ 85625 USA. He is a Member of IEEE.

Vikass Monebhurrun (vikass.monebhurrun@centralesupelec.fr) is with CentraleSupélec, GeePs, 91192 Paris, France. He currently serves as chair of the IEEE Antennas and Propagation

Standards Committee and associate editor of IEEE Transactions on Antennas and Propagation. He is a Senior Member of IEEE.

REFERENCES

- [1] J. Kraus, *Antennas*, 2nd ed. Boston, MA, USA: McGraw-Hill, 1988.
- [2] C. A. Balanis, *Antenna Theory: Analysis and Design*, 2nd ed. New York, NY, USA: Wiley, 1997.
- [3] W. Stutzman and G. Thiele, *Antenna Theory and Design*, 2nd ed. New York, NY, USA: Wiley, 1998.
- [4] IEEE Standard Test Procedures for Antennas, IEEE Standard 149-1979, Nov. 1979.
- [5] V. Rodriguez, L. Foged, and J. Fordham, "Expected changes and additions to the antenna measurement standard IEEE Std149™," in *Proc. IEEE Conf. Antenna Meas. Appl. (CAMA)*, 2018, pp. 1–2, doi: 10.1109/CAMA.2018.8530605.
- [6] V. Rodriguez, J. Fordham, and L. Foged, "A review of the changes and additions to the antenna measurement standard IEEE Std 149," in *Proc. Antenna Meas. Techn. Assoc. Symp. (AMTA)*, 2019, pp. 1–3, doi: 10.23919/AMTAP.2019.8906343.
- [7] IEEE Recommended Practice for Antenna Measurements, IEEE Standard 149-2021, 2021.
- [8] IEEE Standard for Definitions of Terms for Antennas, IEEE Standard 145-2013, 2013.
- [9] IEEE Recommended Practice for Near Field Antenna Measurements, IEEE Standard 1720-2012, 2012.
- [10] R. E. Hiatt, E. F. Knott, and T. B. A. Senior, "A study of VHF absorber and anechoic rooms," University of Michigan, Ann Arbor, MI, USA, Report 5391-1-1-F, Feb. 1963.
- [11] Evaluation of Measurement Data – Guide to the Expression of Uncertainty in Measurement, Switzerland, Geneva, JCGM Standard 100:2008, 2008.
- [12] IEEE Standard for Safety Levels with Respect to Human Exposure to Electric, Magnetic and Electromagnetic Fields, 0 Hz to 300 GHz, IEEE Standard C95.1-2019, 2019.
- [13] General Requirements for the Competence of Testing and Calibration Laboratories, ISO/IEC Standard 17025:2017, 2017.

MEETINGS & SYMPOSIA

(continued from page 76)

IEEE RADIO AND WIRELESS WEEK 2024 (RWW 2024)

21–24 January 2024, San Antonio, TX, USA. Elsie Vega, IEEE MCE, 445 Hoes Lane, Piscataway, NJ 08854 USA. +1 732 981 3428, e-mail: elsie.vega@ieee.org. <http://radiowirelessweek.org>

IEEE INTERNATIONAL CONFERENCE ON COMMUNICATIONS (ICC 2024)

9–13 June 2024, Denver, CO, USA. (Papers: 11 October 2023). <http://icc2024.ieee-icc.org>



Trevor S. Bird

The Role of History in Technology Fields

To paraphrase a quotation of American author James Redfield, the history of fields of endeavor such as antennas and propagation is not just the evolution of technology, but it is the evolution of thought. That is why it is important that organizations such as the IEEE and the Antennas and Propagation Society have History Committees and an IEEE Milestone program and that the editor-in-chief of this magazine supports this column.

I have been asked several times why I am interested in the history of our field, and my answer is usually that you do not really know your field unless you delve deeper into how it came about and why we use the techniques we do. Several members of our Society are enthusiastic about the history of electromagnetics, specific antennas, propagation modeling, and application of numerical methods. My hope is that we can encourage a greater interest in the history of particular techniques and why certain potentially powerful methods were not adopted until later. An awareness of history in our field gives a better sense of awareness, of others' work and of workers in our field, its continuity, and the obvious advantage of not repeating mistakes of the past.

One example of this is the moment method. As a numerical technique, it has been around since the 1940s when it was developed by Yamada and reported

I have been asked several times why I am interested in the history of our field, and my answer is usually that you do not really know your field unless you delve deeper into how it came about and why we use the techniques we do.

more widely in the early 1950s [1]. There are various ways of formulating the method in terms of shape functions and order of moments. The first record of the use of moment methods for antennas was by Barzilai in 1955 [2], when he used a variation of the method to solve Hallen's equation for linear antennas. Others followed with variations of the method. Harrington authored a landmark paper in 1967 on matrix methods in field problems [3]. In this paper, Harrington introduced an appropriate

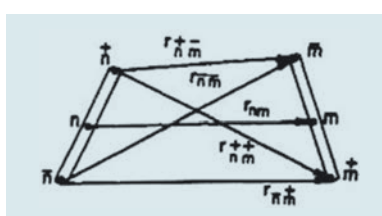


FIGURE 1. Two segments m and n of a wire scatterer in Harrington's moment method formulation described in 1967 [3].

Digital Object Identifier 10.1109/MAP.2023.3280837
Date of current version: 8 August 2023

moment method formulation and gave solutions for a charged conducting plate and radiation from wires of arbitrary shape.

Figure 1 shows two segments n and m of wire scatterers from the paper by Harrington; n^+ and n^- denote the two ends of segment n . The distances from the ends and the midpoints are generally $r_{n^+m^-}$, which is the distance from the top end of segment n and bottom end of m . This was put together in much more detail in his book on moment methods, which appeared in 1968 [4]. This book was cogently written and very influential. I know from experience it caused considerable interest in my first year as a research student in 1971 as I attended a seminar given by a researcher who had visited Harrington and was adopting his methods for arrays. The advantages of Harrington's formulation of the moment method were plain to see, and the computation time was modest. In this instance, it took the development of computers, a suitable formulation of the method, and programs for the computers to achieve the full potential of the method. Since then, the moment method has remained a major tool in the tool kit of many antenna engineers.

Other numerical methods that had been developed in the early part of the 20th century were also adopted about

this time, too. This came about because of the relative ease of computation in the 1970s. As well as moment methods, finite elements, and other subdomain methods, computer packages based on these techniques were developed in the ten to fifteen years following. As an aside, the subdomain methods took a little longer to become commercial as there was the critical problem of achieving a suitable method of discretization, but that is another story. This is an example of a method or approach ahead of its time, and it needed developments in fields outside the original development. The advantage of history is that it shows that sometimes the further development of an idea or concept may need to be looked for in other fields.

Another example of having a grasp of history is to realize stimulation of development may come not from within our field but outside it. There are many instances of this. From my experience, I was part of the transition of reflector antennas and feeds from single to dual

polarization [5]. This requirement came about to double the channel capacity and throughput in both terrestrial microwave links and satellite communications. Another more recent example has been the need for wideband arrays to provide flexibility for next generation communications. The concept of the current sheet introduced by Wheeler [6] has been rediscovered after about 50 years [7] and used in this challenging area along with metamaterials, which also are based on well-known techniques from periodic structures that are well known in other fields [8].

An appreciation of history enables us to better understand the work of others and enables us to comment on proposed advances. The benefit of an improved approach that moves our technology forward will be readily apparent from an appreciation of history for reviews, conference attendance, and purchasing new products. This goes to support another comment on history that it is like having the rear vision mirror

providing input to our advance in a forward direction.

REFERENCES

- [1] H. Yamada, "An approximate method of integration of the laminar boundary-layer equation," *Rep. Res. Inst. Fluid Eng.*, vol. 4, pp. 27–42, 1950. (*Appl. Mech. Rev.*, vol. 5, no. 488).
- [2] G. Barzilai, "On the input construction of thin antennas," *Trans. IRE Prof. Group Antennas Propag.*, vol. 3, no. 1, pp. 29–32, Jan. 1955, doi: 10.1109/TPGAP.1955.5720408.
- [3] R. F. Harrington, "Matrix methods for field problems," *Proc. IEEE*, vol. 55, no. 2, pp. 136–149, Feb. 1967, doi: 10.1109/PROC.1967.5433.
- [4] R. F. Harrington, *Field Computation by Moment Methods*. New York, NY, USA: Macmillan, 1968.
- [5] T. S. Bird, *Fundamentals of Aperture Antennas and Arrays: From Theory to Design, Fabrication and Testing*. Chichester, U.K.: Wiley, 2016.
- [6] H. A. Wheeler, "Simple relations derived for a phased-array antenna made of an infinite current sheet," *IEEE Trans. Antennas Propag.*, vol. 13, no. 4, pp. 506–514, Jul. 1965, doi: 10.1109/TAP.1965.1138456.
- [7] I. Tzanidis, J. P. Doane, K. Sertel, and J. L. Volakis, "Wheeler's current sheet concept and Munk's wideband array," in *Proc. IEEE Symp. Antennas Propag.*, Chicago IL, USA, Jul. 2012, pp. 1–2, doi: 10.1109/APS.2012.6349119.
- [8] C. Kittel, *Introduction to Solid State Physics*, 3rd ed. New York, NY, USA: Wiley, ch. 9, 1968.



COURSES

(continued from page 78)

FAR-FIELD, ANECHOIC CHAMBER, COMPACT AND NEAR-FIELD ANTENNA MEASUREMENT TECHNIQUES

30 October–3 November 2023, Atlanta, GA, USA.

BASIC RF ELECTROMAGNETIC WARFARE CONCEPTS

31 October–2 November 2023, Atlanta, GA, USA. Georgia Institute of Technology, Professional Education, P.O. Box 93686, Atlanta, GA 30377-0686 USA. +1 404 385-3500, fax: +1 404 894-8925. <http://www.pe.gatech.edu>.

RADAR WAVEFORMS: PROPERTIES, ANALYSIS, DESIGN, AND APPLICATION

7–9 November 2023, Atlanta, GA, USA.

MODERN ELECTRONIC AND DIGITAL SCANNED ARRAY ANTENNAS

13–17 November 2023, Lake Buena Vista, FL, USA.

SIGNALS INTELLIGENCE (SIGINT) FUNDAMENTALS

14–15 November 2023, Lake Buena Vista, FL, USA.

BASIC RADAR CONCEPTS

14–16 November 2023, Lake Buena Vista, FL, USA.

TEST AND EVALUATION OF RF SYSTEMS

14–16 November 2023, Lake Buena Vista, FL, USA. Georgia Institute of Technology, Professional Education, P.O. Box 93686, Atlanta, GA 30377-0686 USA. +1 404 385-3500, fax: +1 404 894-8925. <http://www.pe.gatech.edu>.

EMI/EMC IN MILITARY SYSTEMS

14–16 November 2023. ONLINE. Applied Technology Institute, 349 Berkshire Drive, Riva, MD 21140-1433, USA. +1 410 956-8805 or +1 888 501-2100, fax: +1 410 956-5785, e-mail: ati@ATIcourses.com. <http://www.ATIcourses.com>.

TEST AND EVALUATION OF RF SYSTEMS

5–7 December 2023, ONLINE. Georgia Institute of Technology, Professional Education, P.O. Box 93686, Atlanta, GA 30377-0686, USA. +1 404 385-3500, fax: +1 404 894-8925. <http://www.pe.gatech.edu>.



Call for IEEE AP-S Young Professional Ambassador Nominations

Nomination Deadline: October 30, 2023

The objective of this program is to inspire and inform AP-S Young Professionals on a variety of topics both technical and non-technical to enhance their interest and engagement in the field of Antennas and Propagation by delivering the talks at various chapters/sections "on-demand" virtually.

Self-nominations are encouraged, and decisions will normally be made before the end of the year to start term from January following year. All new Ambassadors are required to give at least two lectures during the tenure of one year. The call for candidates will open once a year and Ambassadors are selected for a term of 1 year, with possible extension to a second year. Young Professional Ambassadors are eligible for the IEEE Antennas and Propagation Society Young Professional of the Year Award.

Eligibility:

- Be an IEEE AP-S Member
- Belong to IEEE YP Group as defined by IEEE (IEEE members and volunteers who have graduated from their first professional degree within the past 15 years - <https://yp.ieee.org/>).
- 5 years or more experience reflecting professional maturity.

Nomination Package:

The nomination package should include the following four files. Please note that all four files are mandatory and any additional material, including those beyond the length limit, will not be considered. The entire nomination package should be sent by e-mail (single PDF document with video link) to the Chair of the Committee, with the E-mail Subject of "AP-S Young Professional Ambassador Nomination 2023", by the deadline in order to consider for the one-year term beginning in the following year. The mandatory video clip may be submitted by other means such as YouTube/OneDrive/Googledrive/Dropbox if necessary.

- Resume (2 pages maximum)
- Title (s) / Brief Abstract (s) of the talks (s) (max 2 talks) and a 500-word bio with picture
- A brief writeup (1000 words max) on benefits of the talk (s) proposed to the AP-S YP Community
- A 5 min short video sample of any proposed talk

Selection Criteria:

Candidates will be judged by a Selection Panel on their qualifications and suitability, according to the following selection criteria:

- Presentation skills (35%)
- A growing trajectory of accomplishment in the field of Antennas and Propagation (35%)
- Quality and relevance of proposed lectures to YP (30%)

Nomination Deadline: October 30, 2023

Submit your questions about this program and your nominations to:

Qammer H. Abbasi, *SMIEEE, FRSA, FRET, FRAE (Industry), FEAI*
Chair, IEEE AP-S Young Professional Ambassador Program Sub-Committee
University of Glasgow, UK
Qammer.abbasi@glasgow.ac.uk

Up Close and Personal

Konstantina S. Nikita  and Zoya Popović 

This is the second of three articles in which we give the stage to some outstanding women in our field. So, we asked our colleagues questions that are gender independent, hoping everyone can learn something useful from their answers, or at least be entertained. Here is what we wanted to learn:

Digital Object Identifier 10.1109/MAP2023.3282235
Date of current version: 8 August 2023

EDITOR'S NOTE

The August issue contribution to the "Women in Engineering" column is the second article in a series of three, featuring selected interviews of women in the antennas and propagation field, asking them to answer five gender-independent questions on their role models, mentors, accomplishments, and wishes for the future generation of engineers. This contribution was prepared by Prof. Konstantina S. Nikita, National Technical University of Athens, Greece, and Prof. Zoya Popović, University of Colorado, Boulder, CO USA.



Francesca Vipiana 

Prof. Rodica Ramer, UNSW, Australia

Role Model: As a student, I greatly admired my quantum mechanics professor, S. Titeica, Nobel laureate Heisenberg's PhD student. As a microwave researcher, Roberto Sorrentino became my role model; he reminded me that "electromagnetics is universal" wherever I work, which inspired me to accept the first female academic position in the School of Electrical Engineering at UNSW Sydney. I am now the only female professor of microwave engineering and antennas in Australia.

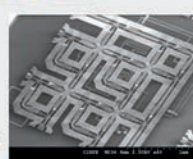
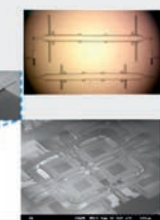


What I would like: During my career, I would like to continue witnessing the success and advancement of my students in the workforce. I am proud to see them as fully-fledged microwave engineers working at Nokia, Ericsson, Amazon, BIT, Huawei, Samsung, NUST, CUS, etc.

Words of wisdom: Always tap and replenish your energy from your IEEE society. You will discover the best, most remarkable professionals, and find friends for the rest of your life.



Mentor: Prof. Raafat Mansour encouraged me to take on RF MEMS research. We learned RF MEMS fabrication at the Centre for Integrated Radio Frequency Engineering (CIRFE) and our MMM laboratory became the centre of RF MEMS devices in Australia.



Biggest Accomplishment: All my microwave device designs (circulators, filters, switches, resonators, phase shifters, antennas), created with different materials (ferrimagnetics, ferroelectrics, HTS) in various technologies (waveguide, coax, microstrip, RF MEMS, LTCC, SIW, inkjet printing, additive manufacturing).

FIGURE 1. Rodica Ramer received her B.E., M.E., and Ph.D. degrees in solid-state physics. She has been with the School of Electrical Engineering and Telecommunications at the University of New South Wales Sydney, Australia, where she is currently a full professor and the head of the research discipline. Her research areas include microwave and millimeter-wave circuits, antennas, and materials technologies for wireless and communications applications.

- Who was/is your role model and why?
- Who was your mentor or someone who made a big impact on your career?
- What do you think is your biggest accomplishment, and what do others think is your biggest accomplishment?
- What would you like to see happen in our profession during your career?
- A word of wisdom for young engineers (women and men).

We hope you will find their answers as inspiring and entertaining as we have! It is such a privilege to have these amazing people as our colleagues and professional friends.

In our three articles, we tried to cover different continents, countries,

Dr. Małgorzata Celuch, QuickWave, Poland

Role Model: My father, a survivor of Soviet deportation during WWII, who completed high school in post-war Poland after only attending primary school in a Siberian hamlet for 3 years. He earned an MSc in Engineering and a PhD in economics and worked for Polish foreign trade, providing me with my first international exposure. And he always had time for me.




Words of wisdom: Max Ehrmann's poem "Desiderata" has become my wisdom, my hope, my reconciliation in all the joys and hardships of life, private and professional alike. "Enjoy your achievements as well as your plans. Keep interested in your own career, however humble; it is a real possession in the changing fortunes of time (...) Be cheerful. Strive to be happy" (Ehrmann)

BIGGEST ACCOMPLISHMENT: Blazing new trails while still maintaining personal relationships and pursuing my passions (dress design, theatre, swimming, and skiing). It's rewarding to have the love and support of my family, including my husband, son, daughter-in-law, and grandchildren.




WHAT OTHERS THINK: When I hear words of appreciation from others, it is usually for implementing research results of my team and me, in the form of commercial products successfully competing on the international arena with those of large corporations.





WHAT I WOULD LIKE: I would like developments in our profession to... slow down and leave space for human and social developments to catch up.

FIGURE 2. Małgorzata Celuch received her Ph.D. (honors) degrees from the Warsaw University of Technology, Poland, in 1996. She coauthored QuickWave software and is cofounder and vice president of QWED and an assistant professor at the Warsaw University of Technology. She has authored more than 150 publications, including 20 journal articles and three book chapters. Her main fields of research are electromagnetic modeling of microwave circuits and numerical methods for computational electromagnetics. The QWED team was the recipient of many prestigious awards, including the European Information Technology Prize.

Role Model: I am inspired by people with deep technical expertise who have contributed to the development of others.

Mentor: None really 😊

What I would like: A lot more women engineers solving challenging technical problems.

BIGGEST ACCOMPLISHMENTS: Two pieces of work:

1. development of a microwave sensor system for multiphase flow metering for oil wells to determine oil, water, and gas fractions
2. design of several customized eddy current sensors for reliable defect detection that help qualify expensive components of power turbines and aviation engines, which otherwise would have been scrapped.

Words of wisdom: Continuous learning, a mindset to delve deep while having a broader perspective along with patience and persistence to solve problems helps build credibility.

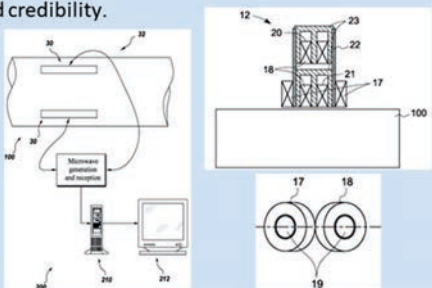


FIGURE 3. Aparna Sheila-Vadde received her undergraduate degree from the College of Engineering at Trivandrum in Kerala, India, and her Ph.D. degree from Carnegie Mellon University. She is a senior engineer at General Electric (GE) in Bangalore, India, where she is in charge of the development of electromagnetic sensor systems for inspection and monitoring.

Prof. Francesca Vipiana, Polytechnic, Torino

Role Model: My role model is the incomparable Marie Skłodowska-Curie for everything she did in her incredible life and, in particular, for her capability to be accepted and well respected in the scientific community that was very closed to women.



Mentor: My mentor is Prof. Donald Wilton from the University of Houston, Texas, US. I remember the first time in 2008 when I visited him in Houston: Don and Joanne, his wife, welcomed me and I felt immediately as at home.



Bigest Accomplishment: My main accomplishment was receiving the 2017 IEEE-APS Lot Shafai Mid-Career Distinguished Achievement Award for my contributions to computational electromagnetics, and in particular to the analysis of multi-scale problems.

What I would like: As part of the academia, I would like to see more opportunities for brilliant researchers that would like to become professors and transfer their passion in the research to the young generations.

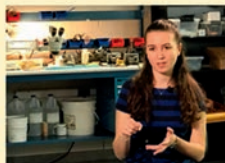
Words of wisdom: My message to young engineers is to choose a work and topic that they really enjoy, without taking care about the initial salary or contract kind: if we can work in something that we really like great results will arrive.

FIGURE 4. Francesca Vipiana received her Laurea and Ph.D. degrees in electronic engineering from POLITO, Italy. She serves as a full professor of electromagnetic fields in the Department of Electronics and Telecommunications of POLITO, Italy. Her focus research areas include computational electromagnetics, antennas, and microwave sensing and imaging.

Prof. Asimina Kiourti, OSU, USA

Role Model: my very first role model in my adolescent years was my English as a foreign language teacher, a meticulous hard-working woman who was highly successful in combining career and family.

Bigest Accomplishment: I think my biggest accomplishment dates back to 2020 when my group's wearable kinematics sensing work won the NSF CAREER grant (which I prepared throughout my pregnancy and finalized within a month after delivery).



Mentors: Both my PhD advisor (Konstantina Nikita, Professor at the National Technical University of Athens) and my post-doc mentor (John Volakis, Dean and Professor at Florida International University) have had and continue to have a tremendous impact on my career, inspiring me to set high standards, seek quality, and collaborate in a way that sees the best in people.

Words of wisdom: Do your best in anything you commit to, no matter how small or insignificant a certain task may be; if you are not willing to put your heart and your soul in a given task, then it's better to decline it at first place.



What others think: Others often consider my biggest accomplishment to be my ~20-student group and their productivity in terms of both research and outreach to the general public.



What I would like: I would like to see more inter- and cross-disciplinary work that takes people out of silos to jointly achieve something bigger than the sum of their individual contributions.

FIGURE 5. Asimina Kiourti received her Ph.D. degree in electrical and computer engineering from the National Technical University of Athens, Greece, and her M.Sc. degree from University College London, U.K. She is an Innovation Scholar Endowed Associate Professor of electrical and computer engineering at The Ohio State University, Columbus, OH, USA. Her research interests lie in bioelectromagnetics, wearable and implantable antennas, sensors for body area applications, and flexible e-textiles.

(continued on page 127)

Resonating Journeys

Exploring personal and professional growth in IEEE conferences on antennas and propagation for young professionals

Miguel Ferrando-Rocher 

This article explores the personal journey and professional growth experienced by a young professional in the field of antennas and propagation through participation in IEEE conferences. It discusses the transformative impact of engaging with IEEE resources, such as the IEEE Xplore Digital Library, the IEEE Young Professionals Program, and the IEEE Antennas and Propagation Society (AP-S) Symposium series. I share personal reflections on the invaluable networking opportunities and knowledge gained, highlighting the profound influence of IEEE conferences on my career development and personal growth.

INTRODUCTION

Challenges as a young professional in the field of antennas and propagation have always been present in my journey to advance my scientific career. However, like many of my peers, I have faced numerous obstacles. From a lack of available resources to limited networking opportunities, navigating the complex landscape of scientific career advancement has been daunting. Fortunately,

EDITOR'S NOTE

In this issue, Dr. Miguel Ferrando-Rocher has contributed an interesting article, "Resonating Journeys: Exploring Personal and Professional Growth in IEEE Conferences on Antennas and Propagation for Young Professionals." Dr. Ferrando-Rocher is also one of the 2022 IEEE Antennas and Propagation Society Young Professional Ambassadors. This article explores the personal journey and professional growth experienced by Dr. Ferrando-Rocher as a young professional in the field of antennas and propagation through participation in IEEE conferences. Young professionals can learn from the article the importance of attending conferences to gain invaluable opportunities for learning, collaboration, and building a strong professional network to aid their career growth in the field of antennas and propagation.

We have many exciting articles planned for this column in future issues. Anyone who would like to contribute to the "Young Professionals" column or has any suggestions on the topics of interest, please contact me at cjreddy@ieee.org. Follow us on LinkedIn at <https://www.linkedin.com/company/ieee-aps-yp> for the latest updates and events that are of interest to AP-S Young Professionals.



CJ Reddy

IEEE conferences have emerged as a vital resource for young AP-S professionals to gain knowledge, make connections, and explore new opportunities. In this article, I explore the profound impact of IEEE resources and opportunities on the personal and professional growth of young professionals in the field of antennas.

In the "Personal Impact of IEEE Resources and Opportunities" section, the article explores the personal impact

of IEEE resources and opportunities. It discusses how access to the IEEE Xplore Digital Library, participation in the IEEE Young Professionals Program, engagement with the AP-S Symposium series, and involvement with IEEE Student Branches play a significant role in the personal and professional growth of young professionals. The section "The Importance of IEEE Conferences in the Scientific Career of Young Professionals" focuses on the

importance of IEEE conferences in shaping the scientific career paths of emerging researchers. It discusses the valuable learning experiences, networking opportunities, professional development resources, and recognition programs offered by these conferences.

The “A Real Experience, My First IEEE AP-S Conference” is dedicated to sharing a personal account of my transformative experience at my first IEEE AP-S conference. I recount the invaluable connections forged, collaborative projects initiated, and lasting impact on my professional growth resulting from attending IEEE conferences. The vibrant interactions and encounters with esteemed researchers have left an indelible mark on my journey. In the final section, the power of diverse perspectives in fostering innovation is examined. Drawing upon various backgrounds, the unexpected connection between engineering and the performing arts is elucidated. By embracing this fusion of disciplines, new realms of creativity, problem solving, and effective communication can be unlocked, pushing the boundaries of antenna research to new horizons.

In conclusion, this article sheds light on the transformative influence of IEEE resources and opportunities

on the journeys of young professionals in the field of antennas. It emphasizes the role of IEEE conferences as valuable platforms for knowledge exchange, highlights the personal experiences that shape individual growth, and underscores the power of diverse perspectives in driving innovation. By sharing these insights, the aim is to inspire and empower the next generation of antenna researchers to achieve remarkable success and make a significant impact in this dynamic field.

PERSONAL IMPACT OF IEEE RESOURCES AND OPPORTUNITIES

As a young professional, I have been fortunate to have access to the resources and opportunities IEEE offers. These resources have played a significant role in my personal and professional growth, beyond just the technical knowledge gained. The IEEE Xplore Digital Library [1] has allowed me to stay up to date with my field's latest research and developments. Still, it has also given me the confidence to participate in technical discussions with my colleagues and peers. The AP-S Young Professional Ambassador Program [2] has provided me with networking opportunities and career development resources

and helped me build a sense of community and belonging within the larger IEEE organization. The AP-S Symposium series [3] has allowed me to present my research, learn from other professionals in the field, experience different cultures, and build friendships with people from around the world. Finally, the IEEE Student Branches have allowed me to participate in IEEE activities, helped me develop my leadership skills, and built my confidence in my abilities.

Overall, the resources and opportunities offered by IEEE have significantly impacted my personal and professional growth beyond just the technical knowledge gained. They have given me the confidence to participate in technical discussions, a sense of community and belonging, exposure to different cultures, and the opportunity to develop my leadership skills.

THE IMPORTANCE OF IEEE CONFERENCES IN THE SCIENTIFIC CAREERS OF YOUNG PROFESSIONALS

I can confidently say that IEEE conferences have been a game changer for my career. These conferences have provided me with a platform to interact with fellow researchers, industry experts, and thought leaders in my field, which has been instrumental in broadening my knowledge and understanding of current research and trends.

Attending IEEE conferences provides a multitude of benefits in the field of antennas and propagation. The technical sessions encompass various topics, including antennas, propagation, electromagnetism, and microwave technology. These sessions have provided valuable insights and inspiration for my work. In addition to technical sessions, IEEE conferences offer a range of professional development opportunities, such as workshops on grant writing, career development, and entrepreneurship. These opportunities have equipped me with essential skills and knowledge to succeed in my professional journey.

As an illustrative example, in 2016, we had the honor of visiting the iconic Arecibo Observatory (Figure 1) in



FIGURE 1. The Arecibo Observatory during a visit organized by the AP-S/URSI 2016 Conference held in Fajardo, Puerto Rico.

Puerto Rico as part of the AP-S/URSI 2016 Conference. It was an unforgettable experience where we had the opportunity to witness firsthand the impressive radiotelescope and its remarkable contributions to science. Despite its closure in 2020, we cherish the special memories of our visit to this prominent scientific facility. In addition, our time in Puerto Rico was further enriched by a truly special event. We had the pleasure of attending a Young Professionals barbecue on the picturesque island of Palomino. This gathering provided a unique opportunity to network and connect with fellow professionals in a relaxed and beautiful setting (Figures 2 and 3). I also fondly remember the “Young Professionals Afloat—A Sail Through Boston Harbor Aboard the *Spirit of Boston*” event. It was a delightful experience sailing through the scenic Boston Harbor with both young and young-at-heart professionals (Figure 4).

In conclusion, I believe that IEEE conferences are an essential tool for developing young professionals in the field of the AP-S. These conferences provide opportunities for learning, networking, and professional development. They are an excellent way for young professionals like me to advance our careers in antennas and propagation.

A REAL EXPERIENCE: MY FIRST AP-S CONFERENCE

Now, I think we should shift our focus to the personal aspects essential to this contribution. I’d like to share some personal experiences that have shaped my journey in this field.

Less than a decade ago, my venture into the world of IEEE conferences began with the memorable experience of attending the IEEE International Symposium on Antennas and Propagation and USNC-URSI Radio Science Meeting in the captivating city of Vancouver, Canada (Figure 5). Year after year, I eagerly anticipate the arrival of this esteemed conference. Despite being part of a small group of Spanish attendees, we always come together for a special dinner known as *ESCORIA* (*Spanish Committee for Research in Antennas*). The name itself carries a clever

double meaning, as “escoria” in Spanish typically denotes negativity, but, for us, it symbolizes the bond of camaraderie and collaborative spirit that unites us.

During these dinners, I had the opportunity to meet professors and students from other universities. Those informal encounters became the starting point for numerous joint research projects, academic exchanges, collaborative work, and reciprocal visits. The connections we forged during those dinners became lasting bonds that transcended academic and

geographical boundaries. Curiously, the *ESCORIA* dinner became a symbol of our unity over the years, and more and more people joined, expanding the network of contacts and collaboration opportunities. However, the conference was not confined to the national realm alone. I was fortunate enough to cross paths with renowned experts in antenna and propagation research whose books I had read and admired. I engaged in conversations with them, shared ideas, and even took advantage of the casual atmosphere during coffee



FIGURE 2. The Young Professionals barbecue on Palomino Island, organized by the AP-S/URSI 2016 Conference.



FIGURE 3. The postdinner celebration at the Young Professionals barbecue during the AP-S/URSI 2016 Conference.

breaks and the gala dinner to have a drink together.

These conversations and informal meetings with prominent figures in the field of antennas and propagation research inspired and motivated me to further explore and deepen my studies in this area. Their knowledge and expertise were invaluable, and the privilege of interacting with them closely was genuinely remarkable. For example, I vividly recall the moment I was introduced to the late Prof. Kildal [4], [5], an

inspirational leader who unknowingly played a significant role in shaping my research career. Looking back, I can confidently state that those dinners and informal encounters during the conference were pivotal catalysts for developing numerous research projects and my professional growth. The significance of networking transcended national boundaries, and I felt fortunate to establish connections with colleagues from different countries, cultures, and academic traditions. The conference was not

merely a platform for presenting results and knowledge but also a conducive environment for exchanging experiences and fostering human connections.

In summary, the IEEE International Symposium on Antennas and Propagation and USNC-URSI Radio Science Meeting as well as the ESCORIA dinner became annual events where collaboration and networking thrived. This conference was not only a space for showcasing research and knowledge but also a nurturing ground for sharing experiences and creating meaningful connections.

EMBRACING PERSONAL PASSIONS: UNLEASHING THE POWER OF DIVERSE PERSPECTIVES

In the realm of telecommunications, technical expertise and knowledge often take center stage. However, there exists a hidden power within each individual, stemming from their personal passions and interests. In this last section, most personal of all, I invite you to explore a different perspective, one that transcends technicality and embraces the enrichment that diverse passions can bring to our professional lives.

UNVEILING THE UNEXPECTED: BALANCING ENGINEERING AND THE PERFORMING ARTS

As a telecommunications engineer with a deep-rooted passion for the performing arts, I embarked on a unique journey that intertwined my two seemingly disparate worlds. Throughout the course of my doctoral studies, I secretly pursued a degree in theatre, directing, and playwriting from the prestigious Spanish School of Dramatic Arts. This duality remained unknown to many of my colleagues, and, for a long time, I felt a sense of unease about blending these seemingly contradictory passions.

However, in retrospect, I have come to appreciate the invaluable lessons that emerged from embracing both sides of my identity. It is through this personal experience that I wish to share a valuable insight: our individual passions, no matter how diverse they may seem, have the potential to enhance our professional growth.



FIGURE 4. The AP-S/URSI 2018 Conference in Boston with colleagues from the Antennas and Propagation Lab.



FIGURE 5. Whistler, British Columbia, during the AP-S/URSI 2015 Conference in Vancouver.

BREAKING BARRIERS: THE POWER OF INTERDISCIPLINARY PERSPECTIVES

In a field often dominated by technical prowess, the incorporation of interdisciplinary perspectives can yield remarkable results. Although the arts and engineering might appear to be worlds apart, they share underlying principles of creativity, problem solving, and effective communication.

My theatrical endeavors taught me the arts of storytelling, harnessing emotions, and understanding human behavior—skills that have proven invaluable in my engineering career. Conversely, my technical expertise provided a structured approach, analytical thinking, and attention to detail that greatly enriched my abilities as a theater director.

Embracing our multifaceted nature fosters innovation and opens doors to new possibilities. By transcending the boundaries of a singular discipline, we tap into a vast reserve of knowledge and creativity that can revolutionize our work.

CULTIVATING A SUPPORTIVE COMMUNITY: INSPIRING GROWTH THROUGH COLLABORATION

One significant takeaway from my personal journey is the importance of building a supportive community. Often, we fear judgment or assume that our personal passions will not be understood or appreciated in professional circles. However, it is precisely these personal facets that can strengthen our professional contributions. By sharing our diverse interests and experiences openly, we create an environment conducive to collaboration and growth. Engaging in conferences, networking, and presenting our work becomes an opportunity to inspire others and learn from their unique perspectives. Together, we can challenge the status quo and foster a culture of open-mindedness, allowing our individual strengths to shine and benefiting the entire community.

CONCLUSIONS

In conclusion, I humbly acknowledge the significant impact that IEEE

conferences have had on my personal and professional growth as a young professional in the field of antennas and propagation. Through the exploration of key aspects in this article, such as the importance of networking, the accessibility of resources, and the transformative experiences I have shared, it becomes evident that IEEE conferences have played a pivotal role in shaping my journey. These conferences have provided invaluable opportunities for learning, collaboration, and building a strong professional network. I am grateful for the diverse perspectives and interdisciplinary intersections within the inclusive IEEE community, which have contributed to my holistic growth and transformative path. I hope that, by sharing my experiences, aspiring researchers can also find inspiration in the abundant resources and opportunities offered by IEEE, leading them to discover their own paths of personal and professional evolution.

AUTHOR INFORMATION

Miguel Ferrando-Rocher (miguel.ferrando@upv.es) is an assistant professor in the Department of Communications, Universitat Politècnica de València, 46010 Valencia, Spain. He is a Member of IEEE.

REFERENCES

- [1] M. Wilde, "IEEE Xplore digital library," *Charleston Advisor*, vol. 17, no. 4, pp. 24–30, Apr. 2016, doi: 10.5260/chara.17.4.24.
- [2] Q. H. Abbasi, "AP-S young professional ambassador program [Young Professionals]," *IEEE Antennas Propag. Mag.*, vol. 64, no. 2, pp. 79–105, Apr. 2022, doi: 10.1109/MAP.2022.3145720.
- [3] S. A. Long, "A brief history of the international symposium on antennas and propagation," in *Proc. IEEE Antennas Propag. Soc. Int. Symp. (APSURSI)*, 2014, pp. 522–523, doi: 10.1109/APS.2014.6904592.
- [4] A. Svensson et al., "In memoriam: Per-Simon Kildal," *Radio Sci. Bull.*, vol. 2016, no. 357, pp. 45–46, Jun. 2016.
- [5] A. Valero-Nogueira and E. Alfonso, "How gap waveguides were conceived," in *Proc. 11th Eur. Conf. Antennas Propag. (EUCAP)*, 2017, pp. 242–246, doi: 10.23919/EuCAP.2017.7928260.



TAP. CONNECT. NETWORK. SHARE.

Download on the App Store | GET IT ON Google Play

IEEE Advancing Technology for Humanity

Connect to IEEE—no matter where you are—with the IEEE App.

- Stay up-to-date with the latest news
- Schedule, manage, or join meetups virtually
- Get geo and interest-based recommendations
- Read and download your IEEE magazines
- Create a personalized experience
- Locate IEEE members by location, interests, and affiliations

Download Today!



2023 IEEE Awards

IEEE-Level Awards

2023 IEEE Richard M. Emberson Award

Ross Stone (*posthumously*)

For distinguished service advancing the technical objectives of the IEEE, with the following citation: "For sustained contributions to and impactful leadership in the IEEE Technical Activities publication enterprise"

IEEE APS Field Awards

2023 Distinguished Achievement Award

Andrea Alù, *City University of New York*

For pioneering contributions to metamaterial technologies and extreme electromagnetic wave phenomena

2023 Chen-To Tai Distinguished Educator Award

Christos Christodoulou, *University of New Mexico*

In recognition of being an outstanding educator and a passionate mentor to both undergraduate and graduate students

Filiberto Bilitotti, *ROMA TRE University*

For being an inspiring educator, mentor, and contributor to the development of electromagnetic metamaterials, metasurfaces, and their applications

2023 John Kraus Antenna Award

Douglas Henry Werner, *The Pennsylvania State University*

For innovative contributions to antenna theory and design including the application of transformation electromagnetics, metamaterials and global optimization techniques

2023 Lot Shafai Mid-Career Distinguished Achievement Award

Asimina Kiourtzi, *The Ohio State University*

For her contributions to body area electromagnetics and her outreach efforts towards boosting women's proclivity to pursue careers in engineering

2023 Harrington-Mitra Award in Computational Electromagnetics

Atef Z. Elsherbini, *Colorado School of Mines*

For contributions to computational electromagnetics with hardware acceleration techniques

2023 Donald G. Dudley Jr. Undergraduate Teaching Award

Hugo G. Espinosa, *Griffith University*

In recognition of his innovations in teaching and curriculum development, successfully equipping emerging generations of engineers with the skills needed to address important sustainability challenges

IEEE Industry Awards

2023 Distinguished Industry Leader Award

Dr. Ing. habil Ulrich L. Rohde, *University of the Armed Forces Federal University, INF3 Institute for Technical Informatics*

For the scientific contribution and leaderships to the field of Antennas and related Communication Systems, leading to development of state-of-the-art Antennas products for industrial, military and aerospace applications

2023 Industrial Innovation Award

Lars J. Foged, *Microwave Vision Group*

For demonstrating visionary leadership in advancing the use of multi-probe technology for antenna measurements, standardization efforts, and pioneering innovation in antenna measurement and post-processing techniques

IEEE APS Awards for papers published in 2022

2022 Sergei A. Schelkunoff Transactions Prize Paper Award

Charles A. Guo and Y. Jay Guo. "A general approach for synthesizing multibeam antenna arrays employing generalized joined coupler matrix." *IEEE Transactions on Antennas and Propagation* 70, no. 9 (2022): 7556-7564.

2022 R. W. P. King Paper Award

Carl Pfeiffer and Jeffrey Massman. "An UWB hemispherical Vivaldi array." *IEEE Transactions on Antennas and Propagation* 70, no. 10 (2022): 9214-9224

2022 Harold A. Wheeler Applications Prize Paper Award

Ilias I. Giannakopoulos, Georgy D. Guryev, José EC Serrallés, Ioannis P. Georgakis, Luca Daniel, Jacob K. White, and Riccardo Lattanzi. "Compression of volume-surface integral equation matrices via Tucker decomposition for magnetic resonance applications." *IEEE transactions on antennas and propagation* 70, no. 1 (2021): 459-471.

2022 Piergiorgio L. E. Uslenghi Letters Prize Paper Award

Lukas Piotrowsky, Jan Barowski, and Nils Pohl. "Near-field effects on micrometer accurate ranging with ultra-wideband mmwave radar." *IEEE Antennas and Wireless Propagation Letters* 21, no. 5 (2022): 938-942.

2022 Edward E. Altshuler AP-S Magazine Prize Paper Award

Miloslav Capek and Kurt Schab. "Computational aspects of characteristic mode decomposition: An overview." *IEEE Antennas and Propagation Magazine* 64, no. 2 (2022): 23-31.

IEEE APS Donor Recognition

A selection of IEEE Antennas and Propagation Society's (APS) world class awards portfolio that recognize excellence in contributions to physics research, service, and teaching are funded through the generosity of donors to the IEEE Foundation. Thanks to these donors, APS has the resources to energize innovation by celebrating technological excellence.

APS Awards supported by giving to the IEEE Foundation include:

IEEE APS Eugene F Knott Memorial Pre-doctoral Research Award

Through the generous support of Terri L. Craig

IEEE Ulrich L. Rohde Technical Field Project Award

Through the generous support of Dr. Ulrich L. Rohde

IEEE APS CJ Reddy Travel Grant for Graduate Students

Through the generous support of Dr. C. J. Reddy

Raj Mittra Travel Grant

Through the generous support of Dr. Raj Mittra

IEEE John Kraus Antenna Award

Through the generous support of Dr. John D. Kraus, Jr.

IEEE Antennas and Propagation Society Edward E. Altshuler Prize Paper Award

Through the generous support of Edward E. Altshuler

IEEE Lot Shafai Mid-Career Distinguished Achievement Award

Through the generous support of Lotfollah Shafai

IEEE Harrington-Mitra Award

Through the generous support of Roger F. Harrington & Dr. Raj Mittra

IEEE Ulrich L. Rohde Innovative Conference Paper Awards on Computational Techniques in Electromagnetics

Through the generous support of Dr. Ulrich L. Rohde

IEEE Ulrich L. Rohde Innovative Conference Paper Awards on Antenna Measurements and Applications

Through the generous support of Dr. Ulrich L. Rohde

Chen-To Tai Distinguished Educator Award

Through the generous support of the Family and Friends of Professor Chen-To Tai

The IEEE Foundation is a leader in transforming lives through the power of technology and education. The IEEE Foundation is committed to transparency and impact, receiving 100/100 points on Charity Navigator and a Gold rating on Guidestar, so you can feel confident that your investment is making an impact.

If you're interested in making or learning more about a philanthropic gift to IEEE, please reach out to the IEEE Foundation team at donate@ieee.org. Learn more about the IEEE Foundation at www.ieefoundation.org

10 Questions . . .

This article features an interview with Dr Yihong Qi, president and chief scientist of General Test Systems, Inc., Shenzhen, China, about his perspectives and experiences.

Rod Waterhouse: Over your career, you have worked at many exciting companies in many roles. Describe for us the first job you undertook as an antenna engineer. Were there any important lessons you can share with us that you learned in that role that are still relevant to your work now?

Yihong Qi: During my 15 and a half years as an engineer at Research In Motion (now BlackBerry), I had the privilege of witnessing the company's remarkable growth from a small team of around 20 individuals to a workforce of approximately 18,000 employees by 2010. Throughout my tenure, I faced various intriguing technical challenges, one of which centered around designing multiband smartphone antennas.

Before 2005, cell phones and early smartphones followed an inverted patch concept, with the antenna positioned on the back of the device. However, as smartphones began to widen, a new issue emerged: the wider the phone, the higher the antenna's quality factor (Q), resulting in a narrower potential bandwidth. This presented a problem as the emerging trend in

EDITOR'S NOTE

In this edition of the column, I "sat down" with Dr. Yihong Qi, president and chief scientist of General Test Systems, Inc., Shenzhen, China. Yihong Qi has founded several antenna technology companies throughout the world and has made significant contributions to the realization of the present day smartphone. Dr. Qi is an IEEE Fellow, a Distinguished Lecturer of the IEEE Antenna and Propagation Society (AP-S), and is also the Distinguished Industry Speaker at the 2023 IEEE AP-S Flagship conference in Portland, Oregon, USA. I hope you find the following an interesting and informative read.



Rod Waterhouse

smartphones was to support quad- or pentaband functionality.

To address this challenge, I designed a pentaband "printed inverted F antenna" that omitted a ground plane on the inverted F section of the antenna. This design innovation allowed for improved bandwidth characteristics, making it suitable for smartphones with wider physical dimensions.

Prior to 2005, cell phone antennas were typically located on the top of the device for wireless communication. However, without a ground plane, the multiband antenna encountered different boundary conditions when the phone was in various talking modes, such as against the ear, using earphones, or in speakerphone mode. These conditions could lead to detuning of the antenna and, more importantly, noncompliance with regulatory requirements for specific absorbing rate (SAR) and hearing aid compatibility (HAC).

To mitigate these concerns, positioning the multiband antenna on the opposite side of the earpiece receiver proved to be a practical solution, resolving detuning, SAR, and HAC issues.

This new antenna positioning arrangement brought forth additional challenges. First, wireless carriers' white papers or "standards" stipulated that the antenna should be positioned on the top of the phone. Second, this change would impact the overall design of the smartphone, including considerations related to electromagnetic (EM) compatibility. Overcoming these challenges necessitated collaboration with the management team and carriers to establish a new antenna arrangement "standard" and involved assisting RF [radio frequency] and mechanical engineering teams in the overall redesign of the phone. Antenna engineering is not a solitary task; effective communication and hands-on work from an RF and

system perspective are vital to making inventions applicable.

My experience with this invention taught me that solving antenna design challenges is just one aspect; equally important is to establish new standards and supporting other teams for overall system design. Antenna engineering is a multidisciplinary effort that requires effective communication and a comprehensive understanding of RF and system considerations to successfully implement innovations. It brings me great pride to witness the widespread utilization of this engineering design in the majority of smartphones. What truly uplifts my spirit is knowing that this design effectively mitigates the risk associated with RF radiation and aids individuals dependent on hearing aids. The ultimate measure of a superior product lies in its ability to positively impact people's lives.

Waterhouse: A classic term often used in the startup world is having "an exit strategy" (note, not my favorite term!). You have been involved with several companies; did you have one for each, or was it more another opportunity arose that you decided to pursue?

Qi: When it comes to launching startup companies, every entrepreneur has their own approach. In my case, I focus on selecting areas where significant challenges, essential needs, and a massive market exist. These are the criteria that guide my decision-making process. Leveraging my knowledge and experience, I aim to assist the team in establishing a unique and advantageous position within the market. By identifying and addressing these key factors, I strive to create a solid foundation for the success of the startup venture.

When a company is operating smoothly and enjoys certain advantages in the market, various opportunities arise. Whether the company chooses to go public, remain privately held, pursue a merger, or be acquired by a larger company depends not only on market opportunities and positioning but also on the vision and execution capabilities of the team.

Market conditions and the company's competitive position play a

The ultimate measure of a superior product lies in its ability to positively impact people's lives.

significant role in determining the available opportunities. However, the ultimate "exit strategy" decision regarding the company's direction is influenced by the team's vision for the future and their ability to execute strategic plans effectively. During the early stages of a startup, the focus is often on building the business, establishing a strong foundation, and achieving sustainable growth. Exit strategies tend to be decisions made at a later stage when the company has reached a certain level of maturity and market presence. By remaining agile and adaptable, the company can navigate the evolving business landscape and seize opportunities that arise, ultimately contributing to its long-term success and the betterment of society.

Factors such as long-term growth potential, financial stability, synergies with potential partners or acquirers, and the overall alignment of goals and values are considered when evaluating these opportunities. It is crucial for the team to assess the market landscape, weigh the potential benefits and risks, and align their vision and capabilities with the chosen path forward.

As a company founder, I firmly believe that growth can only be achieved by helping others. By prioritizing the needs and goals of customers and stakeholders, and by providing value and solutions to their challenges, a company can foster its own growth and success in the market.

Waterhouse: Looking through the diverse set of companies you have worked at (diverse for an antenna engineer!), was your line of thought, "There is a gap in the technology needing to be addressed: I'll start a company in that area," or were you approached to be involved with these new companies due to your previous experience?

Qi: My experience in entrepreneurship, as an engineer, typically begins by identifying market needs through thorough research and analysis. If there is a noticeable gap between existing technology and market demands,

an opportunity arises to form a team and develop new technologies based on theoretical understanding. These new technologies then serve as the foundation for product development.

In this process, the business model plays a critical role in determining how the products will be marketed and sold. Creating an effective and viable business model is essential for successfully bringing the products to market and generating revenue.

There have been instances where my previous experience and expertise have attracted opportunities, leading to the realization that a new team is necessary to pursue those opportunities. This recognition often arises from understanding the specific requirements and challenges of the new opportunity and realizing that assembling a diverse and capable team will be crucial to its success.

Waterhouse: Over the years, have you had close collaborations with universities? If so, can you give us an example?

Qi: In the realm of technology companies, a profound understanding of theoretical breakthroughs is of utmost importance. Collaborating with universities plays a significant role in the success of high-tech companies. I consider myself fortunate to have had the opportunity to work with several universities as an adjunct professor, including the Missouri University of Science and Technology Electromagnetic Compatibility Laboratory, Western University in Canada, Hunan University, and others.

University collaborations offer a multitude of benefits. First, they provide access to deep theoretical research conducted by academic experts. This enables technology companies to stay informed about the latest advancements and cutting-edge knowledge in their respective fields. Such collaborations

foster an environment of continuous learning and ensure that companies remain at the forefront of innovation.

Additionally, university collaborations offer a valuable pipeline of talent. Graduate students who are well-trained and equipped with the latest academic knowledge can serve as a potential new workforce for technology companies. By engaging with universities, companies can establish connections with talented individuals who may bring fresh perspectives and contribute to the growth and success of the organization.

Moreover, university collaborations facilitate knowledge exchange between academia and industry. These partnerships allow for the transfer of practical industry insights to academia, ensuring that academic research aligns with real-world applications and industry needs. Simultaneously, companies benefit from the theoretical expertise and research conducted within the academic realm, which can inspire and inform their innovation and product development processes.

Waterhouse: With the different companies, what's been the hardest challenge? Looking back, were the challenges the same, or unique?

Qi: Technology companies face stiff competition if their products or business models are similar to those of their competitors. The key challenge for these companies, in my opinion, is to innovate either their technology or business models to solve real-world problems. Each company may have its own unique problems to solve, but innovation is crucial to differentiate themselves from the competition and stay ahead in the market. Finance, marketing, sales, and management are very important if the company wants to grow fast.

Waterhouse: In your talk at [the IEEE Antenna and Propagation Society] AP-S this year, you make an observation about academia versus real-world engineering. Both have exciting elements to them, but as you hint, publishing is not considered important for the career of a typical industry engineer. Can you elaborate further on this?

Qi: The goals and priorities of universities, research institutes, and industries significantly differ. Universities and research institutes heavily rely on government funding for fundamental research and industrial projects, which supports their financial needs. Consequently, their focus is often on publishing academic papers and theoretical research, rather than developing real-world products.

In contrast, industries primarily aim to generate revenue in the market. Engineers in industry are typically occupied with solving practical engineering problems, leaving them with limited time to engage with academic papers. Additionally, factors such as intellectual property protection, resource constraints, and confidentiality requirements further limit their ability to dedicate time to writing papers.

As a result, there exists a gap between theoretical research and real-world applications. On the one hand, engineering-related academic research often remains disconnected from real-world engineering practices. On the other hand, engineers working in real-world applications are in need of reliable, cost-effective solutions to address their specific problems. They seek guidance from solid theoretical foundations and practical engineering concepts.

Waterhouse: There is a lot of talk these days about "digital twins." How close to this are we, or do you think experimental tweaking will always be part of antenna engineering?

Qi: The term *digital twin* has gained significant attention in the technology landscape and is being widely discussed across various industries. It encompasses the concept of using digital representations to mirror and simulate real-world systems or phenomena. This concept has practical applications in diverse sectors, including manufacturing, health care, transportation, and infrastructure. Furthermore, I believe it will also find its way into electromagnetic applications, such as integrated measurement-based computational emulation.

Integrated measurement-based computational emulation involves leveraging

critical physical measurements as a basis for employing computational modeling to emulate and simulate real-world systems. This approach combines the benefits of accurate measurements with the flexibility and scalability offered by computational modeling. In the field of antenna measurement, for instance, we utilize an "electromagnetic environment twin" to replicate the real-world MIMO [multiple input/multiple output] channel model within a controlled environment, such as an anechoic chamber. By accurately reproducing the signals and noise that exist in the real world, a controlled environment provides a fast, precise, and cost-effective solution for evaluating integrated systems. This approach, such as the radiated two-stage method for MIMO measurement, allows for efficient and reliable assessments of MIMO radio performance in complex scenarios. This advancement significantly enhanced the accuracy and affordability of measurements for 5G/6G, intelligent connected vehicle, and satellite application.

With respect to "antenna tweaking," owing to the lack of a well-defined common mode return path for the antenna, as well as the nonlinearity exhibited by the system and the uncertainties associated with component modeling, there is a perpetual requirement for experimental fine-tuning in RF and antenna designs. Furthermore, the field of EM engineering is increasingly dependent on simulations, complemented by advancements in theoretical breakthroughs.

Waterhouse: With the companies you have been involved with, was there a common funding approach, for example venture capital funding? Or was each endeavor a different approach?

Qi: The best approach starts with product market fit and market traction. What matters most is growth, customer acquisition, and sales. All of my companies share this common characteristic, as they have been able to scale through revenue and customer fit. Financial funding is a stimulant to accelerate growth, but that can only be achieved after revenue and sales channels have been established.

That said, we worked closely with financial institutions for growth and initial public offerings. The relationship with financial institutions offers two things: expertise and credibility.

For expertise and networking, financial institutions bring valuable expertise and industry knowledge to the table. They have experience working with growth companies and can provide guidance on strategic decisions, business development, and operational efficiency. Additionally, financial institutions often have extensive networks that can connect with potential partners, customers, and other industry influencers, a valuable resource during initial public offering and growth stages.

Financial institutions offer validation and credibility to attract other investors, customers, and key stakeholders. Their endorsement can validate business model, traction, market potential, and team. I've found in my experience financial partners become an essential part of a road show, and in the end, a critical ingredient for growth.

Waterhouse: What's the next big thing in the antenna world?

Qi: Metasurface antennas have garnered significant research interest over the past decade. Despite extensive research in this field, their practical applications have not yet achieved widespread implementation on a large scale. However, it is reasonable to anticipate that new developments and advancements in metasurface technology, along with related antenna technologies, will soon enter the marketplace.

Antenna engineers have made significant contributions to the development of innovative antenna structures that are widely utilized in various systems. Examples of such antennas include the Yagi-Uda antenna, log-periodic antenna, corrugated horns, microstrip patch antenna, and phased array antennas. These antennas have demonstrated their usefulness, leading to their widespread application. The continuous innovations in these areas are still the mainstream application focus.

ABOUT YIHONG QI

Yihong Qi is an engineer, scientist, inventor, and entrepreneur. He is president and chief scientist of General Test Systems, Inc., Shenzhen, China. He is founder of Pontosense Inc., Merku Inc., Canada and Link-E, Zhuhai, China. He is an honorary professor at Xidian University and Southwest Jiaotong University. He is also adjunct professor in the Electromagnetic Compatibility (EMC) Laboratory, Missouri University of Science and Technology, Rolla, MO, USA, and Western University, Ontario, Canada.



Yihong Qi

Qi is an inventor of more than 500 published and pending patents. He has published 150 academic papers. His smartphone antenna design patent significantly reduced harmful radio-wave radiation to the human head, which could potentially help billions of smartphone users reduce potential hazardous electromagnetic radiation. His invention also resolved the hearing aid compatibility issue; there are more than 20-million cell phone users who depend on hearing aid devices. His standards related inventions have made the certification process for 4G, 5G, and potentially 6G wireless communications and autonomous cars more efficient and cost-effective.

Qi was an associate professor in Southeast University, China, in 1992. From 1995 to 2010, he was with Research in Motion (Blackberry), Waterloo, ON, Canada, where he was the director of advanced electromagnetic research. He was founding Chairman of the IEEE EMC Society Technical Committee-12. He is associate editor of *IEEE Internet of Things* and *IEEE Transactions on Electromagnetic Compatibility*. He is Distinguished Lecturer of the IEEE Antenna and Propagation Society and was a Distinguished Lecturer of IEEE EMC Society. He has received an IEEE EMC Society Technical Achievement Award. His inventions won 2019, 2020 CES innovation awards, the 2021 CES Network Product Award, the 2022 CES Wellbeing Product Award, the Red Dot Award, and the IEEE Technical Committee on Hyperintelligence Industrial Award, among other awards. He is a Fellow of the Canadian Academy of Engineering, a Fellow of the National Academy of Inventors, and a Fellow of IEEE.

In recent work, I collaborated with Dr. Lidong Chi and Dr. Zibin Weng to invent a linear array that achieved an approximate bandwidth of 80%. This significant improvement surpassed the classic Yagi-Uda antenna's bandwidth of 10%. Moreover, we successfully reduced the maximum antenna dimensions. These advancements in developing a high-quality, wideband linear array have showcased their immense benefit across various scenarios, which used to be demonstrated by the remarkable performance of the Yagi-Uda antenna over 100 years.

Another noteworthy aspect is the growing prominence of antennas as key system blocks, such as antenna in package, in various applications. This development is expected to gain significant traction. The concerns related to system design, testing, mass production, and time to market will act as driving factors for innovation in this domain.

Waterhouse: How important have community relationships been for you to achieve all the goals you have met to date?

Qi: Throughout my career, I have gained invaluable knowledge and experience from various sources, including my supervisors, mentors, coworkers, students, and partners. The collaborative environment, discussions, and academic explorations have fostered mutual trust, leading to long-term relationships with the shared objective of enhancing the overall well-being and development of the community.

We come together with shared interests, tackling challenges, celebrating discoveries, and finding joy in the engineering profession. It is through our collective efforts and synergy that a group of people can achieve remarkable progress and go far in their endeavors.

EuCAP 2023, AP-S Chapter Activities, COPE Corner, and Distinguished Lecturers

EUCAP 2023 IN FLORENCE, ITALY

THE BIGGEST EUROPEAN AP CONFERENCE EVER

Report by: Juan R. Mosig^{ID}

The European Conference on Antennas and Propagation (EuCAP) is the flagship conference of the European Association on Antennas and Propagation (EurAAP, <https://www.euraap.org>). This year, the 17th edition, EuCAP 2023, took place in Florence, Italy, on 25–31 March 2023 (*). More details and photos in specific sections (marked by an asterisk) can be found in the supplementary material that accompanies this article on IEEE Xplore.

Since their beginning in 2006, EuCAP conferences have attracted a crowd of about 1,000 participants. After the COVID-forced online editions of 2020 and 2021, the EuCAP 2022 conference, held in Madrid, Spain, in a hybrid format, had already almost gone back to the average numbers, despite the restrictions for physical meetings still existing in Europe. This was a clear proof of the solidity of EuCAP conferences, well established in the personal agenda of most members of our antennas and propagation community. The 2023 edition has confirmed this trend. Able to go back to a pure face-to-face physical style, EuCAP 2023 has broken all previous

records. For this, the author, on behalf of the EurAAP Board, wants to thank the EuCAP 2023 chair, Prof. Stefano Maci (Figure 1), his cochairs, Prof. O. Breinbjerg and Prof. A. Freni, and all of the committees, organizing teams, cooperating universities, and volunteering individuals who contributed to the amazing success of this conference (*).

Also, thanks are given to the international associations that have implemented a lasting strong collaboration with the EuCAP conferences, through signed memoranda of understanding with EurAAP. Their names are well known in our community: the Antenna Measurement Techniques Association (AMTA), the European Microwave Association (EuMA), the IEEE Antennas and

Propagation Society (AP-S), the Institution of Engineering and Technology (IET), the International Symposium on Antennas and Propagation (ISAP-IEICE), the International Union of Radio Science (URSI), and three newcomers, the European Conference on Networks and Communications (EuCNC), the Virtual Institute for Artificial Electromagnetic Materials and Metamaterials (METAMORPHOSE), and the European Space Agency (ESA), who signed its agreement with EurAAP during the conference (*).

SOME NUMBERS

EuCAP 2023 welcomed 1,712 (!) registered delegates from 65 countries, the absolute record in the EuCAP series.



FIGURE 1. EuCAP 2023 is presented by its chair, Stefano Maci, University of Siena, Italy, and by EurAAP Chair Stefania Monni, TNO, The Netherlands.

The “big five” European countries (in our domain, France, Germany, Italy, Spain, and the United Kingdom) accounted for roughly half of the participants, with sizable contributions (around 10%) from both North America and the Asian Far East (*).

After a strict revision by a team of more than 1,000 reviewers and metareviewers, 1,046 papers were accepted. Of these, no fewer than 1,013 were actually presented. The papers’ geographical distribution was very close to that of the registered delegates. They were presented both in oral sessions (72%) and as posters (28%). Of the total papers, 66% were unsolicited contributions, presented in regular sessions, while 34% were the outcome of no fewer than 55 convened sessions.

It is also interesting to look at the authors of the papers (there were more than 4,000 different names). Roughly, 59% came from academia, 23% were master’s or Ph.D. students, and the remaining 18% were distributed among industry, government employees, and nongovernmental organizations.

EuCAP always classifies its papers into four traditional topics: antennas (53%), electromagnetics (21%), propagation (15%), and measurements (11%). But in the last editions, an additional and useful classification by “application tracks” has been introduced. This is not only very helpful to organize and distribute the papers in the 65 oral sessions, but it also provides some practical orientation to the attendees. It is worth mentioning that among the 11 predefined application tracks (*), the most popular was “MM-wave and THz cellular” (18% of the papers) followed by “Fundamental Research and Emerging Technologies” (15%).

To pamper this record-breaking number of delegates, EuCAP 2023 offered them a superb exhibition with no fewer than 50 international exhibitors, covering almost the full alphabet, from Airbus to Xphased (*). Add to this 12 short courses, 20 scientific and industrial workshops (both half and full day), a rich social program for both delegates and accompanying persons—and you will start to understand

why EuCAP 2023 was the edition of all superlatives.

All of this was also facilitated by the generosity of the 20 sponsors (*) to whom deeply felt thanks must be given, starting with the two Platinum sponsors, Huawei and Microwave Vision Group.

ORGANIZATION DETAILS

The basic schedule of EuCAP conferences is now well established, although there is always room for innovation and improvement and the need to adjust to the material conditions of every venue.

The venue for the 2023 edition was Fortezza da Basso, a wonderful fortress built by Alessandro de Medici in 1534 and transformed into a congress and exhibition center by the city of Florence. It has a very convenient location in downtown Florence, a few minutes’ walk from the main railways station. But above all, it was perfectly suited for EuCAP and its traditional program (*).

Monday morning started with the usual opening address, followed by a plenary session including three prestigious keynote speakers: Nader Engheta (University of Pennsylvania), Rashaunda Henderson (University of Texas at Dallas), and Marco di Renzo (CNRS and Supélec Paris) (*). A crowded Cavaniglia Pavilion (1,000 people) was the perfect frame for these events.

The main flow of the conference then moved to the two-floor Spadolini Pavilion.

The traditional format of EuCAP includes 11 parallel sessions in the morning and late afternoon. In the early afternoon, between lunch and coffee break, the protagonists are the poster sessions followed by two semiplenary sessions. These sessions include only two presentations per day, resulting in a total of 12 invited papers given by top-notch speakers (*). The Spadolini upper floor provided ample room for the 11 parallel sessions. More importantly, the more than 8,000 m² of the lower floor were a delightful playground for a deep interaction among exhibition, poster sessions, invited papers, lunches, and coffee breaks. This was confirmed by all of the exhibitors, who systematically praised the arrangements and configuration of the venue.

In addition, Fortezza da Basso provided all of the additional rooms needed for workshops, short courses, and ad hoc meetings, with an appreciated touristic supplement: the possibility of visiting the historical areas underneath the modern venue. And last but not least, on Monday evening, the Fortezza hosted a very successful and animated welcome drink event (*).

Of course, several events took place outside this wonderful venue, and the first to be mentioned is the outstanding conference dinner. EuCAP 2023 was able to offer to the conference dinner participants a predinner cocktail in the Salone dei Cinquecento, undoubtedly the grandest and most imposing room in Florence’s Palazzo Vecchio (Figure 2). It



FIGURE 2. Cocktails preceding the conference dinner in the Salone dei Cinquecento, inside Palazzo Vecchio in downtown Florence.

was an amazing feeling to have a drink and chat with colleagues amid paintings and sculptures by the big names of the Italian Renaissance. Then, the participants moved to the no-less-imposing Santa Maria Novella church, where the conference dinner was held in its big Cloister refectory. This was the moment to celebrate the winners of the four prestigious EurAAP Awards (°) (see <https://www.euraap.org/awards> and consider applying for them): the Antennas, Propagation, Felsen, and Kildal Awards, whose 2023 recipients were, respectively, Guy Vandebosch, Vittorio Degli Esposti, Christos Argyropoulos, and Daniel Martínez de Rioja.

Finally, it is worth mentioning that, to compensate for the limited number of conference dinner tickets, the EuCAP organizers kindly offered an alternative to the delegates during the conference—in the form of no less than four get-together dinners.

Other traditional, very successful EuCAP outings in Florence were the two sold-out AMTA technical tours, to the Arcetri Astrophysical Observatory and the Galileo Museum (°).

SOME PERSONAL COMMENTS

This author was impressed by the consistently high technical and scientific level of the conference, from the keynote presentations to the posters. The workshops were also very successful and well attended. Three are worth mentioning: 1) the “History of Electromagnetics and Antennas” session, built around the historic Oersted experiment (whose 200th anniversary we should have celebrated in 2020) and including 10 well-known speakers (°); 2) an innovative workshop on “Disruptive Innovations: The Roadmap of the European Funding Agencies,” where speakers shared the vision of main European Union agencies on disruptive technologies and explained which instruments are available to support innovative ideas (°); and 3) the brand-new EuCAP Perspective Workshop, providing a broad and multidisciplinary view on the current trends, ongoing initiatives, and industrial perspectives in a certain field; this year “Smart Wireless Environments” (°).

Another novel and successful event was the “EuCAP Job Corner,” where students and young researchers were able to discover companies and job opportunities through the short talks of professionals belonging to the exhibition companies.

In summary, EuCAP 2023 was a most successful conference, and I would like to highlight two details that I believe strongly contributed to its success. The phone app was excellent. All attendees were able to set up their personal schedules, to be aware of late-notice changes, and to easily find their way. No more paper! Also, there were enough tables and chairs to enjoy relaxed lunches and coffee breaks and to take full advantage of the excellent Tuscan food (and wine) and the always-satisfying espressos and cappuccinos—nothing better for meeting colleagues, exchanging ideas, and discussing possible collaborations.

EuCAP 2023 ended early afternoon on Friday with the traditional closing ceremony, announcing the future edition (°). Get ready for EuCAP 2024 on 17–22 March 2024, in Glasgow, U.K.!

SUPPLEMENTARY MATERIAL



VIDEO



AP-S CHAPTER ACTIVITY

Committee Chair: Ajay Poddar 
Report by: Mei Song Tong 

NEW AP-S CHAPTERS

The following new Chapters have been formed:

- 1) Raghu Institute of Technology, Antennas and Propagation Society Student Branch Chapter, geocode SBC03240D, 16 February 2023
- 2) Kumaraguru College of Technology, Antennas and Propagation Society Student Branch Chapter, geocode SBC29751B, 22 February 2023
- 3) Bhusanayana Mukundadas Sreenivasaiah (BMS) College of Engineering, Antennas and Propagation Society Student Branch Chapter, geocode SBC04431G, 17 March 2023
- 4) Silchar, IEEE Kolkata Section, Antennas and Propagation Society Chapter, geocode CH11058, 18 March 2023
- 5) Vignan's Foundation for Science, Technology Research, Antennas and Propagation Society Student Branch Chapter, geocode SBC13631A, 23 March 2023
- 6) Wayanad, Antennas and Propagation Society Student Branch Chapter, geocode SBC11161B, 28 March 2023
- 7) Indian Institute of Technology Patna, Antennas and Propagation Society Student Branch Chapter, geocode SBC14591A, 29 March 2023.

If any of you reside in a location where you do not have access to an existing AP-S Chapter and are interested in establishing a new one, please feel free to contact Chapter Activity Committee (CAC) Chair Dr. Ajay Poddar (akpoddar@ieee.org) and the AP-S Chapter Region coordinators for guidance through the petition process. Start by researching your area, and then decide which route will best suit your needs and support a healthy, active Society/Technical Council Chapter environment (<https://mga.ieee.org/resources-operations/geographic-unit/chapters/how-to-create-a-new-ieee-chapter>).

It is very important for an active Chapter to submit its annual report to be eligible to receive financial support for 2023 Chapter events (technical meetings, workshops, and special projects) and for Chapter chair travel grants to attend the annual Chapter Chairs Meeting at the AP-S flagship

and AP-S-supported regional conferences. As of 2022 May, there are 36 independent Chapters, 110 joint Chapters, and 75 Student Branch Chapters for a total of 221 Chapters (<https://tblanalytics.ieee.org/>). Many Chapters have organized numerous technical seminars, workshops, outreach drives, Committee on Promoting Equality (COPE) projects (<http://aps-cope.org/>), IEEE Special Interest Group on Humanitarian Technology (SIGHT) projects (<https://sight.ieee.org/>), and social events at the Chapter and Regional levels. We would like to welcome and express gratitude to the many new Chapter officers for their time and hard work for the benefit of IEEE Members.

AP-S CHAPTER REPORTS

IEEE NORTH JERSEY SECTION AP-S/MTT-S CHAPTER OUTSTANDING ENGINEER AWARD

Figure 3 is a photo of Nina Krikorian-Ezik receiving the North Jersey Section AP-S/ IEEE Microwave Theory and Technology Society (MTT-S) Chapter Outstanding Engineer Award plaque at the award banquet event, 7 May 2023, at Birchwood Manor, Whippany, NJ, USA. Nina Krikorian-Ezik is currently a manager of the Mission Solutions RF Design Group at L3 Harris in Clifton, NJ. She has 25+ years of experience in the aerospace and defense industry and has developed system-level radio-frequency (RF) architecture designs for software-defined radio in addition to developing RF hardware circuit designs, such as up/down converters, antenna interface modules, clock circuits, voltage control oscillators, filters, and antenna designs up to Q-band.

Figure 4 is a photo of Dr. Ajay Poddar, receiving a plaque from Dr. Hong Zhao, a professor at Fairleigh Dickinson University, NJ, and chair of the IEEE North Jersey Section, for serving as chair of the North Jersey Section from 2021 to 2022.

IEEE ULRICH L. ROHDE HUMANITARIAN TECHNICAL FIELD PROJECT AWARD

The SIGHT/IEEE Humanitarian Activities Committee (HAC) project

It was an amazing feeling to have a drink and chat with colleagues amid paintings and sculptures by the big names of the Italian Renaissance.

has a call for proposals. The proposal, consisting of details of the project and budget, can be submitted to Dr. Jawad Siddiqui, AP-S SIGHT Committee chair, e-mail: jys.rpe@gmail.com. The submission deadline for the “IEEE Ulrich L. Rohde Humanitarian Technical Field Project Award” is 30 August 2023. The project selection process is in line with IEEE SIGHT and HAC Project Awards. The evaluation of proposals will be based primarily on technical content. After completion of the project, the awards committee will explore follow-up activities for low-cost production of the proposed technology, which is the key requirement for humanitarian needs.

IEEE AP-S CHAPTER STUDENT DESIGN CONTEST

There is additional funding available for supporting Student Design Contests (SDCs) cosponsored by local AP-S Chapters for the engagement of students and Young Professionals. The template for the SDC is in the category of Special Project, and it can be sent to AP-S CAC Chair Dr. Ajay K. Poddar, e-mail: akpoddar@ieee.org. The SDC and Special Project Form and preparation guidelines are posted on the AP-S Chapter webpage (<https://www.ieeeaps.org/chapters/chapters>). The selected SDC project will be published in *IEEE Antennas and Propagation Magazine* as a part of the “AdCom Corner” column report activities. Please contact your AP-S Chapter Activity Region Coordinator for clarifications and support related to financial support, travel grants, and other concerns. Please click the link for contact details of the AP-S Chapter Activity Region Coordinators: <https://ieeeaps.org/committees/current-committee-members>.



FIGURE 3. Nina Krikorian-Ezik receives the IEEE North Jersey Section AP-S/MTT-S Chapter Outstanding Engineer Award plaque at the award banquet event on 7 May 2023. From left, Dr. Adriaan J. de Lind van Wijngaarden, chair of North Jersey Section IEEE Information Theory Society Chapter; Dr. Ajay K. Poddar, chair of IEEE AP-S CAC; Nina Krikorian-Ezik, L3 Harris Clifton, NJ; Dr. Hong Zhao, chair of IEEE North Jersey Section; and Dr. Anisha M. Apte, IEEE AP-S CAC Region coordinator. Venue: Birchwood Manor, Whippany, NJ, USA.

SUPPLEMENTARY MATERIAL



COPE CORNER

Committee Chair: Weng C. Chew

Report by: Anisha Apte 

SCIENCE, TECHNOLOGY, ENGINEERING, AND MATHEMATICS IN NORTH AMERICA

Members of the AP-S COPE North America subcommittee: David R. Jackson (chair), Charlotte Blair, Niru Nahar, Jose Schutte-Áine, and Karl Warnick.

The AP-S COPE North America subcommittee is providing a brief overview of the stimulating discussions that arose from a presentation by the AP-S COPE North America subcommittee to the AP-S COPE Committee on 1 April 2023, on the subject of science,

technology, engineering, and mathematics (STEM) education in North America. The main purpose was to stimulate discussion and suggestions for furthering STEM in North America and determining how AP-S COPE can help.

BACKGROUND AND NEED FOR STEM INVOLVEMENT IN NORTH AMERICA

We first note that the United States placed 11th out of 79 countries in science, when testing of U.S. students was administered in 2018. Also, the United States was not among the top five math-scoring countries in 2018, and the scores of U.S. math students have remained roughly constant since 2003. Furthermore, in a recent report that lists the top 10 countries with the most educated populations, only one country in North America, Canada, was among the list, ranking at number 9. Clearly, much effort is needed to improve STEM education in the United States, with a disproportionate number of students in underserved, underrepresented, and marginalized communities being especially in need of improved education in the STEM

areas. An improvement of STEM education in the public K-12 system in the United States, especially within marginalized communities, can only serve to increase the overall educational level and quality of life for all U.S. citizens. According to the U.S. Department of Education website, “Research shows how a sense of belonging in rich and rigorous classrooms is directly correlated to students’ long-term academic success.” Moreover, “the Department’s Civil Rights Data Collection continues to demonstrate that students of color and students with disabilities are disproportionately excluded from learning opportunities in STEM,” said U.S. Deputy Secretary of Education Cindy Marten. Furthermore, she says “Today, we are saying unequivocally to all students and educators that they belong in STEM and that they deserve to have rigorous and relevant educational experiences that inspire and empower them to reach their full potential as productive, contributing members of our nation’s workforce.”

HOW CAN AP-S COPE HELP?

Many engineering colleges at universities in the United States and in electrical and computer engineering departments in particular, already have existing STEM-related programs and host STEM-related events. Often they are in the form of special camps or theme-related events to help engage young students in STEM activities. These activities can be very beneficial, especially when they involve outreach to marginalized communities. To give two specific examples, Brigham Young University hosts a “Chip Camp” for youth in seventh and eighth grades. The University of Houston hosts a STEM Technology Camp for grades 3–8. Many other such programs exist throughout the country. The AP-S community can help advocate for such programs and participate in them, as appropriate. This could also be an excellent opportunity for Members of IEEE student branches to become further involved in outreach.

Some universities may also have a special office that pertains to diversity,



FIGURE 4. Dr. Ajay Poddar receives the plaque. From left, Kenneth Oexle, chair of North Jersey Section Award Committee; Russell Pepe, member of North Jersey Section Award Committee; Prof. Durgamadhab Misra, chair of North Jersey IEEE Electron Devices Society/IEEE Circuits and Systems Society Chapter; Dr. Adriaan J. de Lind van Wijngaarden, chair of New Jersey Section IEEE Information Theory Society Chapter; Dr. Ajay Poddar, chair AP-S CAC; Prof. Hong Zhao, chair of IEEE North Jersey Section; Har Dayal, cochair of Engineering in Medicine and Biology; Naresh Chand, chair of North Jersey Section Photonic Society Chapter; Howard Leach, chair of North Jersey Section History Committee; and Kirit Dixit, chair of North Jersey Section IEEE Society on Social Implications of Technology Chapter. Venue: Birchwood Manor, Whippany, NJ, USA.

equity, and inclusion. Working with such offices may be beneficial when planning outreach to marginalized communities, especially when the university is located in or near a marginalized community.

Another way in which AP-S members can get involved with STEM activities is to interact directly with local schools. Members of the AP-S community are experts in electromagnetism, and, as we all know, this area makes for some fascinating demonstrations in the classroom.

Figure 5 shows a Tesla coil and a Van de Graaff generator being demoed for a third-grade class. These kinds of demos are something that AP-S students and students in a local IEEE student branch can easily do, and the students in the classroom will really enjoy it. This is an excellent way to enhance outreach to our local schools. This type of outreach can possibly be coordinated through existing STEM programs that are already in place at our universities.

Another possible way in which AP-S members can get involved in STEM activities at local schools is by working with teachers to help them implement electromagnetism-related classroom projects for their students. Again, this type of activity could possibly be done in conjunction with STEM programs that are already in place at our universities.

By getting more involved, we can all help to advance STEM activities, and our youth will surely benefit. The AP-S COPE North America subcommittee welcomes further suggestions!

AP-S COPE-SPONSORED TERRA NORTH JERSEY STEM FAIR

The Terra North Jersey STEM Fair (TNJSF) is a high school student competition in all STEM fields, in which students, individually or in groups, present a wide variety of projects. Most of the projects are investigative in nature, posing and attempting to answer some question or problem, either through experimentation and design or in a theoretical sense. All areas of science, math, and engineering are included.

The fair accepts entries from 10 counties of Northern New Jersey: Bergen, Essex, Hunterdon, Middlesex, Morris, Passaic, Somerset, Sussex, Union, and Warren. The home page for the TNJSF is <https://tnjsf.zfairs.com>.

The mission of the TNJSF is to support, encourage, and recognize student involvement in scientific research, with the belief that students can only truly appreciate the creative nature of the scientific process if they have actually experienced it themselves. In addition, the TNJSF endeavors to provide resources that further this overarching goal, including giving students various opportunities to interact with professional scientists and engineers. The opportunity to partake of the TNJSF itself as well as the other resources offered is intended to be open to all high school students in the Northern New Jersey Region.

The AP-S sponsors IEEE North Jersey Section Young Engineer Awards for projects in engineering, biomedical engineering, and computer science that demonstrate the use of sound engineering principles. A team of judges from AP-S COPE and the IEEE North Jersey Section has selected nine students (see Table 1) as recipients of the IEEE Young Engineer Award. The awardees were presented with an award check and a certificate of achievement during a personal visit to each of the schools by the IEEE North Jersey Section Chapter officers.

AP-S EPICS COLLABORATION

Another meeting of the COPE was held on 11 May 2023. The main agenda of this meeting was a presentation by Ashley Moran (seen in the top left corner in Figure 6) on the topic Engineering Projects in Community



FIGURE 5. David Jackson having fun in a third-grade classroom, demonstrating a Tesla coil and a Van de Graaff generator.

TABLE 1. RECIPIENTS OF THE IEEE NEW JERSEY YOUNG ENGINEER AWARD.

Category	Student	School
BE.01	Ryan Kwon	Bergen Catholic High School
CS.01	Divya Krishna	Edison High School
CS.05	Zayn Rekhi	Millburn High School
CS.08	Ryan Rong and Curtis J Zhou	The Peddie School
EN.07	Charles Jiang and Diego Pasini	The Pingry School
EN.10	Abhay Bhaskar	Middlesex Academy of Science, Mathematics, and Engineering Technology
EN.11	Kai Song	Tenafly High School

Service (EPICS) in the IEEE program to see if there may be a way for EPICS to partner with AP-S and COPE.

The meeting was initiated by Dr. Ajay Poddar and began with a formal introduction of the COPE members to the speaker. The goals of EPICS in IEEE and some stories about the impact their student lead projects have had on their communities were presented.

All EPICS projects tie back to one of the four pillars of community improvement: access and abilities, environment, human services, and education and outreach. EPICS project teams partner with nonprofit organizations in their community to bring engineering solutions to underserved populations. With these highlights, the different ways in which EPICS could partner with AP-S COPE, given their shared goals, were discussed.

IEEE adopted the philosophy of EPICS from Purdue University by creating the EPICS in IEEE Committee in 2009. EPICS in IEEE empowers students to work with local service organizations to apply technical knowledge to implement solutions for a community's unique challenges. Prof. Weng Chew, the AP-S COPE chair and a professor at Purdue University, stated that he will be discussing with Bill Oakes at Purdue University about a joint collaboration effort in line with COPE's mission. Prof. Yahia Antar, past AP-S president,

Members of the AP-S community are experts in electromagnetism, and, as we all know, this area makes for some fascinating demonstrations in the classroom.

invited Ashley to give a presentation to the AP-S AdCom on Sunday, 23 July 2023, at AP-S URSI in Portland, OR, to help AP-S AdCom and committee members in understanding the AP-S COPE EPIC initiatives. Dr. Anisha Apte and Dr. Jawad Siddiqui recommended that Ashley also give a presentation during the Chapter chair meeting or during the SIGHT/IEEE Member and Geographic Activities meeting on Thursday to reach out to the local Chapter officers attending these meetings, which she has gladly accepted. We look forward to this collaborative effort in addressing the shared vision of IEEE EPICS and AP-S COPE.

AP-S COPE FUNDING REQUEST DEADLINE FOR 2023: 31 JULY 2023

AP-S COPE aims to fund projects that provide good use of IEEE expertise exhibiting a strong technological component, with clear engagement with the community, indicating that the proposed solution is both desired

and feasible. There should be established relationships, ideally documented, with stakeholders who will be involved in the project and implementation with a clear, detailed, and credible Project Assessment Matrix, Project Implementation Plan, and Budget. The team should demonstrate combined experience to credibly execute the project and

identify and address potential risks, and the project should have real, tangible impact. If a proposal is missing the mark on two or more of these areas, it might not be ready for funding.

AREAS OF FOCUS

AP-S COPE is prioritizing immediate impact on poverty mitigation and inequality reduction through the following project areas:

- upgradation of a marginalized population
- STEM education for a marginalized population
- information and communications technology for an underserved population
- sustainable power sources for an underserved population
- water, sanitation, and hygiene for an underserved population.

Projects must be successfully completed and submitted to AP-S through final reporting indicating the status of



FIGURE 6. Screenshot of the AP-S COPE Zoom meeting held on 11 May 2023.

the project and utilization of funds at the end of each calendar year. Expense vouchers should be submitted as supporting documents for audit. An “APS COPE Project Budget Template 2023” spreadsheet should be submitted for budget proposal during application and an expense report on completion of the project. Fund utilization should be clearly indicated. Each AP-S Chapter/Joint Chapter/Student Branch Chapter may submit multiple proposals. Proposals are subject to review and scrutiny, and the total project funding will not exceed US\$3,000 for any calendar year. For additional funding, teams are encouraged to submit proposals to AP-S SIGHT and AP-S CAC.

AP-S Chapter officers/members can fill out and submit the IEEE AP-S COPE - Special Project Funding Request Form 2023 using the online submission link. Please use the link given next to the Google Form to submit your project proposals under the COPE mission: 2023 AP-S COPE Special-Project Funding Request Application (Google Form: <https://forms.gle/T6rQJNV2v7E7a73Q8>).

If Google Forms is not available in your Region, you may use “AP-S Special Project Request Form” (MS Word, PDF) or “2023 AP-S COPE (Committee on Promoting Equality) Special Purpose Fund Request Form” (MS Word), found on the IEEE AP-S website (ieeeps.org). Chapter officers can submit their write-ups, photos, and videos of COPE events

It was one of my main ambitions and goals when applying for the Distinguished Lecturer program to deliver interesting lectures in the Middle East and Central Asia.

to be uploaded to the COPE website (aps-cope.org) and/or to be published in *IEEE Antennas and Propagation Magazine* in the “AdCom Corner” column.

DISTINGUISHED LECTURERS

Committee Chair: Kwai Man Luk 

I am delighted to report that our Distinguished Lecturers, including Prof. Reyhan Baktur, Prof. Yongxin Guo, Prof. Debatosh Guha, Prof. Zhongxiang Shen, Prof. Ahmad Hoorfar, and Prof. Levent Sevgi, have arranged or planned their talks, both online and in person, over the past few months. AP-S Chapters are always most welcome to invite our present and past Distinguished Lecturers to visit your locations and meet your colleagues and students.

One of my major tasks recently is the selection of the MTT-S and AP-S Inter-Society Distinguished Lecturer, working with Prof. Luca Pierantoni, the MTT-S representative. This is a new initiative proposed by Prof. Ke Wu. The call for nomination of the

AP-S Distinguished Lecturers serving the period from 2024 to 2026 has been announced. Members are welcome to nominate outstanding candidates or themselves for this important position in our AP-S. The deadline for nomination is 31 August 2023.

REYHAN BAKTUR'S MIDDLE EAST LECTURE TOUR

Reyhan Baktur, IEEE APS Distinguished Lecturer (2022–2024)

I returned from a one-week lecture tour in Egypt on 17 December 2022. This concluded a Middle East lecture trip that included lectures across Turkey and Egypt. It was one of my main ambitions and goals when applying for the Distinguished Lecturer program to deliver interesting lectures in the Middle East and Central Asia. I hoped that, with my cultural background, students, especially female students, could find a resemblance and kinship and would be inspired to engage in graduate studies in the antennas and propagation field. When I received an invitation to visit Egypt in December, I was on board in no time.

Earlier in June, I was asked to deliver lectures at three top universities in Turkey. In addition to the in-person Middle East lectures, I also delivered eight online lectures to Chapters in the United States, Canada, India, and



FIGURE 7. After the lecture at the Higher Institute of Engineering and Technology in Dumyat.



FIGURE 8. At Mediterranean University, Turkey.

France. This report presents a retrospective highlight of my visit to Egypt and Turkey.

My lectures in Egypt started with the Air Defense College in Alexandria on 13 December 2022. The lecture focused on CubeSats and their development cycle, from concept to orbit. The topic was chosen in consideration of the curriculum and interest of the host institute, which is active in organizing the International Conference on Telecommunications.

The second lecture was on 14 December 2022, at the Higher Institute of Engineering and Technology in Dumyat, which is a young yet quite vibrant engineering school. The lecture focused on optically transparent antennas and had almost 300 people in attendance. I was very happy to see responses and reactions from students and was pleased to see a good portion of female enrollment in the program. After the lecture, students walked me around their innovation design laboratory, where many student-led projects are in progress. The projects include energy harvesting, robotics, and artificial intelligence-based sensing. In addition to my lecture, I talked to the students and young faculty

about IEEE, for example, on becoming members and the paper formats of IEEE conferences. I could see the interest and ambition in those bright young eyes, and I hope our Society will keep on growing.

On 15 December 2022, I delivered my last lecture at The Innovation Hub, Silicon Waha, in New Borg El-Arab City. The lecture was open to engineers and students in nearby institutes. The hub is quite fascinating with its fabrication facility and outreach nature. The audience included a high school student working on his design project at the facility.

My lecture in Turkey started at Bosphorus University in Istanbul on 6 June 2022, where two lectures were delivered on the same day, followed by visits to the antenna laboratory and robotics facility. Two more lectures followed at Middle East Technical University on 8 and 13 June, where the presentations were attended by entrepreneurs of small businesses in addition to students and faculty.

My last stop in Turkey was at Mediterranean University on 20 June. It was heartwarming to see many students at the last lecture even though their final exams were over by then.

The lecture turned into an interactive flipped-classroom style activity, where we wrote down background equations with students' initiatives and generated some interesting future project ideas. I was given a tour to see a few graduate research projects after the lecture.

I value all of my experiences and interactions with the audiences in my Middle East lecture tour. I think the presentations are well received as reflected by the feedback I got. I look forward to a fruitful new year.

Figures 7 and 8 are photos of some of the attendees from my 2022 Middle East lecture tour. Additional photos are provided in the supplementary material.

SUPPLEMENTARY MATERIAL





The National Academies of
SCIENCES • ENGINEERING • MEDICINE



National Radio Science Meeting

50th Anniversary Event

January 9-13, 2024 at the University of Colorado at Boulder: www.nrsmboulder.org
Archive website: www.usnc-ursi-archive.org USNC-URSI website: <http://www.usnc-ursi.org/>

You are cordially invited to the in-person 2024 National Radio Science Meeting. This meeting is sponsored by the U.S. National Committee (USNC) for the International Union of Radio Science (URSI), and it is technically co-sponsored by the IEEE Antennas and Propagation Society. It will include plenary speakers, workshops / short courses, exhibits, a student paper competition, a student luncheon, and special events to celebrate the 50th anniversary of holding this meeting in Boulder, CO.

USNC-URSI Chair (2022-2023): Michael Newkirk, Michael.Newkirk@jhuapl.edu

USNC-URSI Chair (2024-2026): Jamesina J. Simpson, Jamesina.Simpson@utah.edu

ABSTRACT AND SUMMARY SUBMISSIONS

Abstract and summary preparation and submission instructions are [posted](#). Authors have their choice of submitting one-page abstracts or two-page summaries, both of which may be archived in IEEE Xplore. Abstracts must have a minimum of 250 words and summaries are limited to two pages. The deadline to submit is **Wednesday, September 13, 2023**. In order for an abstract / summary to be included in the proceedings and submitted to IEEE Xplore, at least one author must be registered and the corresponding presentation must be delivered in person. Registration is also required to attend any session of the meeting. If you have any questions relating to abstract / summary submissions or the technical program, please direct them to the USNC-URSI officers listed above.

Abstracts or summaries on any topic relating to the ten Commissions listed below are welcome. Special sessions will also be organized and are listed on the conference site. Contact the appropriate USNC-URSI Commission Chair listed below or visit the [Topics](#) page on the meeting website for a list of topics and special sessions.

COMMISSIONS

A: Electromagnetic Metrology <i>Chair:</i> Chris Anderson; canderson@ntia.gov	F: Wave Propagation and Remote Sensing <i>Chair:</i> Thomas Hanley; thomas.hanley@jhuapl.edu
B: Fields and Waves <i>Chair:</i> Branislav Notaros; notaros@colostate.edu	G: Ionospheric Radio and Propagation <i>Chair:</i> Thomas Gussiran; gauss@utexas.edu
C: Radio-Communication Systems and Signal Processing <i>Chair:</i> Greg Huff; ghuff@psu.edu	H: Waves in Plasmas <i>Chair:</i> Mark Golkowski; mark.golkowski@ucdenver.edu
D: Electronics and Photonics <i>Chair:</i> Jonathan Chisum; jchisum@nd.edu	J: Radio Astronomy <i>Chair:</i> Alyson Ford; alysonford@arizona.edu
E: Electromagnetic Environment and Interference <i>Chair:</i> Robert Gardner; robert.gardner@gtri.gatech.edu	K: Electromagnetics in Biology and Medicine <i>Chair:</i> Asimina Kiourti; kiourti.1@osu.edu

STUDENT TRAVEL SUPPORT

[Travel support](#) is available for students.

ERNEST K. SMITH USNC-URSI STUDENT PAPER COMPETITION

Prizes are available: First Prize in the amount of \$1000, Second Prize \$750, and Third Prize \$500. The deadline for students to submit [full papers](#) to this [competition](#) is the same as the regular submission deadline.

Questions?

For questions concerning conference logistics, please contact Christina Patarino at:
Phone: (303) 492-5151
E-mail: nrsmboulder@colorado.edu

Abstract / Summary Submissions and
Student Paper Competition Submissions
are due by
September 13, 2023
Please visit www.nrsmboulder.org

Remembering Prof. Rodolfo S. Zich

Roberto D. Graglia 

Rodolfo S. Zich, professor emeritus at Politecnico di Torino, Italy, passed away on 8 May 2023, at the age of 83, after a long illness.

Prof. Zich was the rector of Politecnico di Torino from 1987 to 2001, where he was a full professor of electromagnetic fields and circuits in the Department of Electronics until his retirement in 2011. Among his many honors, he was elected a member of the Accademia Delle Scienze di Torino in 1987 and an Honorary Member of IEEE in 2016.

He was the head of numerous prestigious institutional and entrepreneurial offices. He was extraordinary commissioner of the Galileo Ferraris National Electronic Institute from 1991 to 1993 and a member of the board of directors of the École Polytechnique de Paris from 1997 to 2001. From 1999 to 2003, he was president of CSELT, the research center of the Italian telephone company, during the period of its transformation into TILab, and later, he was the director of the Telecom Italia Mobile joint stock company from 2001 to 2005. He was president of the Torino Wireless Foundation (now Piemonte Innova), which he founded in 2002 to promote information and communications technology innovation in Turin and Piedmont, and president and founder of the Istituto Superiore Mario Boella, now the Links Foundation. He



Prof. Rodolfo S. Zich

was president of the NETTUNO consortium, the first Italian telematic university, now UniNettuno University, and vice president of the supervisory board of Intesa Sanpaolo Bank from 2006 to 2010. Furthermore, his contribution in the 1990s to the reform of university studies in Italy was notable, and his role in promoting digital innovation was extremely important, so much so that he held the position of president of the Italian Association for Informatics and Automatic Calculation from 2010 to 2013.

His contributions to the development of Politecnico di Torino during the years of his rectorship and beyond were fundamental, thanks, above all, to the conception and implementation of the new “Cittadella Politecnica” (“Polytechnic Citadel”), which resulted

in doubling the size of the Politecnico. This achievement placed the Politecnico at the center of Turin city life and played a fundamental role in the post-industrial urban restructuring of the city of Turin, contributing to its transformation into a city dedicated to innovation and research. Several start-ups and the Innovative Enterprise Incubator (I3P) are, in fact, based in the “Cittadella Politecnica.” The I3P was founded in 1999, during the rectorate of Prof. Zich, and is now the best public incubator in the world, as established by the 2019–2020 “UBI World Rankings of Business Incubators and Accelerators.”

Among other things, we cannot forget that Prof. Zich was also the founder and president of the steering committee, on an ongoing basis, of the International Conference on Electromagnetics in Advanced Applications, which is well known to many members of the IEEE Antennas and Propagation Society and whose first edition dates back to 1989.

The solemn greeting to the coffin of Prof. Zich was addressed on 10 May 2023, in the courtyard of honor of Politecnico di Torino, by his family members; Rector Prof. Guido Saracco; Prof. Stefano Lo Russo, mayor of the city of Turin; former Rector Prof. Francesco Profumo, president of the Compagnia di San Paolo Foundation and former minister of university and research; Prof. Marco Mezzalama, president of the Links Foundation and vice president of

the Academy of Sciences of Turin; and all academic authorities and many of his former students.

All those who had the privilege of sharing part of their professional career with Prof. Zich are immensely grateful to

him for his inspired guidance and friendship. His numerous former students join all of the members of the Politecnico di Torino Applied Electromagnetics research group in expressing their deepest condolences to his family and friends.

AUTHOR INFORMATION

Roberto D. Graglia (roberto.graglia@polito.it) is the 2015 past president of the IEEE Antennas and Propagation Society. He is a Life Fellow of IEEE.



WOMEN IN ENGINEERING

(continued from page 104)

Role Model: My role model is Ruth Bader Ginsburg because she worked hard on projects she believed in, and never let anyone stop her from breaking barriers.



What others think: I would say that others think my greatest accomplishment is re-building NIST's traceability path in S-parameter measurements since this has a major impact on global microwave metrology.

Dr. Angela Stelson, NIST, Boulder, USA

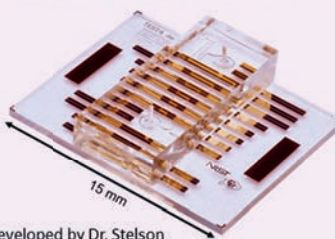
Mentors: Nathan Orloff and Christian Long have both been excellent technical and professional mentors, and their unfailing belief in my ability as a scientist has had an incalculable impact on my career.



What I would like: I hope to see microwave engineering become more interdisciplinary, with other fields using and teaching microwave techniques, and microwave engineers becoming more integrated with physics, chemistry, biology and medicine.

Biggest Accomplishment: Creating an inclusive and welcoming interdisciplinary research environment on the project I lead—people volunteer their time for these projects and want to attend project meetings because they like the environment and the work, and to me that is the sign of good science.

Microfluidics chip developed by Dr. Stelson



Words of wisdom: Surround yourself with people who support you and want you to succeed. It is a sign of strength to be able to walk away from unhealthy situations.

FIGURE 6. Angela Stelson received her undergraduate degree from the University of Oregon and her Ph.D. degree from Cornell University, where she was a Lester B. Knight Nanotechnology Fellow. As a National Research Council (NRC) Postdoctoral Fellow at the National Institute of Standards and Technology (NIST) Boulder, CO, USA, she developed microwave microfluidic measurements, calibrations, and packaged devices for chemical and biological applications. She is currently a physicist at the National Institute of Standards and Technology (NIST), where she is leading the microwave S-parameter measurement project.

and technical strengths. Stay tuned for the last installment later this year!

AUTHOR INFORMATION

Konstantina S. Nikita (knikita@ece.ntua.gr) is a professor at the National Technical University of Athens, 15780 Athens, Greece, and an Irene McCulloch Distinguished Adjunct Professor of Bio-

medical Engineering and Medicine with the Keck School of Medicine and Viterbi School of Engineering, University of Southern California, Los Angeles, CA 90089 USA. She is editor-in-chief of *IEEE Transactions on Antennas and Propagation*. She is a recipient of various honors/awards, including the Bodossaki Foundation Academic Prize.

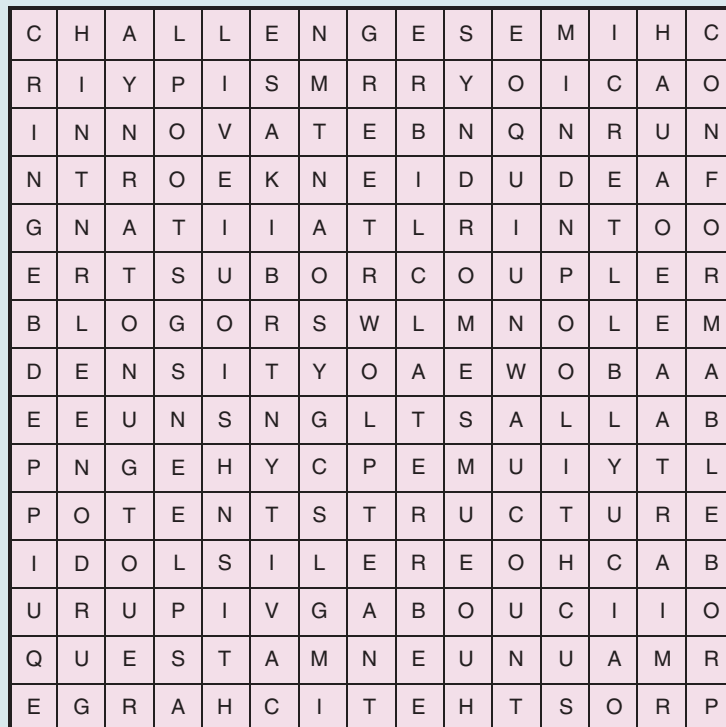
Zoya Popović (zoya@colorado.edu) is a Distinguished Professor and Lockheed Martin Chair of RF Engineering at the University of Colorado, Boulder, CO 80309 USA. She is a member of the National Academy of Engineering. Her research is in analog radio-frequency front ends for various microwave engineering applications.





Fred E. Gardiol

Cross out, in the grid, all the words that appear in the list below — they may appear horizontally, vertically, or diagonally. Seven letters should then remain, referring to an active research field in computing and communication.



Bach	Chimp	Equipped	Labour	Plow	Spleen
Ballast	Clam	Erbil	Later	Potent	Structure
Bias	Conformable	Esaki	Live	Probe	Such
Bionic	Count	Germ	Lynn	Prosthetic	Syndrome
Blog	Coupler	Gross	Loop	Quest	Tang
Bosun	Cringe	Greet	Melon	Raton	Team
Cardiology	Crunch	Health	Malice	Rictus	Tests
Cavity	Deaf	Hint	Mind	Robust	Tubes
Challenge	Density	Idols	Monitoring	Sith	Wolof
Charge	Drug	Innovate	Ooty	Stoop	
Chimes	Engine	Into	Penguin	Snort	



The Advertisers Index contained in this issue is compiled as a service to our readers and advertisers: the publisher is not liable for errors or omissions although every effort is made to ensure its accuracy. Be sure to let our advertisers know you found them through *IEEE Antennas & Propagation Magazine*.

COMPANY	PAGE NUMBER	WEBSITE	PHONE
AR/RF	5	www.arworld.us/sunarrfmotion	+1 215 723 8181
Comsol	3	comsol.com/feature/rf-innovation	
EMCoS	7	www.emcos.com	
Remcom	Cover 4	www.remcom.com/wireless-insite	+1 888 7 REMCOM
WIPL-D	9	www.wipl-d.com	

445 Hoes Lane, Piscataway, NJ 08854

IEEE ANTENNAS & PROPAGATION MAGAZINE REPRESENTATIVE

Mike Sroka
Media Consultant
Naylor Association Solutions
Phone: +1 352 333 3378
msroka@naylor.com

Digital Object Identifier 10.1109/MAP.2023.3295972

SOCIETY OFFICERS & ADMINISTRATIVE COMMITTEE

OFFICERS

Stefano Maci—President
Department of Information Engineering
and Mathematics
Via Roma, 56, 53100 Siena, Italy
E-mail: macis@dii.unisi.it

Branislav M. Notaros—President-Elect
Department of Electrical and Computer Engineering
Colorado State University
Fort Collins, CO, 80523
E-mail: notaros@colostate.edu

Néstor D. López—Treasurer
BAE Systems, Inc.
Nashua, NH
E-mail: nestor.lopez@ieee.org

Felix Vega—Secretary

National University of Colombia, Bogota, Colombia
Electrical and Electronic Engineering Department
Edificio 411 off 210
Ciudad Universitaria, Bogota, Colombia
E-mail: jfvegas@unal.edu.co

ADMINISTRATIVE COMMITTEE

2023
Magda El-Shenawee
Branislav M. Notaros
Kamal Sarabandi
Kwai Man Luk

2024
Anisha M. Apte
Reyhan Bakur
Ashwin K. Iyer
Jiro Hirokawa

2025

Sima Noghanian
C.J. Reddy
Camila Albuquerque
Zhi Ning Chen

HONORARY LIFE MEMBER

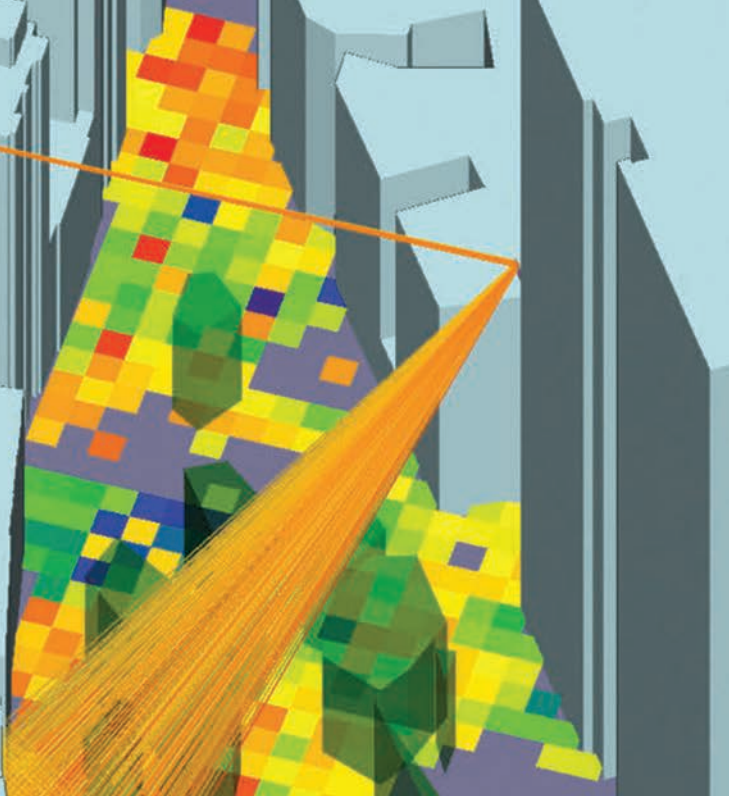
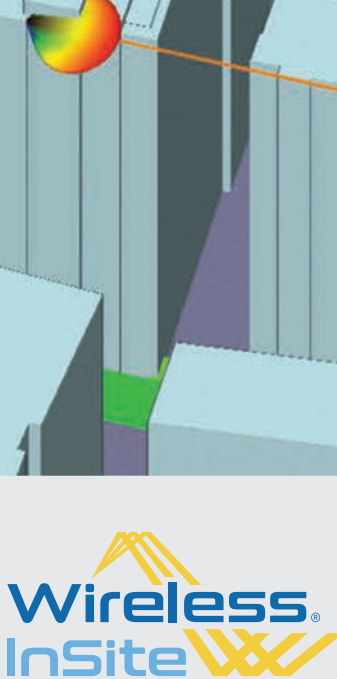
W. Ross Stone

PAST PRESIDENTS

Gianluca Lazzi, 2022
Yahia M.M. Antar, 2021
Mahta Moghaddam, 2020
Koichi Ito, 2019

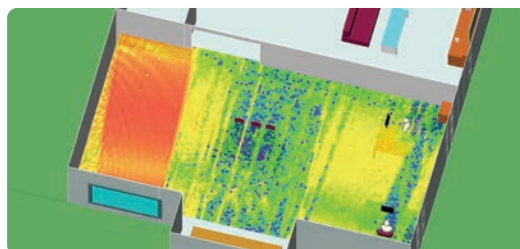


Digital Object Identifier 10.1109/MAP.2023.3291188
Date of current version: 8 August 2023

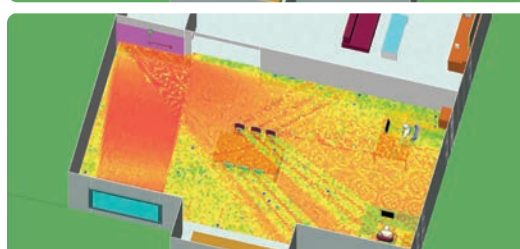


Optimize Wireless Communication Coverage with Wireless InSite®

Now with Engineered Electromagnetic Surface Modeling



Model passive metasurfaces designed to optimize wireless communication coverage by manipulating how signals propagate through a scene.



Evaluate how the EES modifies the propagation environment to improve connectivity.



Learn more and request a demonstration at
www.remcom.com/wireless-insite

Wireless InSite simulates propagation in a scene with sub-optimal signal coverage (top) and reveals the improvement with the addition of an EES (bottom).

REMCOM®

+1.888.7.REMCOM (US/CAN) | +1.814.861.1299 | www.remcom.com

Improve the design process | Reduce development costs | Deliver superior results